STATISTICS OF POLYCHROMATIC SPECKLE PROPAGATION THROUGH THE TURBULENT ATMOSPHERE

Venkata Subba Rao Gudimetla
B. E. Andhra University, Waltair, 1971
M. Tech, Indian Institute of Technology, Kharagpur, 1975

A dissertation submitted to the faculty
of the Oregon Graduate Center
in partial fulfillment of the
requirements for the degree
Doctor of Philosophy
in
Applied Physics

April 1982

The dissertation "Statistics of Polychromatic Speckle Propagation Through the Turbulent Atmospere" by Venkata Subba Rao Gudimetla, has been examined and approved by the following Examiantion Committee:

J. Fred Holmes, Thesis Advisor
Professor

Richard A. Elliott
Associate Professor

Paul R. Davis

William E. Wood
Professor

ACKNOWLEDGMENTS

I gratefully acknowledge my debt to my research advisor, Dr. J. Fred Holmes for suggesting this research problem and for many valuable discussions. I am very thankful to Dr. R. A. Elliott, who taught me Mathematical Physics that improved my mathematical skills and to Dr. Jon Orloff, who taught me Statistical Mechanics, that gave me many new viewpoints in physics. Both these subjects played a major role in shaping this dissertation.

I take this opportunity to express my gratitude to my examination committee members, Dr. Holmes, Dr. Elliott, Dr. Davis and Dr. Wood for their very careful examination and criticism of this manuscript and to my student program committee members, Dr. Rasmussen, Dr. Swanson and Dr. Holmes for helping me plan my Ph.D. program.

During my research work I have enjoyed very much discussing with Dr. M. H. Lee, several problems in the area of Atmospheric Optics. A very special note of thanks to John Hunt for his help whenever there were problems with the computer. I appreciate very much the invaluable cooperation I received from fellow students, Mark Gesley, Jack Biles and Rick DeFreez.

Chris, Maureen and Steve must also be thanked for their help in the Library.

typing of this dissertation and her help as the administrative secretary of the Applied Physics and Electrical Engineering Department.

TABLE OF CONTENTS

LIST OF TABLES

LIST OF ILLUSTRATIONS

ABSTRACT

STATISTICS OF POLYCHROMATIC SPECKLE PROPAGATION THROUGH THE TURBULENT ATMOSPHERE

V. S. Rao Gudimetla
Oregon Graduate Center

Supervising Professor: Dr. J. Fred Holmes

Using the extended Huygens Fresnel principle, the effect of the atmospheric turbulence on the statistical properties of a polychromatic speckle field, generated by a diffuse target, is studied in detail. The results, substantiated by experimental data, indicate that the atmospheric perturbation increases the variance of the received intensity substantially and is sensitive to the wavelength, beam size and beam geometry. The results for the covariance of the received intensity, normalized to the variance, indicate that, at low turbulence levels, reduction in vacuum speckle contrast ratio (VSCR) also reduces the normalized covariance but, with further increase in the turbulence level, reduction in the vacuum speckle contrast ratio increases the normalized covariance. Also it is found that for small detector spacings, the normalized covariance remains approximately constant even with substantial increase in the turbulence level. By resolving the time delayed covariance of the received intensity (TDC), into coherent and incoherent terms, it is shown that for large time delays, the time delayed covariance is determined by the incoherent fluctuations and for poor vacuum speckle contrast ratio, the time delayed covariance is not very sensitive to the wind velocity. Finally it is shown that due to the atmospheric perturbation that the probability density function of the received intensity changes from an M-distribution or a sum of exponential distributions in vacuum to a K-distribution or a weighted sum of K-distributions in the presence of the turbulent atmosphere.

CHAPTER I

INTRODUCTION

Of the two types of flow of liquids and gases, turbulent flow, characterized by the random spatial and temporal fluctuations of fluid mechanical parameters such as pressure, temperature and velocity, is more common in nature as well as in technological applications than laminar flow. A turbulent flow is characterized by its rotational, three-dimensional, nonlinear, diffusive and stochastic nature.[1] As examples, one can consider the turbulent atmosphere around us, the spreading of admixtures in the air, flow of gases in the interstellar nebulae, turbulent flow of water in pipes, high speed jets from nozzles, etc. Monin and Yaglom[2] list several other examples and consider the theory of turbulent fields in detail in their monumental treatise.

Since the turbulent environment is so common around us, it is essential to understand the nature of turbulent fields and their interaction with electromagnetic and acoustic waves. This is either to find the limitations on designing electromagnetic and acoustic systems in the turbulent environment or to use the effects of the turbulent environment on them to understand the nature of the turbulent fields. For example, the performance of a line of sight optical communication link or optical coherent radar is severely limited by the turbulent nature of the atmosphere. However, one can use the effects of the turbulent atmosphere to remotely sense wind velocities and the strength of turbulence. Other applications exist in connection with magnetohydrodynamics and turbulent jets.

Great contributions to the theory of turbulence are made by Reynolds, G. I. Taylor, Keller, Friedmann, Prandtl, Von Karman, Richardson, Kolmogorov, Obukhov and more recently by Kraichnan and Malkus. The treatise by Monin and Yaglom[2] should be consulted for the vast amount of literature and diversity of problems in the theory of turbulence. More recently Hill[3,4] proposed a new spectrum for the refractive index fluctuations of the turbulent atmosphere which seems very useful. This model is used by Elliott, et al.[5] to describe the turbulence simulated in the laboratory.

Before the development of the ruby laser in 1960, two monographs on the propagation of acoustic and radio waves in random media were written by Chernov,[6] and Tatarskii.[7] These works are useful to understand laser beam propagation through the turbulent atmosphere. After translation of these works into English by Silverman in 1961, very extensive theoretical and experimental work was accomplished on the effects of the turbulent atmosphere on the laser beam propagation. This work was reviewed by Lee and Harp,[8] by Lawrence and Strohbehn[9] in 1970, by

Fante,[10] and by Prokhorov, et al.[11] in 1975. More recently Fante[12] updated his earlier review. In addition there is an updated monograph by Tatarskii,[13] a textbook by Ishimaru[14] and an edited monograph by Strohbehn.[15] As stated earlier, most of these works are about the effects of the turbulent medium on a laser beam (on plane and spherical waves) in a line of sight geometry in the context of single scattering. However, Livingstone[16] considered the effects of multiple scattering in the turbulent atmosphere while Dashen,[17] more recently developed path integrals for waves in random media and considered turbulence, characterized by more than two scales.

The problem of speckle propagation through the turbulent atmosphere, which is immediately applicable to such problems as Optical Radar, remote sensing of wind and Coherent Adaptive Optical Systems (COAT systems), was considered by Holmes et al.[19] Assuming a spatially coherent and monochromatic laser source as the transmitter and a diffuse target at the other end of the path, Lee, Holmes and Kerr[18] estimated the effects of the turbulent atmosphere and the cross wind on the propagation of the speckle, generated by the diffuse target. Later this work was generalized by Holmes et al.[19] to include the effects of the log-amplitude fluctuations and the feasibility of remote sensing of wind determined.[20] This work is by far the most complete formulation presented on the speckle propagation through the turbulent atmosphere as it includes all the necessary formulations for the useful first and second order statistics. In this thesis, the monochromatic work cited will be extended by assuming the source to be polychromatic. Fante[21] calculated multiple frequency axial coherence functions and Carl Leader[22] studied the propagation of the spatially partial coherent sources but both works concern line of sight propagation of a laser beam rather than speckle propagation.

1.1 Outlines of the Thesis

In the next chapter, an introduction to speckle phenomena and the reduction of speckle contrast due to the presence of a large number of modes in the laser and due to the lack of coherence of the laser source, when several frequencies are present, is discussed. An important contribution, regarding the number of patterns into which a given polychromatic speckle pattern can be resolved is developed.

In Chapter III, the four point two-frequency amplitude, phase, and cross correlation functions and the corresponding structure functions are derived for a spherical wave. These are generalizations of the results of Yura[23] and Ishimaru.[24] Limitations on the validity of these results are discussed at the end of that chapter.

In Chapter IV, a formulation for the time delayed correlation function of the received intensity for a polychromatic speckle field after propagation through the turbulent atmosphere is given. This formulation will be used to develop all other statistical parameters of the received field in the subsequent chapters.

In Chapter V, using the results from the previous chapters, expressions for the mean and the variance for the received intensity are given and the results are compared with experimental data. The effects of the source parameters (beam size, number of modes, beam geometry, and wave length) and the propagation parameters (path length and turbulence level) on the atmospheric perturbation are discussed in detail and a very useful phenomenological explanation for the behavior of the variance is given.

In Chapter VI, the covariance of the received intensity is derived and the results are compared with experimental data. The relation of the covariance scale size to the Fresnel zone size, the beam size at the transmitter and the lateral coherence length at the target plane is discussed for a given value of the vacuum speckle contrast ratio. Also variation of the covariance (normalized to the variance) for different turbulence levels for several values of the vacuum speckle contrast ratio is discussed. Extensive numerical calculations have been used to obtain the correct behavior of the covariance scale size for several values of the vacuum speckle contrast ratio to estimate the relative effects of the partial coherence of the transmitter.

In Chapter VII, an approximate numerical approach to estimate the time delayed covariance of the intensity is described. Since previously no numerical results were presented for the monochromatic case, this method was applied to the monochromatic case first and then extended to the problem of the polychromatic case. Using the time delayed covariance function to measure the cross wind along the path and the effects of the detector integration time are also discussed. In addition the results for the autocorrelation function of the received intensity and the spectrum of the received intensity fluctuations are given.

In Chapter VIII, the probability density function of the received intensity after propagation through the turbulent atmosphere is considered and the results are compared with the experimental data. Since the previously proposed exponential probability density function[18] for the intensity of a speckle pattern in the turbulent atmosphere is correct under the phase dominance assumption, only if the log-amplitude effects are not considered, a new probability density function for the received intensity fluctuations of the speckle pattern, including log-amplitude effects, was derived first for the monochromatic case and the results are extended to the polychromatic case.

In Chapter IX, final conclusions for the theoretical and experimental work in this thesis are given and the future directions for the extension of this work are discussed.

The appendices include several programs, written by the author for the numerical evaluation of the various statistical parameters developed in this thesis.

CHAPTER II

EFFECT OF THE COHERENCE OF A LASER SOURCE ON THE CONTRAST AND THE NUMBER OF THE DOMINANT EIGENVALUES IN ITS SPECKLE PATTERN

A speckle pattern is formed when partially coherent light is scattered off a rough surface or when coherent light propagates through a turbulent medium. Statistical properties of speckle patterns are dependent on the coherence properties of the laser source and the relevant turbulence parameters. If a surface is very rough i.e. the standard deviation of the optical path differences involved on the surface is very much greater than the wave length of the incident light and the source is coherent as in the case of most lasers, running in a single axial and transverse mode, the contrast of the speckle pattern is unity and the pattern has a striking granular appearance. If the surface is not sufficiently rough or if the incident light is not spatially or temporally coherent, the pattern gets washed out and the speckle contrast reduces (note it is difficult to see speckles in white light). Even though speckle-like phenomena are known elsewhere in physics, for example the temporal statistics of incoherent light,[25] theory of narrow band electrical noise[26] and radio wave propagation,[27] interest in speckle phenomena started with the working of lasers. There was some work on the polychromatic speckle patterns by Ramachandran.[28] Also Goodman[29] in an unpublished but well-known report, developed the statistics of the speckle patterns and related the contrast of the speckle pattern to the roughness of the surface and bandwidth of the incident light. He showed that in case of very rough surfaces, if the incident light is spatially and temporally coherent, the statistics of the field is Complex-Gaussian and so the intensity follows an exponential distribution. Among other workers, Parry,[30,31] Pedersen[32,33] McKechnie[34] and Dainty[35] studied the effects of polychromatic and partially coherent speckle patterns. The state of art in the theory and applications of the laser speckle pattern is summarized in an excellent monograph edited by Dainty.[36] A more general theory of electromagnetic scattering off rough surfaces is discussed in detail by Beckmann and Sphizhichono.[37]

In this chapter the effects of surface roughness and coherence properties of the incident light on the contrast and the number and magnitudes of dominant eigenvalues of the speckle will be studied.

2.1 Effects of Surface Roughness and Bandwidth of the Incident Light on the contrast and Number of the Dominant Eigenvalues of the Speckle Pattern

The determination of the probability density function of the intensity for a speckle pattern formed when a polychromatic source of known spectral distribution is incident on a very rough surface has been considered by various authors.

Using a Karhunen-Loeve expansion, the complex speckle field $A(x,k)$ at a point x in the polychromatic speckle pattern when incident light is of unit intensity and wave number k can be expressed as[38,39]

$$A(x,k) = \sum_{i=1}^{\infty} a_i \Psi_i(k) \tag{2.1}$$

where the a_i's are the random coefficients of the deterministic functions Ψ_i. The Ψ_i's are chosen to be complete orthonormal functions with respect to the source spectral distribution $S(k)$ by requiring that

$$\int \Psi_i(k) \Psi_j(k) S(k)dk = \delta_{ij} \tag{2.2}$$

If the speckle field due to any wavelength in the range where $S(k)$ is nonzero is normally distributed, then the random coefficients will also be normally distributed. In addition, they will be uncorrelated and independent if the expansion functions are chosen to satisfy the Fredholm equation[40]

$$\int S(k)\ \Gamma_A\ (k,k')\ \Psi_i^*(k')dk' = \lambda_i\ \Psi_i(k) \tag{2.3}$$

where

$$\Gamma_A(k,k') = \langle A(x,k)\rangle\ A^*(x,k')\rangle$$

and is the correlation function of the complex random fields. The kernel of Eq.(2.3) is not symmetric but it can be made symmetric by choosing a modified set of orthogonal functions, ϕ_i, such that the eigenvalue equation then becomes

$$\lambda_i \phi_i(k) = \int \sqrt{S(k)}\ \sqrt{S(k')}\ \Gamma_A(k,k')\ \phi_i(k')\ dk' \tag{2.4}$$

It follows that the mean intensity and the variance are given by

$$\langle I(x)\rangle = \sum_{i=1}^{\infty} \lambda_i \quad \text{and } \sigma_I^{\ 2} = \sum_{i=1}^{\infty} \lambda_i^{\ 2} \tag{2.5}$$

Having solved Eq.(2.4) for the eigenvalues, the probability density function for the intensity is given by[29]

$$P_I(I) = \sum_{i=1}^{N} \frac{C_i}{\lambda_i} \quad e^{-I/\lambda_i} \tag{2.6}$$

where

$$C_i = \prod_{j\neq i}^{N} \lambda_i/(\lambda_i - \lambda_j)$$

One method of solving Eq.(2.4) for the N dominant eigenvalues is to take N samples at appropriate wave numbers k_i and solve the resulting N linear equations for the corresponding eigenvalues. Since the system of equations is homogenous, this can be accomplished by diagonalizing the correlation matrix S,

$$[S] = \begin{bmatrix} R(k_1,k_1) & R(k_1,k_2) & \dots & R(k_1,k_N) \\ R(k_2,k_1) & R(k_2,k_2) & \dots & R(k_2,k_N) \\ \vdots & & & \\ R(k_N,k_1) & R(k_N,k_2) & \dots & R(k_N,k_N) \end{bmatrix} \tag{2.7}$$

where

$$R(k_i,k_j) = \sqrt{S(k_i)}\,\sqrt{S(k_j)}\,\Gamma_A(k_i,k_k) \tag{2.8}$$

However since N is not known a priori, either N must be initially very large or successively increased, S diagonalized and the resultant eigenvalues compared to determine if all the dominant eigenvalues have been determined. Either approach could be very time consuming and consequently a method of determining N without first having to solve for the eigenvalues is needed.

Let J_N be equal to the ratio of the sum of the N smallest eigenvalues out of a total of 2N eigenvalues to the sum of all 2N eigenvalues. Then since $\lambda_i < 1$, if $J_N \ll 1$, all the dominant eigenvalues will have been included. It should be noted that J_N equals the fractional error in the mean intensity that will result if only the N largest eigenvalues are considered. Fukunaga[41] considered a similar problem and using his results it can be shown that

$$J_N = \sum_{i=1}^{N} \{R(k_{2i},k_{2i}) - R(k_{2i},k_{2i-1}) - R(k_{2i-1},k_{2i}) + R(k_{2i-1},k_{2i-1})\} / \sum_{i=1}^{N} \{R(k_{2i},k_{2i}) + R(k_{2i-1},k_{2i-1})\} \qquad (2.9)$$

It should be noted that Eq.(2.9) approaches the ratio described above only for N large enough such that J_N is small. If J_N is now calculated using Eq.(2.9) for successively increasing values of N, a point will be reached where J_N is suitably small and N has been determined. At this point the N dominant eigenvalues are determined by diagonalizing the matrix in Eq.(2.7) and then used in Eq.(2.6) to determine the probability density function of the intensity. The question of what is a suitably small value of J_N will be addressed in the next paragraph. The eigenvalues of matrix Eq.(2.7) are determined numerically using the computer program given in Appendix A.

In order to investigate the question of what is an appropriate value of J_N to use as a cutoff point in determining N, the method has been applied to the case of a Gaussian spectral distribution given by

$$S(k) = \frac{1}{\sqrt{2\pi}\, W} \exp\left[-(k - k_o)^2/2W^2\right] \tag{2.10}$$

where W is the bandwidth and k is the wave vector. The rough surface is assumed to have a Gaussian spectral correlation function with $2W\sigma_z$ equal to $\sqrt{15}$, and where $\sigma_z^{\,2}$ is the optical path variance on the surface. The results are shown in Figure 2.1 which shows the probability density functions for several values of N and Table 2.1 which lists the corresponding eigenvalues and J_N's. It appears that since all the normalized eigenvalues are less than unity, from Eq.(2.5) it follows that an error of 5% in the mean value of intensity corresponds to an error, less than 5%, in the variance, the actual reduction depending on the magnitudes of the eigenvalues. This was investigated for the cases where $2W\sigma_z = \sqrt{3}$, $\sqrt{15}$, $\sqrt{63}$, and $\sqrt{99}$ and it is noticed that the optimum choice of samples for this example is approximately given by

$$J_N = 3\sqrt{1 + (2W\sigma_z)^2}$$

In fact by substituting Eq.(2.8) for $R(k_i,k_j)$ in Eq.(2.9) and rearranging the terms, it can be shown that the above choice of N corresponds to about 6% error in the mean value of the intensity. Also from Table 2.1 it is noticed that choosing N greater than the number given by Eq.(2.9) in general does not change the

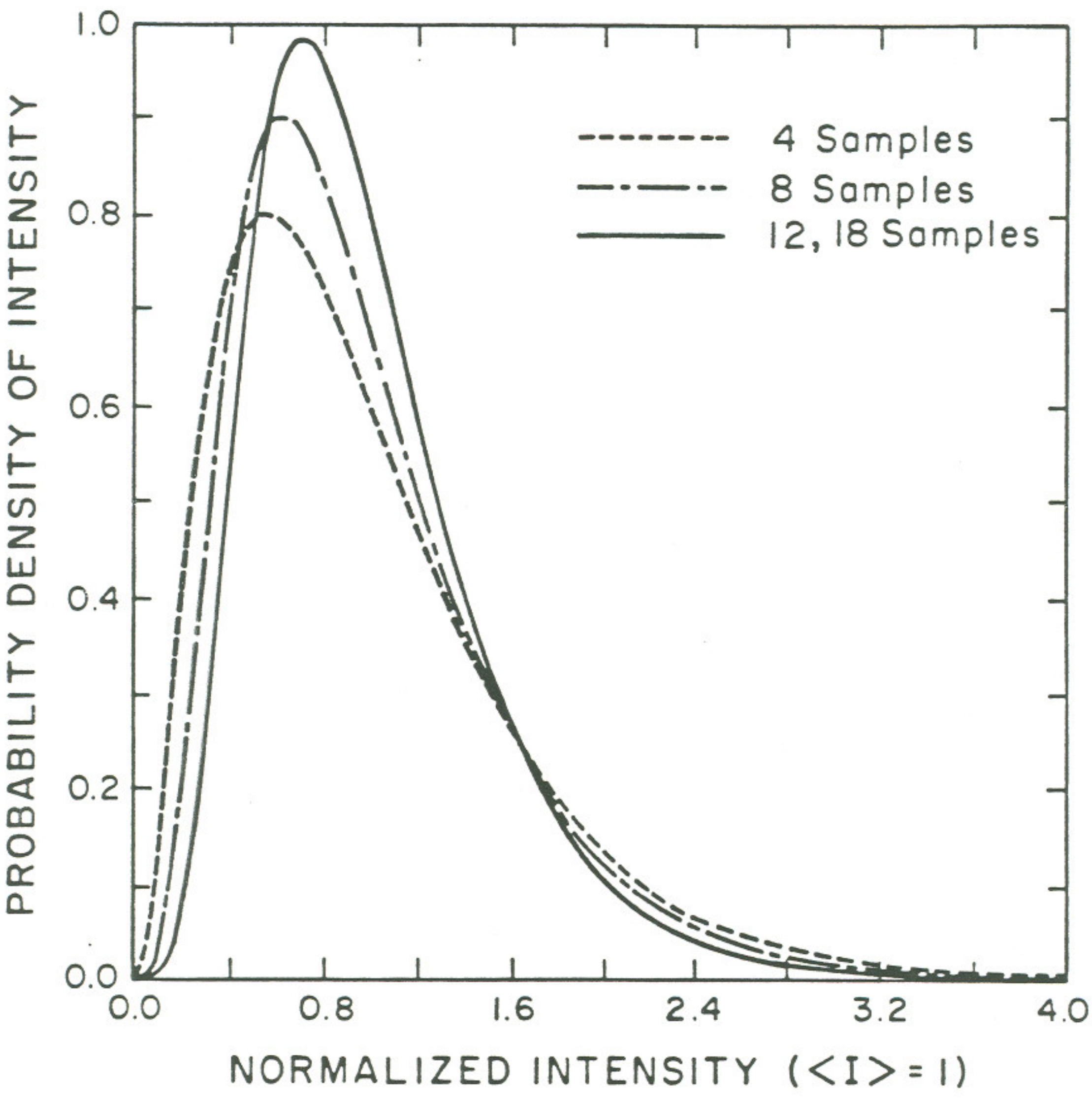

Figure 2.1 Probability density function of the intensity, on the basis of the eigenvalues in Table 2.1 for different values of N.

Table 2.1. Dominant eigenvalues of a polychromatic speckle pattern with Gaussian spectral density and Gaussian spectral correlation on the surface corresponding to equally spaced samples with N = 4, 8, 12 and 18 for $2W\sigma_z = \sqrt{15}$ (sampling range -3W to +3W).

Eigenvalues	N = 4	N = 8	N = 12	N = 18
λ_1	.458272	.510685	.399915	.39910
λ_2	.444980	.249931	.239950	.239947
λ_3	.047588	.121985	.143972	.143968
λ_4	.047590	.061233	.086394	.086380
λ_5		.027674	.051834	.051824
λ_6		.017809	.031208	.031081
λ_7		.004421	.018553	.018611
λ_8		.003915	.011746	.011087
λ_9			.006182	.006520
λ_{10}			.004879	.003741
λ_{11}			.001399	.002066
λ_{12}			.001323	.001085
λ_{13}				.000525
λ_{14}				.000111
λ_{15}				.000047
λ_{16}				.000016
λ_{17}				.000009
λ_{18}				.000000
J_N	.337549	.122425	.058665	.026977
Normalized Variance from above eigenvalues	.41384978	.34839531	.2558	.25116
Normalized Variance from the Theory	.25	.25	.25	.25

eigenvalues significantly. For comparison, the normalized variance from the actual theory and as calculated from each set of eigenvalues are also listed in the table.

An approximate probability density function for the intensity that has been suggested by Parry,[43] Goodman[42] and Barakat[40] is an M-distribution given by

$$P(I) = \frac{M^M \, I^{M-1} \, e^{-MI/\langle I \rangle}}{\langle I \rangle^M \, \Gamma(M)} \tag{2.11}$$

where $\Gamma(....)$ is the gamma function. It is derived by assuming that all the M dominant eigenvalues are equal. When this is not true, then considerable errors can occur, particularly for values of intensity around its mean value. This is illustrated in Figure 2.2 which shows the actual distribution and the corresponding M-distribution ($M = 4$). Since the eigenvalues tend to be equal as M becomes larger, the M-distribution is accurate only if M is large. For the example given, there is substantial difference between the actual and the approximate distribution for the values of the intensity around the mean value.

Using a Gaussian model for the rough surface, the normalized variance of the received intensity is given by[32]

$$\sigma_I^{\,2}/\langle I \rangle^2 = 1/\sqrt{1 + (2W\sigma_z)^2} \tag{2.12}$$

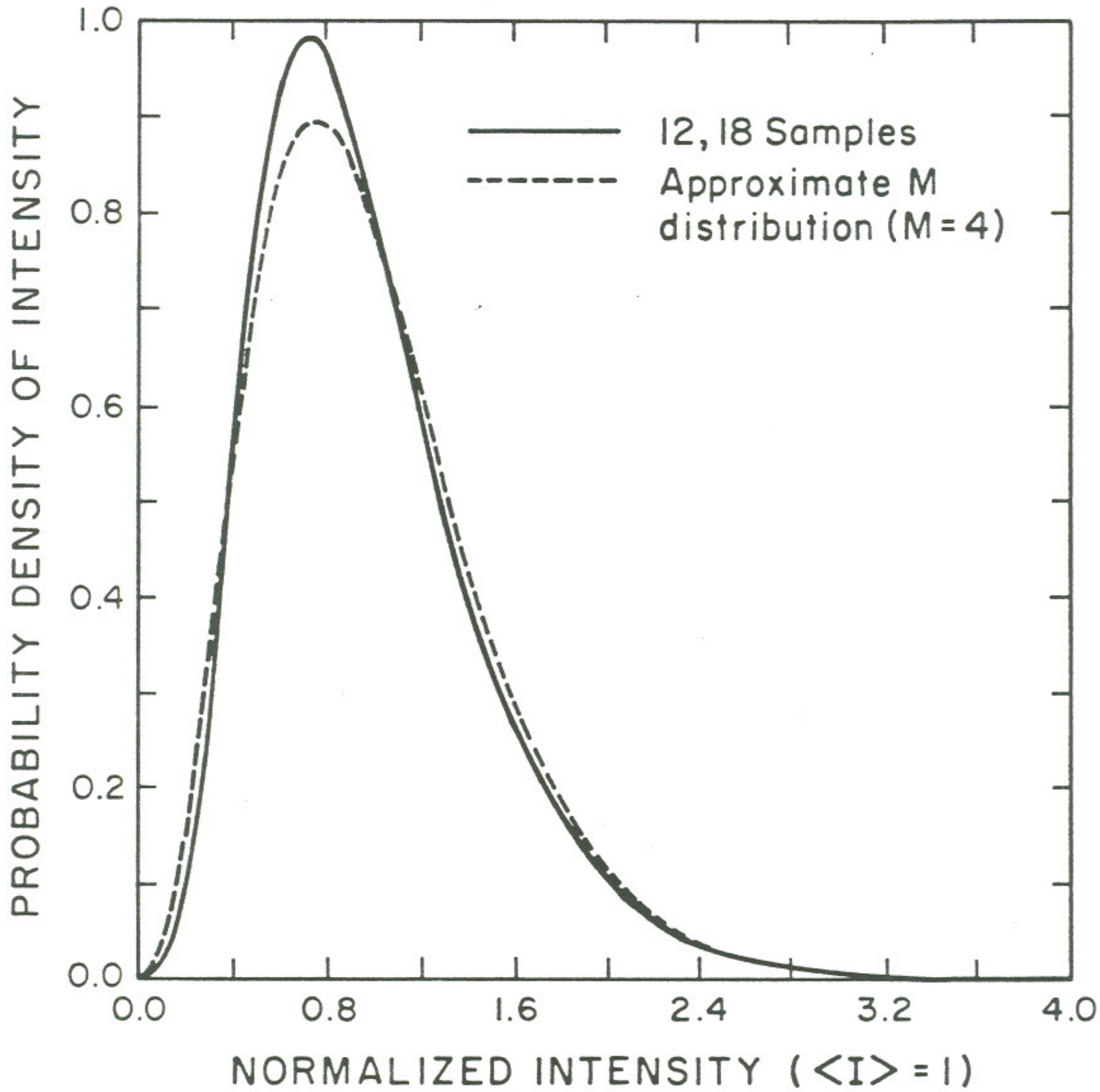

Figure 2.2 Comparison of the probability density function using actual eigenvalues with the approximate M-distribution.

where 2W is the bandwidth and $\sigma_z{}^2$ is the optical path variance. So either as the bandwidth increases or as σ_z increases, the normalized variance reduces. This effect has been used to measure the roughness of the surfaces.[33] Additional representations and characterizations of Gaussian random processes in terms of independent random variables are discussed by Pierre[44] and Ray and Driver.[45]

2.2 Dependence of Speckle Contrast on the Coherence of the Incident Light

It has been shown by several workers[36] that the contrast of a speckle pattern reduces as the coherence of the incident laser light reduces. McKechnie[34] actually used this property to reduce the contrast of speckle patterns. Lasers exhibit poor spatial as well as temporal coherence properties, when running in several longitudinal or transverse modes either in a pulsed or in a continuous mode. Coherence properties of a ruby laser were first studied by Collins, Nelson, Schalow, Bond, Barret and Kaiser.[46] Berkeley and Wolga[47] studied a pulsed ruby laser and noticed that the fringe visibility, in a Young's interference experiment, is dependent on the number of modes present in the laser. Chang and Kilcoyne[48] studied the partial coherence of pulsed multimode radiation from a ruby laser and concluded that the pulsed radiation is not coherent across the beam cross section and it should be treated as a sum of several coherent patches. This reduces the fringe contrast in a Young's interference experiment as they had noticed. Also the effect of the path differences involved when several longitudinal modes are present in the laser beam and its effects on the visibility of the fringes is well known in holography and has been worked out by Foreman[49] and Cathey.[50] Fringe visibility in this case is a periodic function of L/N where L is the length of the cavity and N is the number of the longitudinal modes (all modes are assumed to be of equal amplitude). Collier[51] et al. considered use of gas lasers in interferometry and showed that the fringe visibility is strongly dependent on the number of modes present in the laser. When many modes are present, the laser output may not be coherent across its beam size as the beam size may be substantial compared to L/N. In this section, a simple analysis, following Sotskii and Goncharenko,[52] is presented to relate the degree of the coherence of the laser and the number of modes present in the laser emission.

Assuming that the emission of the laser consists of N plane harmonic waves with different frequencies (ω's) and directions of propagation (wave vectors k's) but with equal amplitude (unity), the analytical signal V(x,t) of such a field is given by[53]

$$V(x,t) = \sum_{j=1}^{N_1} e^{i(k_j x - w_j t)} \tag{2.13}$$

The mutual coherence function at two space time points, $\Gamma(x_1,t_1;x_2,t_2)$ following Wolf[53] is given by

$$\Gamma(x_1,t_1;\ x_2,t_2) = \langle V(x_1,t_1)\ V^*(x_2,t_2)\rangle \tag{2.14}$$

where the angle brackets <....> in this case indicate averaging over time following the ergodic assumption. Using Eqs.(2.13) and (2.14), the mutual coherence function is given by

$$\Gamma_{12}(x_1,t_1:x_2,t_2) = \sum_{j=1} e^{i\{k_j \overline{x_1 - x_2} - w_j \overline{t_1 - t_2}\}} \tag{2.15}$$

For a stationary process, writing $x_1 - x_2 = x$ and $t_2 - t_1 = \tau$ the normalized complex degree of coherence is given by

$$y_{12}(x,\tau) = \Gamma_{12}(x,\tau)/\Gamma_{12}(0,0) = (1/N) \sum_{j=1}^{N} e^{i\{k_j x - w_j t\}} \tag{2.16}$$

The modulus of the above function is then given by

$$\left|y_{12}(x,\tau)\right|^2 = (1/N^2) \sum_{n,s=1}^{N} e^{i(\overline{w_n - w_s}\ \tau + \overline{k_n - k_s}\ x)} \tag{2.17}$$

The effect of the spatial modes will now be considered. Assuming the laser radiation spreads in a small angle and $\tau = 0$, the spatial wave vector of the s th mode is approximately given by

$$k_s = k_o + \Delta k_s$$

where

$$\Delta k_s = \lambda_o s/(2\alpha_o n) \tag{2.18}$$

where α_o is the beam size, n is the refractive index of the medium and λ_o is the wavelength. From this the spatial coherence of the laser beam is given as

$$\left|\gamma_{12}(x)\right|^2 = \sin^2[\Pi Nx/4\alpha_o n]/(N^2 \sin^2[\Pi x/4\alpha_o n]) \tag{2.19}$$

Consider now the temporal coherence by assuming $x = 0$ in Eq.(2.17). For the longitudinal modes in a cavity of length L, it is known

$$w_q - w_s = \Pi c/[nL(q - s)] \tag{2.20}$$

where q and s refer to mode numbers, n is the refractive index and c is the velocity of light. Then the temporal coherence of the emission is given by

$$\left|\gamma_{12}(\tau)\right|^2 = \sin^2[N\Pi c\tau/2nL]/(N^2 \sin^2[\Pi c\tau/2nL]) \tag{2.21}$$

It is clear from the above expressions that the radiation is completely coherent if and only if the emission consists of a single longitudinal and transverse mode and that the coherence length (time) quickly reduces as the number of modes increases. The above theory is derived assuming a stationary laser emission. For non-stationary emission, the mutual coherence function from Eqs.(2.13) and (2.14), is given by

$$\left|\gamma_{12}(\tau)\right|^2 = (1/N^2)\left[N + 2 \sum_{n>s=1}^{N} \cos\{\overline{k_n - k_s}\, x - \overline{w_n - w_s}\, \tau\}\right] \qquad (2.22)$$

Since the distribution of the frequencies (within the limits of the width of the emission line) and the propagation directions of the modes will be completely random for all the modes, the second term in the numerator of Eq.(2.22) will be zero and the coherence of the laser emission is given by

$$\left|\gamma_{12}(\tau)\right|^2 = 1/N \qquad (2.23)$$

Thus for non-stationary emission, the laser radiation will be partially coherent, the degree of coherence being determined by the number of the modes.

As the degree of coherence of the incident laser source reduces, the speckle contrast also reduces for a given roughness of the surface. In applications, such as remote sensing of the crosswind, pulsed lasers such as CO_2, Nd:YAG lasers are being used. Coherence properties of these lasers are very poor and the contrast of a speckle pattern, formed when these lasers are scattered off an extremely diffuse target, is very low. Holmes et al.[54] report a contrast of .142 for the speckle pattern, generated when a pulsed Nd:YAG laser is scattered off a diffuse target, located at a distance of 500 meters from the transmitter-receiver plane and attributed it to a large number of longitudinal and transverse modes. Fossey et al.[55] reported a speckle contrast of .55 when using an Argon laser (without etalon in the cavity) in the same experiment and they attributed it to the presence of several longitudinal modes in the laser. In addition the following experiments were conducted by the author. Two almost identical laser beams are superimposed and the resultant beam scattered off white paper. Initially the contrast of the speckle pattern due to each beam was found to be very high by blocking the other beam. But when the contrast of the total speckle pattern was measured with both the laser beams present, it was found to be poor (the corresponding normalized variance is .45). This result was independent of the fact whether the bright and dark patches of the speckles due to each beam overlap or not. This indicates that both patterns behave as if they are statistically independent. This is true because there is no interference between two independent lasers, when the detector integration time is too large to resolve the beats between them. These results are summarized in Table 2.2, where the mean, the second moment and the normalized variance of the intensity of each speckle pattern and the total speckle pattern are given (the slight variation in the normalized

Table 2.2 DATA ON THE TWO BEAM SPECKLE EXPERIMENT

	Average Intensity	Second Moment	Variance	Normalized Variance
First Beam (I_1)	187.39	67395	32280	.92
Second Beam (I_2)	182.39	63622	30356	.91
Superimposed Two Beams				
Position #1	372.59	203744	64291	.47
Position #2	349.59	174697	52484	.43
Position #3	397.99	228892	70486	.445

variance is due to the fact that in order to decorrelate the speckle patterns by an order of speckle size, one of the beams has to strike the target at a very small angle to the normal and the resultant speckle pattern falls on the detector at an angle). Figures 2.3 and 2.4 give the probability density function of the intensity of the speckle pattern due to each beam separately. It can be seen that the resultant statistics in each case is approximately exponential. Figure 2.5 gives the probability density function of the total speckle pattern when both laser beams are superimposed for 3 different positions, such that in position (1), the speckles due to each beam only overlap, in position (2) the speckles due to each beam only partially overlap and in position (3), the speckle patterns are completely decorrelated. It is noticed that there is no significant difference in the nature of the probability density function or in the normalized variance. This reduction in speckle contrast is due to the fact that both the laser beams, however identical they may be, are statistically independent and thus remain incoherent with respect to each other. In this case, the complex speckle field is no longer Gaussian and so the fields due to each beam should be added on intensity basis. In addition, the contrast of the speckle pattern, generated when an argon laser beam, at .488 μm, without an etalon in the cavity is scattered off a white paper target, was measured and was found to be .34. Figure 2.6 gives the probability density function of the

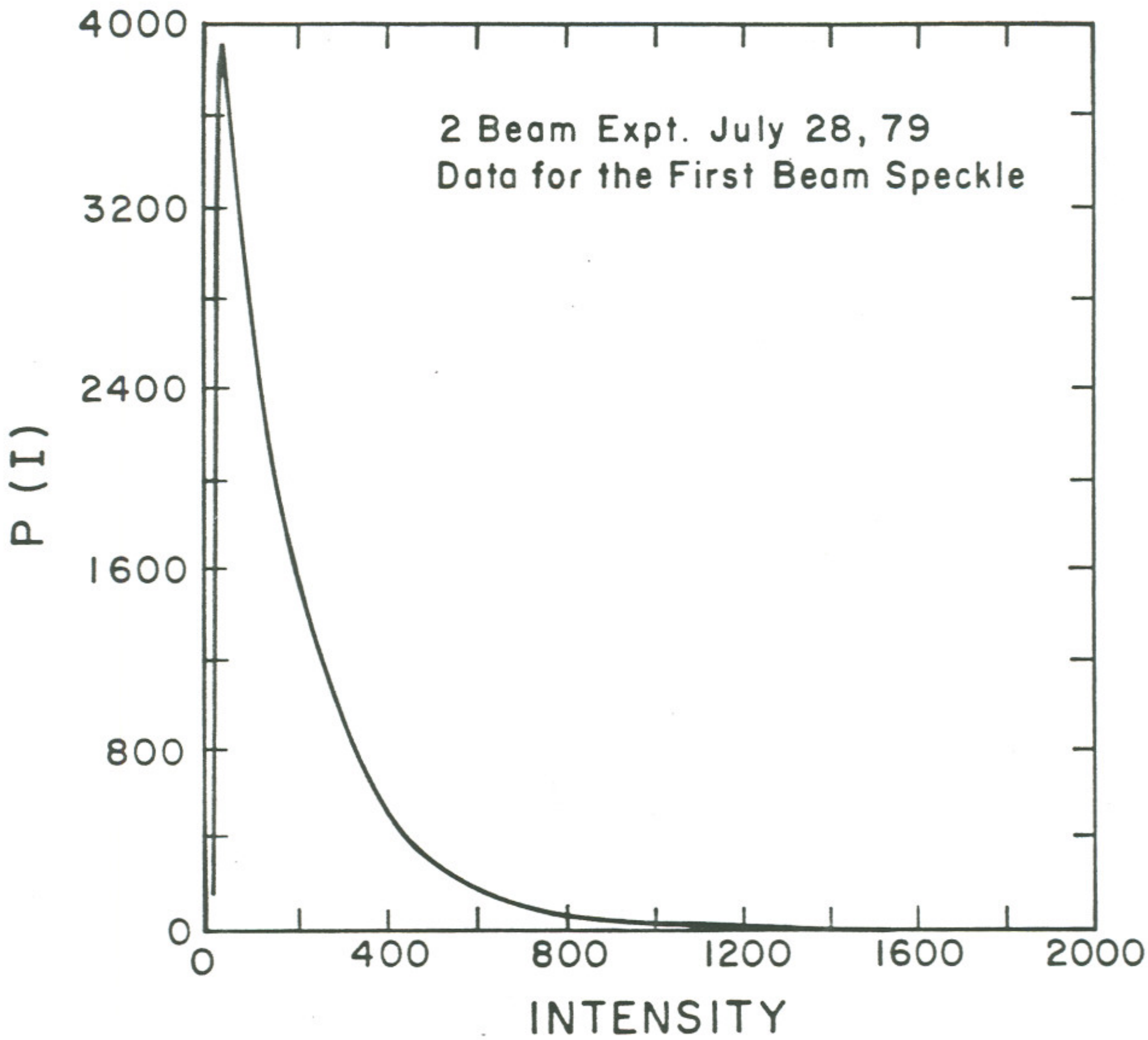

Figure 2.3. Probability density function of the intensity of speckle pattern when only one beam is present (Beam 1).

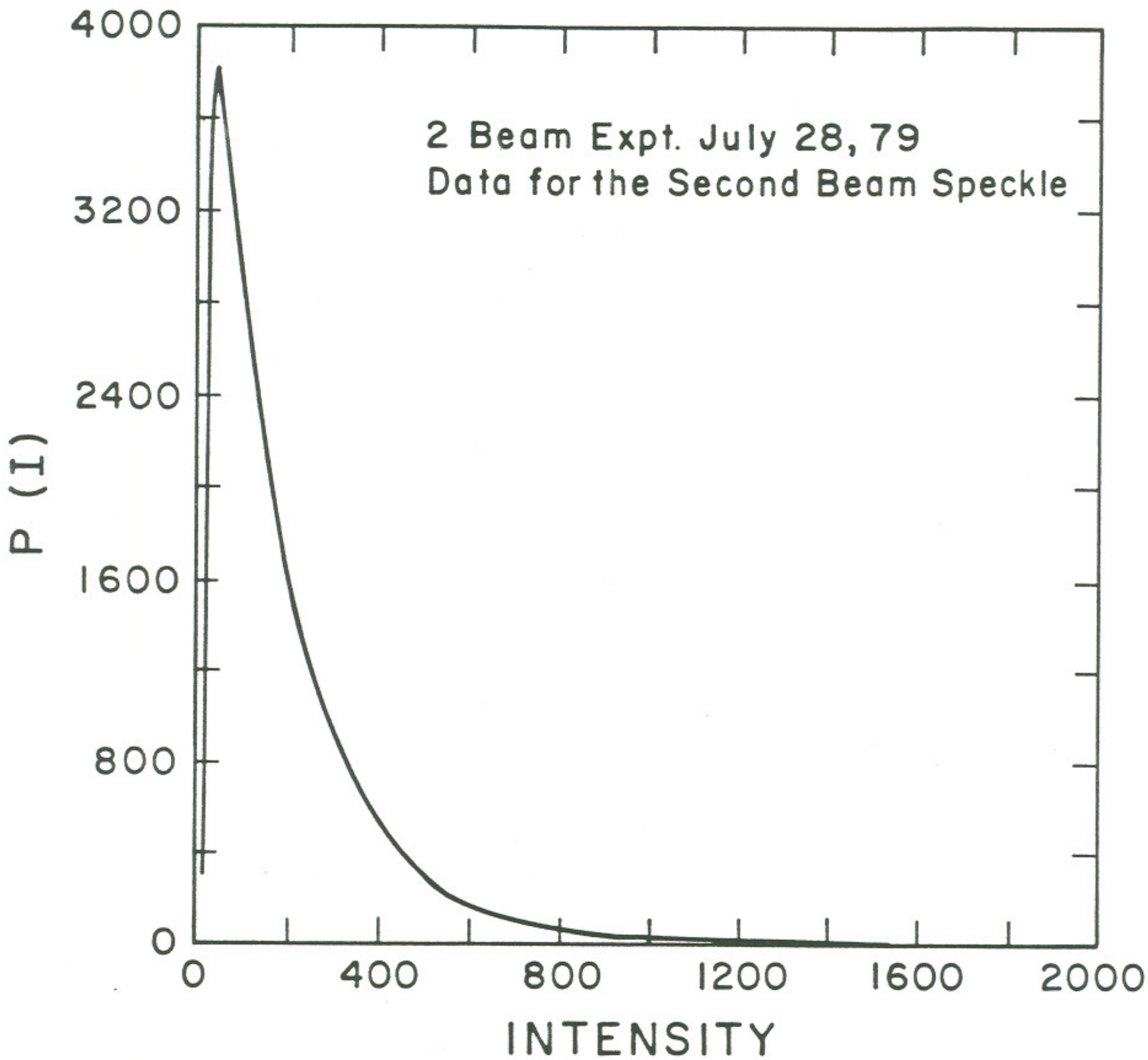

Figure 2.4. Probability density function of intensity of speckle pattern when only one beam is present (Beam 2).

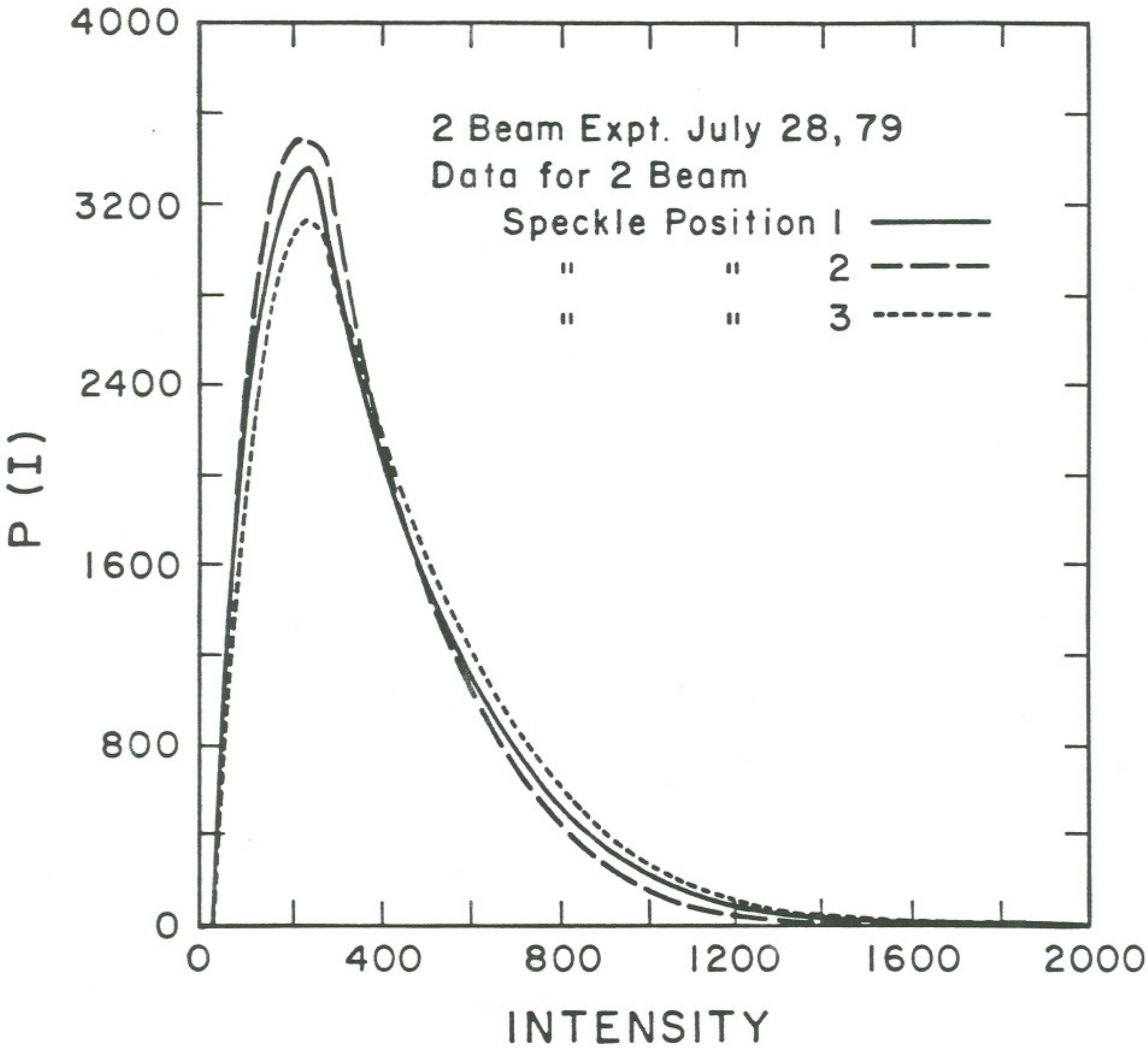

Figure 2.5 . Probability density function of the intensity of speckle pattern when two laser beams are superimposed. Positions refer to the conditions when the speckle patterns are completely correlated, partially correlated and completely decorrelated.

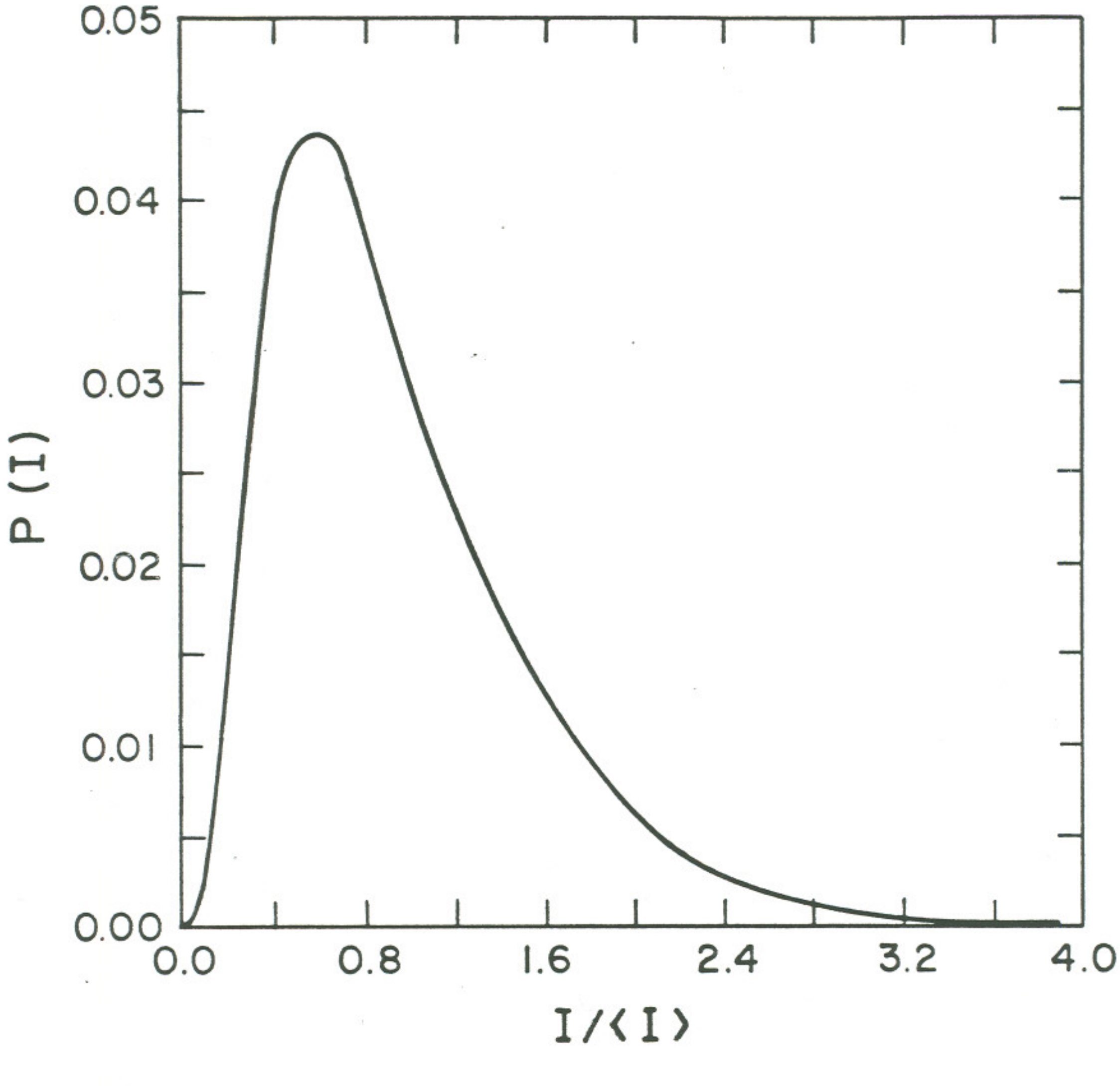

Figure 2.6. Probability density function of the intensity of a speckle pattern formed, when a multimode argon laser is scattered off a white paper.

speckle pattern, generated in this case. In Figure 2.7, the cumulative experimental probability values are compared with the theoretical values, using an M-distribution with M = 2.875. It can be seen that there is an excellent agreement between the theory and the experiment.

In the above experiments, an ensemble average over a set of rough surfaces was achieved by rotating the target very slowly. The reduction in speckle contrast of the superimposed beam cannot be due to the target rotation since for a single beam very high contrast was observed. The intensity correlation between the two speckle patterns is related to the correlation between the corresponding field correlations. The correlation between the fields from two different sources is zero. Had there been correlation between the fields, a single speckle pattern of very high contrast would have been observed. Over an ensemble of patterns, the fields due to both beams would be added incoherently. That both the speckle patterns are fundamentally independent can be observed from Table 2.2 where the total average is the sum of averages of both beams and the total variance is the sum of variances. In addition, additional reduction in speckle contrast can be due to the fact that individual longitudinal modes may have a different phase curvature.

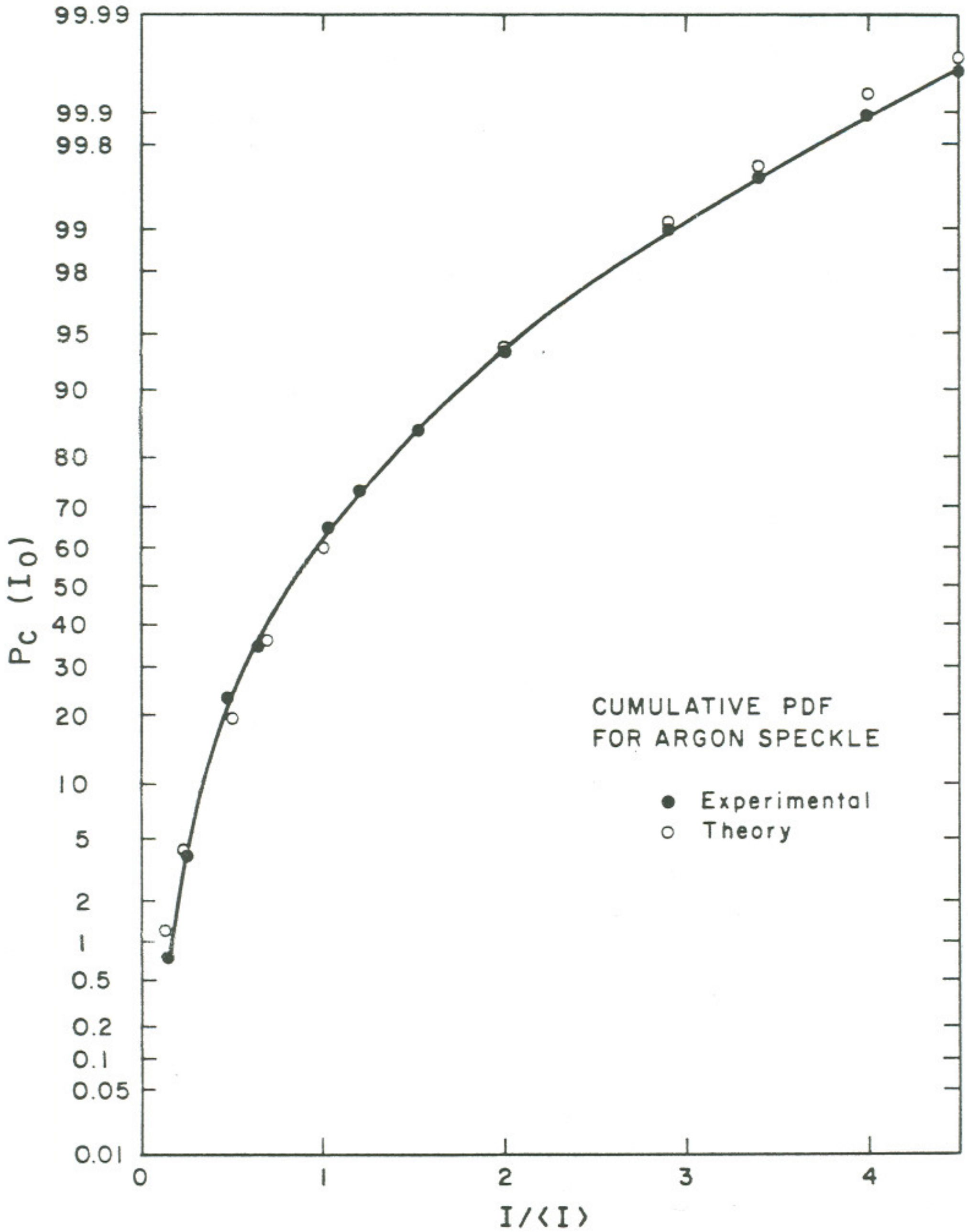

Figure 2.7. Comparison of theoretical and experimental values of the cumulative density function of the intensity for a multimode argon laser on probability paper.

2.3 Speckle Averaging

The speckle theory is closely related to the theory of coherence. An important work in the theory of coherence is the quantum mechanical representation of optical fields due to Glauber[56] who also showed that incoherent light of very narrow bandwidth can be formed by superimposing several identical but statistically independent lasers. In addition, classical models were developed by Mandel and Wolf.[57] The role of coherence concepts in the speckle theory was examined recently by Goodman.[58] Goodman also showed that a speckle pattern is only locally stationary and thus the average of a speckle over an ensemble of surfaces is not the same as the spatial average over the pattern. Similarly due to nonergodicity, the average of the speckle patterns over time is also not an ensemble average. So one must, while studying the statistical properties of the speckle averaging over both ensembles (sources and rough surfaces) must be used.

2.4 Conclusions

In this chapter important aspects of speckle theory were detailed. In particular, a very useful method for determining the eigenvalues of a polychromatic or partially coherent speckle pattern was developed. It must be noted that the criterion for N in Eq.(2.9) is not just a matter of selecting sufficient samples for solving the Eq.(2.4) but emphasizes the fact that a polychromatic or partially coherent speckle pattern can be resolved into a few dominant Gaussian speckle patterns. Also the effects of laser coherence on the contrast of speckle were discussed. Since most of the sources for applications such as COAT systems, wind sensing systems, etc., are pulsed laser sources, which run in several longitudinal and transverse modes, the speckle contrast from diffuse targets will be poor. Then the received speckle pattern can be treated as a sum of several independent Gaussian speckle patterns. This fact is used in the subsequent chapters to study the effects of the turbulent atmosphere on a speckle pattern with a poor vacuum speckle contrast ratio.

CHAPTER III

FOUR POINT TWO FREQUENCY CORRELATION AND STRUCTURE FUNCTIONS IN THE TURBULENT ATMOSPHERE

In order to develop the theory of polychromatic speckle propagation through the turbulent atmosphere, the four point two frequency amplitude correlation function, the four point two frequency phase correlation function, the four point two frequency correlation function for amplitude at one frequency and phase at another frequency and finally the two frequency amplitude, phase and wave structure functions are needed. Since the extended Huygens Fresnel approximation is used in the subsequent theory, all the above formulations should be developed for a spherical wave. Since the four point two frequency correlations have not yet been reported in the literature, these formulations are developed in this chapter from fundamentals. The results in this chapter are generalizations of the results of Yura[23] and Ishimaru.[24]

3.1 FOUR POINT TWO FREQUENCY CORRELATION FUNCTIONS

Consider a spherical wave propagating through a random medium, the refractive index of which is given by

$$n(r) = 1 + n_1(r) \tag{3.1}$$

here $n_1(r)$ is the fluctuating part and $n_1 << 1$. Choosing the z axis as the direction of propagation, the electrical field satisfies the Helmholtz wave equation given by

$$[\nabla^2 + k^2\{1 + n_1(r)\}^2]U_1 = 0 \qquad (3.2)$$

Under frozen turbulence conditions, when a vector cross wind of velocity V is present, the fluctuation part of the refractive index term n_1 at time t, in plane z' is related to the random spectral amplitude $d\nu(K,z')$ by the relation[63]

$$n_1(\overline{\rho}', \overline{z}', t) = \int_{-\infty}^{\infty} e^{i\overline{K}\cdot(\overline{\rho}' - \overline{V}t)} \, d\nu(K, z') \qquad (3.3)$$

where $\overline{\rho}'$ is the transverse vector at z' and K is the spatial wave vector of the refractive index fluctuatons. The random spectral amplitude $d\nu(K,z)$ satisfies the relation[59]

$$\langle d\nu(K,z)d\nu^*(K',z')\rangle = F_n(K,z-z')\ \delta(K-K')dK'dK \qquad (3.4)$$

where the angle brackets $\langle\ \rangle$ indicate the ensemble average and $F_n(K,z)$ is the two-dimensional spectral density of the refractive index fluctuations. If the random medium is assumed to be stationary and dispersion is negligible, the spatial correlation of refractive index fluctuations $B_n(\overline{x}_1,\overline{x}_2)$ is given by using Eqs.(3.3) and (3.4), as

$$B_n(\bar{x}_1,\bar{x}_2) = \langle n_1(\bar{x}_1)\; n_1^*(\bar{x}_2)\rangle$$

$$= \int d^2K\; F_n(K,z_1-z_2)\; e^{-iK\cdot[(\bar{\rho}_1-\bar{\rho}_2) - V(t_1-t_2)]} \tag{3.5}$$

the coordinate $\bar{x}$ being $(\bar{\rho},z)$. Let $\bar{r}$ be a coordinate vector in the transmitter plane and $\bar{p}$ be a vector in the receiver plane, both planes being perpendicular to the direction of propagation, the z-axis. To derive the correlation functions, it is enough to consider only the line of sight geometry.

By using the Rytov method,[60] the solution for Eq.(3.2) is

$$U_1(\bar{r},\bar{p}) = U_o(\bar{r},\bar{p})e^{i\psi(\bar{r},\bar{p})} \tag{3.6}$$

where $U_o(\bar{r},\bar{p})$ is the solution in free space and $\psi(\bar{r},\bar{p})$ is the effect of the random medium. Then from the results of Tatarskii,[60]

$$U_1(\bar{r},\bar{p}) = (k^2/2\pi)\int d^3x\; n_1(\bar{x})\; U_o(\bar{r},\bar{x})\; \frac{e^{ikR(\bar{x},\bar{p})}}{R(\bar{x},\bar{p})}$$

and

$$U_o(\bar{r},\bar{x}) = \frac{e^{ikR(\bar{x},\bar{r})}}{R(\bar{x},\bar{r})} \tag{3.7}$$

where $R(\bar{x},\bar{r})$ is the distance between the vector coordinates $\bar{x}$ and $\bar{r}$. By using the Hygens Fresnel approximation for $\psi(\bar{r},\bar{p})$[62,63] and using Eq.(3.3) for $n_1(\bar{x})$, as $\psi = U_1/U_0$

$$\Psi(\bar{r},\bar{p}) = \frac{k^2}{2\pi}\, e^{\frac{ik|\bar{r}_1-\bar{p}_1|^2}{2L}} \int d^3x_1\, e^{\frac{ik|\bar{\rho}_1-\bar{r}_1|^2}{2z_1}}$$

$$e^{\frac{ik|\bar{\rho}_1-\bar{p}_1|^2}{2(L-z_1)}} \int e^{-iK\cdot(\bar{\rho}_1-\bar{V}t_1)}\, d\nu(K,z_1) \tag{3.8}$$

In the above integral, $\bar{\rho}_1$ is the transverse vector coordinate in the plane z_1. The integration over $\bar{\rho}_1$ can be extended to $\pm\,\infty$, even though the approximation is not valid for sufficiently large values of $|\rho|$. This is because, the integral over the region, where $|\rho|$ is large, is zero due to the rapid oscillations of the integrand in this region. Then completing the integral over ρ_1, we get

$$\Psi(\bar{r},\bar{p}) = ik \int_0^L dz_1 \int_{-\infty}^{\infty} d\nu(K,z_1)\, e^{(iK^2/2k)z_1(1 - z_1/L)}$$

$$e^{-i[(z_1/L)\bar{p}_1 + (1 - z_1/L)\bar{r} - \bar{V}t_1]\cdot\bar{K}} \tag{3.9}$$

The complex function $\Psi(\bar{r},\bar{p})$ can be resolved into a real part $\chi(\bar{r},\bar{p})$, which represents the amplitude fluctuations and $\phi(\bar{r},\bar{p})$, which represents the phase fluctuations. Then from Eq.(3.9), we get

$$\chi(\bar{r},\bar{p}) = [\Psi(\bar{r},\bar{p}) + \Psi^*(\bar{r},\bar{p})]/2$$

$$= k \int_0^L dz_1 \int_{-\infty}^{\infty} d\nu(K,z_1)\, e^{-i[(z_1/L)\,\bar{p} + (1 - z_1/L)\,\bar{r} - \bar{V}t_1]\cdot\bar{K}}$$

$$\sin[K^2 z_1(1 - z_1/L)/2k] \tag{3.10}$$

and

$$\phi(\bar{r},\bar{p}) = (1/2i)[\Psi(\bar{r},\bar{p}) - \Psi^*(\bar{r},\bar{p})]$$

$$= k \int_0^L dz_1 \int_{-\infty}^{\infty} d\nu(K,z_1)\, e^{-i[(z_1/L)\bar{p} + (1 - z_1/L)\,\bar{r}_1 - \bar{V}t_1]\cdot\bar{K}}$$

$$\cos[K^2 z_1(1 - z_1/L)/2k] \tag{3.11}$$

To find the four point, two frequency correlation functions, consider two point sources at different frequencies k_1 and k_2, the positions of which are at coordinate vectors $\bar{r}_1$ and $\bar{r}_2$, in the plane $z = 0$. Consider now two points in the receiver plane, their positions being given by the transverse coordinates $\bar{p}_1$ and $\bar{p}_2$ in the receiver plane $z = L$. The four point two frequency amplitude correlation function, is the correlation between the amplitude fluctuations at a point $\bar{p}_1$ in the receiver plane at a time t_1 due to a point source at $\bar{r}_1$ in the transmitter plane at a frequency k_1 and the amplitude fluctuations at a point $\bar{p}_2$ in the receiver plane at time t_2 due to a point source at $\bar{r}_2$ in the transmitter plane at a frequency k_2 and is denoted as $C_\chi(\bar{r}_1,\bar{p}_1,t_1,k_1;\ \bar{r}_2,\bar{p}_2,t_2,k_2)$.

$$C_\chi(\bar{r}_1,\bar{p}_1,t_1,k_1;\ \bar{r}_2,\bar{p}_2,t_2,k_2) = \langle\chi(\bar{r}_1,\bar{p}_1,t_1,k_1)\ \chi^*(\bar{r}_2,\bar{p}_2,t_2,k_2)\rangle$$

$$= k_1k_2 \int_0^L dz_1 \int_0^L dz_2 \int_0^{\infty} F_n(K,\ z_1 - z_2)\ d^2K$$

$$+ (1 - z_2/L)\,\bar{r}_2 - \bar{V}t_2] \cdot \bar{K}]\}$$

$$\sin[K^2 z_1(1 - z_1/L)/2k_1]\ \sin[K^2 z_2(1 - z_2/L)/2k_2] \qquad (3.12)$$

Changing the variables z_1 and z_2 to ξ and η where $2\eta = z_1 + z_2$ and $\xi = z_1 - z_2$ and noting that $F_n(K,\xi) = 0$ for $|\xi| > L_o$ where L_o is the scale length of inhomogeneties (outer scale), we get

$$C_\chi(\bar{r}_1,\bar{p}_1,t_1,k_1\!: \bar{r}_2,\bar{p}_2,t_2,k_2)$$

$$= 2k_1k_2 \int_o^L d\eta \int_o^L d\xi \int_o^\infty F_n(K,\xi)\ d^2K$$

$$e^{-i[\{(\eta + \xi/2)/L\}\bar{p}_1 + \{(1 - \eta + \xi/2)/L\}\bar{r}_1 - \bar{V}t_2] \cdot \bar{K}}$$

$$e^{i[\{(\eta - \xi/2)L\}\bar{p}_2 + \{(1 - \eta - \xi/2)/L\}\ \bar{r}_2 - \bar{V}t_2] \cdot \bar{K}}$$

$$\sin[K^2(\eta + \xi/2)(L - \eta + \xi/2)/(2Lk_1)]$$

$$\sin[K^2(\eta - \xi/2)(L - \eta - \xi/2)/(2Lk_2)]$$

Since in the region of important integration, the terms involving ξ may be neglected except in the spectral density $F_n(K,\xi)$. As $\xi = 0$ for $|\xi| > L_o$ the limits of integration can be extended to ∞. Since

$$\int_o^\infty F_n(K,\xi)\ d\xi = \pi\phi_n(K)$$

where $\phi_n(K)$ is the three-dimensional spectral density of refractive index fluctuations, the four point two frequency amplitude correlation function is given by

$$C_\chi(\bar{r}_1,\bar{p}_1,t_1,k_1:\ \bar{r}_2,\bar{p}_2,t_2,k_2)$$

$$= 2\pi\, k_1 k_2 \int_0^L d\eta \int_0^\infty d^2K\ \phi_n(K)\ e^{-i[(\eta/L)(\bar{p}_1-\bar{p}_2)\ +\ (1-\eta/L)(\bar{r}_1-\bar{r}_2)-\bar{v}\tau]\cdot\bar{K}}$$

$$\sin[K^2\eta(1-\eta/L)/2k_1]\ \sin[K^2\eta(1-\eta/L)/2k_2] \qquad (3.14)$$

where $\tau = t_1-t_2$, by assuming the fluctuations are stationary. For isotropic turbulence this reduces to

$$C_\chi(\bar{r}_1,\bar{p}_1,t_1,k_1;\ \bar{r}_2,\bar{p}_2,t_2k_2)$$

$$= C_\chi(\bar{r}_1-\bar{r}_2,\bar{p}_1-\bar{p}_2,t_1-t_2,k_1,k_2) = C_\chi(\bar{r},\bar{p},\tau,k_1,k_2)$$

$$= 4\pi^2 k_1 k_2 \int_0^L d\eta \int_0^\infty K\ dK\ \phi_n(K)$$

$$J_o(K\left|\frac{\eta}{L}\,\bar{p} + (1-\frac{\eta}{L})\ \bar{r}-\bar{v}\tau\right|)$$

$$\sin[K^2\eta(1-\eta/L)/2k_1]\ \sin[K^2\eta(1-\eta/L)/2k_2] \qquad (3.15)$$

where $\bar{p} = \bar{p}_1-\bar{p}_2$ and $\bar{r} = \bar{r}_1-\bar{r}_2$. By substituting the proper spectrum of refractive index fluctuations in Eq.(3.14) or (3.15), depending on whether the refractive index fluctuations are isotropic or not, the amplitude correlation function for the two frequency, four point case can be evaluated.

Now using Eqs.(3.11) and (3.4) and following the same arguments used to derive the amplitude correlation function, it can be shown that the four point two frequency phase correlation function for the isotropic case is given by

$$C_{\phi}(\bar{r}_1,\bar{p}_1,t_1,k_1;\ \bar{r}_2,\bar{p}_2,t_2,k_2)$$

$$= 4\pi^2 k_1 k_2 \int_o^L d\eta \int_o^\infty K\ \phi_n(K)dK\ J_o\left(K\left|\frac{\eta}{L}(\bar{p}_1-\bar{p}_2) + (1-\frac{\eta}{L})\ (\bar{r}_1-\bar{r}_2) - v\tau\right|\right)$$

$$\cos[K^2\ \eta(1-\eta/L)/2k_1]\ \cos[K^2\ \eta(1-\eta/L)/2k_2] \tag{3.16}$$

Similarly the cross correlation function for the amplitude at a frequency k_1 at a point p_1 in the receiver plane at a time t_1 due to a point source at r_1 in the transmitter plane and the phase at a frequency k_2 at a point p_2 in the receiver plane at time t_2 due to a point source at r_2 in the transmitter plane is derived using Eqs.(3.10), (3.11) and (3.4). Following the same arguments as earlier and considering the case of isotropic turbulence the cross correlation function is given as

$$C_{\chi\phi}(\bar{r}_1,\bar{p}_1,t_1,k_1:\ \bar{r}_2,\bar{p}_2,t_2,k_2)$$

$$= 4\pi^2 k_1 k_2 \int_o^L d\eta \int_o^\infty K\ \phi_n(K)\ dK\ \cos[K^2\ \eta(1-\eta/L)/2k_2]$$

$$J_o\left(K\left|(\eta/L)\ \overline{p_1-p_2} + (1-\eta/L)(\overline{r_1-r_2}) - \bar{v}\tau\right|\right)\ \sin[K^2\eta(1-\eta/L)/2k_1] \tag{3.17}$$

Using these correlation functions the two frequency structure functions can be evaluated.

3.2 FOUR POINT TWO FREQUENCY STRUCTURE FUNCTIONS

The four point two frequency amplitude structure function is defined as

$$D_\chi(\bar{r}_1,\bar{p}_1,t_1,k_1 : \bar{r}_2,\bar{p}_2,t_2,k_2)$$

$$= \langle[\chi(\bar{r}_1,\bar{p}_1,t_1,k_1) - \chi(\bar{r}_2,\bar{p}_2,t_2,k_2)]^2\rangle$$

$$= C_\chi(o,k_1) + C_\chi(o,k_2) - 2C_\chi(\bar{r}_1-\bar{r}_2,\bar{p}_1-\bar{p}_2,t_1-t_2,k_1,k_2)$$

Using Eq.(3.15), we get

$$D_\chi = 4\pi^2 k_1{}^2 \int_o^L d\eta \int_o^\infty K\, dK\, \phi_n(k)\, \sin^2[k^2\eta(1-\eta/L)/2k_1]$$

$$+ 4\pi^2 k_2{}^2 \int_o^L d\eta \int_o^\infty K\, dK\, \phi_n(K)\, \sin^2[K^2\eta(1-\eta/L)/2k_2]$$

$$-8\pi^2 k_1 k_2 \int_o^L d\eta \int_o^\infty K\, dK\, \phi_n(K)\, \sin[K^2\eta(1-\eta/L)/2k_1]$$

$$\sin[K^2\eta(1-\eta/L)/2k_2]\; J_o(K\left|(\eta/L)(\bar{p}_1-\bar{p}_2) + (1-\eta/L)(\bar{r}_1-\bar{r}_2) - \bar{v}\tau\right|) \quad (3.18)$$

Similarly, the four point two frequency phase structure function is defined as

$$D_\phi(\bar{r}_1,\bar{p}_1,t_1,k_1; \bar{r}_2,\bar{p}_2,t_2,k_2)$$

$$= \langle[\phi(\bar{r}_1,\bar{p}_1,t_1,k_1) - \phi(\bar{r}_2,\bar{p}_2,t_2,k_2)]^2\rangle$$

and using Eq.(3.16), this is derived as

$$D_\phi = 4\pi^2 k_1{}^2 \int_o^L d\eta \int_o^\infty dK\, \phi_\eta(K)\, \cos^2[K^2\eta(1-\eta/L)/2k_1]$$

$$+ 4\pi^2 k_2{}^2 \int_o^L d\eta \int_o^\infty dK\, \phi_n(K)\, \cos^2[K^2\eta(1-\eta/L)/2k_2]$$

$$-8\pi^2 k_1 k_2 \int_o^L d\eta \int_o^\infty dK\ \phi_n(K)\ \cos[K^2\eta(1-\eta/L)/2k_1]$$

$$\cos[K^2\eta(1-\eta/L)/2k_2]\ J_o(K\left|(\eta/L)(p_1-p_2) + (1-\eta/L)(r_1-r_2)-v\tau\right|) \quad (3.19)$$

Finally the two frequency wave structure function is defined as

$D\psi = D_\chi + D\psi$

and using Eqs.(3.18) and (3.19), this is given as

$$D_\Psi = D_\chi + D_\Psi$$

$$= 4\pi^2 k_1^2 \int_o^L d\eta \int_o^\infty K\ dK\ \phi_n(K)$$

$$+ 4\pi^2 k_2^2 \int_o^L d\eta \int_o^\infty dK\ K\ \phi_n(K)$$

$$- 8\pi^2 k_1 k_2 \int_o^L d\eta \int_o^\infty dK\ K\ \phi_n(K)\ \cos[K^2\eta(1-\eta/L)(1/k_1-1/k_2)]$$

$$J_o(K\left|(p_1-p_2)(\eta/L) + (1-\eta/L)(r_1-r_2) - v\tau\right|) \quad (3.20)$$

All the above correlation and the structure functions are required in order to assess the effects of the turbulent atmosphere on the polychromatic speckle propagation.

3.3 CHOICE OF THE SPECTRUM OF FLUCTUATIONS

In order to numerically evaluate the above functions for any given data, the three-dimensional spatial spectrum for the refractive index fluctuations in the turbulent atmosphere is needed. The most famous and often used spectrum for optical propagation through the turbulent atmosphere is the Kolmogorov spectrum, given by[63]

$$\phi_n(K) = .033\ C_n^{\ 2}\ K^{-11/3}\ . \tag{3.21}$$

The above spectrum has been modified by Tatarskii[63] as

$$\phi_n(K) = .033\ C_n^{\ 2}\ K^{-11/3}\ e^{-K^2/K_m^{\ 2}} \tag{3.22}$$

where $k_m = 5.92/\ell_o$ to take into consideration the dissipation of energy due to viscosity effects for eddy sizes less than the inner scale of turbulence. For eddy sizes greater than the outer scale of turbulence, the energy in the eddies must be less than that predicted by the Kolmogorov spectrum. This effect is taken into consideration by the Von-Karman spectrum given by[63]

$$\phi_n(K) = .033\ C_n^{\ 2}(K^2 + 1/L_o^{\ 2})^{-11/6}\ e^{-K^2/K_m^{\ 2}} \tag{3.23}$$

where $k_o = 2\pi/L_o$. The spectra (3.22) and 3.23) are good models only in the inertial sub-range, $2\pi/L_o \leq K \leq 2\pi/\ell_o$. In this they behave like the Kolmogorov spectrum. Outside this range as there is little theoretical basis and scant observational support for these spectra, any predicted effects due to scale sizes outside the inner and outer scales of the turbulence may not be valid. More recently, Hill[3,4] proposed a new spectrum which takes into consideration the effects of the inner scale. The three-dimensional Hill spectrum is given by

$$\phi_n(K) = (C_n^{\;2}/4\pi)(1/K^3)(1 + K\ell_1)\; e^{-K\ell_1} \tag{3.24}$$

Elliott et al.[5] used this spectrum to describe the temperature fluctuations of turbulence, in a heated tank and studied the effects on the laser beam propagation. They also compared the relative merits of the various spectra for describing the temperature fluctuations of a turbulent medium.

A serious defect of the Hill spectrum is that there is no outer scale term in the final expression for the spectrum. Since phase covariance is strongly dependent on the outer scale size, it is not possible to calculate the phase covariance even for monochromatic wave propagation using the Hill spectrum. Similar difficulties exist while calculating the phase covariance or the structure functions for the two frequency case, if we use the Hill spectrum. The Hill spectrum should be modified to include the outer scale effects, in analogy with the Von Karman spectrum, for use in phase calculations.

3.4 CONCLUSIONS

In this chapter all the necessary four point two frequency correlation functions and the structure functions, are developed starting from fundamentals and including the effects of the time delay. Substituting $k_1 = k_2$, in all the expressions (where k is a wave number), corresponding results of the monochromatic case are obtained. The Hill spectrum is radically different from the rest as it predicts larger values for the variance and the covariance of log-amplitude fluctuations for some values of the ratio of Fresnel zone size to the inner scale of turbulence. For most of the experimental data used in this thesis, the results predicted by the Hill spectrum are approximately the same as the Kolmogorov spectrum. Since the Kolmogorov spectrum is well tested and widely used, all the computer programs in this thesis (except for the phase calculations) were written using this spectrum. For phase calculations, the Von Karman spectrum is used. Additional remarks regarding the Hill spectrum follow at the end of Chapters V and VI.

The two frequency correlation and structure functions have not been derived, even for simple cases for saturation conditions of turbulence (i.e. Rytov variance $\geq$ .3). However, following Clifford[64] who derived a form of log-amplitude covariance function in saturation regime by convolving the unsaturated form of log-amplitude covariance function at each point along the path with the short term modulation transfer function, it may be possible to derive the saturated turbulence forms by knowing the two frequency short term modulation transfer function. However it will be shown in Chapter V that for speckle propagation through turbulence, a two frequency turbulence theory in saturation regime is rarely needed. Also there is not enough experimental data to substantiate any theory proposed. For speckle propagation through turbulence, the unsaturated forms of log-amplitude covariance and wave structure functions are sufficient to develop a good theory.

CHAPTER IV

THE INTENSITY CORRELATION FUNCTION FOR A POLYCHROMATIC SPECKLE PATTERN IN THE TURBULENT ATMOSPHERE

In the design of atmospheric optical systems, using speckle patterns, such as compensation for atmospheric distortion, remote sensing of cross wind, etc. the nature of the speckle pattern produced by a diffuse target at the receiver plane is very important. A very important statistical parameter in this connection is the correlation function of the received intensity at two space time points in the receiver plane. As will be shown later, by knowing this correlation function and the mean intensity at the receiver, all the necessary statistical parameters of the intensity can be determined. The correlation function of the received intensity for two space time points is defined as

$$B_I(\overline{p}_1,t_1;\ \overline{p}_2,t_2) = \langle I(\overline{p}_1,t_1)I(\overline{p}_2,t_2)\rangle$$

where $I(\overline{p}_i,t_i)$ is the intensity at a point $\overline{p}_i$ at time t_i in the receiver plane. This generalized correlation function is evaluated by determining the intensity at two space time points and taking an ensemble average over both space and time as well as over an ensemble of rough surfaces and atmospheres.

4.1 ANALYSIS

The path geometry for the problem under consideration is shown in Fig. 4.1. The transmitter and the receiver are located at one end of the path and the laser beam from the transmitter illuminates a diffuse target at the other end of the path after propagation through the turbulent atmosphere. The speckle pattern, formed after the laser beam scattered from the diffuse target, propagates back to the receiver through the turbulent atmosphere. It is assumed that the back scattering is negligible and the outgoing and the incoming radiation experience independent turbulence regions. Also it is assumed that the transmitter consists of a number of discrete frequencies given by k_i, $i = 1,2,\ldots,N$ and that the receiver bandwidth is very much smaller than any difference frequency present in the transmitter ($\Delta\omega << \omega_i - \omega_j$) but large enough to recover all the amplitude fluctuations in the turbulent atmosphere. Let $\overline{p}$, $\overline{\rho}$ and $\overline{r}$ denote the transverse coordinates in the receiver, target and the transmitter planes respectively which are perpendicular to the line of sight path if the receiver and the transmitter are sufficiently close. It is known that the intensity fluctuations in the turbulent atmosphere at different frequencies are perfectly correlated for small bandwidths of the transmitter.[65,66] In order that the intensity fluctuations at two different frequencies be decorrelated, very large bandwidth of light or widely separated frequencies are needed.

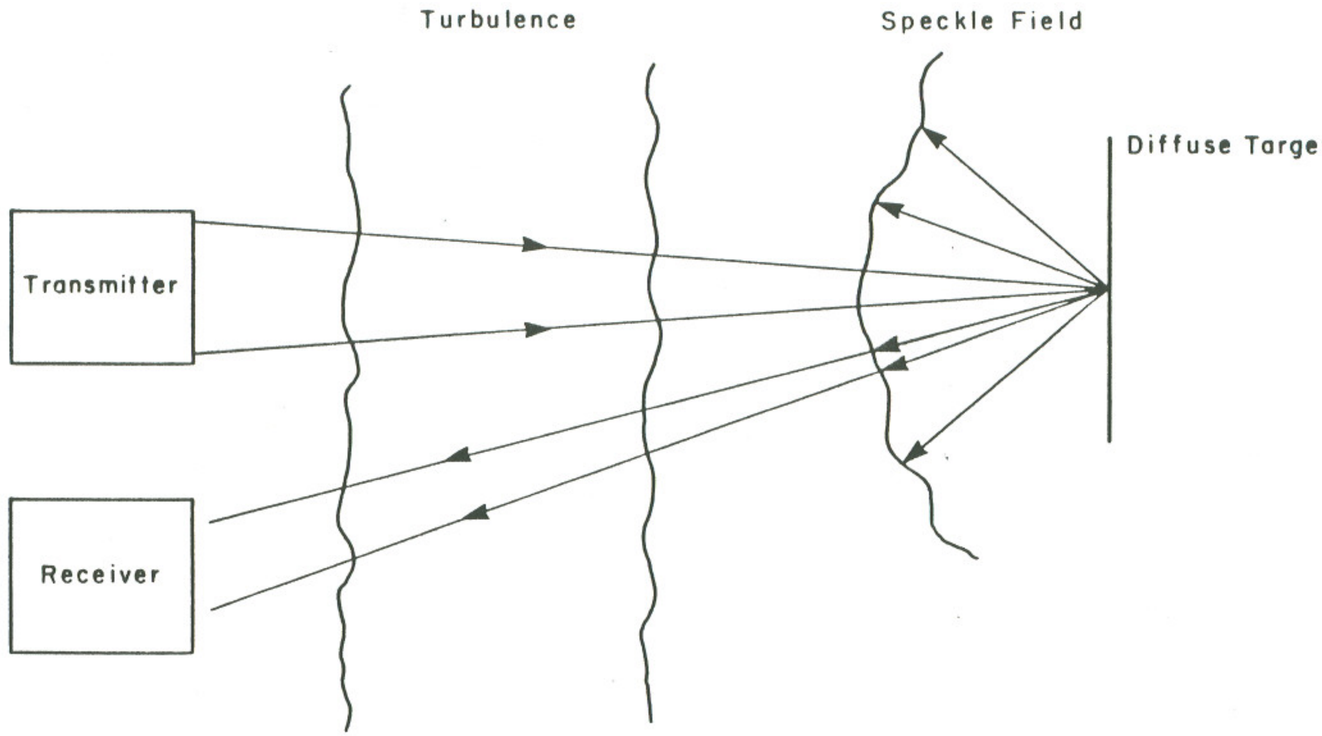

Figure 4.1. Experimental and theoretical configuration of the path geometry for target generated speckle pattern.

A widely used method of generating speckle field is to illuminate a very diffuse target with the TEM_{00} laser beam at several frequencies as shown in Fig. 4.1. The field distribution at the transmitter is given as

$$U_o(r) = \sum_{j=1}^{N} U_o(r,k_j)$$

$$= \sum_{j=1}^{N} U_{oj} \exp\{-r^2/2\alpha_o^2 - ik_j r^2/2F\} \qquad (4.1)$$

where $U_o(r,k_j)$ corresponds to the field distribution at the frequency k_j and α_o and F are the characteristic beam radius and focal length (assumed to be the same at all frequencies without any loss of generality) respectively. The field at the target plane before scattering from the target can be written, using the extended Huygens Fresnel theory,[23,62] as

$$U'(\rho) = \sum_{j=1}^{N} U'(\rho,k_j)$$

$$= \sum_{j=1}^{N} \left((k_j U_{oj})/(i2\pi L)\right)\exp\{ik_j(L + \rho^2/2L)\}$$

$$\times \int \exp\{-(r^2/2\alpha_o^2) - ir^2(k_j/2L)(1 - L/F)$$

$$- ik_j(\overline{r}\cdot\overline{\rho})/L + \Psi_1(\rho,r,k_j)\}d\overline{r} \qquad (4.2)$$

where the random function $\Psi_1(\ldots)$ represents the effect of the turbulent atmosphere on the propagation of a spherical wave from a point located at a point r in the transmitter plane to a point ρ in the target plane, k is the wave number and L is the path length.

Similarly the field at the receiver can be written in terms of the fields $U(\rho,k_j)$ at the target after scattering as

$$U(p) = \sum_{j=1}^{N} \left(k_j/i2\pi L\right)e^{ik_j(L + p^2/2L)}$$

$$\times \int d\overline{\rho}\; U(\rho,k_j)\; e^{i(k_j/2L)(\rho^2-2p\cdot\rho) + \Psi_2(p,\rho,k_j)} \tag{4.3}$$

The fields before and after scattering from the target are related by the properties of the target. The complex random function is given as

$$\Psi = x + i\phi \tag{4.4}$$

where x represents the log-amplitude perturbation of a spherical wave due to the atmospheric turbulence and ϕ, the phase perturbation. Using the above three equations, the expressions for the two point space-time correlation of the received intensity can be developed. When N discrete frequencies are present as in Eq.(4.1), the correlation of the received intensity is given as

$B_I(p_1,p_2,\tau)$

$$= \langle U(\overline{p}_1,o)U^*(\overline{p}_1,o)U(p_2,\tau)U^*(p_2,\tau)\rangle$$

$$= \sum_{i=1}^{N} \sum_{j=1}^{N} [(k_i^2\ k_j^2)/(2\pi L)^4] \iiiint d\overline{\rho}_1\ d\overline{\rho}_2\ d\overline{\rho}_3\ d\overline{\rho}_4$$

$$\langle U(\overline{\rho}_1,o,k_i)U^*(\overline{\rho}_2,o,k_i)U(\overline{\rho}_3,\tau,k_j)U^*(\overline{\rho}_4,\tau,k_j)\rangle$$

$$\exp\{(ik_i/2L)[\rho_1^2-\rho_2^2-2\overline{p}_1\cdot(\overline{\rho}_1-\overline{\rho}_2)] + (ik_j/2L)[\rho_3^2-\rho_4^2-2\overline{p}_2\cdot(\overline{\rho}_3-\overline{\rho}_4)]\}$$

$$H(p_1,p_2;\rho_1,\rho_2,\rho_3,\rho_4;\ \tau;\ k_i,k_j) \tag{4.5}$$

where, using the generalized spherical wave mutual coherence function,[67] the function H(....) is given by

$$H(p_1,p_2;\rho_1,\rho_2,\rho_3,\rho_4;\tau;k_i,k_j)$$

$$= \langle\exp[\Psi(p_1,\rho_1,o,k_i) + \Psi^*(p_1,\rho_2,o,k_i)$$

$$+ \Psi(p_2,\rho_3,\tau,k_j) + \Psi^*(p_2,\rho_4,\tau,k_j)]\rangle$$

$$= \exp[-1/2\{D_\Psi(o,\rho_2-\rho_1,o,k_i,k_i) - D_\Psi(p_2-p_1,\rho_3-\rho_1,\tau,k_i,k_j)$$

$$+ D_\psi(p_2-p_1, \rho_4-\rho_1, \tau, k_i, k_j) + D_\psi(p_2-p_1, \rho_3-\rho_2, \tau, k_i, k_i)$$

$$- D_\psi(p_2-p_1, \rho_4-\rho_2, \tau, k_i, k_j) + D_\psi(o, \rho_4-\rho_3, o, k_j, k_j)\}$$

$$+ 2C_\chi(p_2-p_1, \rho_3-\rho_1, \tau, k_i, k_j)$$

$$+ 2C_\chi(p_2-p_1, \rho_4-\rho_2, \tau, k_i, k_j)] \quad (4.6)$$

The two frequency structure function $D\psi$ and the two frequency log-amplitude covariance function C_χ are given using the results of the previous chapter for the Kolmogorov spectrum as,

$$D_\psi = \cdot 132\ \pi^2 L \int_0^1 du\ C_n^{\ 2}\ (t) \int_o^\infty du\ u^{-8/3}$$

$$\times \left[k_1^{\ 2} + k_2^{\ 2} - 2k_1k_2 \cos\{(u^2 t(1-t)L/2)(1/k_1-1/k_2)\}\right.$$

$$\left. J_o\{u\left|t\overline{p_2-p_1} + (1-t)\overline{\rho_2-\rho_1}-\overline{V}(t_2-t_1)\right|\}\right] \quad (4.7)$$

and

$$C_\chi = \cdot 132\ \pi^2\ k_1k_2L \int_0^1 dt\ C_n^{\ 2}(t) \int_o^\infty du\ u^{-8/3}$$

$$\sin[u^2 t(1-t)L/2k_1]\ \sin[u^2 t(1-t)L/2k_2]\ J_o\{u\left|t(\overline{p}_2-\overline{p}_1) + (1-t)(\overline{\rho}_2-\overline{\rho}_1)\right.$$

$$\left.-\overline{V}(t_2-t_1)\right|\} \quad (4.8)$$

The dummy variable t represents the distance from the source to the field point normalized by the total path L. The function H(....)

is the two frequency fourth order mutual coherence function. Since the target is perfectly diffuse, it can be assumed that at the target the fields due to any particular frequency are gaussian (spatially incoherent). If the coherence length of the source is larger than the surface correlation length, the fields before and after scattering can be related as

$$\langle U(\overline{\rho}_1,o,k_i)U^*(\overline{\rho}_2,o,k_i)U(\overline{\rho}_3,\tau,k_j)U^*(\overline{\rho}_4,\tau,k_j)\rangle$$

$$= (4\pi/k^2)^2 \langle I(\overline{\rho}_1,o)\rangle\langle I(\overline{\rho}_3,\tau)\rangle \; \delta(\overline{\rho}_1-\overline{\rho}_2) \; \delta(\overline{\rho}_3-\overline{\rho}_4)$$

$$+ (4\pi/k^2)^2 \langle U(\overline{\rho}_4,o)U^*(\overline{\rho}_4,\tau)\rangle\langle U(\overline{\rho}_2,\tau)U^*(\overline{\rho}_2,o)\rangle$$

$$\delta(\overline{\rho}_1-\overline{\rho}_4) \; \delta(\overline{\rho}_3-\overline{\rho}_2) \quad \text{if } k_i = k_j$$

$$= (4\pi/k_i k_j)^2 \langle I(\overline{\rho}_1,o,k_i)\rangle\langle I(\overline{\rho}_3,\tau,k_j)\rangle$$

$$\delta(\overline{\rho}_1-\overline{\rho}_2) \; \delta(\overline{\rho}_3-\overline{\rho}_4) \quad \text{if } k_i \neq k_j$$

Substituting this result in Eq.(4.5) and completing the $d\overline{\rho}_1$ and $d\overline{\rho}_3$ integrations, the correlation of the received intensity is given by

$$B_I(p,\tau) = C_{I_1}(p,\tau) + C_{I_2}(p,\tau) \tag{4.10}$$

$$C_{I_1}(p,\tau)$$

$$= (1/\pi^2 L^4) \sum_{i=1}^{N} \sum_{j=1}^{N} \iint d\overline{\rho}_2 \; d\overline{\rho}_4 \; \langle I(\overline{\rho}_2, o, k_i)\rangle$$

$$\langle I(\overline{\rho}_4, \tau, k_j)\rangle \; d^{\,4C_\chi(p_1-p_2,\rho_2-\rho_4,\tau,k_i,k_j)} \tag{4.11}$$

and

$$C_{I_2}(p,\tau)$$

$$= (1/\pi^2 L^4) \sum_{j=1}^{N} \iint d\overline{\rho}_2 d\overline{\rho}_4 \; \langle U(\overline{\rho}_4, o, k_i) U^*(\overline{\rho}_4, \tau, k_i)\rangle$$

$$\langle U(\overline{\rho}_2, \tau, k_i) U^*(\overline{\rho}_2, o, k_i)\rangle \; e^{i(k/L)\overline{p}\cdot\overline{\rho}} \; H_2(p_1, p_2; \rho_2, \rho_4; \tau : k_i, k_j) \tag{4.12}$$

In order to evaluate Eqs.(4.11) and (4.12), the quantity $\langle U(\overline{\rho}_4, o, k_i) U^*(\overline{\rho}_4, \tau, k_i)\rangle$, which is related to the incoherent speckle field at the target, must be calculated. Using Eqs.(4.1) and (4.2),

$$\langle U(\overline{\rho}_4,o)U^*(\overline{\rho}_4,\tau)\rangle$$

$$= \left(k_i^{\,2}/4\pi^2L^2\right)U_{oi}^{\,2} \iint d\overline{r}_1\, d\overline{r}_2\, \exp\left[-(r_1^{\,2}+r_2^{\,2})/2\alpha_o^{\,2} + i(k_i/2L)(1-L/F)\right.$$

$$\left.(r_1^{\,2}-r_2^{\,2}) - i(k_i/L)\overline{\rho}_4\cdot(\overline{r}_1-\overline{r}_2)\right] \langle\exp\left[\Psi(\overline{\rho}_4,\overline{r}_1,o) + \Psi^*(\overline{\rho}_4,\overline{r}_2,\tau)\right]\rangle \quad (4.13)$$

where the two frequency mutual coherence function is given by

$$\langle\exp\left[\Psi(\overline{\rho}_4,\overline{r}_1,o) + \Psi^*(\overline{\rho}_4,\overline{r}_2,\tau)\right]\rangle$$

$$= \exp\left[-\ (1/2)D_\Psi(o,\overline{r}_2-\overline{r}_1,\tau)\right] \quad (4.14)$$

In Eq.(4.13), changing the variables r_1 and r_2 to R and r where

$2R = r_1 + r_2$ and $r = r_1 - r_2$

we get

$$\langle U(\overline{\rho}_4,o)U^*(\overline{\rho}_4,\tau)\rangle$$

$$= (1/2\pi)k_i^{\,2}\ U_{oi}^{\,2}(\alpha_o^{\,2}/2L^2) \int d\overline{r}\ \exp\left[-r^2/4\alpha_o^{\,2} - i(k_i/L)\overline{\rho}_4\cdot\overline{r}\right.$$

$$\left.-\ (1/2)D_\Psi(o,-\overline{r},\tau) - (k_i^{\,2}/L^2)(\alpha_o^{\,2}/4)(1 - L/F)^2r^2\right] \quad (4.15)$$

where the following relations are used.

$$\int_0^{2\pi} d\theta\ e^{-ia\overline{\rho}\cdot\overline{r}} = 2\pi\ J_o(a\rho r)$$

$$\int_0^\infty R\, e^{-aR^2}\, J_o(bR)\, dR = (1/2a^2)\, e^{-b^2/4a^2}$$

The mean intensity at the target, is needed to complete Eq.(4.11) and can be evaluated by putting $\tau = 0$ in Eq.(4.15) and it is given by

$$\langle I(\rho_4, k_i)\rangle$$

$$= \left(k_i^{\,2}/L^2\right) U_{oi}^{\,2} \left(\alpha_o^{\,2}/2\right) \int r dr\, J_o(\overline{k_i/L}\, \rho_4 r)\, \exp\left[-r^2/4\alpha_o^{\,2} - (r/\rho_{oi})^{5/3}\right.$$

$$\left. - \left(k_i^{\,2}/L^2\right) \left(\alpha_o^{\,2}/4\right) (1 - L/F)^2 r^2\right] \qquad (4.16)$$

where $\rho_o = (.545625\ C_n^{\,2}\ k^2 L)^{-3/5}$ is the lateral coherence length. Substituting Eq.(4.16) in Eq.(4.11) gives,

$$C_{I_1}(p, \tau)$$

$$= \left(1/\pi^2 L^4\right) \sum_{i=1}^{N} \sum_{j=1}^{N} \iint d\overline{\rho}_2\ d\overline{\rho}_4\ k_i^{\,2}\ k_j^{\,2}\ U_{oi}^{\,2}\ U_{oj}^{\,2} \left(\alpha_o^{\,2}/4L^4\right)$$

$$\int r_1 dr_1\, J_o(\overline{k_i/L}\, \rho_4 r_1) \int r_2 dr_2\, J_o(\overline{k_j/L}\, \rho_2 r_2)$$

$$\times \exp\left[-r_1^{\,2}/4\alpha_o^{\,2} - r_2^{\,2}/4\alpha_o^{\,2} - (r_1/\rho_{oi})^{5/3} - (r_2/\rho_{oj})^{5/3}\right.$$

$$\left. - \left((k_i^{\,2}\alpha_o^{\,2}/4L^2)(1-L/F)^2 r_1^{\,2} - (k_j^{\,2}\alpha_o^{\,2})/4L^2\right)(1-L/F)^2\ r_2^{\,2}\right]$$

$$\times \exp\left\{4C_\chi(p, \rho_2-\rho_4, \tau, k_i, k_j)\right\} \qquad (4.17)$$

By changing the coordinates p_2 and ρ_4 to R and ρ where $\rho = \rho_2 - \rho_4$ and $2R = \rho_2 + \rho_4$ and using the expansion[68]

$$J_o(k/L\ r_1|\overline{R} \pm \overline{\rho}/2|)\ \sum_{m=o}^{\infty} \varepsilon_m(\mp 1)^m\ J_m(\overline{k/L}\ r_1\ R)\ J_m(\overline{k/L}\ r_1\ \rho/2)\ \cos(m\phi) \tag{4.18}$$

where

$\phi = \phi_R - \phi_\rho \qquad \varepsilon_o = 1$ and $\varepsilon_m = 2$ if $m = 0$

C_{I_1} is given by

$$C_{I_1}(p,\tau) = [\alpha_o^{\,4}/(4\pi^2L^8)]\ \sum_{i=1}^{N}\ \sum_{j=1}^{N}\ U_{oi}^{\ 2}\ U_{oj}^{\ 2}\ k_i^{\ 2}\ k_j^{\ 2}$$

$$\int d\overline{\rho}\ \int d\overline{R}\ \int r_1\ dr_1\ \int dr_2 \sum_{m_1=o}^{\infty} \{\varepsilon_{m_1}(-1)^{m_1} J_{m_1}(\overline{k_i/L}\ \rho/2\ r_1) J_{m_1}(\overline{k_i/L} R r_1)$$

$$\cos\overline{m_1(\phi_R-\phi_\rho)}\}\{\sum_{m_2=o}^{\infty}\ \varepsilon_{m_2}(+1)^{m_2}\ J_{m_2}(\overline{k_i/L}\ \rho/_2 V_2)\ J_{m_2}(\overline{k_j/L}\ R\ r_2)$$

$$\cos\overline{m_2(\phi_R-\theta_\rho)}\}\ \exp[-r_1^{\,2}/2\alpha_o^{\,2} - r_2^{\,2}/4\alpha_o^{\,2} - (r_1/\rho_{oi})^{5/3} - (r_2/\rho_{oj})^{5/3}$$

$$-\ (k_i^{\,2}\alpha_o^{\,2}/4L^2)(1-L/F)^2\ r_1^{\,2} - ((k_j^{\,2}\ \alpha_o^{\,2})/4L^2)(1-L/F)r_2^{\,2}]$$

$$\times \exp\{4\ C_\chi\ (p,\rho,\tau,k_i,k_j)\} \tag{4.19}$$

Completing the integral over $d\theta_R$ gives us,

$$C_{I_1}(p,\tau) = \left(\alpha_o^{\ 4}/L^8\right) \sum_{i=1}^{N} \sum_{j=1}^{N} U_{oi}^{\ 2}\, U_{oj}^{\ 2}\, k_i^{\ 2}\, k_j^{\ 2}$$

$$\times \int d\overline{\rho} \int RdR \int r_1\, dr_1 \int r_2\, dr_2 \left[\sum_{m_1=o}^{\infty} \varepsilon_{m_1} (-1)^{m_1} \right.$$

$$\left. J_{m_1}\left(\overline{k_i/L}\ \overline{\rho/2}\ r_1\right) J_{m_1}\left(\overline{k_i/L}\ R\ r_1\right) J_{m_1}\left(\overline{k_j/L}\ \overline{\rho/2}\ r_2\right) J_{m_1}\left(\overline{k_j/L}\ R\ r_2\right)\right]$$

$$\exp\left\{-r_1^{\ 2}/4\alpha_o^{\ 2} - r_2^{\ 2}/4\alpha_o^{\ 2} - \left(r_1/\rho_{oi}\right)^{5/3} - \overline{k_i^{\ 2}/L^2}\ \overline{\alpha_o^{\ 2}/4}\ (1-L/F) r_1^{\ 2}\right.$$

$$\left. - \overline{\left(k_j^{\ 2}\ \alpha_o^{\ 2}\right)/4L^2}\ (1-L/F)^2\ r_2^{\ 2}\right\} \exp\left\{4C_\chi(p,\rho,\tau,k_i,k_j)\right\} \qquad (4.20)$$

Changing the variables r_1 and r_2 to r_3 and r_4 where

$\left(k_i/L\right) r_1 = r_3$ and $\left(k_j/L\right) r_2 = r_4$

Eq.(4.20) can be rewritten as

$$C_{I_1}(p,\tau) = \left(\alpha_o^{\ 4}/2\pi L^4\right) \sum_{i=1}^{N} \sum_{j=1}^{N} U_{oi}^{\ 2}\, U_{oj}^{\ 2} \int d\overline{\rho} \int RdR \int r_3 dr_3$$

$$\times \int r_4\, dr_4 \left[\sum_{m=o}^{\infty} \varepsilon_m\, (-1)^m\, J_m(\overline{\rho/2}\ r_3)\, J_m(Rr_3)\, J_m(\overline{\rho/2}\ r_4)\right)$$

$$J_m(Rr_4)\,]\ \exp\{-r_3^2\ L^2/k_i^2\ 4\alpha_o^2\ -r_4^2L^2/4\alpha_o^2\ k_j^2 - (\overline{r_3L}/\overline{k_i\rho_{oi}})^{5/3}$$

$$-(\overline{r_4L}/\overline{k_j\ \rho_{oj}})^{5/3}\ -r_3^2(\alpha_o^2/4)(1-L/F)^2\ -r_4^2(\alpha_o^2/4)(1-L/F)^2\}$$

$$\exp\{4C_\chi(p,\rho,\tau,k_i,k_j)\} \tag{4.21}$$

The integral over R can be accomplished by using the relation

$$\int RdR\ J_m(r_3R)\ J_m(r_4R) = 2\delta(r_3-r_4)/(r_3+r_4) \tag{4.22}$$

Substituting Eq.(4.22) into Eq.(4.21) and completing the integral over dr_3,

$$C_{I_1}(p,\tau) = (\alpha_o^4/2\pi L^4)\ \sum_{i=1}^{N}\ \sum_{j=1}^{N}\ U_{oi}^2\ U_{oj}^2 \int d\overline{\rho} \int r_3dr_3$$

$$\times\ [\sum_{m=o}^{\infty}\ (-1)^m\ \varepsilon_m\ J_m^2(\overline{\rho/2}\ r_3)]\ \exp\{-(\overline{r_3^2\ L^2)/(4\alpha_o^2})(1/k_i^2 + 1/k_j^2)$$

$$-\ (\overline{r_3L}/\overline{k_i\rho_{oi}})^{5/3}\quad -(\overline{r_3L}/\overline{k_j\ \rho_{oj}})^{5/3}\ -r_3^2(\alpha_o^2/2)(1-L/F)^2\}$$

$$\times\ \exp\{4C_\chi(p,\rho,\tau,k_ik_j)\} \tag{4.23}$$

Using the summation

$$\sum_{m=o}^{\infty} (-1)^m \varepsilon_m J_m^2(x) = J_o(2x)$$

and dropping the index 3, the final result for C_{I_1} as a double integral is given by

$$C_{I_1}(p,\tau) = \left(\alpha_o^4/2\pi L^4\right) \sum_{i=1}^{N} \sum_{j=1}^{N} U_{oi}^2 U_{oj}^2 \int d\bar{\rho} \int rdr$$

$$J_o(\rho r) \exp\left\{-\left(r^2L^2/4\alpha_o^2\right) (1/k_i^2 + 1/k_j^2) - (\overline{rL/k_i\rho_{oi}})^{5/3}\right.$$

$$\left.-(\overline{rL/k_j\rho_{oj}})^{5/3} - r^2(\alpha_o^2/2)(1-L/F)^2\right\} \exp\left\{4C_\chi(p,\rho,\tau,k_i,k_j)\right\} \quad (4.24)$$

Similarly, using the Eqs.(4.12) and (4.13) and following the same arguments, C_{I_2} is given by

$$C_{I_2}(p,\tau) = \sum_{i=1}^{N} (k_i^2/4\pi^2L^2)U_{oi}^4(\alpha_o^4/L^4) \int d\bar{r}_2 \int d\bar{\rho}$$

$$\times \exp[-r_2^2/2\alpha_o^2 - D_\Psi(o,-\bar{r}_2,-\tau) - r_2^2 k_i^2(\alpha_o^2/2L^2)(1-L/F)^2]$$

$$\times \exp[\overline{ik_i/L}\ \bar{\rho}\cdot(\bar{p}+\bar{r}_2)]\ H_2(\bar{p},\rho,\tau) \quad (4.25)$$

By changing r_2 to r_3 where $\overline{k_i/L}\ r_2 = r_3$, C_{I_2} can also be written as

$C_{I_2}(p,2)$

$$= \sum^{N} U_{oi}{}^4(\alpha_o{}^4/4\ \pi^2)\sum d\overline{r}_3 \int d\overline{\rho}$$

$$\times \exp\left[-r_3{}^2L^2/(2k^2\alpha_o{}^2) - D_\Psi(o,-Lr_3/k_i - \tau) - (r_3{}^2/2)\alpha_o{}^2\ (1 - L/F)^2\right]$$

$$\times \exp\left[i\ \overline{k_i/L}\ \overline{\rho}\cdot\overline{p}+i\ \overline{\rho}\cdot r_3\right] H_2(\overline{p},\overline{\rho},\tau) \tag{4.26}$$

where

$$H_2(\overline{\rho},\overline{p},\tau) = \exp\left[-D_\Psi(o,\overline{\rho},o) - D_\Psi(\overline{p},o,\tau)\right.$$

$$+ (1/2)D_\Psi(\overline{p},-\overline{\rho},\tau) + (1/2)\ D_\Psi(\overline{p},\overline{\rho},\tau) + 2C_\chi(\overline{p},-\overline{\rho},\tau)$$

$$\left.+ 2\ C_\chi(\overline{p},\overline{\rho},\tau)\right] \tag{4.27}$$

The term C_{I_2} term is not derived in detail as it is a straightforward generalization of the corresponding term for the monochromatic case, worked out by Holmes et al.[19]

By adding Eqs.(4.25) and (4.26), the two point space time correlation function of the intensity of a polychromatic speckle pattern is given.

4.2 CONCLUSIONS

The numerical evaluation of C_{I_2} was not accomplished previously when τ is not zero for the monochromatic case. So the two point space time correlation function of the speckle was not numerically evaluated even for the monochromatic case to compare with experimental data. In Chapter VII, an approximate method to evaluate the above expression numerically is described. In the next two chapters, expressions for the variance and the covariance of the received intensity are developed using the above expression and the mean intensity to be calculated later.

In summary, in this chapter, a very general second order statistical parameter, the correlation function of the received intensity when the transmitter consists of N discrete frequencies is evaluated. This will be used in the subsequent formulations to develop all the necessary statistical parameters.

CHAPTER V

THE MEAN AND THE VARIANCE OF THE RECEIVED INTENSITY

In the previous chapter, a general formulation is developed for the two point space time correlation function of the received intensity. From this correlation function and the mean value, the variance of the received intensity can be obtained. A more meaningful parameter is the variance of the received intensity, normalized to the square of the mean of the received intensity. However the mean intensity cannot be evaluated from the two point space time correlation function. In this chapter, we develop the expressions for the mean and the variance and compare the results with experimental data. The variance of the received intensity can be used to obtain the turbulence level C_n^2 of the atmosphere and this can be used to compensate for the turbulence in the remote sensing of wind.

5.1 MEAN INTENSITY

When the polychromatic speckle field has N discrete frequencies, as described in the earlier chapter, the mean intensity at a point p in the receiver plane is given for the folded path geometry of Fig. 4.1 as

$$\langle I(p)\rangle = \langle U(p)\ U^{*}(p)\rangle \tag{5.1}$$

$$\langle I(p)\rangle = \sum_{j=1}^{N} \sum_{i=1}^{N} k_j\, k_i/4\pi^2 L^2\, e^{i(k_j-k_i)(L + p^2/2L)}$$

$$\times \iint \langle U(p_1,k_j)U^*(\rho_2,k_i)\rangle\, d\overline{\rho}_1\, d\overline{\rho}_2$$

$$\times \exp\left[i\, k_j/2L\, (\rho_1{}^2 - 2p\cdot\rho_1 - i\, k_i/2L\, (\rho_2{}^2 - 2p\cdot\rho_2)\right]$$

$$\times \langle\exp\left[\Psi_2(p,\rho_1,k_j) + \Psi_2{}^*(p,\rho_2,k_i)\right]\rangle \tag{5.2}$$

Under the assumption that the fields due to different frequencies are uncorrelated, the fields at the target before and after scattering are related as

$$\langle U(\rho_1,k_j)\; U^*(\rho_2,k_i)\rangle = \delta(\rho_1-\rho_2)\; 4\pi/k_i{}^2\; \langle I(\rho,k_i)\rangle \text{ if } k_i = k_j$$

$$= o \text{ if } k_i \neq k_j \tag{5.3}$$

Substituting Eq.(5.3) in Eq.(5.2),

$$\langle I(p)\rangle = 1/\pi L^2 \mathop{\varepsilon}_{j=1}^{N} \int d\overline{\rho}\, \langle I(p,k_j)\rangle \tag{5.4}$$

Substituting for $\langle I(\rho,k_j)\rangle$ from Eq.(4.16),

$$\langle I(p)\rangle = \sum_{j=1}^{N} 1/\pi L^2 \int \rho\cdot d\rho\; k_j{}^2\; U_{oj}{}^2\; \alpha_o{}^2/2L^2 \int rdr \int_o^{2\pi} d\theta_e$$

$$\langle I(p)\rangle = \sum_{j=1}^{N} (1/\pi L^2) \int \rho \, d\rho \, k_j^2 \, U_{oj}^2(\alpha_o^2/2L^2) \int r dr \int_o^{2\pi} d\theta_\rho$$

$$\times J_o[(k_j/L)\rho r] \exp[-r^2/4\alpha_o^2 - (r/\rho_{oj})^{5/3} - (k_j^2/L^2)(\alpha_o^2/4)\ (1-L/F)^2 r^2] \tag{5.5}$$

Using the integral

$$\int_o^{\infty} \rho \, J_o(\rho r) \, d\rho = \delta(r)/r$$

the mean intensity is given by

$$\langle I(p)\rangle = \sum_{j=1}^{N} U_{oj}^2(\alpha_o^2/L^2) = \sum_{j=1}^{N} \langle I_j\rangle \tag{5.6}$$

where $\langle I_j\rangle$ is the average intensity at the receiver due to the field at the frequency k_j in the transmitter. It is clear from the above expression that the average intensity is independent of the turbulence level and is sum of average intensities due to each transmitted frequency k_i.

5.2 THE VARIANCE OF THE RECEIVED INTENSITY

The variance of the received intensity is, by definition, given by

$$\sigma_I^2 = \langle I^2\rangle - \langle I\rangle^2 \tag{5.7}$$

where $\langle I^2\rangle$ is the second moment of the intensity and it is a special case of the correlation function when the two space time points are the same. Therefore, $\langle I^2\rangle$ can be calculated by putting $p = 0$ and $\tau = 0$ in the equations for $B_I(p,\tau)$ in the previous chapter. Thus

$$\langle I^2\rangle = C_{I_1}(0,0) + C_{I_2}(0,0) \tag{5.8}$$

where

$$C_{I_1} = \left(\alpha_o^{\,4}/2\pi L^4\right) \sum_{i=1}^{N} \sum_{j=1}^{N} U_{oi}^{\;2}\, U_{oj}^{\;2} \int d\overline{\rho} \int r dr\, J_o(\rho r)$$

$$\times \exp\left[- r^2(L^2/4\alpha_o^{\,2})(1/k_i^{\,2} + 1/k_j^{\,2}) - (rL/\overline{k_i\rho_{oj}})^{5/3} - (rL/\overline{k_j\rho_{oj}})^{5/3}\right.$$

$$\left. - (r^2\alpha_o^{\,2}/2)(1-L/F)^2\right] \times \exp\left[4\, C_\chi(\rho,k_i,k_j)\right] \tag{5.9}$$

and

$$C_{I_2} = \sum_{i=1}^{N} \left(U_{oi}^{\;4}\; \alpha_o^{\,4}/2\pi L^4\right) \int d\overline{r} \int \rho d\rho\, J_o(\rho r)$$

$$\times \exp\left[-r^2(L^2/2k_i^{\,2})\; \alpha_o^{\,2} - 2(rL/\overline{k\rho_{oi}})^{5/3} - (r^2\; \alpha_o^{\,2}/2)\; (1-L/F)^2\right]$$

$$\times \exp[4C_\chi(\rho,k_i)] \tag{5.10}$$

Since $p=0$, integration over $d\theta_\rho$ can be completed in Eq.(5.9) and C_{I_1} is given by

$$C_{I_1} = (\alpha_o^{4}/L^{4}) \sum_{i=1}^{N} \sum_{j=1}^{N} U_{oi}^{2} U_{oj}^{2} \int \rho d\rho \int r dr\, J_o(\rho r)$$

$$\times \exp\left[-r^2(L^2/4\alpha_o^{2})(1/k_i^{2} + 1/k_j^{2}) - (rL/\overline{k_i\rho_{oi}})^{5/3} - (rL/\overline{k_j\rho_{oj}})^{5/3} - (r^2\alpha_o^{2}/2)(1-L/F)^2\right] \times \exp\left[4C_\chi(\rho,k_i,k_j)\right] \quad (5.11)$$

Since $\tau = 0$ $d\theta_\rho$ and $d\theta_{r2}$ integrations can be completed in Eq.(5.10) and C_{I_2} is given by

$$C_{I_2} = \sum_{i=1}^{N} (U_{oi}^{4}\, \alpha_o^{4}/L^4) \int r dr \int \rho d\rho\, J_o(\rho r)$$

$$\times \exp\left[-r^2L^2/(2k_i^{2}\,\alpha_o^{2}) - 2(rL/\overline{k\rho_{oi}})^{5/3} - r^2(\alpha_o^{2}/2)(1-L/F)^2\right]$$

$$\times \exp\left[4C_\chi(\rho,k_i)\right] \quad (5.12)$$

Since the expectation value of the intensity at each frequency is given as

$$\langle I_i \rangle = U_{oi}^{2}(\alpha_o^{2}/L^2) \quad (5.13)$$

if the final expression for the variance of the received intensity can be written as

$$\sigma_I{}^2 = \sum_{i=1}^{N} \sum_{j=1}^{N} \langle I_i \rangle \langle I_j \rangle \int \rho d\rho \int r dr\; J_o(\rho r)$$

$$\times\; f_1(r,k_i,k_j)\; \exp\left[4C_\chi(\rho,k_i,k_j)\right]$$

$$+ \sum_{i=1}^{N} \langle I_i \rangle^2 \int r dr \int \rho d\rho\; J_o(\rho r)$$

$$f_2(r,k_i)\; \exp\left[4C_\chi(\rho,k_i)\right] - \{\sum \langle I_i \rangle\}^2 \tag{5.14}$$

where

$$f_1(r,k_i,k_j)$$

$$= \exp\left[-(r^2L^2/4\alpha_o{}^2)\{1/k_j{}^2 + 1/k_j{}^2\} - (rL/\overline{k_i\rho_{oi}})^{5/3} - (rL/\overline{k_j\rho_{oj}})^{5/3}\right.$$

$$\left. -r^2(\alpha_o{}^2/2)(1-L/F)^2\right] \tag{5.15}$$

and

$$f_2(r,k)$$

$$= \exp\left[-r^2(L^2/2\alpha_o{}^2)k^2 - 2(rL/\overline{k\rho_{oi}})^{5/3} - (r^2\alpha_o{}^2/2)(1-L/F)^2\right] \tag{5.16}$$

The normalized variance of the received intensity can be obtained now by dividing Eq.(5.14) on both sides by the square of the expectation value of the total received intensity.

5.3 NUMERICAL ANALYSIS

The term C_{I_1} can be evaluated by expanding the function f_1 in a Fourier-Bessel series[70] as

$$f_1(r,k_i,k_j) = \sum_m b_m(k_i,k_j)\, J_o\left(p_m r/A_1(k_i,k_j)\right) \tag{5.17}$$

where the coefficients b_m's are given by

$$b_m(k_i,k_j) = \left[2/\left\{A_1{}^2(k_i,k_j)J_1{}^2(p_m)\right\}\right] \int_o^{A_1(k_i,k_j)} f_1(r,k_i,k_j)$$

$$J_o\left[p_m r/A_1(k_i,k_j)\right]rdr \tag{5.18}$$

$$J_o(p_m) = 0 \tag{5.19}$$

and A_1 is chosen such that $f_1(r)$ is negligible for some value of $r=A_1$, which is dependent on both k_i and k_j. Then C_{I_1} is given as

$$C_{I_1} = \sum_m b_m(k_i,k_j)\, \exp\left[4C_\chi\left(p_m/A_1(k_i,k_j),\ k_i,k_j\right)\right] \tag{5.20}$$

Similarly C_{I_2} can be evaluated by expanding the function f_2 in a

$$f_2(r,k_i) = \sum_m C_m(k_i)\, J_o\left(P_m r/A_2(k_i)\right) \tag{5.21}$$

where

$$C_m(k_i) = \int_o^{A_2(k_i)} f_2(r,k_i)\, J_o\left(p_m r/A_2(k_i)\right) r\,dr \tag{5.22}$$

$$J_o(p_m) = 0 \tag{5.23}$$

and A_2 is chosen such that f_2 is negligible for some value of $r = A_2$. Then C_{I_2} is given as

$$C_I^{\,2} = \sum_m C_m(k_i)\, \exp\left[4C_\chi\left(p_m/A_2(k_i),k_i\right)\right] \tag{5.24}$$

It is convenient to let $\langle I_i\rangle = G_i\langle I\rangle$
so that $\sum G_i = 1$. The normalized variance of the received intensity is then given as

$$\sigma_{I_N}^{\,2} = \sigma_I^{\,2}/\langle I\rangle^2$$

$$= \sum_{i=1}^{N} \sum_{j=1}^{N} G_i G_j \left\{\sum_m b_m(k_i,k_j)\, \exp\left[4C_\chi\left(p_m/A_1(k_i,k_j),k_i,k_j\right)\right]\right\}$$

$$+ \sum_{i=1}^{N} G_i^{\,2} \left\{\sum_m C_m(k_i)\exp\left[4C_\chi\left(p_m/A_2(k_i),\ k_i\right)\right]\right\} - 1 \tag{5.25}$$

For several problems of practical interest, all the frequencies are sufficiently near enough that we can replace all the frequencies under consideration by the center frequency. This approximation is valid at least for pulsed sources which give a poor vacuum speckle contrast when scattered off a rough target.

By defining an atmospheric perturbation term $AP(k_i,k_j)$ as

$$AP(k_i,k_j) = \langle I_i I_j \rangle / \langle I_i \rangle \langle I_j \rangle$$

$$= \sum_m b_m(k_i,k_j) \exp\left[4C_\chi\left(P_m/A_1(k_i,k_j),\ k_i,k_j\right)\right] \tag{5.26}$$

the normalized variance of the received intensity $\sigma_{I_N}{}^2$ can be written as

$$\sigma_{I_N}{}^2 = \sum_i G_i{}^2\, AP(k_i,k_i) + \sum_i \sum_j G_i\, AP(k_i,k_j) - 1. \tag{5.27}$$

Eq.(5.27) can be used to predict the effect of the atmospheric turbulence on the polychromatic speckle if the intensities of each line or mode in the laser is known. If the bandwidth of the source is small, a more convenient form, for Eq.(5.27) can be written in terms of the vacuum speckle contrast ratio (VSCR), as

$$\sigma_{I_N}{}^2 = \left\{\sum_m b_m \exp\left[4C_\chi\left(p_m/A,k,k\right)\right]\right\} \left[1 + (\mathrm{VSCR})^2\right] - 1. \tag{5.28}$$

where k is the center frequency.

The VSCR is the square root of the normalized variance as measured in vacuum. This measurement can be made in the laboratory or over a short propagation path at almost zero turbulence level. Eq.(5.28) is particularly useful in that knowledge of the distribution of the modes making up the laser source need not be known. In order to determine when Eq.(5.28) can be used, the parameter

$$AP(k_i,k_j)/AP\left[(k_i + k_j)/2,\ (k_i + k_j)/2)\right]$$

has been calculated for various ratios of k_i to k_j. The results are shown in Table 5.1. As can be seen, a large wavelength difference is required before the complete form of the atmospheric perturbation is required. Consequently Eq.(5.28) can be used for most applications.

5.4 EXPERIMENTAL RESULTS

Experimental measurements of the normalized variance of a polychromatic speckle field were made at 1.06 μm by Holmes et al.[54] Their results are compared with the theory developed here in Fig. 5.1. A pulsed Nd:YAG laser running in several axial and transverse modes at 10 pulses per second and focused onto a target at 500 meters range was used as a polychromatic source. The data shown in Fig. 5.1 represent a total of 12,200 pulses. A measured VSCR of .135 was used to generate the theoretical values from Eq.(5.28) for comparison. Good agreement was obtained between the theory and experiment within about 5% error in the atmospheric perturbation (this error may be due to spatial modes). The theory developed in this chapter explains this result satisfactorily.

TABLE 5.1. COMPARISON OF THE TWO-FREQUENCY ATMOSPHERIC PERTURBATIONS. FOCUSED TRANSMITTER, L = 500 METERS, α_o = 1.35 cm.

$\frac{k_i - k_j}{k_o}$	$\frac{AP(k_i, k_j)}{AP\left(\frac{k_i + k_j}{2}, \frac{k_i + k_j}{2}\right)}$	
	$\sigma_\chi^2 = .1$	$\sigma_\chi^2 = .2$
.1	1.000	1.000
.2	.99964	1.000
.3	.9968	.9976
.4	.99484	.9986
.5	.990725	.9984
.6	.9872	.99253

σ_χ^2 is specified at $k_o = \frac{k_i + k_j}{2}$

λ_o = 0.488 μm

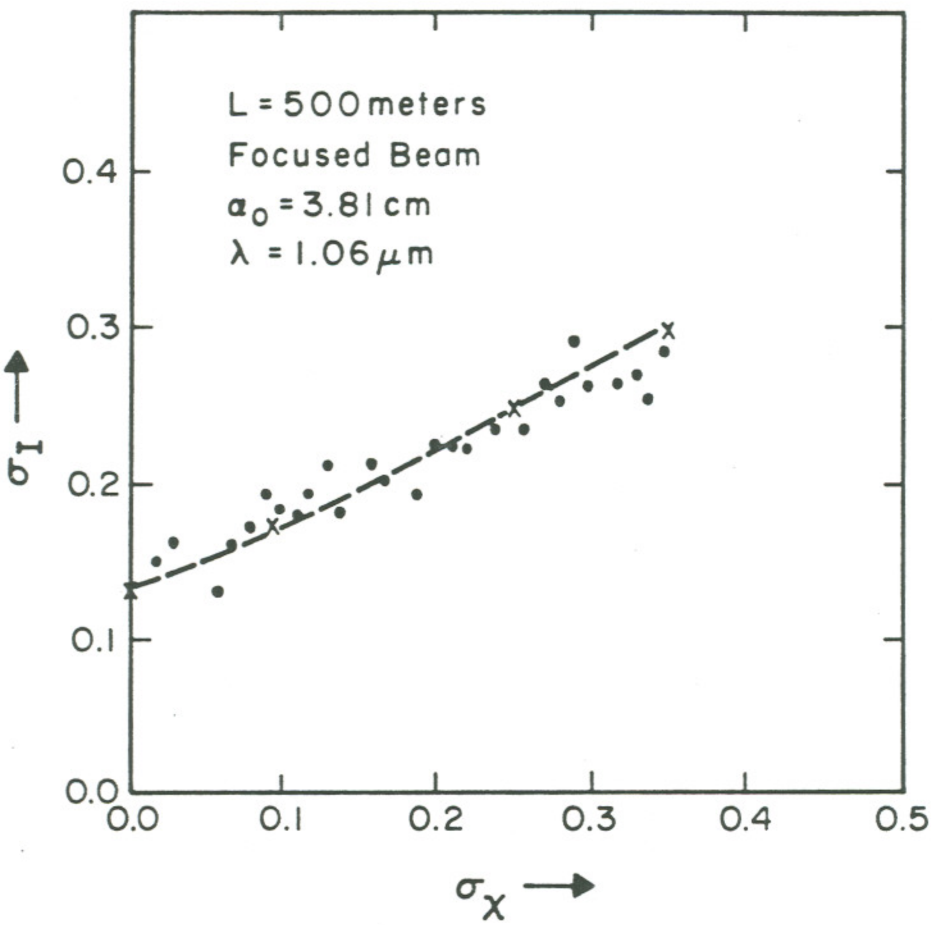

Figure 5.1. Contrast ratio of the received intensity for a polychromatic speckle field generated by a multimode Nd:YAG laser versus the log-amplitude standard deviation. Dots indicate the experimental data. Solid line is the theoretical curve.

5.5 DISCUSSION

As remarked earlier, the theory developed here correctly explains the variance data, collected by Holmes[54] et al. In addition the theory predicts substantial increase in the variance even for incoherent sources as will be shown later.

Evaluations of the theoretical formulation, given by Eq.(5.28) are shown in Fig. 5.2 for several values of the VSCR. It is interesting to note that at high values of integrated turbulence, the normalized variance returns to its vacuum value. This return of the normalized variance is caused not by the saturation of the turbulent atmosphere but by a transition from the dominance of atmospheric perturbation by log-amplitude effects to dominance by phase effects. From Eq.(5.28), it is obvious that the normalized variance depends on the log-amplitude covariance. It is obvious that it also depends on the transverse coherence lengths ρ_{oi} and ρ_{oj} through parameters A_1 and A_2.

In order to obtain the Eqs.(5.20) and (5.24), the functions f_1 and f_2 were expanded in a Fourier-Bessel series. These expansions required that they become negligible for some values $r = A_1$, A_2 and beyond. From examining the Eq.(5.25), it is clear that there are three scale sizes, α_o the speckle size at the receiver (same as the beam size at low turbulence levels for a focused beam geometry)

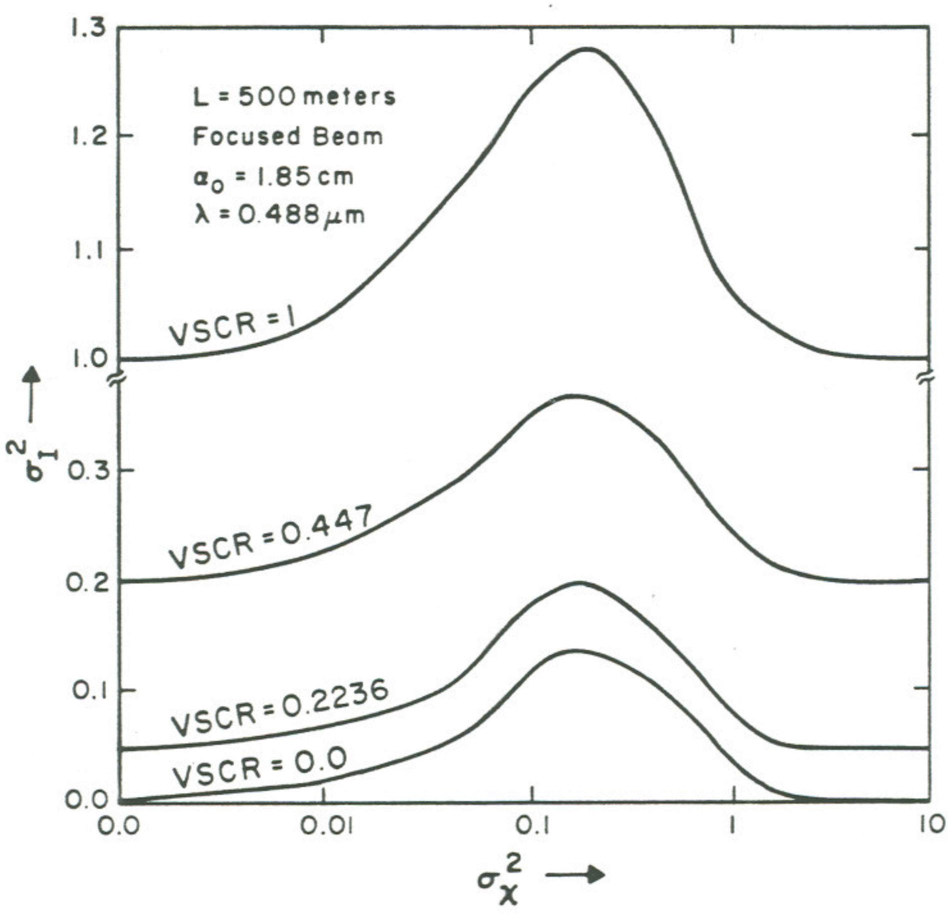

Figure 5.2. Normalized variance of the received intensity versus log-amplitude variance for several values of vacuum speckle contrast ratio.

and the transverse coherence lengths ρ_{oi} and ρ_{oj}. At low turbulence levels α_o dominates f_1 and f_2 and A_1 and A_2 are constants. Under these conditions, the normalized variance tends to increase exponentially with the turbulence level since C_χ is proportional to $\sigma_\chi{}^2$. However as the turbulence level $C_n{}^2$ increases, ρ_{oi} and ρ_{oj} decrease and at some point they will start to affect A_1 and A_2 significantly. Now with further increase in the turbulence level, the parameters A_1 and A_2 rapidly decrease in value. This will cause C_χ to be sampled further and further out on the tail of the covariance curve. In the limit, as C_χ approaches zero, the atmospheric perturbation is unity and the normalized variance returns to the vacuum value. Consequently, the behavior illustrated in Fig. 5.2 does not require saturation to occur. However if saturation does occur before the normalized variance returns to a point near its vacuum value, the process proceeds more rapidly because of the saturation effects in C_χ and the shape of the bump in Fig. 5.2 is affected. Consequently, if the functions f_1 and f_2 are dominated by ρ_{oi} and ρ_{oj} before the onset of saturation, then a form of C_χ that includes the saturation effects does not need to be used (this saves a substantial amount of computation time). Otherwise the saturation form of C_χ should be used in Eq.(5.28). When the functions f_1 and f_2 are not dominated by ρ_{oi} and ρ_{oj}, the assumption that amplitude fluctuations are normally distributed and the use of the generalized spherical wave mutual coherence function is strictly valid. In order to substantiate the arguments further and to estimate the effects of the other propagation parameters, the term AP is calculated for different conditions of turbulence. Figure 5.3 shows the effect of the transmitter size on the atmospheric perturbation term. As the beam size reduces, the term AP also reduces. Mathematically as $\alpha \to 0$, f_1 and $f_2 \to 0$. Phenomenologically, this means that at the target the beam has become large and smooths the effect of the amplitude fluctuations. Such smoothing can also be achieved by defocusing or collimating the transmitted beam so that the beam on the target becomes large. This result is shown in Fig. 5.4 which shows that defocusing reduces the atmospheric perturbation.

In the analysis above, the coordinate r is actually of dimensions 1/length. This is because the spatial coordinate at the transmitter was normalized by k/L. In the actual analysis, the log-amplitude covariance is dependent on the relative size of r with respect to the Fresnel zone size $\sqrt{L/K}$. Therefore the important parameter is $r = (P_m/A)\sqrt{L/K}$. In the region, where the beam size α_o is either completely or partially dominant, the AP term is also affected by the wavelength via the Fresnel zone size. This effect is very substantial as can be seen in Figs. 5.5 and 5.6, where the AP term was calculated for two different path lengths at

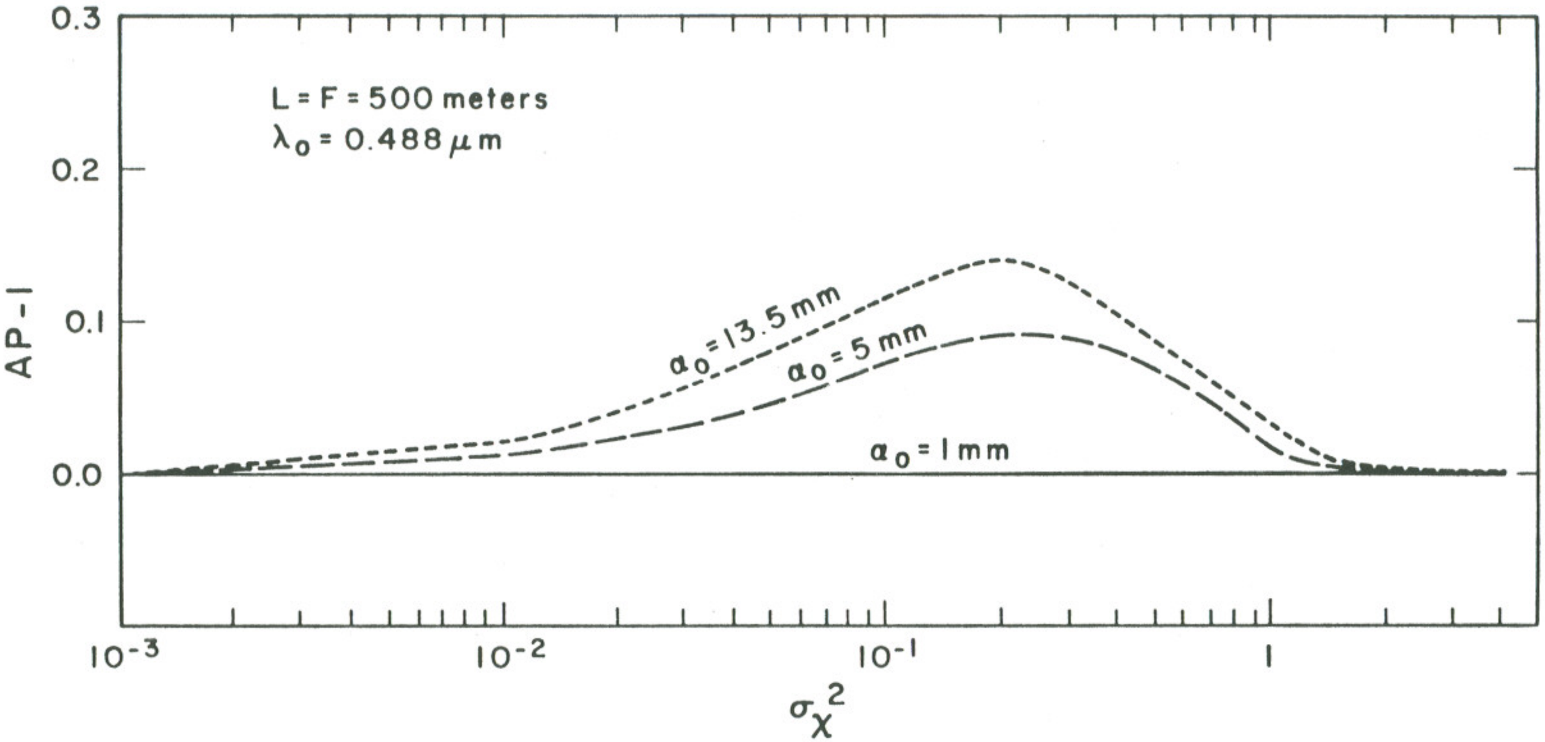

Figure 5.3. Atmospheric perturbation on an argon laser versus log-amplitude variance for several values of the beam size at the transmitter to illustrate the effect of the beam size.

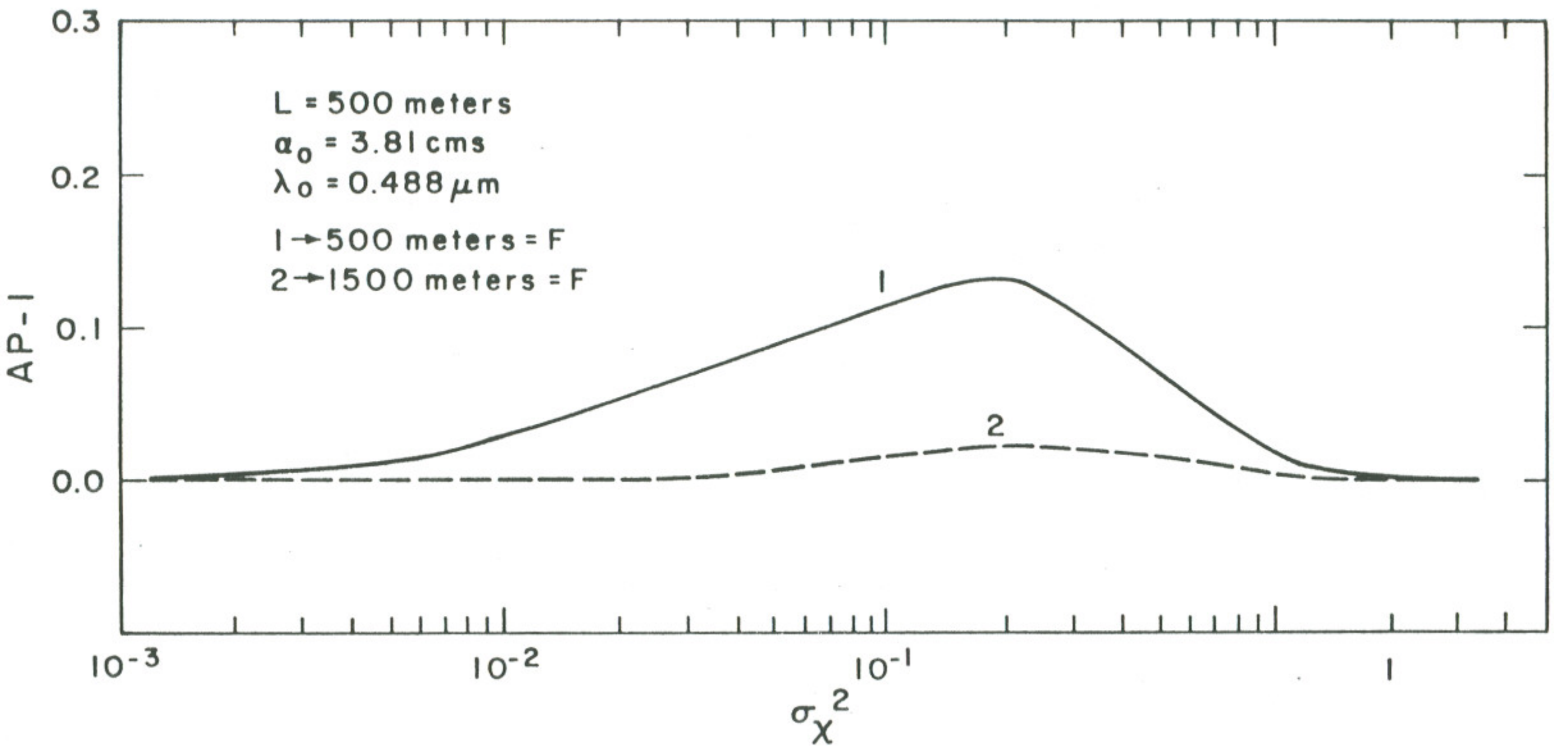

Figure 5.4. The effect of defocusing on the atmospheric perturbation at several values of the log-amplitude variance.

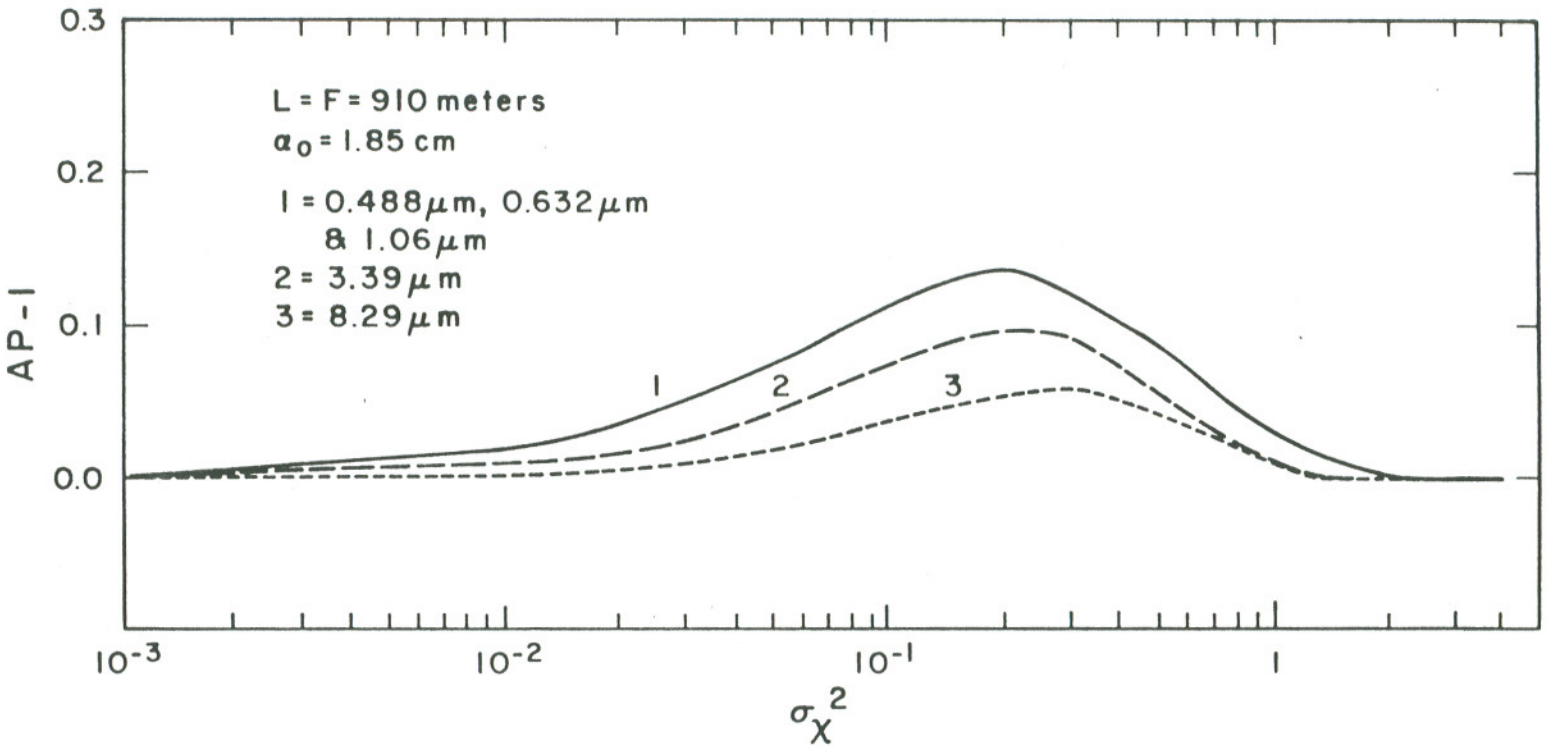

Figure 5.5. Atmospheric perturbation versus log-amplitude variance for several values of wavelength to consider the effect of the wavelength on the atmospheric perturbation at a path length of 910 meters.

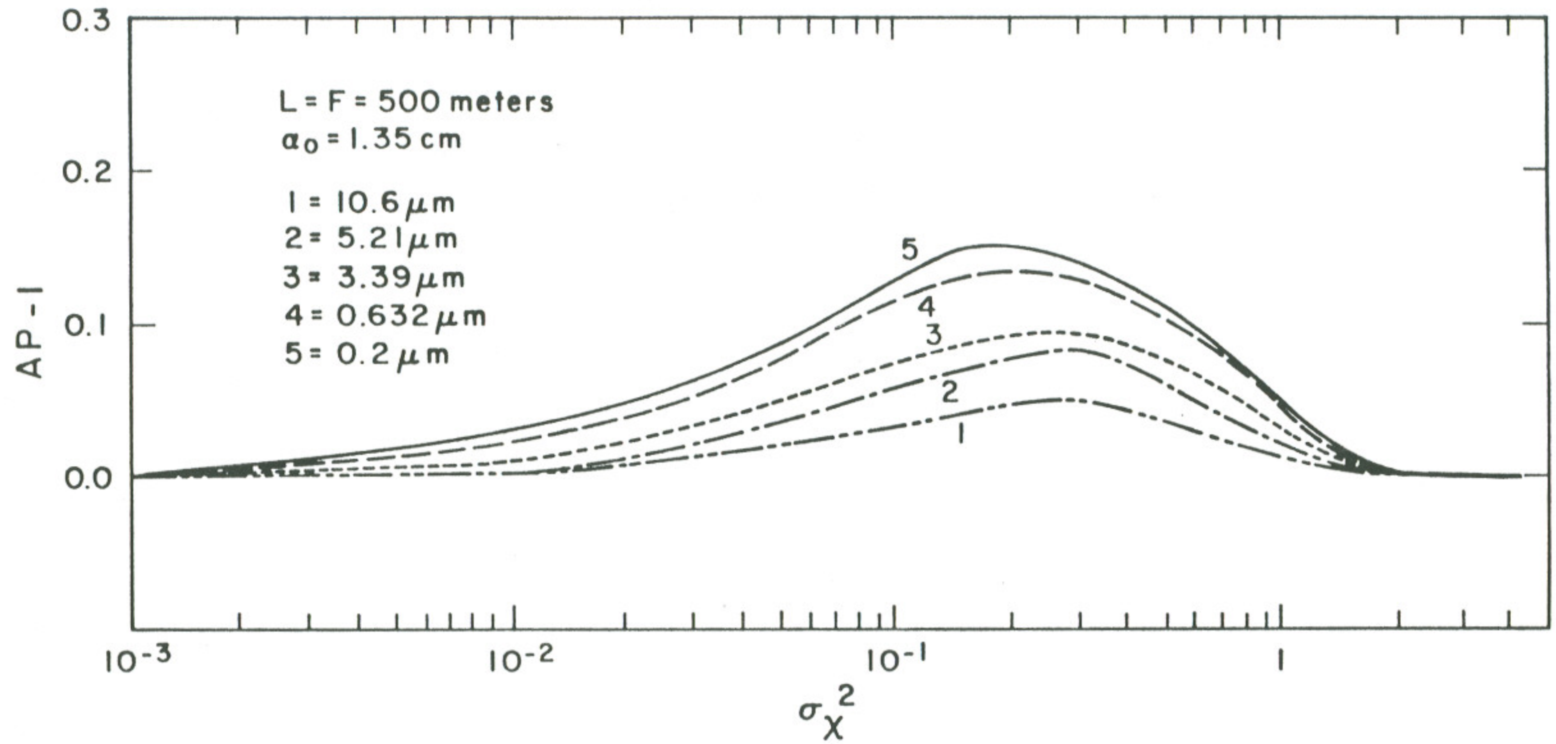

Figure 5.6. Atmospheric perturbation versus log-amplitude variance for several values of wavelength to consider the effect of the wavelength on the atmospheric perturbation at a path length of 500 meters.

various wavelengths. As the wavelength decreases, the Fresnel zone size increases and correspondingly C_χ is reduced, thereby reducing the atmospheric perturbation. Further in the case when widely separated frequencies are present, the scale size A_l is dominated by the larger wavelength which tries to smooth the amplitude fluctuations. Thus most of the AP term comes from the fluctuations at the short wavelengths. The above theory does not take into account the effect of the inner scale size of the turbulent atmosphere. When the speckle size is of order of the inner scale size, the effects may be very substantial. It is expected following the works of Hill and Clifford,[73,74] that the normalized variance may increase substantially depending on the ratio of the Fresnel zone size to the inner scale.

CHAPTER VI

COVARIANCE OF THE RECEIVED INTENSITY OF A POLYCHROMATIC SPECKLE PATTERN IN THE TURBULENT ATMOSPHERE

The covariance of the received intensity of a speckle pattern produced by a diffuse target in the presence of the turbulent atmosphere is an important consideration in the design of adaptive optics and remote sensing systems. For example, by choosing a proper spacing between the detectors, the covariance function can be made less sensitive to the wind velocity fluctuations along the path. In the monochromatic case, the measurements by Pincus et al.[75] and the theoretical work of Holmes et al.[54] show that the covariance scale size is dominated by the beam size at low turbulence levels and by the lateral coherence length (ρ_o) at the target at very high turbulence levels. Thus the speckle size at the receiver is of the order of the beam size (for the focused geometry) at low turbulence levels and is of the order of the lateral coherence length at very high turbulence levels. In addition, knowledge of the proper choice of detector spacing is required so that wind sensing is feasible either by the time delayed covariance method or the slope method.Also knowledge of the covariance scale sizes is required to obtain the joint probability density function of the fields at the target.

6.1 Analysis

The spatial covariance of the received intensity of a speckle pattern is a measure of the correlation between the intensity fluctuations at two points in space and is by definition, given by

$$C_I(P_1,P_2) = \langle I(P_1)I(P_2)\rangle - \langle I\rangle^2 \tag{6.1}$$

The intensity correlation term can be obtained from the general correlation function, developed in the fourth chapter by assuming a zero time difference. Then

$$\begin{aligned} C_I(P) &= B_I(P,\ \tau = 0) - \langle I\rangle^2 \\ &= C_{I_1}(P) + C_{I_2}(P) - \langle I\rangle^2 \end{aligned} \tag{6.2}$$

where $P = P_1 - P_2$. The terms C_{I_1} and C_{I_2} are given as

$$C_{I_1}(P)$$

$$= \sum_{j=1}^{N} \sum_{i=1}^{N} \frac{\langle I_i\rangle\langle I_j\rangle}{2\pi} \int \rho d\rho \int r dr \int d\theta_\rho \; J_o(\rho r)$$

$$f_1(r,k_i,k_j) \exp\{4\ C_\chi(P,\rho,k_i,k_j)\} \tag{6.3}$$

and

$$C_{I_2}(P) = \sum_{i=1}^{N} \frac{\langle I_i\rangle^2}{2\pi} \int r dr \int \rho d\rho \int_o^{2\pi} d\theta_\rho$$

$$f_2(r,k_i) \exp\left[i \frac{k_i}{L} \rho\ P \cos(\theta_P - \theta_\rho)\right]$$

$$H_2(\overline{P},\overline{\rho},\tau=o) \tag{6.4}$$

where the functions f_1 and f_2 are given by Eqs.(5.15) and (5.17). The mutual coherence function H(....) is given by

$$H_2(\overline{P},\overline{\rho},\tau = 0)$$

$$= \exp\Big[-2\Big(\frac{\rho}{\rho_{oi}}\Big)^{5/3} - 2\Big(\frac{P}{\rho_{oi}}\Big)^{5/3} + \frac{1}{2}\ D_\psi(\overline{P},-\overline{\rho},\tau = 0)$$

$$+ \frac{1}{2}\ D_\psi(\overline{P},\overline{\rho},\tau = 0) + 2C_\chi(\overline{P},\overline{\rho},\tau = 0) + 2C_\chi(\overline{P},\overline{\rho},\tau = 0) \qquad (6.5)$$

Using the same Fourier-Bessel series as earlier, the covariance of the received intensity is reduced to a simple one fold integral given by

$$C_{I_N}(P)$$

$$= \sum_{i=1}^{N} \sum_{j=1}^{N} \frac{G_i G_j}{2\pi} \int_o^{2\pi} d\theta_\rho \ \{\sum_m b_m(k_i,k_j) \times$$

$$\exp\Big[4C_\chi\Big(\overline{P},\rho = \frac{P_m}{A_1(k_i,k_j)}\ ,\ k_i,\ k_j\Big)\Big]\}$$

$$+ \sum_{i=1}^{N} \frac{G_i^{\ 2}}{2\pi} \int_o^{2\pi} d\theta_\rho \{\sum_m C_m(k_i) \times$$

$$\exp\Big[i\ \frac{k_i}{L}\ \frac{P_m}{A_2(k_i)}\cos(\theta_p - \theta_\rho)\Big]\ H_2\Big(P,\rho = \frac{P_m}{A_2(k_i)}\ ,\ \tau = 0\Big)\} - 1 \qquad (6.6)$$

When all the frequencies are sufficiently near, the calculations can be done at the midpoint of the band and this is given as

$$C_{I_N}(P)$$

$$= \sum_{i=1}^{N} \sum_{j=1}^{N} \frac{G_i G_j}{2\pi} \int_o^{2\pi} d\theta_\rho \; \{\sum C_m \exp[4C_\chi(P, \rho = \frac{P_m}{A}, k)\}$$

$$+ \sum_{i=1}^{N} \frac{G_i^{\,2}}{2\pi} \int_o^{2\pi} d\theta_\rho \; \{\sum C_m \exp[i \frac{k_i}{L} \frac{P_m}{A} \cos(\theta_p - \theta_\rho)$$

$$\times H_2(P, \rho = \frac{P_m}{A}, \tau = 0)\} - 1 \qquad (6.7)$$

Let

$$\text{AINT1} = \frac{1}{2\pi} \int_o^{2\pi} d\theta_\rho \; \{\sum C_m \exp[4C_\chi(P, \rho = \frac{P_m}{A}, k)]\} \qquad (6.8)$$

and

$$\text{AINT2} = \frac{1}{2\pi} \int_o^{2\pi} d\theta_\rho \; \{\sum C_m \exp[\frac{ik}{L} \frac{P_m}{A} \cos(\theta_p - \theta_\rho)]$$

$$\times H_2\left(P, \rho = \frac{P_m}{A}, \tau = 0\right)\} \qquad (6.9)$$

Then the covariance, normalized to the square of the mean intensity is given as

$$C_{I_N}(P) = \sum_{i=1}^{N} \sum_{j=1}^{N} G_i G_j \; (\text{AINT1}) + \sum_{i=1}^{N} G_i^{\,2} \; (\text{AINT2}) - 1 \qquad (6.10)$$

As discussed earlier, for most problems of practical interest, the frequencies are sufficiently near that the knowledge of the mode distribution of the laser is not necessary and Eq.(6.10) can be written in terms of the vacuum speckle contrast ratio as

$$C_{I_N}(P) = \mathrm{AINT1} + (\mathrm{VSCR})^2 \cdot (\mathrm{AINT2}) - 1 \qquad (6.11)$$

In several problems of practical interest, a more useful parameter is the covariance, normalized to the variance and this is given by

$$C_{I\sigma}(P) = \frac{C_I(P)}{\sigma_I^{\,2}} \qquad (6.12)$$

In this case, the results of Eq.(6.10) or (6.11) are divided by the variance given by Eq.(5.25) or (5.28) to obtain the normalized variance.

Calculation of the covariance curve from Eq.(6.11) in general requires a formulation for the four point two frequency log-amplitude covariance function and the corresponding wave structure function, which are valid for all turbulence levels. For the path lengths and the parameters of the turbulence under consideration here, it may be noted that using the unsaturated form beyond the range of its validity still gives good results. The reason for this is the same as discussed in the chapter on the variance of the intensity. When all frequencies are sufficiently near, a saturated form[72] of the log-amplitude covariance function at the midpoint of the band can be used if it is required.

6.2 NUMERICAL CALCULATIONS AND COMPARISON WITH THE EXPERIMENTAL DATA

Figure 6.1 represents the comparison of the theory with the experimental data collected by Holmes[54] et al., using a Nd:YAG laser, running in several axial and transverse modes for a detector spacing of 4.5 millimeters for several turbulence levels. Using a vacuum speckle contrast ratio of .135, as earlier, the theoretical values for the variance and the covariance at each turbulence level were calculated and from these values a theoretical curve for the normalized covariance (normalized to the variance) was generated in Figure 6.1 for comparison with experimental data. Good agreement between the theoretical and experimental values was obtained within 5% error, thereby satisfactorily explaining the data. Since a VSCR of .135 corresponds to a normalized variance of .015, it corresponds to an almost incoherent source. The normalized covariance in Figure 6.1 is almost constant for a very substantial increase in the turbulence level. There is slight discrepancy between the theory and experiment for values of $\sigma_\chi > 4$. It can be shown using the present results that the normalized covariance remains constant for substantial increase in the turbulence level. In Figures 6.2, 6.3 and 6.4, the experimental data collected by Fossey and Holmes[55] over a 910 meter path is compared with the theory for different turbulence levels. Figure 6.5 represents the comparison of theory with experiment over a 500 meter path.

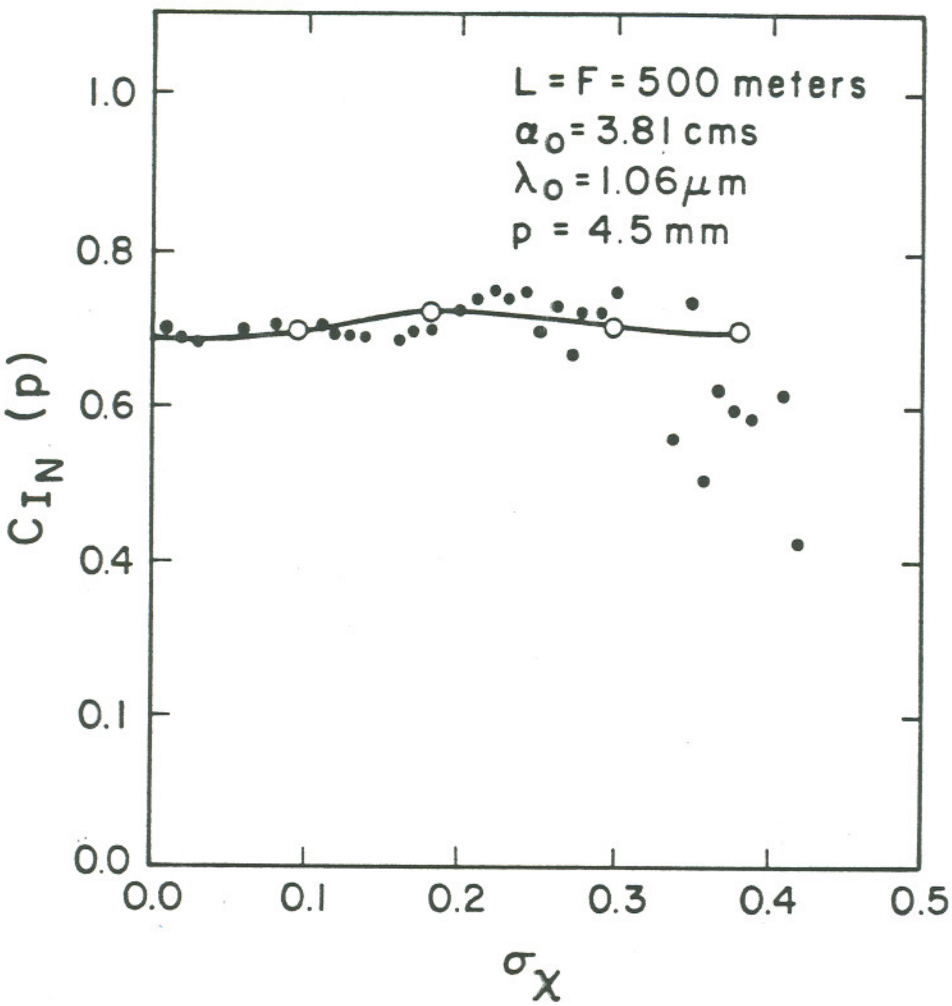

Figure 6.1. Normalized covariance of the received intensity for a polychromatic speckle field generated by a multimode Nd:YAG laser versus the log-amplitude standard deviation. Dots indicate experimental data. Solid line with circle indicates the theoretical values.

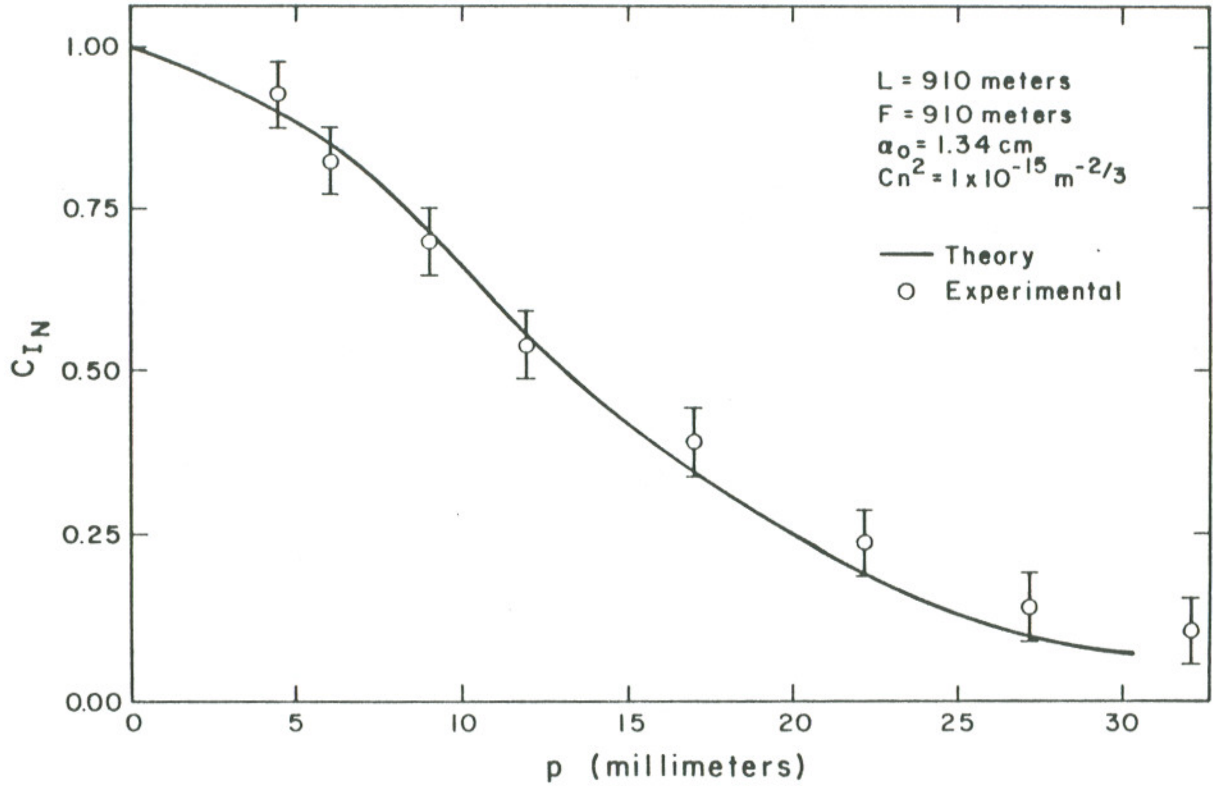

Figure 6.2. Normalized covariance of the received intensity of a multimode argon laser versus the detector spacing for a focused beam geometry.

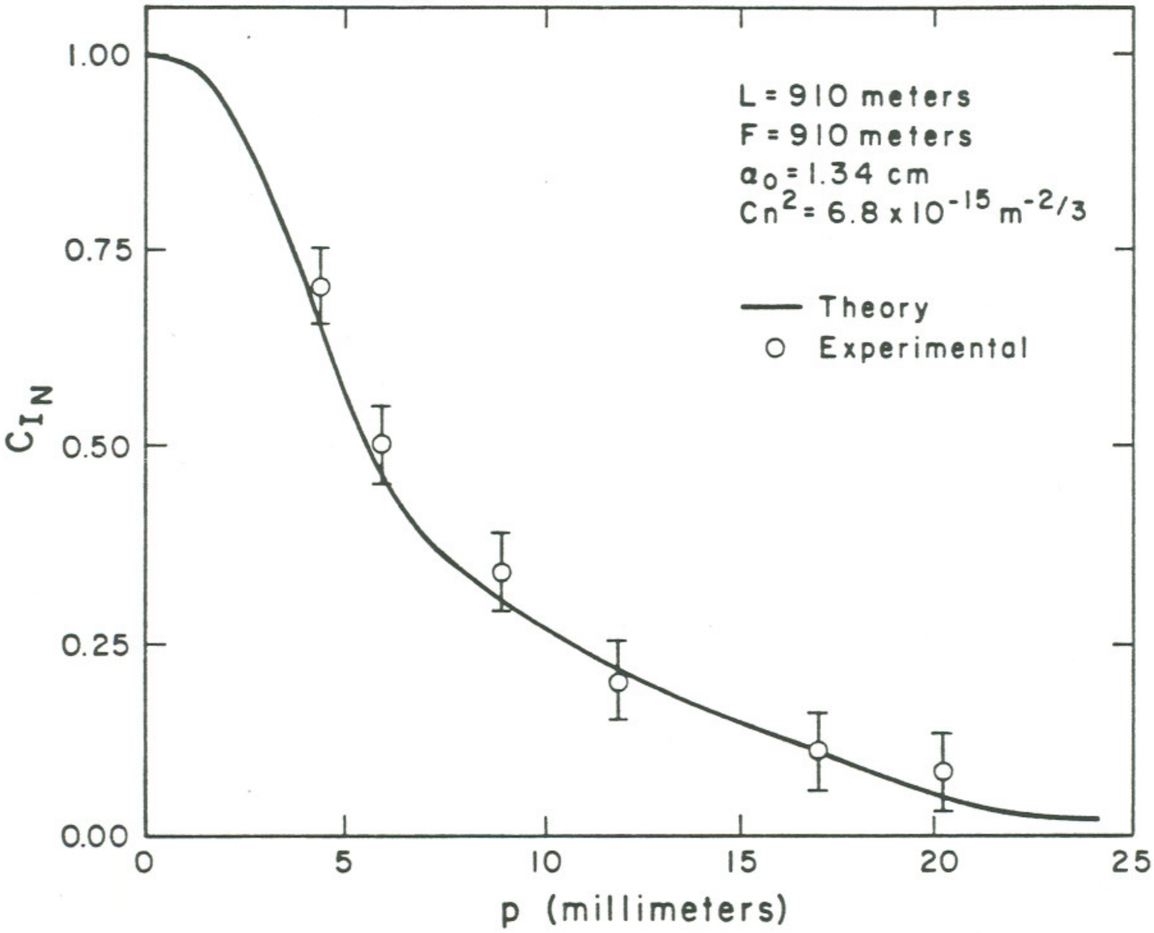

Figure 6.3. Normalized covariance of the received intensity of a multimode argon laser versus the detector spacing for a focused beam geometry.

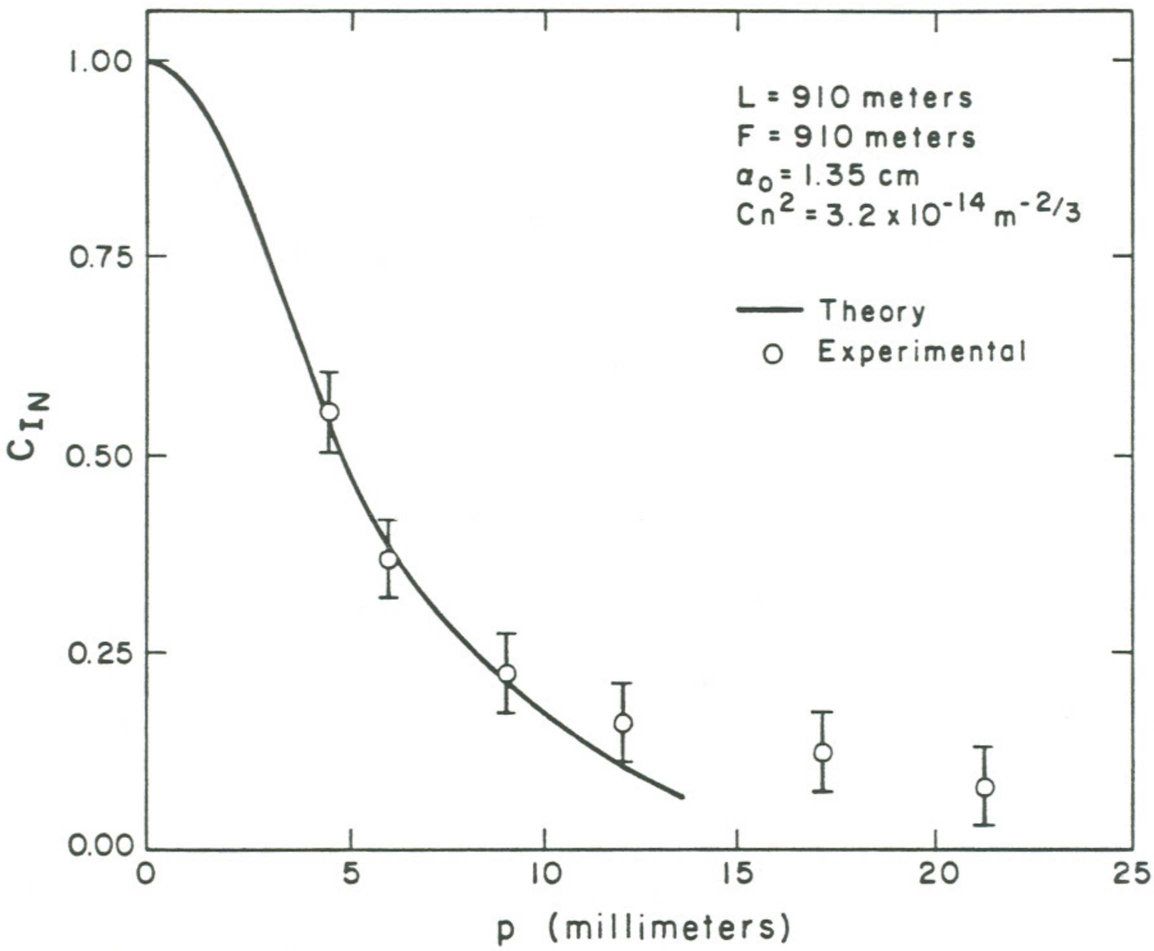

Figure 6.4. Normalized covariance of the received intensity of a multimode argon laser versus detector spacing for a focused beam geometry.

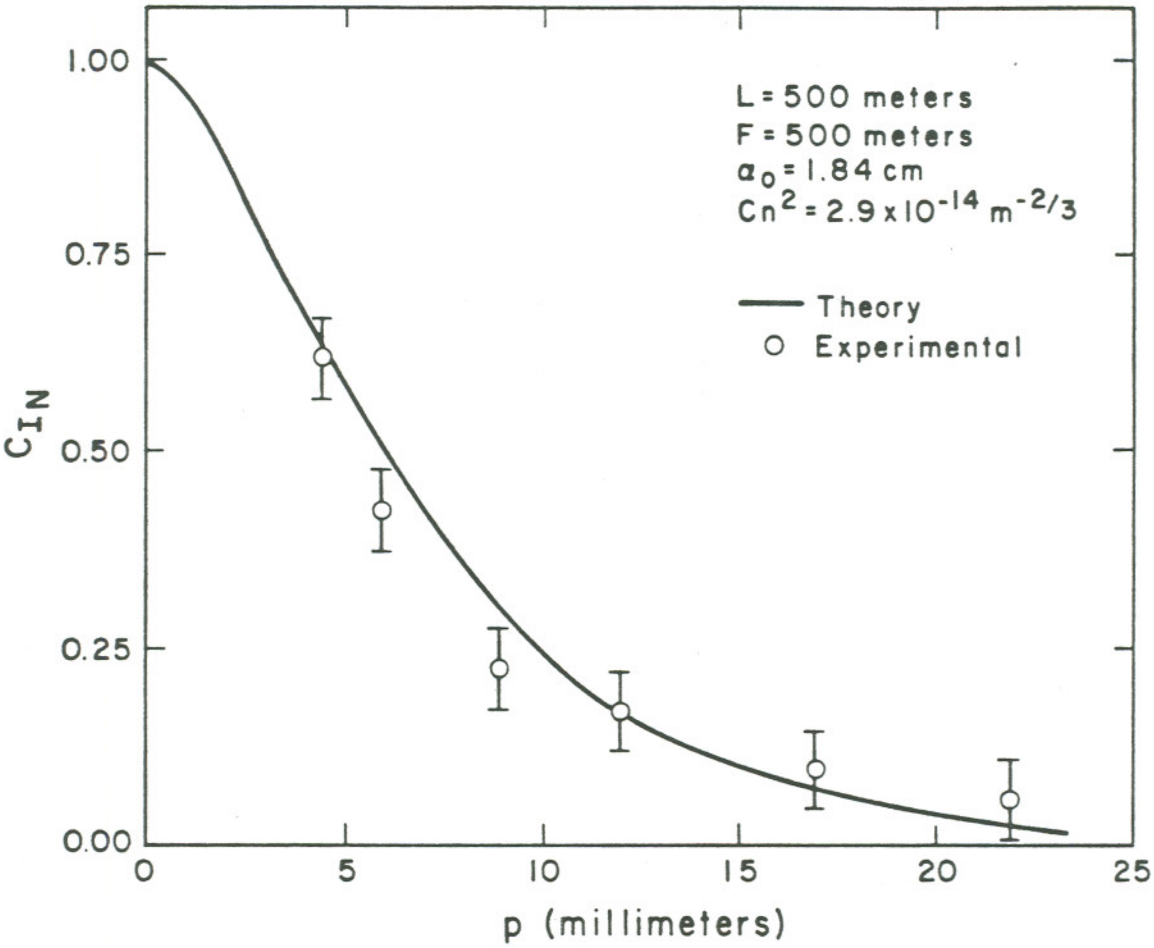

Figure 6.5. Normalized covariance of the received intensity of a multimode argon laser versus the detector spacing.

All the above data sets correspond to the focused beam geometry. Figure 6.6 compares the theory with experimental data for a defocused beam geometry. From these six figures, it is concluded that at low turbulence levels, for focused beam geometry, there is good agreement between the theory and the experiment. At high turbulence levels, the agreement is not very good even for the focused case. Also the defocused geometry did not give good results for large detector spacings.

6.3 Discussion

The theory has correctly predicted the covariance behavior. In order to obtain a deeper understanding of the covariance behavior, the normalized covariance was calculated for a 500 meter path length, with the beam focused on the target. The beam size was assumed to be 3.81 centimeters and a wave length of 1.06 μm was used. The normalized covariance of the received intensity versus the detector spacing is plotted for several values of VSCR in Figures 6.7-6.12. It is noticed that at low turbulence levels as the VSCR decreases, the normalized covariance also reduces for a given value of detector spacing. With an increase in the turbulence level, for some value of C_n^2, the VSCR does not affect the normalized covariance. This is seen for the example, in Figure 6.9 where $\sigma_\chi^2 = .0877$; all VSCR values give approximately the same normalized covariance over a very large range of detector

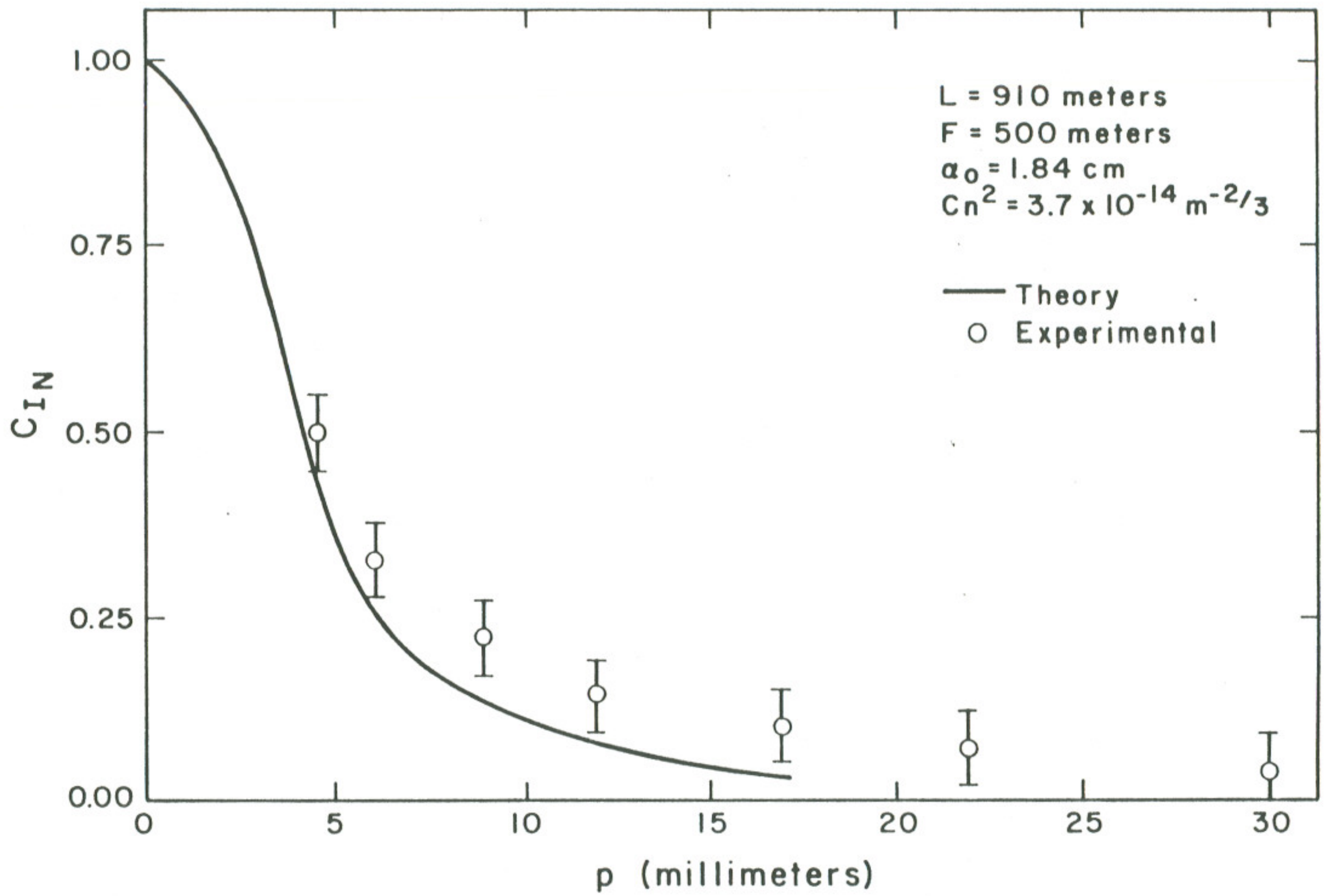

Figure 6.6. Normalized covariance of the received intensity of an argon laser versus detector spacing for a defocused beam geometry.

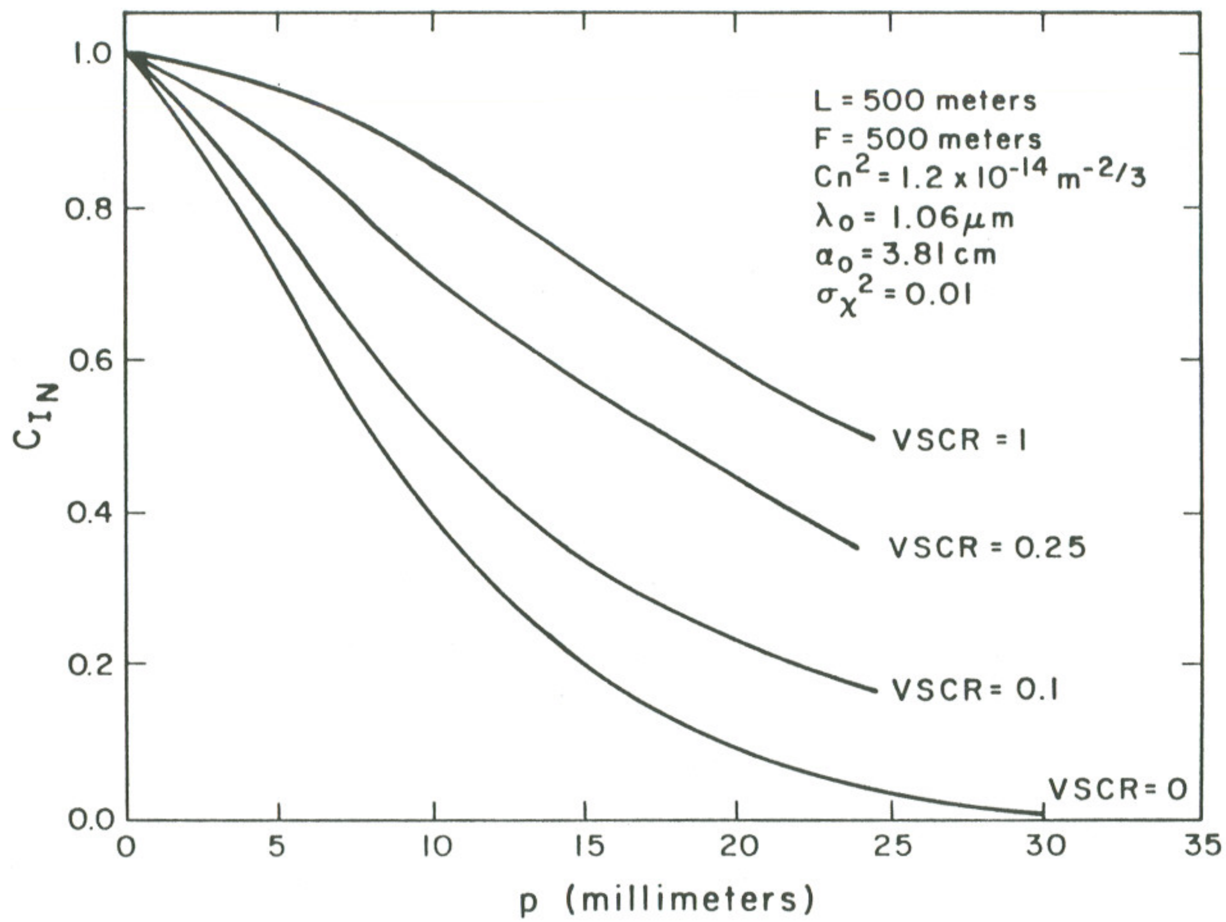

Figure 6.7. Normalized covariance of the received intensity versus detector spacing for several values of vacuum speckle contrast ratio at low turbulence level for a Nd:YAG laser.

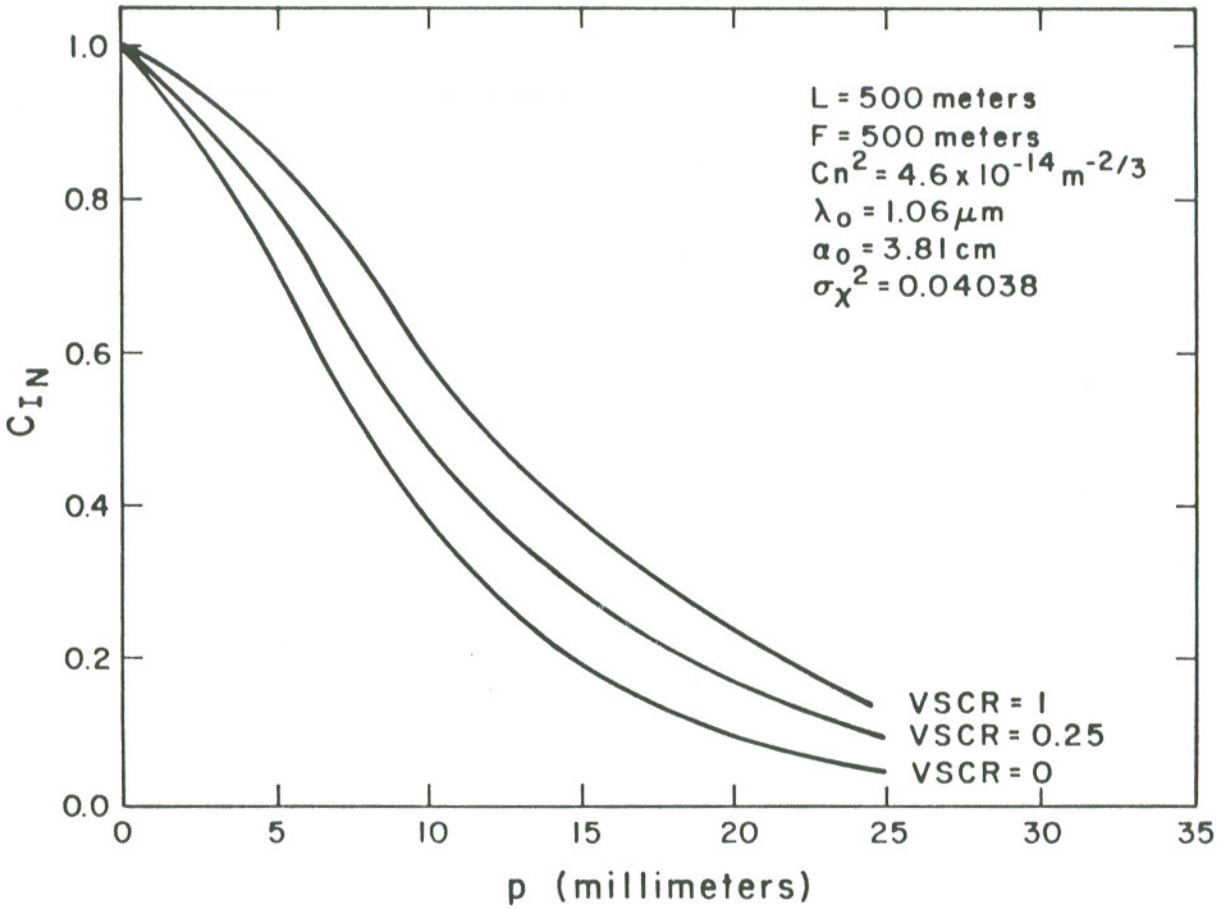

Figure 6.8. Normalized covariance of the received intensity versus detector spacing for Nd:YAG laser for several values of vacuum speckle contrast ratio at low turbulence level.

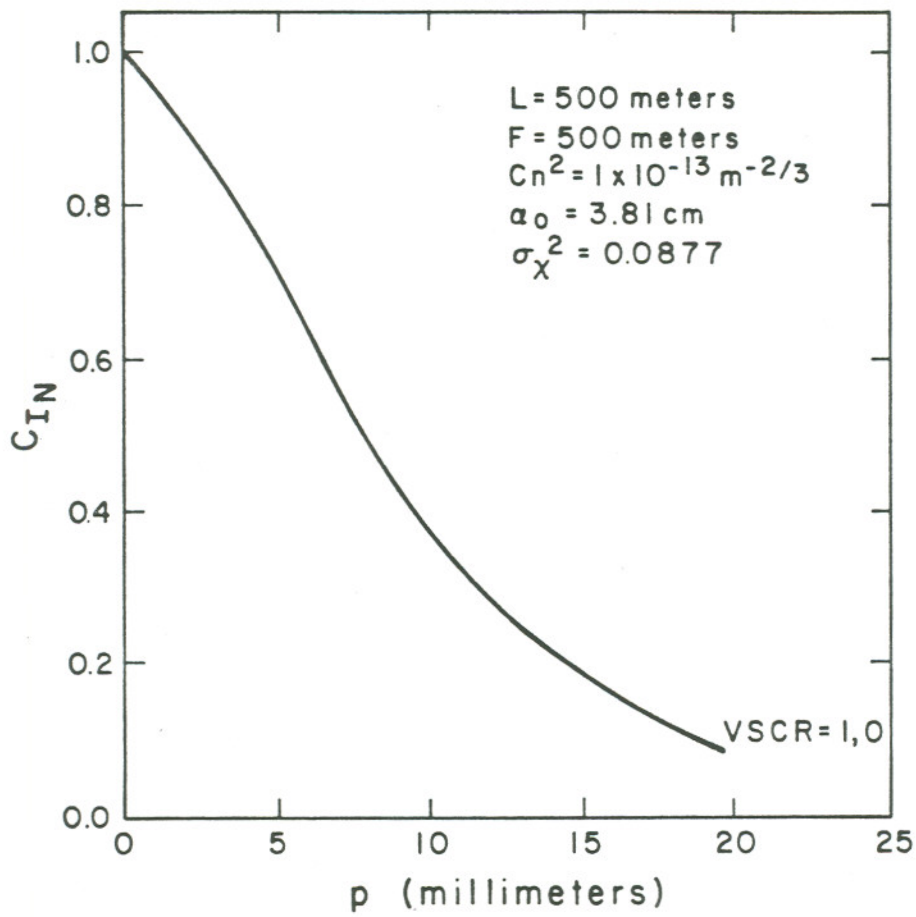

Figure 6.9. Normalized covariance of the received intensity of a Nd:YAG laser versus detector spacing for two values of vacuum speckle contrast ratio in the unsaturated region of turbulence.

spacings. With a further increase in the turbulence level, reducing the VSCR does in fact increase the normalized covariance for all values of detector spacings. This is seen in Figures 6.10-6.12. Figures 6.13 and 6.14 describe the variation of the normalized covariance with respect to the turbulence level, characterized by the Rytov variance, for different values of detector spacing. In these two curves, it is noted that as the VSCR reduces, the sensitivity of the normalized covariance to the variations in the turbulence levels also decreases. This is indeed the nature of the experimental data, observed in Figure 6.1. In order to understand the behavior of the covariance, the total contribution to the normalized covariance of the intensity of a polychromatic speckle pattern can be resolved into a coherent contribution (AINT2) and an incoherent contribution (AINT1 -1.) From the expression for the covariance of the polychromatic speckle field, it can be seen that the coherent term is weighted by the normalized variance (square of VSCR). At low turbulence levels, the coherent term contributes more and thus, as the weighting factor VSCR decreases, the net coherent contribution also reduces. But the variance is still determined by the incoherent term. The net result is that the normalized covariance is strongly dependent on the coherent term. In this regime, the covariance scale size is also dominated by the beam size. With further increase in the turbulence level, the contribution of the incoherent term is more

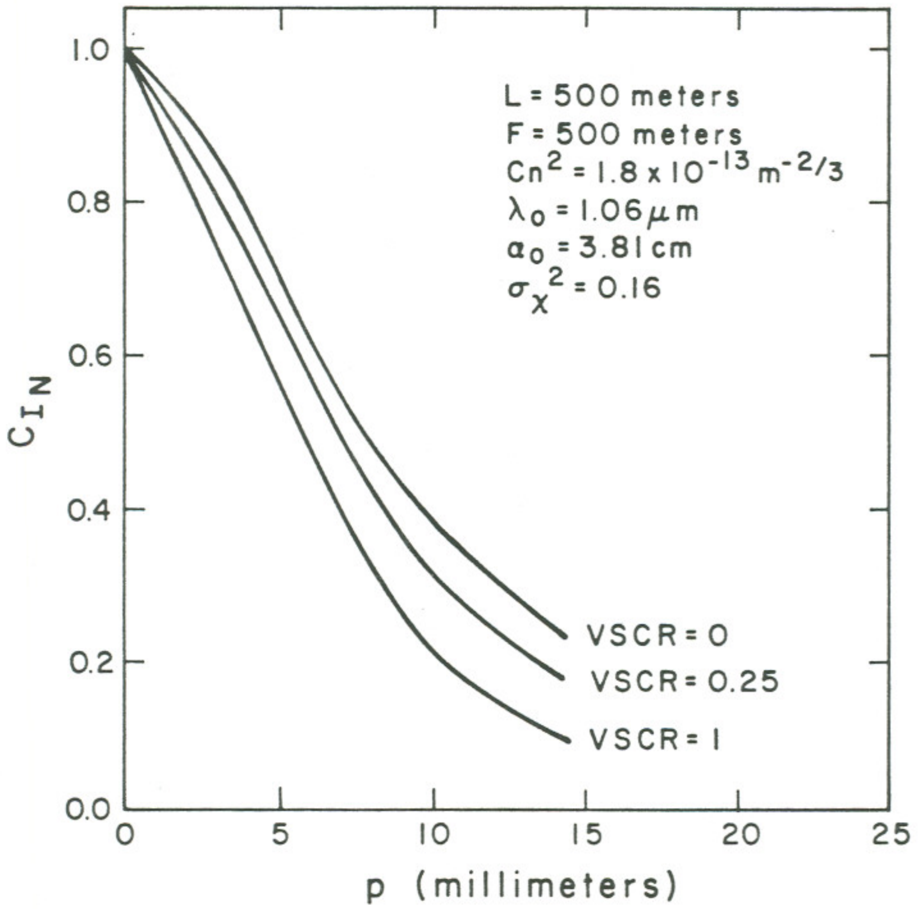

Figure 6.10. Normalized covariance of the received intensity of a Nd:YAG laser versus detector spacing for three different values of vacuum speckle contrast ratio in the unsaturated region of turbulence.

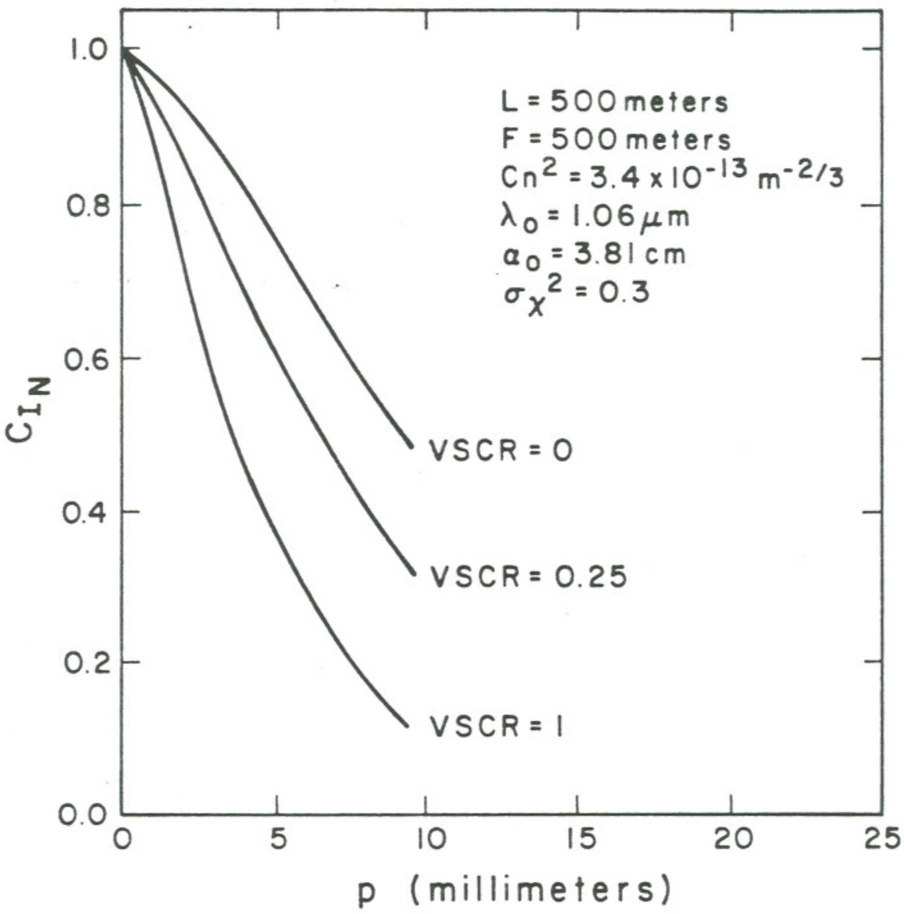

Figure 6.11. Normalized covariance of the received intensity of a Nd:YAG laser versus detector spacing for three different values of vacuum speckle contrast ratio for a turbulence level just at saturation.

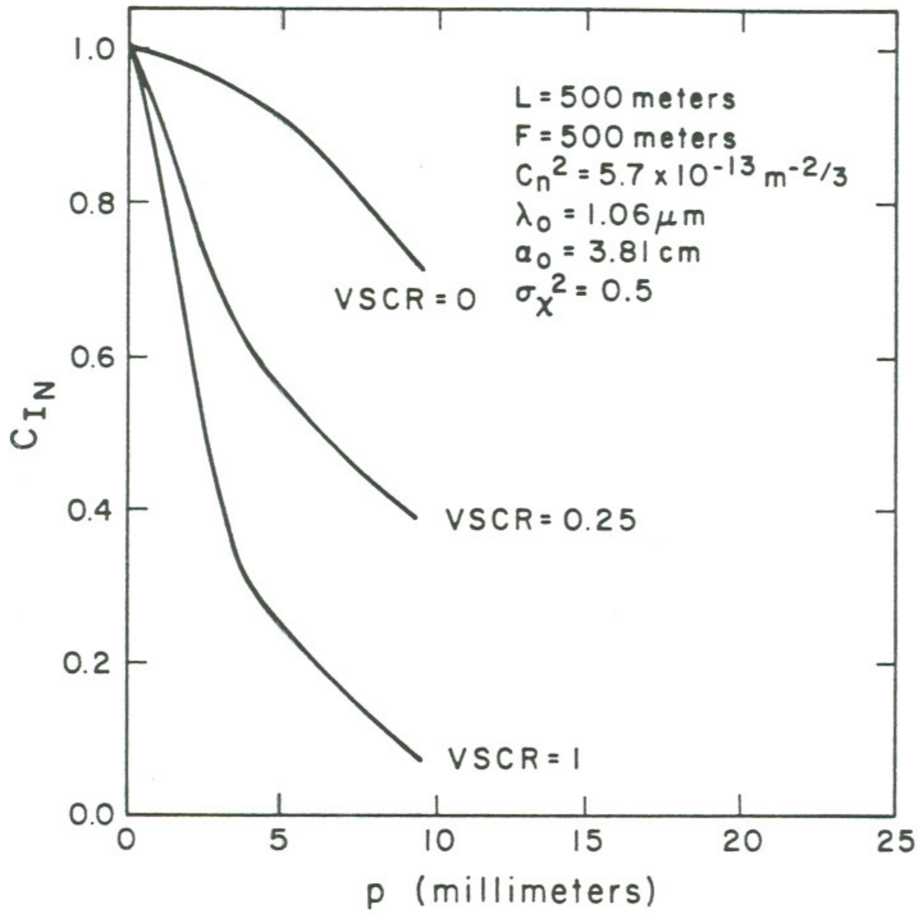

Figure 6.12. Normalized covariance of the received intensity of a Nd:YAG laser versus detector spacing for three different values of vacuum speckle contrast ratio in the saturated region of turbulence.

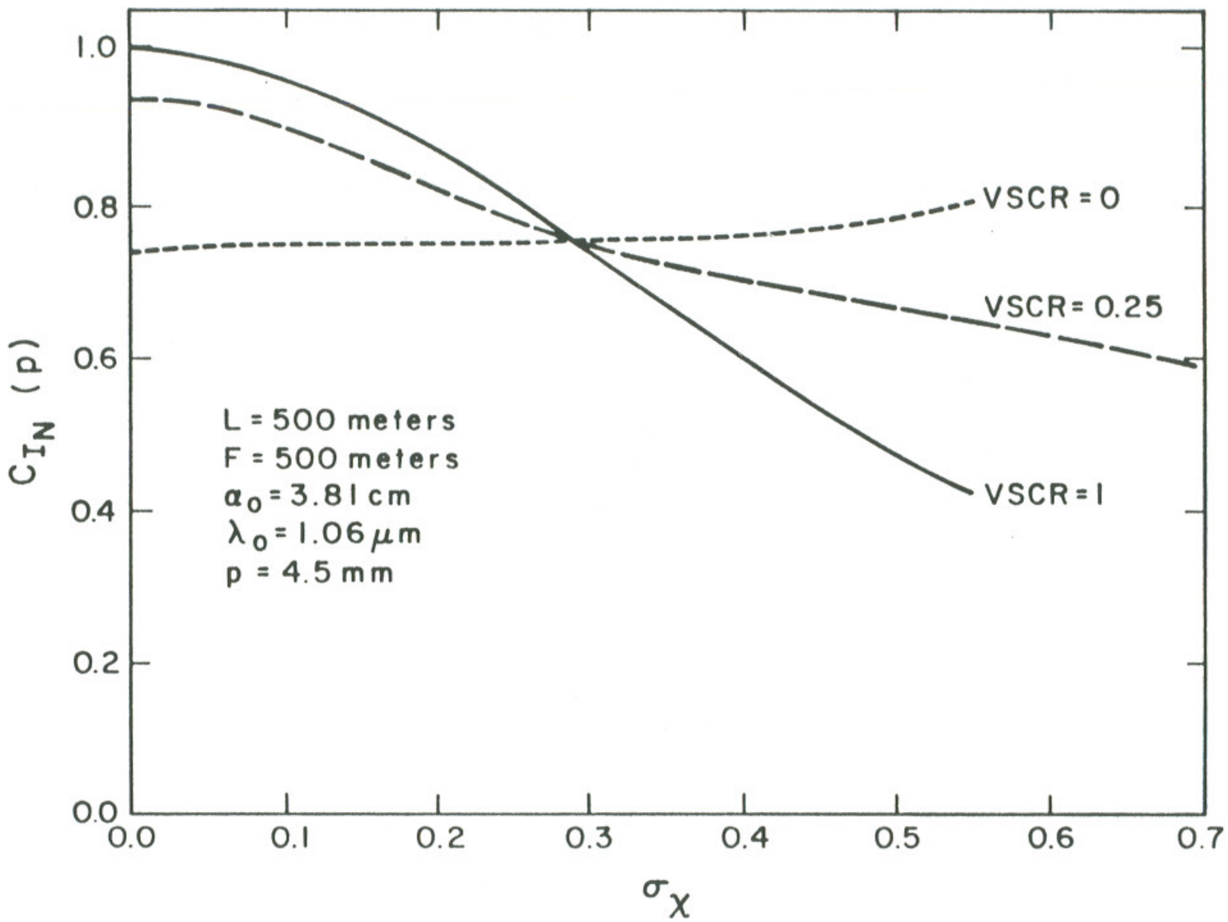

Figure 6.13. Normalized covariance of the received intensity of a Nd:YAG laser versus log-amplitude standard deviation for three different values of vacuum speckle contrast ratio for a detector spacing of 4.5 mm.

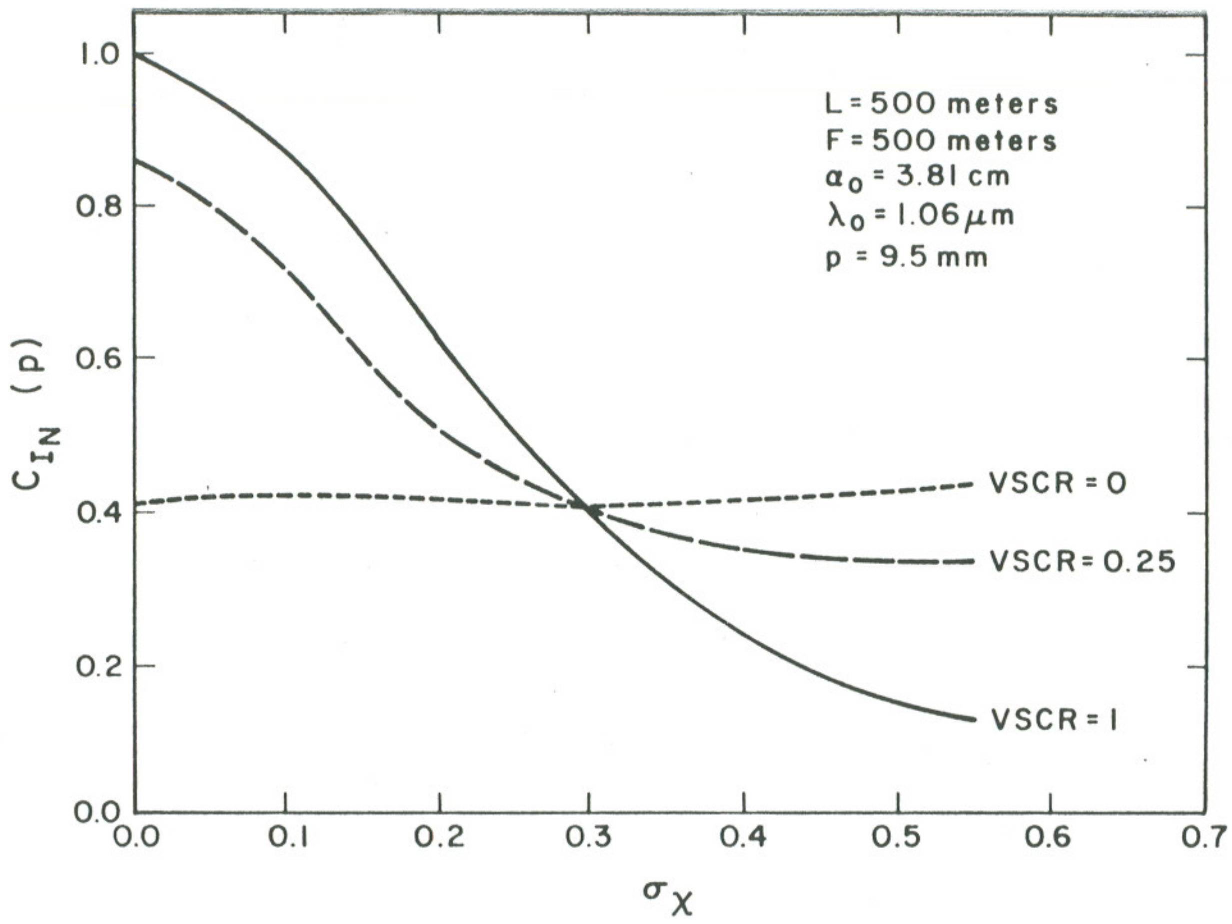

Figure 6.14. Normalized covariance of the received intensity of a Nd:YAG laser versus the log-amplitude standard deviation for three different values of vacuum speckle contrast ratio at a detector spacing of 9.5 mm.

substantial than the coherent term and thus reducing the VSCR does not affect the covariance as much. With further increase in the turbulence level, the contribution due to the incoherent term is substantial and the fluctuations are correlated over larger detector spacings for a partially coherent speckle pattern than for a coherent speckle pattern. Thus as the VSCR reduces, the normalized covariance increases. Extensive numerical calculations support this argument very strongly. From this the insensitivity of the normalized covariance for the variations in the turbulence level at low values of VSCR can be explained. It now remains to remark on the size of the speckle at the receiver both as a function of both the turbulence level and of the VSCR. For a given value of VSCR, the speckle size is dominated by the beam size α_o at low turbulence levels and by ρ_o, the lateral coherence length, at very high turbulence levels. For intermediate levels of turbulence, it is dependent on both α_o and ρ_o. For a given turbulence level, as the VSCR reduces, the covariance is more dominated by the amplitude fluctuations and the speckle size is determined by the Fresnel zone size as well as the lateral coherence lengths. Thus in the turbulence regimes ($\sigma_\chi^2 \approx .1$ to $.3$) where the amplitude fluctuations are most important, the normalized covariance scale size essentially increases with the reduction in VSCR. For widely separated frequencies, the covariance scale size is dominated by the larger wave length as the coefficients b_m are dominated by it and the lateral coherence length at this wave length plays a more dominant role.

CHAPTER VII

TEMPORAL STATISTICAL PARAMETERS

The important temporal statistical parameters are the time delayed covariance, the autocorrelation of the received intensity and the temporal frequency spectrum of the fluctuations of the received intensity. These parameters are necessary to estimate the cross wind velocity and in the design of the remote sensing systems.

In Chapter IV, a formulation was developed for the general correlation of the received intensity. Using this, the time delayed covariance can be estimated. Unfortunately, it is not possible within a reasonable computation time to evaluate exactly a part of the 2 point-space-time correlation function of the intensity (C_{I_2}) which involves a fourfold integral. In this chapter, an approximate numerical method to evaluate the time delayed covariance of the received intensity and the autocorrelation of the intensity is presented. Since the time delayed covariance was not numerically evaluated even for the monochromatic case previously and much experimental data was available for this case, the theoretical results are compared with this case to check the validity of formulation. The theory was then extended to the polychromatic case. It must be noted that the numerical evaluation in this chapter is only approximate and one should be careful in using this method elsewhere. In addition expressions are given for the autocorrelation, which can also be evaluated by using similar numerical techniques, and for the power spectrum of the intensity fluctuations.

7.1 Analysis

The time delayed covariance of the received intensity, by definition, is given by

$$\begin{aligned} &C\,(\overline{P}_2,t_2;\ \overline{P}_1,t_1) \\ &= \langle I(P_2,t_2)I(P_1,t_1)\rangle - \langle I\rangle^2 \\ &= C_{I_1}(P,\tau) + C_{I_2}(P,\tau) - \langle I\rangle^2 \qquad (7.1) \end{aligned}$$

where $I(P_i,t_i)$ is the intensity in the receiver plane at a space time point (P_i,t_i). The time delayed covariance (TDC) of the received intensity can be normalized either to the square of the mean or to the variance of the received intensity. In Eq.(7.1), the terms C_{I_1} and C_{I_2} are given by Eqs.(4.24) and (4.26). The term C_{I_1} is given by

$$\begin{aligned} C_{I_1} = \frac{1}{2\pi} &\sum_i \sum_j G_i G_j \int d\overline{\rho} \int r dr\ J_o(\rho r)\ f_1(r,k_i,k_j) \\ &\times \exp\left[4\ C_\chi(\overline{P},\overline{\rho},\tau,k_i,k_j)\right] \qquad (7.2) \end{aligned}$$

$$f_1(r) = \exp\left[-\frac{r^2L^2}{4\alpha_o^2}\left(\frac{1}{k_i^2} + \frac{1}{k_j^2}\right) - \left(\frac{rL}{k_i\rho_{oi}}\right)^{5/3} - \left(\frac{rL}{k_j\rho_{oj}}\right)^{5/3}\right.$$

$$\left. - \frac{r^2\alpha^2}{2}\left(1 - \frac{L}{F}\right)^2\right]$$

and

$$\frac{C_{I_2}(P,\tau)}{\langle I\rangle^2} = \sum_{i=1}^{N} G_i^2\left(\frac{k_i}{2\pi L}\right)^2 \int r_2\, dr_2 \int d\theta_{r_2} \int \rho d\rho \int d\theta_\rho$$

$$\times f_2(r_2,\theta_{r_2}) \exp\left[\frac{ik_i}{L}\,\overline{\rho}\cdot(\overline{P} + \overline{r}_2)\right] H_2(\overline{P},\overline{\rho},\tau) \tag{7.3}$$

where

$$f_2(r_2,\theta_{r_2}) = \exp\left[-\frac{r_2^2}{2\alpha_o^2} - D_\psi(P,-r_2,-\tau) - \frac{r_2^2k_i^2}{2L^2}\,\alpha_o^2\left(1 - \frac{L}{F}\right)^2\right] \tag{7.4}$$

and

$$H_2(\overline{P},\overline{\rho},\tau) = \exp\left[-D_\psi(o,\rho,o) - D_\psi(\overline{P},o,\tau)\right]$$

$$\times \exp\left[\frac{1}{2}D_\psi(\overline{P},\overline{\rho},\tau) + \frac{1}{2}D_\psi(\overline{P},-\overline{\rho},\tau)\right.$$

$$\left. + 2C_\chi(\overline{P},\overline{\rho},\tau) + 2C_\chi(\overline{P},-\overline{\rho},\tau)\right] \tag{7.5}$$

and θ_{r_2} is the angle between the vectors $\overline{r}_2$ and $\overline{V}$ and θ_ρ is the angle between the vectors $\overline{\rho}$ and $\overline{V}$.

C_{I_1} in Eq.(7.2) can be evaluated by expanding $f_1(r)$ in a Fourier-Bessel series as was done earlier and this is given as

$$\frac{C_{I_1}(P,\tau)}{\langle I\rangle^2} = \frac{1}{2\pi} \sum_{i=1}^{N} \sum_{j=1}^{N} G_i G_j \int_o^{2\pi} d\theta_\rho \{\sum_m b_m(k_i,k_j)$$

$$\times \exp\left[4C_\chi(P,\rho = \frac{P_m}{A_1(K_i,k_j)}, \tau,k_i,k_j)\right]\} \tag{7.6}$$

where the b_m's are coefficients in the Fourier-Bessel series in (5.17). Even though this method was successful in evaluating C_{I_2} in Eq.(6.4) for the covariance case, it cannot be successfully used again as the angle θ_{r_2} is present in the exponential term of $f_2(r)$ and thus the integration over $d\theta_{r_2}$ is not possible. Thus the estimation of C_{I_2} involves a fourfold integral and the integrand, again involves the double integrals due to log-amplitude covariance function and the wave structure functions. Evaluation of these integrals would require a very large amount of computation time. However to estimate C_{I_2} approximately, in the integrand the mutual coherence function H_2 in the integrand can be rewritten by using the relations

$$D_\psi = D_\chi + D_\phi \text{ and}$$

$$D_\chi(\rho) = 2\left[C_\chi(o) - C_\chi(\rho)\right] \tag{7.7}$$

$$H = \exp\left[-D_\psi(o,\overline{\rho},o) - D_\psi(\overline{P},o,\tau) + 4\ \sigma_\chi^{\ 2}\right.$$

$$+ \left\{\frac{1}{2} D_\phi(\overline{P},\overline{\rho},\tau) + C_\chi(\overline{P},\overline{\rho},\tau) - C_\chi(\overline{P},\overline{\rho},\tau) - C_\chi(o)\right.$$

$$\left.\left. + \frac{1}{2} D_\phi(\overline{P},-\overline{\rho},\tau) + C_\chi(\overline{P},-\overline{\rho},\tau) - C_\chi(o)\right\}\right] \tag{7.8}$$

The term in brackets $\{\}$ is dependent on θ_ρ and can be written as

$$8\pi^2\ k_i^{\ 2}\ L\ C_n^{\ 2} \int_o^\infty X^{-8/3}\ dx \int_0^1 du\ \cos^2\left[\frac{x^2 u(1-u)L}{k_i}\right]$$

$$*\left[1 - \frac{J_o\left(\left|Pu + \rho(1-u) - v\tau\right|x\right) + J_o\left(\left|Pu - \rho(1-u) - v\tau\right|x\right)}{2}\right] \tag{7.9}$$

In Eq.(7.9), one can consider that $\left|Pu-v\tau\right|$ is one vector and $\rho(1-u)$ is another vector and then use Graf's addition theorems[68] for the Bessel functions. We then get

$$J_o\left(\left|Pu + \rho(1-u) - v\tau\right|x\right) + J_o\left(\left|Pu - \rho(1-u) - v\tau\right|x\right)$$

$$= 2\ J_o\left(x\left|Pu - v\tau\right|\right)\ J_o\left(x\rho(1-u)\right)$$

$$+ 2 \sum_{m=1}^{\infty} J_{2m}\left[\left|Pu - v\tau\right|x\right]\ J_{2m}\left[x\rho(1-u)\right] \cos\ 2m\theta_\rho \tag{7.10}$$

where θ_ρ is the angle between the vectors $\overline{\rho}$ and $\overline{P}$. Using this result, Eq.(7.9) is written as

$$8\pi^2 k_i^{\ 2} C_n^{\ 2} L \int_o x^{-8/3} dx \int_0 du \cos\left[\frac{x^2 u(1-u)L}{k_i}\right]$$

$$\times \left[1 - J_o\left(x\left|Pu-v\tau\right|\right) J_o\left(x\rho\left|1-u\right|\right)\right.$$

$$\left. - \sum_{m=1}^{\infty} J_{2m}\left(x\left|Pu-v\tau\right|\right) J_{2m}\left(x\rho\left|1-u\right|\right) \cos 2m\ \theta_\rho\right] \qquad (7.11)$$

In the integral (7.11), it can be shown that as x changes from 0 to $2\pi/\sqrt{\lambda L}$, $\cos\left[\frac{x^2 Lu(1-u)}{k}\right]$ decreases to a negligible value and $x^{-8/3}$ decreases from a very high value to a negligible value. This is true for all values of u. We therefore conclude that the maximum contribution comes from the values of x ranging from 0 to $\frac{2\pi}{\sqrt{\lambda L}}$. For a path length of 500 meters and a wave length of .488 μm, the range of importance is 0 to 160. Numerical calculations confirm this. Under this condition, if ρ and Vτ are limited to a few millimeters, the argument of the Bessel function is of the order of .5 or less. For these values of the argument, $J_2(z)$ is less than 3% of $J_0(z)$. So, neglecting the higher order Bessel functions ($m > 1$) in Eq.(7.11) does not lead to significant errors and Eq.(7.11) is rewritten as

$$= 8\pi^2 k_i^{\ 2} C_n^{\ 2} L \int_o^{\infty} x^{-8/3} dx \int_0^1 du \cos\left[\frac{x^2 u(1-u)L}{k_i}\right]$$

$$\times \left[1 - J_o(x\left|Pu-v\tau\right|) J_o(x\rho\left|1-u\right|)\right] \qquad (7.12)$$

Using this equation, H is approximately independent of θ_ρ and Eq.(7.8) can be written as

$$H_a = \exp\Big[- D_\psi(o,\rho,o) - D_\psi(\overline{P},o,\tau) + 4\sigma_\chi^{\ 2}$$

$$+ 8\pi^2 k_i^{\ 2} C_n^{\ 2} L \int_0^\infty x^{-8/3}\, dx \int_0^1 du \cos\Big[\frac{x^2 Lu(1-u)}{2k}\Big]$$

$$\times \Big\{1 - J_o(x\left|Pu-v\tau\right|)\, J_o(x\rho\left|1-u\right|)\Big\}\Big] \qquad (7.13)$$

Substituting this in Eq.(7.3) and using Neumann expansions for sine and cosine functions, we get

$$\frac{C_{I_2}(p,\tau)}{\langle I\rangle^2}$$

$$= \sum_{i=1}^{N} \frac{G_i^{\,2}}{(2\pi)^2} \left(\frac{k_i}{L}\right)^2 \int r_2\, dr_2 \int d\theta_{r_2} \int \rho d\rho \int d\theta_\rho\, f_2(r_2,\, \theta_{r_2})$$

$$\times \Big[J_o\Big(\frac{k_i}{L}\,\rho P\Big)\, J_o\Big(\frac{k_i}{L}\,\rho r_2\Big) + 2 \sum_{n=1}^{\infty} (-1)^n\, J_{2n}\Big(\frac{k}{L}\,\rho P\Big)\, J_o\Big(\frac{k}{L}\,\rho r_2\Big)$$

$$\cos 2\, n\theta_\rho + 2J_o\Big(\frac{k_i}{L}\,\rho P\Big) \sum_{n=1}^{\infty} (-1)^n\, J_{2n}\Big(\frac{k_i}{L}\,\rho r_2\Big) \cos 2n(\theta_\rho - \theta_{r_2})$$

$$+ 4 \sum_{n=1}^{\infty} \sum_{m=1}^{\infty} J_{2n}\Big(\frac{k_i}{L}\,\rho P\Big) \cos(2\, n\, \theta_\rho) J_{2m}\Big(\frac{k_i}{L}\,\rho r_2\Big) \cos \overline{2m(\theta_\rho - \theta_{r_2}})$$

$$-4 \sum_{n=o}^{\infty} \sum_{m=o}^{\infty} (-1)^{n+m}\, J_{2n+1}\, \Big(\frac{k_i}{L}\,\rho P\Big) \cos(\overline{2n+1}\;\theta_\rho) J_{2m+1}\, \Big(\frac{k_i}{L}\,\rho r_2\Big)$$

$$\cos\, \overline{2m+1(\theta_\rho - \theta_{r_2}})\Big] \times H_a(\overline{P},\overline{\rho},\tau) \tag{7.14}$$

completing the integral over $d\theta_\rho$, we get

$$\frac{C_{I_2}(P,\tau)}{\langle I\rangle^2} = \sum_{i=1}^{N} \frac{G_i^{\,2}}{2\pi} \left(\frac{k_i}{L}\right)^2 \int r_2\, dr_2 \int d\theta_{r_2} \int \rho d\rho\, f_2(r_2,\theta_{r_2})$$

$$\times \Big[J_o\Big(\frac{k_i}{L}\,\rho P\Big)\, J_o\Big(\frac{k_i}{L}\,\rho r_2\Big) + \sum_{n=1}^{\infty} (-1)^n\, J_n\, \Big(\frac{k_i}{L}\,\rho P\Big)\, J_n\Big(\frac{k_i}{L}\,\rho r_2\Big)$$

$$\cos(n\theta_{r_2})\Big]\, H_a(P,\rho,\tau) \tag{7.15}$$

where

$f_2(r_2,\ \theta_2)$

$$= \exp\left[\frac{-r_2^{\,2}}{2\alpha_o^{\,2}} - \frac{r_2^{\,2}\ k_i^{\,2}\ \alpha_o^{\,2}}{2L^2}\ \left(1 - \frac{L}{F}\right)^2 - D_\psi(o,-r_2,-\tau)\right] \qquad (7.16)$$

The first term in the integral can be evaluated by expanding the function $f_2(r_2,\theta_{r2})$ into a Fourier-Bessel series for several values of θ_{r2} over 0 to 2π and numerically integrating using these values. This yields

$$\frac{1}{2\pi}\int_o^{2\pi}\left[\sum_m b_m(\theta_{r2})\ \left\{J_o\left(\frac{k}{L}\,\rho P\right)\times H_a(P,\rho,\tau)\right\}\right]d\theta_{r2} \qquad (7.17)$$

with $\rho = (p_m L)/(Ak)$.

The second term in the integral has θ_{r2} both in f_2 as well as in the function $\cos(n\theta_{r2})$. If the variation of f_2 is very slow compared with the variation of $\cos n\theta_{r2}$ or if f_2 does not change much over the region of integration 0 to 2π, the second, the third, etc. integral can be neglected as the $\cos(n\theta_{r2})$ term dominates. For higher values of n this is true. For moderate values of n (for example n = 2,3,4, etc.), the integrals may contribute to the total term substantially. In fact it is found that at moderate values of Rytov variance ($\sigma_\chi^{\,2} \approx .15$), the coefficients are strongly dependent on θ_{r2}. Finally the time delayed covariance of the received intensity can be calculated using Eq.(7.1). The above equations are normalized to the square of the mean received intensity. Normalization to the variance can be similarly obtained. In the numerical analysis, the f_2 was expanded in the Fourier-Bessel series for several values of θ_{r_2} and at each θ_{r_2}, the remaining integrals were evaluated.

7.2 The Autocorrelation and Frequency Spectrum of Intensity Fluctuations

The autocorrelation of the received intensity can be obtained by putting P = 0 in the expression for the time delayed covariance of the intensity. The normalized autocorrelation can similarly be obtained. The corresponding frequency spectrum of the fluctuations is given by taking the Fourier transform of the autocorrelation of the received intensity and this is given as

$$S(W) = \int_{-\infty}^{\infty} e^{-iw\tau} \left[C_{I_1}(o,\tau) + C_{I_2}(o,\tau) - 1\right] d\tau \qquad (7.18)$$

7.3 Theoretical Results and Comparison with the Experimental Data

Using Eqs.(7.6) and (7.15), numerical results are obtained and compared with the experimental data in Figures 7.1, 7.2, and 7.3 for several values of the turbulence level (C_n^2) for a path length of 500 meters and different conditions of the beam geometry (focused or collimated) and for different values of VSCR. The results are compared with the available data for the monochromatic case.[54] Comparison of the theory with experimental data for a

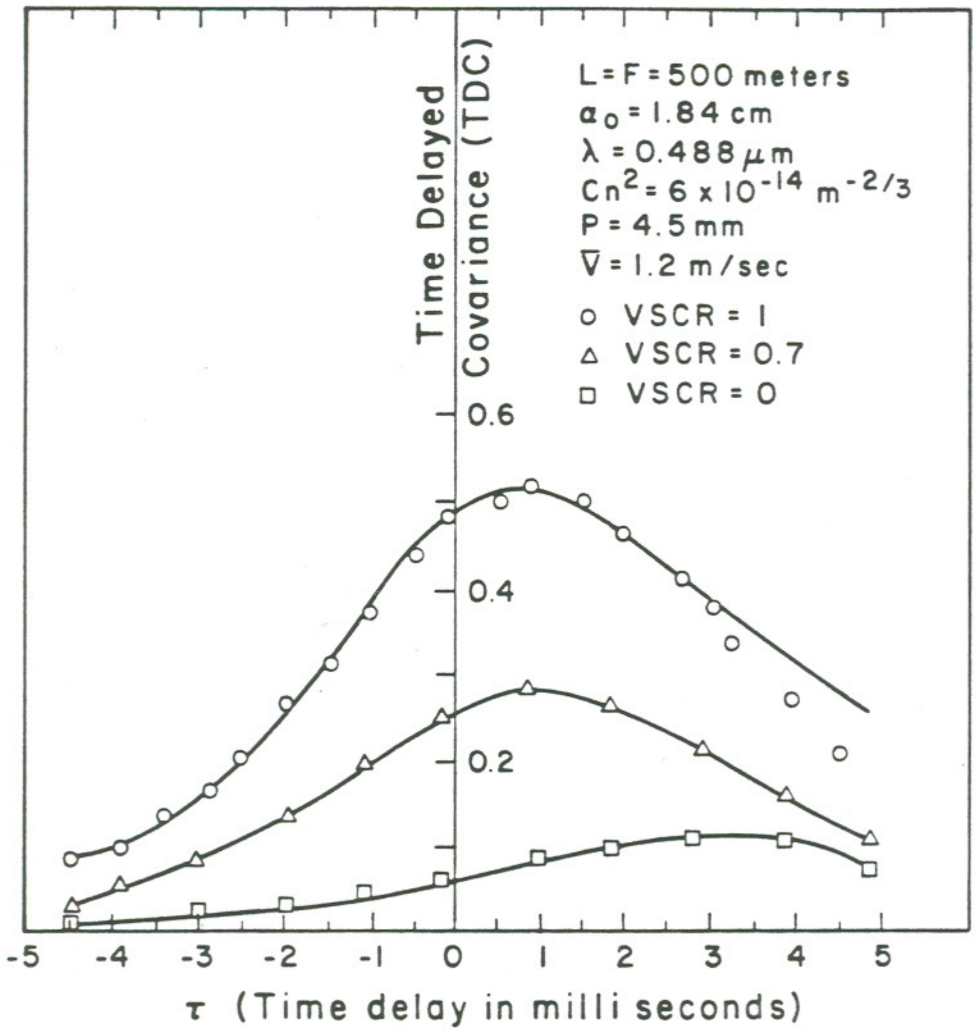

Figure 7.1. Time delayed covariance of the received intensity versus the time delay at a detector spacing of 4.5 mm for an argon laser at several values of vacuum speckle contrast ratio. The smooth curve for VSCR = 1 refers to the experimental data.

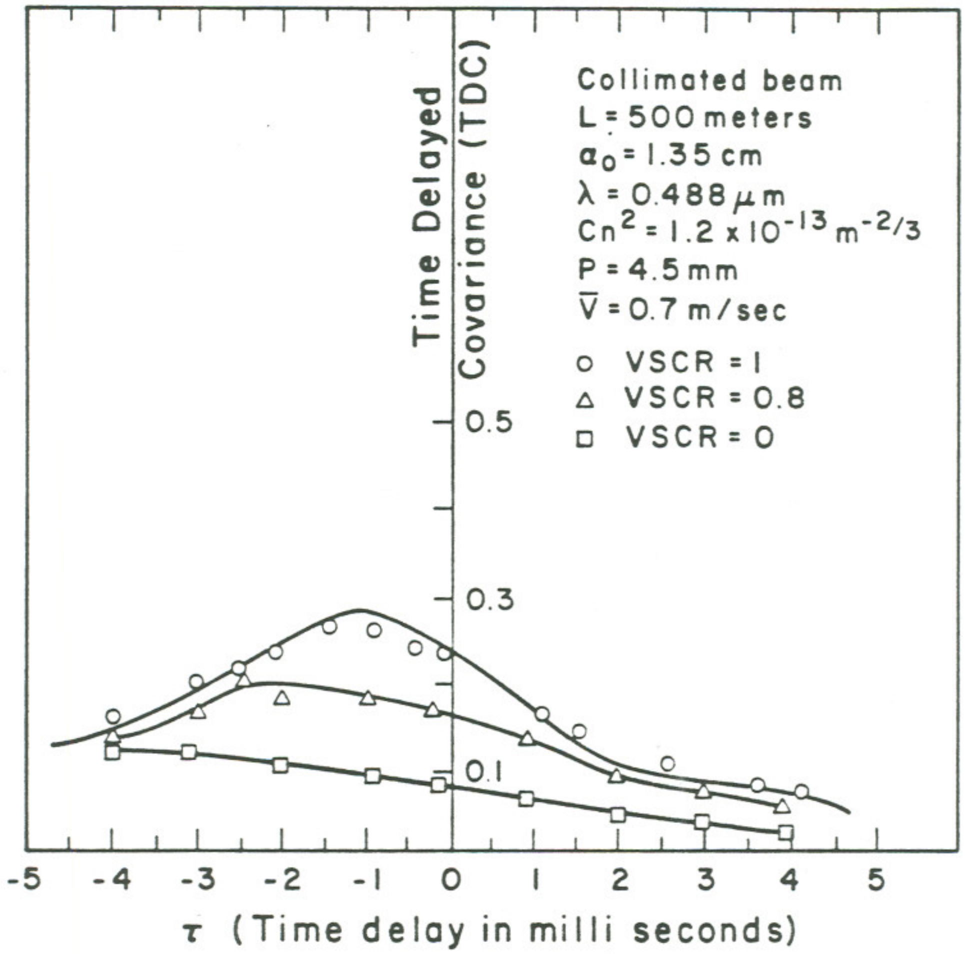

Figure 7.2. The time delayed covariance of the received intensity versus time delay for an argon laser at three values of VSCR at a detector spacing of 4.5 mm (collimated beam). The smooth curve for VSCR = 1 refers to the experimental data.

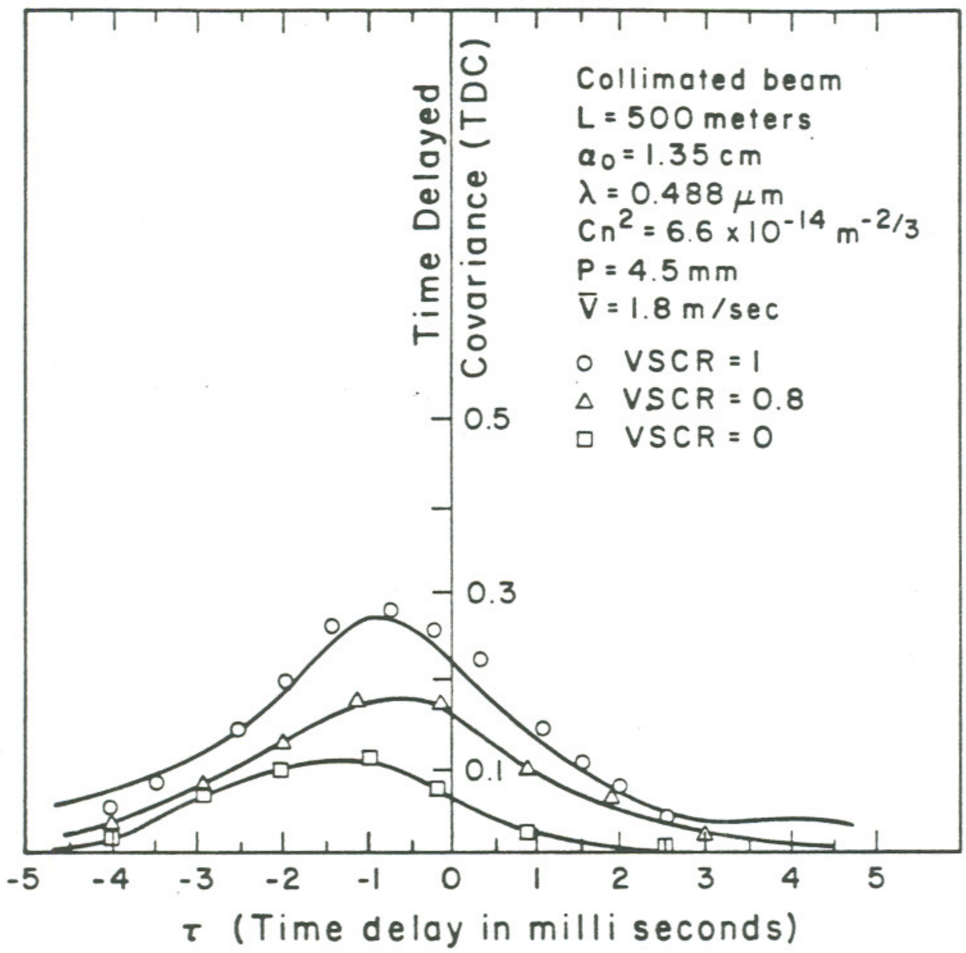

Figure 7.3. The time delayed covariance of the received intensity versus time delay for an argon laser at three values of VSCR at a detector spacing of 4.5 mm (collimated beam). The smooth curve for VSCR = 1 refers to the experimental data.

focused path of 500 meters shows that the approximate evaluation is reasonably good for small time delays. Figures 7.2 and 7.3 compare the theory with the experimental data for a collimated beam. As expected earlier time delayed covariance is substantially less than that of a focused beam. When the effective time delay $V\tau$ is positive, there is substantial difference between the theory and the experiment for large time delays. When effective delay $V\tau$ is negative good agreement is obtained between the theory and experiment consistently over all sets of the data. Consequently it is concluded that the approximate numerical evaluation is not accurate at large time delays. This lack of agreement may also be due to the fact that the time delay is comparable with the detector integration time. The shapes of both theoretical and experimental curves are consistent with the phenomenological theory and peaks are on the opposite sides of zero time delay for the opposite directions of the wind. It was observed experimentally that the sensitivity of the time delayed covariance of intensity to the wind fluctuations along the path is very substantial. Figure 7.4 compares the theoretical autocorrelation function of the intensity with the corresponding experimental data. The agreement is not good at all. No attempts have been made to get the frequency spectrum of the fluctuations due to the same reason and the additional complexity of one more integration from zero to infinity.

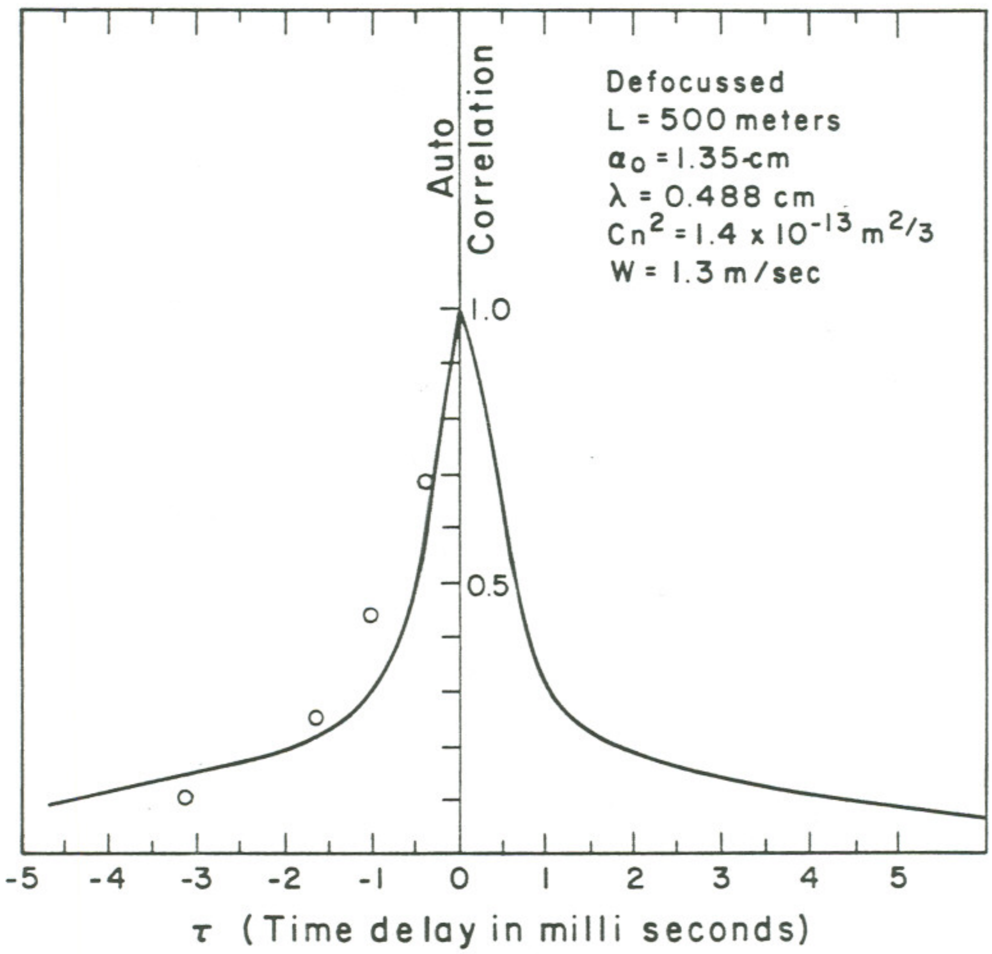

Figure 7.4. The autocorrelation of the received intensity versus time delay for an argon laser. The smooth curve refers to experimental data. Circles indicate theoretical points.

7.4 Discussion

As in the case of the covariance, the time delayed covariance of intensity can be resolved into an incoherent part and a coherent part. The coherent part will be weighted by the square of the VSCR. For very low values of VSCR, the coherent term is no longer a dominant term and the variation of the time delayed covariance of intensity depends on the incoherent term. Thus the ability to sense the cross wind will be very poor even for small detector spacings. For moderate values of VSCR, the shapes of VSCR, the shapes of the TDC versus time delay curves resembles that of the monochromatic case and for very large time delays the time delayed covariance of intensity asymptotically approaches the incoherent term. Phenomenologically, the received intensity pattern is dependent on the target and is controlled by the turbulence level as well as the wind speed. However the statistical features of this pattern such as TDC are strongly dependent on the turbulence level and the angle between the transmitter coordinate V and the wind direction and the correlation is maximum if both of them are in the same direction and least if they are in the opposite direction. The speckle size at the receiver is the same as the covariance scale size (being dominated by the beam size at the low turbulence level and by the lateral coherence length at very high turbulence levels). Initially, for very small $|V\tau|$, both the space time points are in the same speckle and thus correlation is maximum, or order of the covariance. However when $|V\tau|$ becomes very large, both the same points are not in the same speckle and thus the correlation is decided by the correlation between the amplitude fluctuations (incoherent fluctuations). That is why, in all sets of data, the time delayed covariance of intensity curve approaches the incoherent term asymptotically even for the case when the VSCR is unity. The time delayed covariance of intensity becomes zero when the effective space-time distance between the two points under consideration exceeds the correlation distance of the amplitude fluctuations. It is further noted that for very low values of VSCR, the incoherent term dominates and the wind effects are not substantial.

CHAPTER VIII

PROBABILITY DENSITY FUNCTION OF THE INTENSITY FOR A LASER SPECKLE PATTERN IN THE TURBULENT ATMOSPHERE

In this chapter, the theory of wave propagation through the turbulent atmosphere and speckle theory will be used to derive the probability density function for the intensity of a polychromatic speckle pattern after propagation through the turbulent atmosphere. Since the previously proposed probability density function of the intensity of a monochromatic speckle pattern is correct only if the phase but not the amplitude effects are considered and since the amplitude effects are very strong, in this chapter, the probability density function is developed first for the monochromatic case and the results are then generalized to include the polychromatic case. The analysis that follows assumes that both the log-amplitude and phase fluctuations are Gaussian distributed and that the intensity fluctuations of a spherical wave, after propagation through the turbulent atmoshere, can be described by a log-normal or Rice-Nakagami distribution. This will be used to derive the probability density function of the intensity of the speckle field after propagation through the turbulent atmosphere. The results so derived will then be extended to the case of the polychromatic or partially coherent speckle patterns and finally the analytical results will be compared with experimental data, available for both monochromatic and polychromatic speckle patterns.

8.1 Analysis

Goodman[29] has shown that the probability density function of the intensity for a fully developed (i.e. Gaussian) speckle pattern is given by

$$P(I) = \frac{1}{\lambda} e^{-I/\lambda} \tag{8.1}$$

where λ is the average intensity and λ^2 is the variance of the intensity. If however such a speckle pattern is propagating through the turbulent atmosphere, then it is known[75] that the nature of the probability density function is changed from its vacuum value by the turbulent atmosphere. When there is no turbulence, the speckle pattern is stationary and does not evolve. However, when turbulence is present, it has been observed that the brightness of each speckle seems to be modulated by the turbulence. At low turbulence levels, the transverse coherence length in the receiver plane due to turbulence is much larger than the vacuum speckle size. This gives rise to large turbulence induced speckles that encompass groups of smaller target induced speckles. If the same target induced speckle field is observed for an ensemble of atmospheres, the target speckle field will remain the same since the target and the atmosphere are independent; but the atmospheric speckle will change from sample to sample in the ensemble and will modulate in a random manner the brightness of the target induced speckles. Consequently, the model proposed is that the conditional statistics (given the mean value) of the target induced speckles have the same statistics as the vacuum speckle field but now the mean value is a parameter, whose statistics are determined by the turbulence. The joint density function for the intensity and the mean value, which is now a parameter, can be formed from the conditional density function for the target speckle intensity by multiplying it by the marginal density function of the mean. This result can then be integrated over the mean value to find the marginal density function for the received intensity and can be expressed as

$$P_I(I) = \int_0^\infty P_I(I/\lambda = x)\ P_\lambda(x)dx \tag{8.2}$$

where $P_I(I/\lambda = x)$ is the vacuum speckle density function for the intensity and $P_\lambda(x)$ is the density function for the turbulence induced fluctuations of the parameter λ. Problems of this type where one or more of the parameters of the distribution take on different values for different samples in the ensemble are called problems of compound distribution.[81]

For a coherent spherical wave propagating through the atmosphere, it is well known that the probability density function (PDF) of the received intensity can be approximated at turbulence levels below saturation by Rice-Nakagami or log-normal distribution.[77,78,79] However, saturation of scintillations never comes strongly into play in the problem of speckle propagation through turbulence because the received intensity becomes dominated by the turbulence induced phase fluctuations, which are log-normal and never saturate at a Rytov variance below that at which saturation of the log-amplitude fluctuations occurs. A more detailed explanation of this effect is contained in Chapter V. Consequently it is proposed that the distribution of the intensity of a spherical wave in the turbulent atmosphere be used for the distribution of the mean intensity parameter in Eq.(8.1) and it should be valid for all turbulence levels. This leads to a K-distribution for the PDF of the intensity for a monochromatic speckle pattern after propagation through the turbulent atmosphere with the parameters of the distribution dependent on the propagation variables. The above described model is based on the phenomenological observations of the effects of the turbulence on the speckle and therefore may not be rigorously correct. However it leads to very useful results that agree with experimental data for both monochromatic and polychromatic cases in a regime where maximum deviation from the model is expected.

The PDF for a Rice-Nakagami distribution is given by

$$P_x(x) = \frac{1}{\beta} e^{-\frac{\alpha + x}{\beta}} I_o\left(2\frac{\sqrt{x\alpha}}{\beta}\right) \tag{8.3}$$

where

$$\langle x \rangle = \alpha + \beta$$

and

$$\sigma_x^{\ 2} = \beta^2 + 2\alpha\beta$$

Nakagami[27] has shown that the Rice-Nakagami distribution can be approximated by an equivalent M-distribution given by

$$P_x(x) = \frac{M^M x^{M-1} e^{-\frac{Mx}{\langle x \rangle}}}{\Gamma(M) \langle x \rangle^M} \tag{8.4}$$

If the parameters of the distribution are related as

$$\langle x \rangle = \alpha + \beta$$

$$M = \frac{(\alpha + \beta)^2}{\beta^2 + 2\alpha\beta}$$

The higher order moments of the M-distribution are given by

$$\langle x^n \rangle = \frac{\langle x \rangle^n \Gamma(n + M)}{M^n \Gamma(M)} \tag{8.5}$$

It is desirable to use the M-distribution as an approximation to the Rice-Nakagami distribution because its use results in a form of solution that can be readily reduced to numbers and also it is much easier to relate the parameters of the distribution to the propagation variables. In order to assess how well the M-distribution approximates the PDF of the intensity in Eq.(8.2), the mean square error given by

$$E^2 = \int_o^\infty \left[P_I(I/_{\lambda = x})\, P_{RN}(x) - P_I(I/_{\lambda = x})\, P_M(x)\right]^2 dx$$

where $P_{RN}(x)$ is the PDF for a spherical wave propagating through the turbulence and $P_M(x)$ is the M-distribution should be evaluated. This has been done using a Rice-Nakagami distribution for $P_{RN}(x)$ and Eq.(1) for $P_I(I/_{\lambda = x})$. It was found that the RMS error decreases as M increases and that for M greater than 5, the error is less than 3%.

For the M-distribution of Eq.(4), the corresponding PDF for $y = \ell n(\frac{x}{\langle x\rangle})$ can be written as

$$P_y(y) = \frac{M^M\, e^{My - Me^y}}{\Gamma(M)}$$

Then for y small and M becoming very large, the above equation approaches

$$P_y(y) = \frac{1}{\sqrt{\frac{2\pi}{M}}}\quad e^{-My^2}$$

which shows that $y = \ln(\frac{I}{\langle I \rangle})$ is normally distributed with normalized variance equal to 1/M. Thus the log-normal distribution can also be approximated by an M-distribution.

Utilizing Eq.(8.2) with Eq.(8.1) for $P_I(I/_{\lambda = x})$ and Eq.(8.4) for $P_x(x)$, the PDF for a fully developed speckle pattern after propagation through the turbulent atmosphere is given by

$$P_I(I) = \frac{M^M}{\langle x \rangle^M \, \Gamma(M)} \int_o^\infty x^{M-2} \, e^{-\frac{I}{x} - \frac{Mx}{\langle x \rangle}} dx \tag{8.6}$$

Completing the integral in Eq.(8.6),[30] it becomes,

$$P_I(I) = 2\left(\frac{M}{\langle x \rangle}\right)^{\frac{M+1}{2}} \frac{I^{\frac{M-1}{2}}}{\Gamma(M)} K_{M-1}\left(2\sqrt{\frac{M}{\langle x \rangle} I}\right) \tag{8.7}$$

where K_{M-1} is a modified Bessel function of order M-1. Eq.(8.7) is the K-distribution proposed by Jakeman and Pusey[82] elsewhere to model the non-Gaussian fluctuations in optical scattering on the basis of analogy with random walk. Parry and Pusey[83] used the same distributon to describe the fluctuations of laser beam in moderately strong turbulence regimes. The moments of the K-distribution are given by

$$\langle I^n \rangle = \frac{\Gamma(n + M)}{\Gamma(M)} \Gamma(1 + n) \left(\frac{\langle x \rangle}{M}\right)^n \tag{8.8}$$

Using Eq.(8.8)

$\langle I \rangle = \langle x \rangle = \lambda$

and the normalized variance is given by

$$\sigma_{IN}^{\;2} = \frac{\sigma_I^{\;2}}{\langle I \rangle^2} = 1 + \frac{2}{M} \tag{8.9}$$

It should be noted that $\sigma_I^{\;2}$ in Eq.(8.9) is due to the combined effects of the speckle and the turbulence and can be obtained in terms of the strength of turbulence, path length, wavelength and beam size from Chapter V.

The cumulative PDF of the intensity will also be needed for comparison with the experimental data. It is given by

$$F_I(I) = \int_o^I P_I(I)\, dI$$

$$= 1 - \left(\frac{M}{\langle I \rangle} I\right)^{\frac{M}{2}} \frac{2}{\Gamma(M)} K_M\left(2\sqrt{M\frac{I}{\langle I \rangle}}\right) \tag{8.10}$$

From previous work,[19] it is known that for the case under consideration the normalized variance of the intensity starts at unity with no turbulence and as the turbulence increases, it rises above unity and reaches a peak value near 1.25 around a Rytov variance of .1 to .15. As the level of turbulence increases further, the normalized variance decreases and asymptotically approaches unity again at very high turbulence levels. From

Eq.(8.9), it can be seen that the corresponding value of M starts off at infinity and decreases to about 8 and then increases to infinity again as the turbulence increases. Clifford and Hill[84] have shown that as M approaches infinity, the K-distribution asymptotically reduces to an exponential distribution. Consequently the result, given by Eq.(8.7) for the PDF, asymptotically approaches the correct distributions, known at very high and very low turbulence levels.

8.2 Extension to Polychromatic and Partially Developed Speckle Patterns

The intensity of a polychromatic speckle in vacuum follows an M-distribution.[40] This is determined by resolving the total speckle pattern into a set of (fully developed) Gaussian speckle patterns, each having an exponential PDF for its intensity. If all the N patterns are of equal average intensity, then the PDF of the intensity for the total polychromatic speckle pattern is given by an M-distribution with $M = M_1 = N$. If all the component speckle patterns are of equal average intensity, then the PDF of the total intensity is given by[29]

$$P(I) = \sum_{i=1}^{N} \frac{\alpha_i^{N-2}}{\prod_{\substack{j=1 \\ j=i}}^{N} (\alpha_i - \alpha_j)} \frac{e^{-I/\alpha_i \lambda}}{\lambda} \tag{8.11}$$

where the mean intensity is given by

$$\lambda = \sum_{i=1}^{N} \lambda_i$$

and where the average intensity of each component speckle pattern is given by $\lambda_i = \alpha_i \lambda$ and where the average intensity of each component speckle pattern is given bM-distribution. Using an M-distribution with $M = M_2$ for the turbulence effects and combining this with Eq.(8.4), the overall PDF of the intensity for the polychromatic speckle patterns is given by

$$P_I(I) = \frac{M_2^{M_1} M_2^{M_2} I^{M_1-1}}{\langle x \rangle^{M_2} \Gamma(M_2)\Gamma(M_1)} \int_0^\infty x^{M_2-M_1-1} e^{-\frac{M_1 I}{x} - \frac{M_2 x}{\langle x \rangle}} dx$$

$$P_I(I)$$

$$= \frac{(M_1 M_2)^{\frac{M_1 + M_2}{2}}}{\Gamma(M_1)\Gamma(M_1)} \frac{2}{\langle x \rangle^{\frac{M_1 + M_2}{2}}} I^{\frac{M_1 + M_2}{2} - 1}$$

$$* K_{M_2 - M_1} \left(2\sqrt{\frac{M_1 M_2 I}{\langle x \rangle}}\right) \tag{8.12}$$

The moments of the intensity of the above distribution will also be needed later for comparison with experimental measurements. They are given by

$$\langle I^n \rangle = \frac{\langle x \rangle^n \Gamma(n + M_2)\ \Gamma(n + M_1)}{M_1{}^n\ M_2{}^n\ \Gamma(M_2)\ \Gamma(M_1)} \tag{8.13}$$

from which $\langle I \rangle = \langle x \rangle = \lambda$

$$\langle I^2 \rangle = \langle I \rangle^2 \left(1 + \frac{1}{M_2}\right) \left(1 + \frac{1}{M_1}\right)$$

$$\langle I^3 \rangle = \langle I \rangle^3 \left(1 + \frac{2}{M_2}\right) \left(1 + \frac{1}{M_1}\right) \left(1 + \frac{2}{M_2}\right) \left(1 + \frac{1}{M_1}\right)$$

$$\langle I^4 \rangle = \langle I \rangle^4 \left(1 + \frac{3}{M_2}\right) \left(1 + \frac{2}{M_2}\right) \left(1 + \frac{1}{M_1}\right)$$

$$* \left(1 + \frac{3}{M_1}\right) \left(1 + \frac{2}{M_1}\right) \left(1 + \frac{1}{M_1}\right)$$

and the normalized variance of the received intensity is given by

$$\sigma_{IN}{}^2 = \left(1 + \frac{1}{M_2}\right) \left(1 + \frac{1}{M_1}\right) - 1 \tag{8.14}$$

If the PDF for the polychromatic speckle intensity is a sum of exponentials as in Eq.(8.11), then Eq.(8.12) will be modified to

$$P_I(I) = 2 \frac{M_2^{\frac{M_2+1}{2}} I^{\frac{M_2-1}{2}}}{\Gamma(M_2)\ \langle x\rangle^{\frac{M_2}{2}+\frac{5}{2}-N}}$$

$$\times \sum_{i=1}^{N} \frac{\alpha_i^{N-\frac{M_2}{2}-\frac{3}{2}}}{\prod_{\substack{j=1\\ j\neq i}}^{N} (\alpha_i - \alpha_j)}\ K_{1-M_2}\left(2\sqrt{\frac{M}{\alpha_i\langle x\rangle} I}\right) \tag{8.15}$$

where the corresponding moments of the intensity are given by

$$\langle I^n\rangle = \frac{\Gamma(n + M_2)}{\Gamma(M_2)\ {M_2}^n} \langle I^n\rangle_{vacuum} \tag{8.16}$$

and where

$$\langle I^n\rangle_{vacuum} = \Gamma(n + 1) \sum_{i=1}^{N} \frac{\lambda_i^{N-1+n}}{\prod_{\substack{j=1\\ j\neq i}}^{N} (\lambda_i - \lambda_j)} \tag{8.17}$$

Goodman[42] has shown that a partially developed speckle pattern can be resolved into a sum of Gaussian speckle patterns and therefore the PDF of the intensity follows either an M-distribution or a sum of exponential distributions as in the case of the polychromatic speckle patterns. Consequently the above work also applies to the case of the propagation of partially developed speckle patterns throughout the turbulent atmosphere. As was the case for a monochromatic speckle, when the strength of turbulence approaches zero or infinity, the PDF approaches the vacuum result for the target induced speckle.

8.3 Relation Between The Distribution Parameters and the Propagation Variables

The required parameters for the distribution are the average intensity and M or M_1 and M_2. The average intensity is independent of the turbulence level, and so can be calculated using the speckle theory. The parameters M and M_2 however are determined by the atmospheric fluctuations and thus are dependent on the strength of the turbulence, path length, beam size, focal length and the wave length. In accordance with the theory developed herein, M and M_2 can be derived using Eq.(8.9) and Eq.(8.14) or Eq.(8.16) respectively. Consequently, if the relationship between the normalized variance of the received intensity and the propagation variables is known, M or M_2 can be determined and the PDF defined.

A very useful path geometry was considered in previous chapters, in which the laser receiver and the transmitter are located at one end of the path and a target is located at the other end of the path. For this problem in Chapter V, expressions for the variance have been developed. By using the expressions for the variance from Chapter V and the expression for the variance from (8.14), the M_1 and M_2 can be related to the propagation variables.

8.4 Experimental Data and Comparison with Theory

The theory proposed here is compared with the experimental data collected by Fossey and Holmes.[55] The previously proposed PDF[18] did not agree with the experimental data as it did not take into account the amplitude effects. As will be shown here, K-distributions are very good approximations for the intensity fluctuations of both monochromatic and polychromatic speckle patterns.

Experiments were conducted at a height of 2 meters above flat agricultural land. The transmitter consists of an argon ion laser, operating at .488 μm Coherent Radiation Lab Model 52) with an intracavity etalon to yield an output in single longitudinal mode for the monochromatic experiments. The etalon was removed for the polychromatic experiments to allow the laser run in several longitudinal modes. In order to separate the received signal from the background illumination, the outgoing beam was moduated at 100 kHz. Scotchlite (3M sprint marking paper) was used as the target material because it provides a directional return with a gain of 1000 to 1 over a perfect Lambertian surface but still imparts random phase to an incident monochromatic laser beam to form a speckle contrast of unity in the absence of turbulence. Measurements were made with a focused beam at two turbulence levels and with path lengths of 300, 500 and 900 meters. The polychromatic source was used in the 500 meter path measurements and the monochromatic source for other path lengths.

In each case the received normalized variance of the intensity was close to the peak of the curve of the variance of intensity versus the Rytov variance, at which point the maximum deviation of the PDF from the vacuum speckle result should occur and provide the best test of the theory. In order to compare the experimental data with theory in each case, the mean and the variance of the received intensity were used to calculate the proper parameter values of the distribution (since the line strength of the distribution of the laser source is not known, it is assumed that all the lines are of equal strength). Then using the formulations, derived for the PDF and the moments, the third and the fourth moments of the intensity and the cumulative PDF were calculated and compared with experimental data. The results are summarized in tables 8.1 and 8.2 and Figures 8.1 through 8.4. Except for one set of the data at 300 meter path length, which has shown significant deviation for the fourth moment of the intensity, the results are very good. All the cumulative density plots show good agreement between the theory and the experiment.

8.5 Discussion

In this chapter, a very important result, which will be useful in several applications of speckle propagation through turbulence

TABLE 8.1. COMPARISON OF CALCULATED AND MEASURED MOMENTS OF THE INTENSITY FOR A MONOCHROMATIC SPECKLE PATTERN IN THE TURBULENT ATMOSPHERE

Experimental Conditions	Normalized Variance	n	$\langle I^n \rangle_{Theory}$	$\langle I^n \rangle_{Experiment}$	$\dfrac{\langle I^n \rangle_{Theory}}{\langle I^n \rangle_{Experiment}}$
L = 9.10 meters, F = 910 meters, α_o = 1.35 cms, λ = .488 μms	1.2504	3	4.773×10^3	4.564×10^3	.9566
		4	2.171×10^5	2.168×10^5	.9983
	1.17	3	4.086×10^3	3.910×10^3	.9569
		4	1.675×10^5	1.692×10^5	1.010
L = 300 meters, F = 300 meters, α_o = 2.52 cms, λ = .488 μms	1.37	3	2.291×10^4	2.085×10^4	.9101
		4	1.896×10^6	1.741×10^6	.9183
	1.2049	3	4.761×10^4	4.339×10^4	.9114
		4	4.517×10^6	3.521×10^6	.78

TABLE 8.2 COMPARISON OF CALCULATED AND MEASURED MOMENTS OF THE INTENSITY FOR A POLYCHROMATIC SPECKLE PATTERN IN THE TURBULENT ATMOSPHERE

Experimental Conditions		Experimental Values		Higher Moments of the Intensity	
L = 500 meters F = 500 meters α_o = 1.35 cms λ^o = .488 μms		Normalized Variance	M	$\frac{\langle I^3\rangle_{Experiment}}{\langle I^3\rangle_{Theory}}$	$\frac{\langle I^4\rangle_{Experiment}}{\langle I^4\rangle_{Theory}}$
Data in Vacuum		.328667	M_1 = 3.043	.9949	.9814
Data in the Turbulent Atmosphere	Set 1	.638057	M_2 = 4.295	1.081	1.282
	Set 2	.487012	M_2 = 8.390	1.036	1.162
	Set 3	.453380	M_2 = 10.650	1.026	1.093

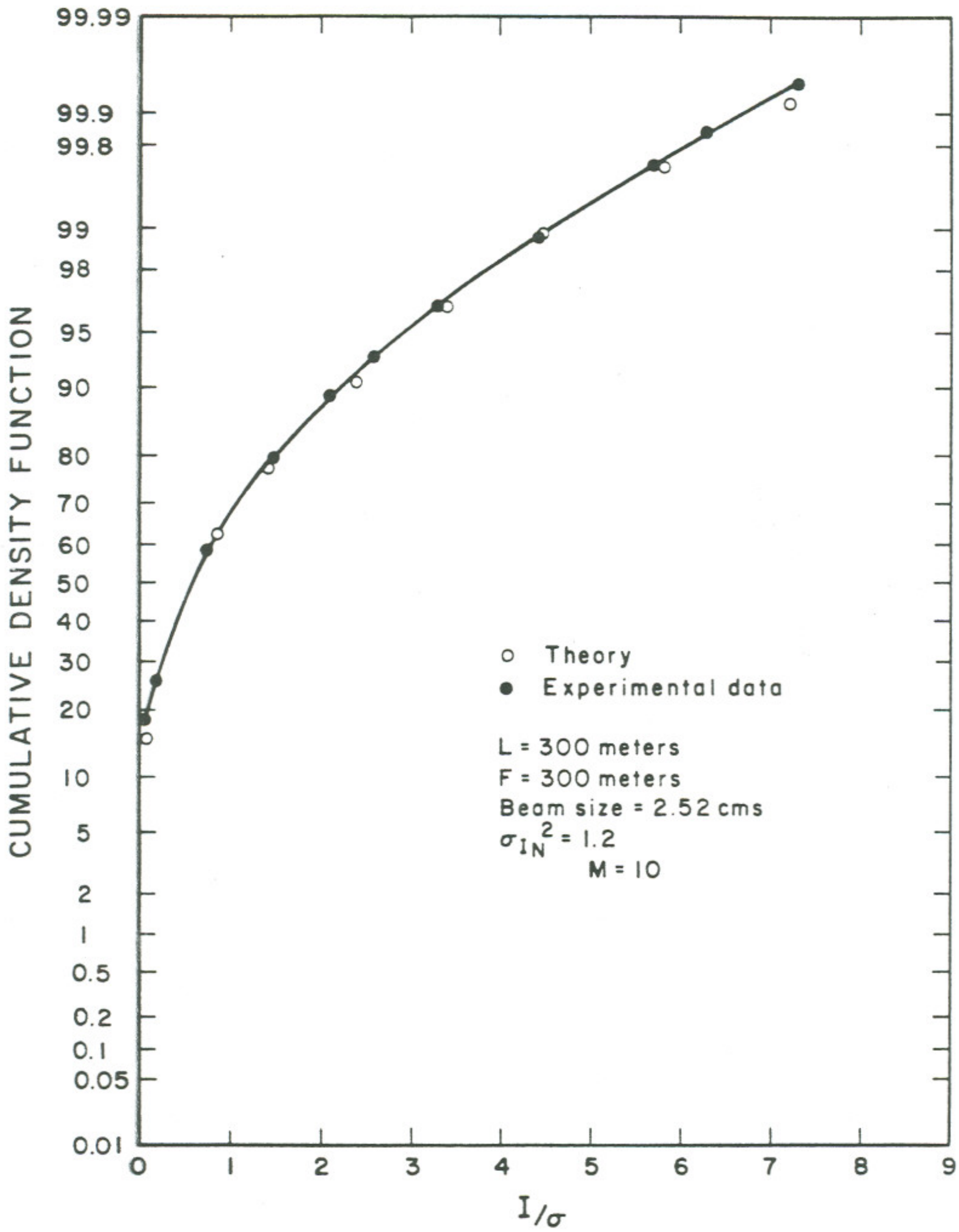

Figure 8.1. Comparison of theoretical and experimental probability functions for a monochromatic speckle pattern.

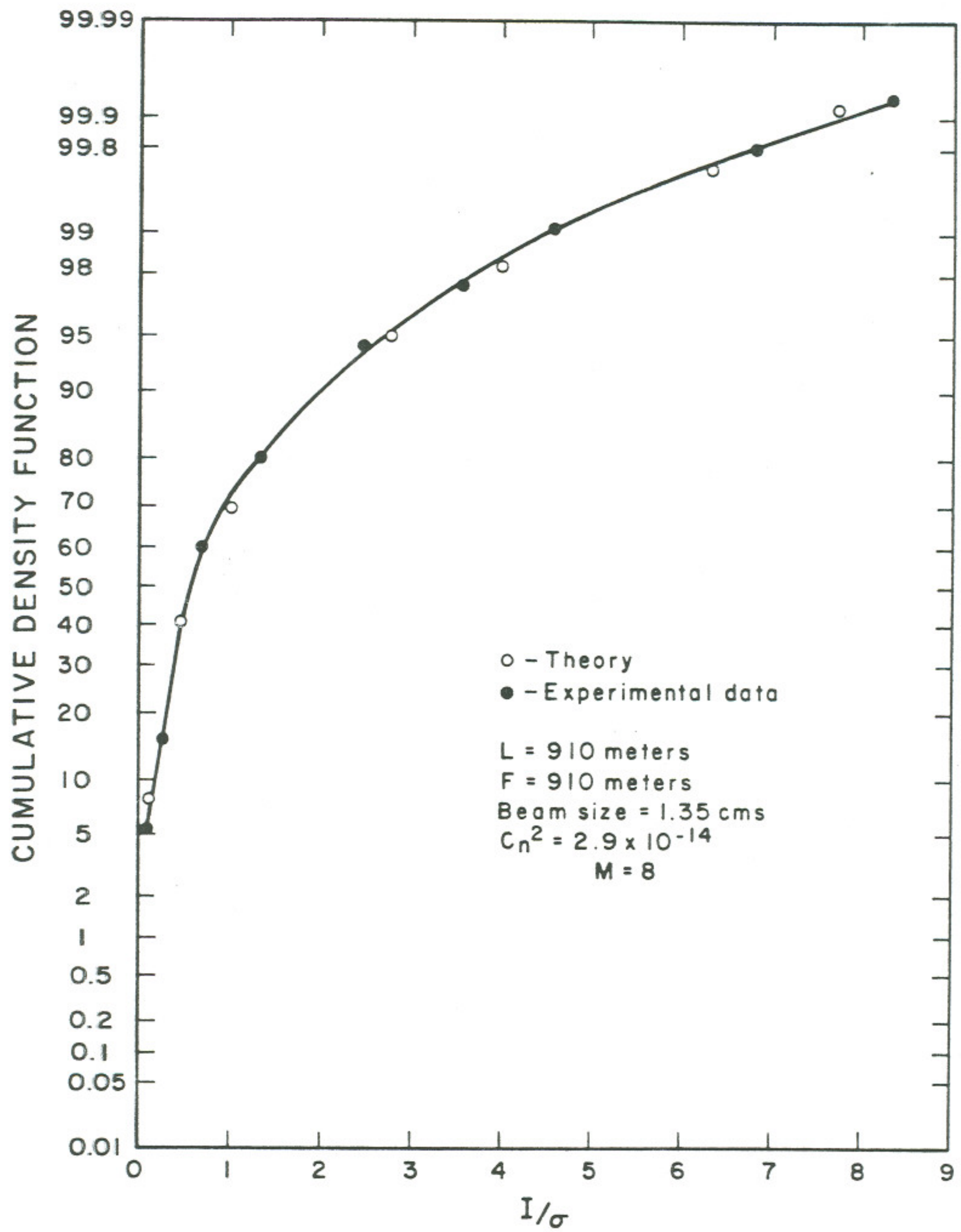

Figure 8.2. Comparison of theoretical and experimental cumulative density functions for a monochromatic speckle pattern.

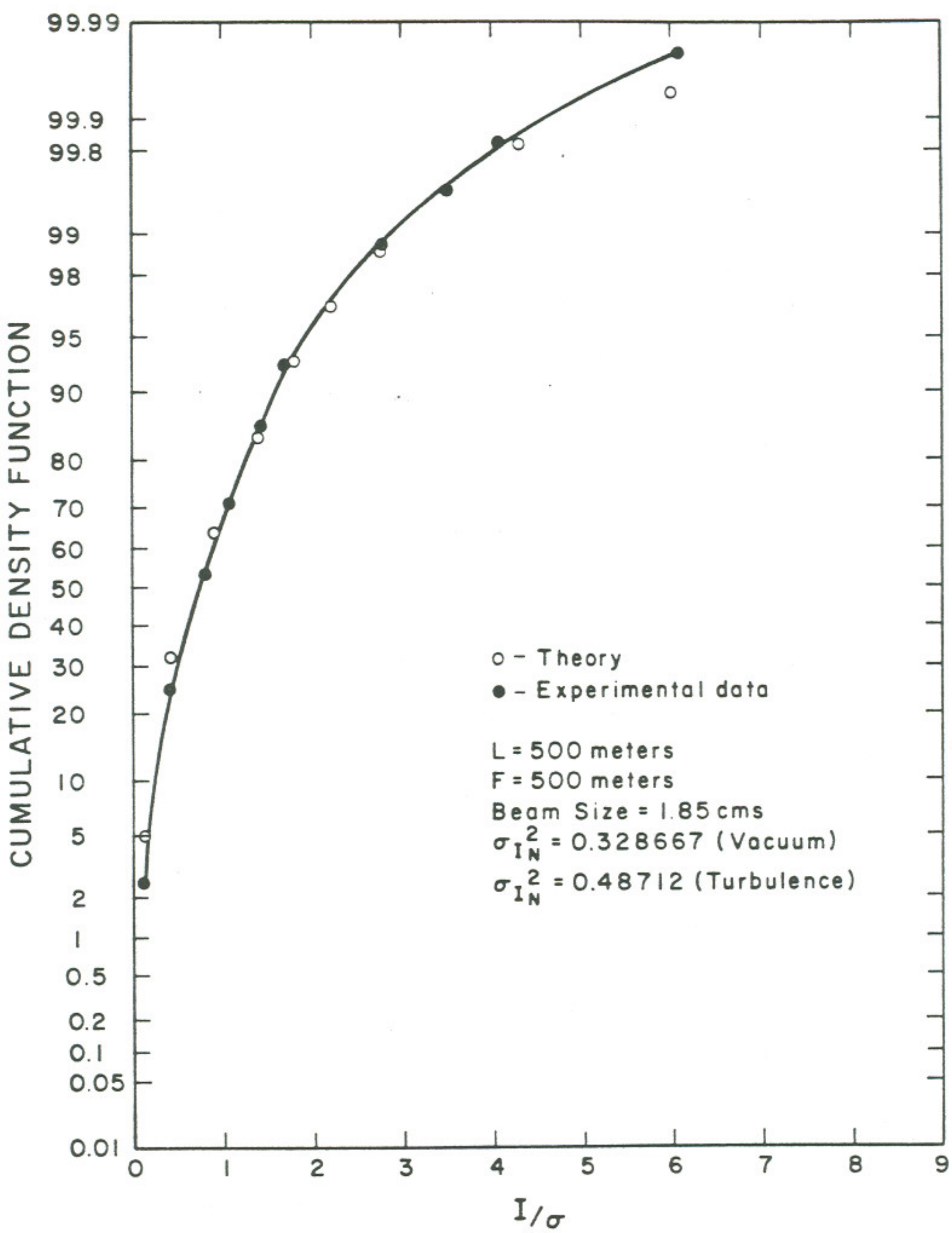

Figure 8.3. Comparison of theoretical and experimental cumulative density functions for a polychromatic speckle pattern.

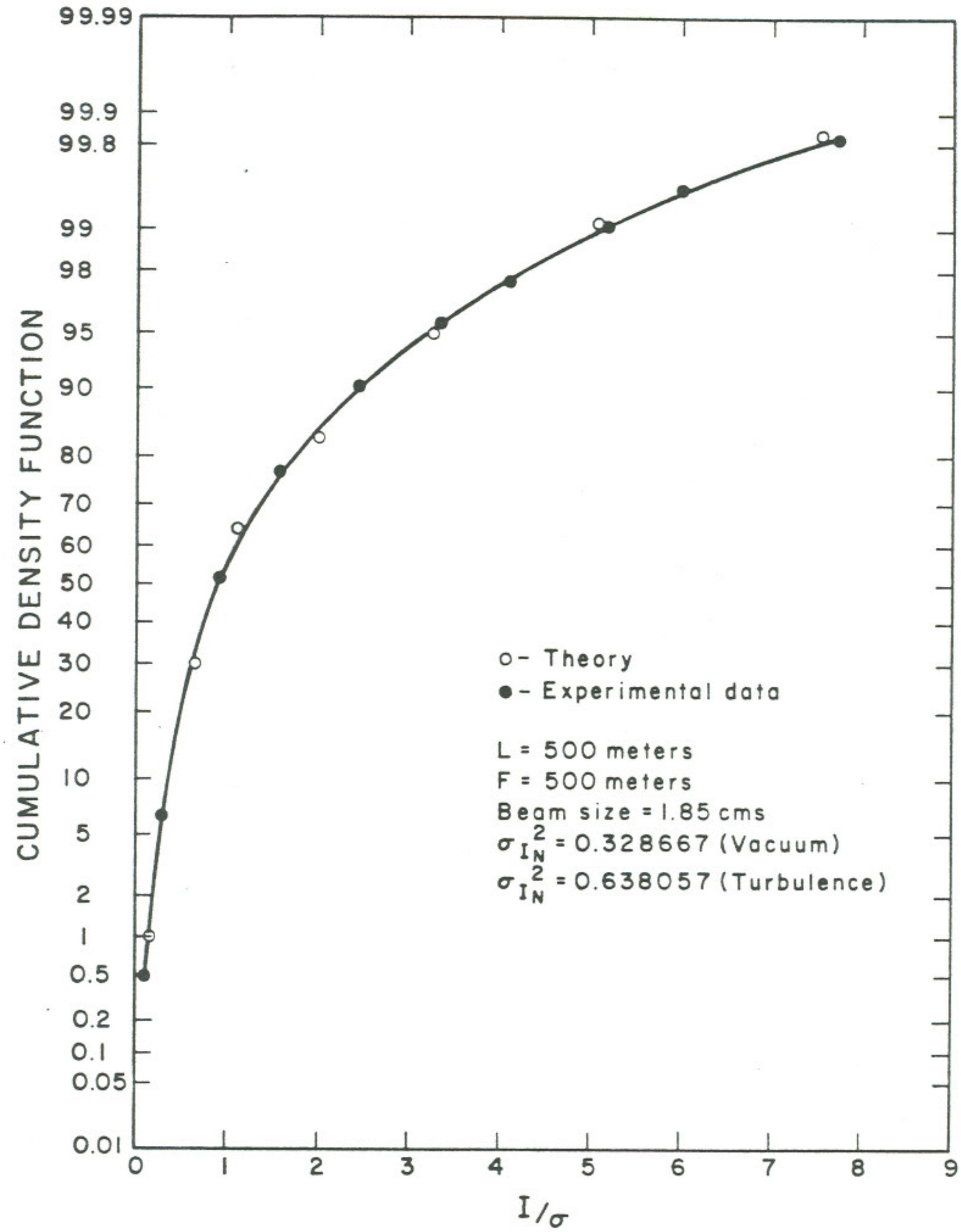

Figure 8.4. Comparison of theoretical and experimental cumulative density functions of a polychromatic speckle pattern.

has been developed. An alternate approach is to assume that the phase and the amplitude fluctuations are independent and due to phase randomization, the intensity follows an exponential distribution and due to log-amplitude fluctuations, the intensity follows an M-distribution. Then since phase and amplitude effects are multiplicative, the overall intensity can be treated as a product of two random variables, suitably normalized. This also then leads to a K-distribution as this formulation is equivalent to what was developed earlier in this chapter.

CHAPTER IX

CONCLUSIONS AND FUTURE WORK

In this chapter, the results obtained in the previous chapters and their limitations and directions for future work will be summarized. Using the Huygens Fresnel approximation the manner in which the turbulent atmosphere effects a polychromatic speckle field, generated by a diffuse target was studied in detail. The effects of the atmospheric perturbation on the various statistical parameters of a polychromatic speckle parameters such as the variance, covariance, time delayed covariance, autocorrelation and the probability density function of the received intensity, was studied in detail.

The results, substantiated by the experimental data suggest that the variance can be significantly increased by the atmospheric perturbation. The dependence of the atmospheric perturbation on the beam size, focusing geometry and wavelengths, was also studied.

It was found that the covariance, normalized to the variance, remains pratically unchanged for a substantial increase in the turbulence level for small separations. Also for low values of the turbulence level, it is found that reducing the vacuum speckle contrast ratio in fact reduces the normalized covariance while for higher levels of turbulence, it increases the normalized covariance. In fact there is a turbulence level at which the vacuum speckle contrast ratio does not effect the normalized covariance. Also the relative roles of the various scale sizes were studied.

By resolving the total contribution to the time delayed covariance, into a coherent and an incoherent contribution, an approximate method for calculating the time delayed covariance to compare with the experimental data was developed. It is found that at low values of VSCR, the time delayed covariance is not affected substantially by the wind velocity. Also it is noticed for very large time delays, the incoherent fluctuations determine the time delayed covariance.

Finally it was shown that the atmospheric perturbation changes the exponential statistics in vacuum to a K-distribution, whose order is dependent on the normalized variance, in case of the monochromatic speckle pattern. For the polychromatic case, the PDF of the intensity in the turbulent atmosphere, follows a K-distribution of higher order or a weighted sum of K-distributions, as shown in the last chapter. The theory is accurate in that it reduces asymptotically to the monochromatic case, worked out by Holmes et al.[19] for a vacuum speckle contrast ratio of unity and to the results of Clifford et al.[85] for the incoherent case when the vacuum speckle contrast ratio tends to be zero.

Additional results can be obtained by assuming other possible three-dimensional spectra for other applications. Results in this thesis are approximately valid for the propagation of partially coherent speckle pattern. Since in most applications pulsed sources are used and their coherence properties are very poor, the effect of the turbulent atmosphere can be best described by using the methods in this thesis. In addition related speckle problems, such as the number of the dominant eigenvalues of a polychromatic speckle pattern, the effect of the laser coherence on the contrast of the speckle pattern and the problem of averaging in the theory of the speckle pattern were discussed in detail. It is further shown that for several problems of practical interest, the source can be completely characterized by the vacuum speckle contrast ratio.

There are some important extensions to this work. For example, the Hill spectrum could be used to obtain the effects of the inner scale on the variance and the covariance. Also two frequency saturated forms for the log-amplitude covariance and other correlation functions can be developed from fundamentals since they have not yet been evaluated. The results developed in this work on PDFs can be used to understand the nature of the fluctuatoins of the laser beam in the turbulent atmosphere. Another promising area is multifrequency adaptive optics. Also, the effects of the turbulent medium, characterized by more than two scales of turbulence is not known. The applicability of the results in this thesis for other problems such as magnetohydrodynamics, should be investigated.

APPENDIX A

This appendix consists of a program called EIGENS which estimates the eigenvalues of a symmetrical matrix. This program was used for the results of Chapter II.

The input matrix A(i,j) was defined in the program since this program was written to solve Eq.(2.7). Otherwise, it can be defined by input data. Matrix dimensions are 12 by 12. This can also be changed by changing the dimension statement. The output is given by the output matrix A(i,j) itself.

```
C       PROGRAM NAME IS EIGENS
        DIMENSION A(12,12),B(12,12),R(12,12)
        DIMENSION H(12,12),G(12,12)
C       PROGRAM TO CALCULATE THE EIGENVALUES OF THE
C       MATRIX IN CHAPTER II.
        CALL CONTRL(2,'EUCLID',8,0)
        CALL CONTRL(2,'GGGGGG',9,0)
        N=12
        AN=N
        X=SQRT(48.)/2.
        DEL=2./AN
        WRITE(8,19)
 19     FORMAT('SPECKLE INPUT MATRIX')
        P3=4./49.
        DO 101  I=1,12
        DO 102  J=1,12
        A(I,J)=EXP(-(I-J)**2*X*X*P3/2.)
 102    CONTINUE
 101    CONTINUE
        DO 401 I=1,12
        WRITE(8,21) (A(I,J),J=1,12)
 21     FORMAT(8(2X,F10.6))
 401    CONTINUE
        ANORM=0.
        DO 103 I=1,12
        DO 104 J=1,12
        IF(I.EQ.J)  GO TO 22
        ANORM=ANORM+A(I,J)**2
 22     CONTINUE
 104    CONTINUE
 103    CONTINUE
        FTH=.1E-07
        ATH=SQRT(ANORM)/AN
 45     DO 601 I=1,12
        I1=I+1
        DO 602  J=I1,12
        P=ABS(A(I,J))-ATH
 70     IF(ABS(A(I,J))-ATH) 602,602,32
 32     DO 105 L=1,12
        DO 106 M=1,12
        IF(L.EQ.M)  GO TO 23
        R(L,M)=0.
        GO TO 106
 23     R(L,M)=1.
        GO TO 106
 106    CONTINUE
 105    CONTINUE
        AL=-A(I,J)
        AMU=0.5*(A(I,I)-A(J,J))
        IF(AL.EQ.0.) GO TO 602
        F=SIGN(1.,AMU)
        OMEGA=F*AL/(ABS(SQRT(AL*AL+AMU*AMU)))
        X=OMEGA/ABS(SQRT(2.*((1.+SQRT((1.-OMEGA**2))))))
```

```
      Y=ABS(SQRT(1.-X*X))
      R(I,I)=Y
      R(J,J)=Y
      R(I,J)=X
      R(J,I)=-X
      CALL MMLT(G,A,R,12,12,12)
      CALL MTRN(H,R,12)
      CALL MMLT(B,H,G,12,12,12)
      DO 107 L1=1,12
      DO 108 L2=1,12
      A(L1,L2)=B(L1,L2)
108   CONTINUE
107   CONTINUE
602   CONTINUE
601   CONTINUE
      TH=(ATH-FTH)*1000.
      IF(TH) 90,90,91
91    CONTINUE
      ATH=ATH/AN
      GO TO 45
90    CONTINUE
      WRITE(8,18)
18    FORMAT('EIGENVALUES THE MATRIX OUTPUT')
      PHI=22./7.
      DO 501 I=1,12
      DO 502 J=1,12
      A(I,J)=DEL*A(I,J)/2.
502   CONTINUE
501   CONTINUE
      WRITE(9,33) N
33    FORMAT(I2)
      DO 201 I=1,12
      DO 203 J=1,12
      IF(A(I,J)-.00001) 203,77,77
77    WRITE(8,29) I,J,A(I,J)
29    FORMAT(2X,I4,2X,I4,2X,F10.6)
      WRITE(9,34) A(I,J)
34    FORMAT(F8.6)
203   CONTINUE
201   CONTINUE
      CALL CONTRL(4,0,8,0)
      CALL CONTRL(4,0,9,0)
      CALL EXIT
      END
```

APPENDIX B

This appendix consists of three programs. The first program is called VAR111. This evaluates the atmospheric perturbation term of Chapter V, for the Kolmogorov spectrum of refractive index fluctuations. The input data is the the path length, wave length, focal length, beam size called alph0, the value at which function f_1 of Chapter V should be chopped and also number of data points and the corresponding Rytov variance values (for a maximum of 14 points). For more data points, the program can be suitably modified. Further details are given at the beginning of the program. This program uses the saturated form of log-amplitude variance for Rytov variance .3 and the unsaturated form for > .3. It is found however that using unsaturated form in the saturated region did not change the atmospheric perturbation values much and in fact saved a lot of time. Some approximations of log-amplitude covariance functions are due to Dr. R. A. Elliott of OGC. The second program, called RAO2FF, is used to calculate Table 5.1 in this thesis. This program calculates the correlation of intensity fluctuations at two different frequencies. Input data is path length, wave length, beam size, focal length and turbulence level. The program evaluates the intensity correlation for about 60% bandwidth in the center frequency k_0. The third program is called

RAOGXX. This program is written to calculate the atmospheric perturbation using the Hill spectrum especially for the turbulence simulation facility developed and tested by R. A. Elliott, et al. The program was written to evaluate the atmospheric perturbation for the possible values of ${C_n}^2$ reached in the tank.

```
C       NAME OF PROGRAM IS VAR111
C       PROGRAM TO CALCULATE THE ATMOSPHERIC PERTURBATION
C       FOR ALL LEVELS OF TURBULENCE
C       PROGRAM USES THE UNSATURATED FORM OF LOG-AMPLITUDE
C       COVARIANCE FUNCTION FOR LOW TURBULENCE VALUES AND
C       SATURATED FORM OF LOG-AMPLITUDE COVARIANCE FUNCTION
C       DUE TO YURA AND CLIFFORD AT HIGH TURBULENCE LEVELS.
C       SOME APPROXIMATE NUMERICAL SERIES FOR THE
C       LOG-AMPLITUDE COVARIANCE FUNCTIONS ARE DEVELOPED
C       BY DR.R.A.ELLIOTT OF O.G.C. AND THESE FORMS
C       ARE USED IN THE SUBROUTINE H AND FUNCTION
C       SUBPROGRAM F3(Y).
C       OUTPUT CONSISTS OF THE  PROPAGATION DATA AND EACH
C       ARGUMENT AND THE CORRESPONDING  MAGNITUDE OF THE
C       LOG-AMPLITUDE COVARIANCE.ALSO EACH
C       BM AND FINAL VALUE OF THE ATMOSPHERIC PERTURBATION
C       (GIVEN AS SIGMA) ARE PRINTED.
C       IF THE FREQUENCIES ARE WIDELY SEPERATED
C       THE PROGRAM SHOULD BE MODIFIED USING THE PROGRAMS
C       RAO2FF AND CX2FF .
        DIMENSION PM(15),AJ1(15),CX(6),CN2I(14)
        DIMENSION BM(10),SIGMAX(14)
        DATA PM /2.4048,5.5201,8.6537,11.7915,14.9309,
       C18.0711,21.2116,24.3525,27.4935,30.6346,33.7758,
       136.9171,40.0584,43.1998,46.3412/
        DATA AJ1 /.51915,-.34206,.27145,-.23246,-.20635,
       1-.18773,.17327,-.16170,-.15218,.144166,-.1373,
       1.131325,-.12607,.1239,-.11721/
C       IN THE  ABOVE DATA  PM'S ARE ZEROS OF ZEROTH ORDER
C       BESSEL FUNCTION. AJ1'S ARE THE VALUES OF FIRST ORDER
C       BESSEL FUNCTION AT VALUES OF PM.
C       PROGRAM GENERATES ATMOSPHERIC PERTURBATION VERSUS
C       RYTOV VARIANCE FOR A MAXIMUM OF 14 DATA POINTS.
C       IF YOU NEED MORE DATA POINTS, PROGRAM CAN BE
C       MODIFIED ACCORDINGLY.
C       INPUT DATA FIRST LINE IS PATH LENGTH, FOCUS, BEAM
C       SIZE AND  WAVELENGTH
        READ(5,702) PATH,FOCUS,ALPH0,AWAVE
  702   FORMAT(2X,F7.2,2X,F7.2,2X,F6.4,2X,E11.4)
C       CHOP IS THE NEGLIGIBLE VALUE ASSIGNED TO THE
C       FUNCTION F1 IN THE THEORY
        READ(5,703) CHOP
  703   FORMAT(F7.5)
        READ(5,704)  NDATA
  704   FORMAT(I2)
C       NDATA IS THE NUMBER OF POINTS SPECIFYING THE RYTOV
C       VARIANCE WHERE THE VARIANCE IS CALCULATED
C       SIGMAX IS THE RYTOV VARIANCE
        DO 866 I=1,NDATA
        READ(5,687)  SIGMAX(I)
  687   FORMAT(F5.2)
  866   CONTINUE
        DO 701 ICN2=1,NDATA
```

```
      CONST1=PATH**(11./6.)
      CONST2=(44./(7.*AWAVE))**(7./6.)
      CN2I(ICN2)=SIGMAX(ICN2)/(CONST1*CONST2*.124)
 701  CONTINUE
      DO 99 INDEX=1,NDATA,1
      CN2=CN2I(INDEX)
      WRITE(4,40)   PATH,FOCUS,ALPH0
      WRITE(6,40)   PATH,FOCUS,ALPH0
  40  FORMAT(2X,'PATH=',F5.0,2X,'FOCUS=',3X,F5.0,2X,'ALPH0
      WRITE(4,41)   CN2,AWAVE
      WRITE(6,41)    CN2,AWAVE
  41  FORMAT(4X,'CN2=',4X,E10.4,2X,'AWAVE=',2X,E10.4)
      PHI=22./7.
      AK=2.*PHI/(AWAVE)
      ARHO=1.09215*CN2*AK*AK*PATH
C     THE NEXT STEP DECIDES THE RANGE TO GET BMS
      A1=1./(2.*ALPH0**2)
      A2=1./(ARHO**(1.2))
      A=(A1+A2)**(-.5)/100.
 22   X=F1(PATH,CN2,AWAVE,ALPH0,FOCUS,A)
      IF(ABS(X).LT.CHOP)   GO TO 23
      A=A*1.1
      GO TO 22
  23  WRITE(4,175)    A
  175 FORMAT(2X,'A=',2X,E14.6)
C     CALCULATION OF BMS FOLLOWS
C     GENERALLY 6 COFFECIENTS ARE ENOUGH,IF MORE REQUIRED
C     CHANGE 6 IN STATEMENT 29 TO THE REQUIRED NUMBER
      M=1
 29   IF(M.GT.6) GO TO 25
C     TRAPEZOIDAL INTEGRATION TO GET BMS
      AR=0.
      BR=A
      DR=(BR-AR)*.5
      PXM=PM(M)
      SUM1=FX(PATH,CN2,AWAVE,ALPH0,FOCUS,PXM,A,AR)+2.*
     1FX(PATH,CN2,AWAVE,ALPH0,FOCUS,PXM,A,DR)+FX(PATH,CN2,
     2AWAVE,ALPH0,FOCUS,PXM,A,BR)
      SUMA=SUM1*DR*.5
      NR=1
 26   NR=2*NR
      TDR=DR
      DR=DR*.5
      R=AR+DR
      DO 101   IR=1,NR
      SUM1=SUM1+2.*FX(PATH,CN2,AWAVE,ALPH0,FOCUS,PXM,A,R)
      R=R+TDR
 101  CONTINUE
      SUM2=SUM1*DR*.5
      IF(ABS(SUM2-SUMA).LE.ABS(.01*SUM2))  GO TO 666
      SUMA=SUM2
      GO TO 26
 666  IF(NR.GT.16)  GO TO 667
      SUMA=SUM2
```

```
      GO TO 26
 667  BM(M)=SUM2*2./((A*AJ1(M))**2)
      M=M+1
      GO TO 29
 25   CONTINUE
      SUMC=0.
      DO 103  M=1,6
      WRITE(4,28)  M,BM(M)
      WRITE(6,28)  M,BM(M)
      SUMC=SUMC+BM(M)
  28  FORMAT(4X,'M=',I4,5X,'BM(M)=',F10.7)
 103  CONTINUE
      WRITE(6,94)    SUMC
      WRITE(4,94)   SUMC
 94   FORMAT(10X,'SUMC=',F10.7)
C     CALCULATIONS FOR CX(M)  FOLLOW
C     SIMPLE EXPRESSION IS USED FOR SIGMAT LESS THAN
C     OR EQ.  .3 AND CLIFFORD EXPRESIION FOR GT OR EQ.  .3
      MC=1
 32   IF(MC.GT.6)   GO TO 33
      RHO=PATH*PM(MC)/(A*AK)
      SIGMAT=.124*AK**(7./6.)*PATH**(11./6.)*CN2
      WRITE(4,93)  SIGMAT
      WRITE(6,93)  SIGMAT
 93   FORMAT(4X,'SIGMAT=',E14.6)
C     SIGMAT IS THE SAME AS SIGMAX
      IF(SIGMAT.LE..3)    GO TO 920
      CX(MC)=FYY(RHO,SIGMAT,AWAVE,PATH)
C     CX(MC) IS THE LOG-AMPLITUDE COVARIANCE FUNCTION
C     FYY IS THE LOG-AMPLITUDE COVRAINCE IN STRONG
C     TURBULENCE REGIME , DEVELOPED BY YURA AND CLIFFORD.
C     THIS IS A DOUBLE INTEGRAL. ONE OF THE INTEGRALS IS
C     APPROXIMATED BY  AN ASYMPTOTIC  SERIES BY
C     DR.R.A.ELLIOTT OF OGC.
C     FOR DETAILS SEE REFERENCES 54 AND 72 OF THIS THESIS
      GO TO 921
 921  CONTINUE
 920  CX(MC)=FGX(RHO,CN2,AWAVE,PATH)
C     FGX IS THE LOG-AMPLITUDE COVARIANCE FUNCTION IN
C     LOW TURBULENCE LEVEL AND IS AGAIN A DOUBLE INTEGRAL.
C     ONE OF THE INTEGRALS WAS APPROXIMATED BY A SERIES
C    BY DR.R.A.ELLIOT . THIS IS  SUBROUTINE H BELOW.
      WRITE(4,511)  MC,CX(MC),RHO
      WRITE(6,511)  MC,CX(MC),RHO
 511  FORMAT(4X,'MC=',I4,5X,'CX(MC)=',E14.6,2X,'RHO=',E14.
      IF(CX(MC).LE..001)  GO TO 520
      MC=MC+1
      GO TO 32
 520  MC1=MC+1
      DO 521 IM=MC1,6
      CX(IM)=0.
 521  CONTINUE
 33   CONTINUE
      COFFSM=0.
```

```
      DO 522  M=1,6
      COFFSM=COFFSM+BM(M)*EXP(4.*CX(M))
522   CONTINUE
      SIGMA=COFFSM+1.-SUMC
C     SIGMA IS THE ATMOSPHERIC PERTURBATION
      WRITE(4,524)    SIGMAT,SIGMA
      WRITE(6,524)   SIGMAT,SIGMA
 524  FORMAT(4X, 'SIGMAT=',E18.6,5X,'SIGMA=',E14.6)
C     THE NORMALIZED VARIANCE OF THE RECEIVED INTENSITY
C     FOR A MONOCHROMATIC SPECKLE IS GIVEN BY
C     VAR=2.*SIGMA-1.
C     FOR A POLYCHROMATIC SPECKLE , THE VARIANCE
C     OF INTENSITY IS GIVEN AS
C     VAR=(1.+VSCR*VSCR)*SIGMA-1.
 99   CONTINUE
      STOP
      END
      FUNCTION AJ0(X)
C     AJ0 IS THE BESSEL FUNCTION OF ZEROTH ORDER AND FIRST
      IF(X.GT.3.) GO TO 71
      X1=X/3.
      AJ0=1.-2.2499997*X1**2+1.2656208*X1**4-.3163866*X1**
     16+.0444479*X1**8-.0039444*X1**10+.00021*X1**12
      GO TO 72
 71   X2=3./X
      FO=.79788456-.00000077*X2-.0055274*X2**2-.0000951*X2
     1**3+.00137237*X2**4-.00072805*X2**5+.00014476*X2**6
      THETA=X-.78539816-.04166397*X2-.00003954*X2**2+
     1.00262573*X2**3-.00054125*X2**4-.00029333*X2**5+
     1.00013558*X2**6
      AJ0=FO*COS(THETA)/SQRT(X)
      GO TO 72
 72   CONTINUE
      RETURN
      END
      FUNCTION F3(Y)
      Q=.7*Y
      IF(Q.GT.4.712389)   GO TO 61
      Q1=Q**(1./3.)
      GQ=3.*(.37278-Q1/4.+Q1**7/448.-Q1**13/29952
     1+Q1**19/(2801.664E03)-Q1**25/(36864.E04))
      FF4=7.02*Y**(5./6.)*GQ
      GO TO 62
 61   Q2=Q**(-1./6.)
      GQ1=.6*Q**(-5./3.)
      GQ2=.79788456*COS(Q+.78539816)*(Q2**(19.)-
     113.194444*Q2**(31.)+420.38966*Q2**(43.))
      GQ3=.79788456*SIN(Q+.78539816)*(3.1666667*Q2**(25)
     1-68.171296*Q2**(37.)+3012.7926*Q2**(49))
      GQ=GQ1-GQ2-GQ3
      FF4=9.45*Q**(5./6.)*GQ
      GO TO 62
 62   F3=FF4
      RETURN
```

```
      END
      FUNCTION FF2(Y)
      IF(Y.LT..01)   GO TO 65
      FF2=SIN(Y)**2/(Y**(11./6.))
      GO TO 66
 65   YP=Y**(1./6.)
      FF2=YP-.3333333*YP**13+.04444444*YP**25
      GO TO 66
66    CONTINUE
      RETURN
      END
      FUNCTION F1(PATH,CN2,AWAVE,ALPH0,FOCUS,Z2)
      ZZ=Z2/ALPH0
      X1=EXP(-ZZ*ZZ/2.)
      AK=44./(7.*AWAVE)
      X3=1.09215*CN2*PATH*AK**2
      Z3=Z2**(5./3.)
      X2=EXP(-X3*Z3)
      X4=AK*(1.-PATH/FOCUS)*Z2*ALPH0/(2.*PATH)
      X5=EXP(-X4*X4*2.)
      F1=X1*X2*X5
      RETURN
      END
      SUBROUTINE GAUSSU(RHO,SIG,AWAVE,PATH,A1,A2,Y,ANSU1)
      C1=(A1+A2)*.5
      C2=(A2-A1)*.5
      U1=-.2386915*C2+C1
      U2=.2386915*C2+C1
      U3=-.6612094*C2+C1
      U4=.6612094*C2+C1
      U5=-.9324695*C2+C1
      U6=.9324695*C2+C1
      W1=.4679139
      W2=W1
      W3=.3607616
      W4=W3
      W5=.1713245
      W6=W5
      UA1=W1*FM(RHO,SIG,AWAVE,PATH,U1,Y)
      UA2=W2*FM(RHO,SIG,AWAVE,PATH,U2,Y)
      UA3=W3*FM(RHO,SIG,AWAVE,PATH,U3,Y)
      UA4=W4*FM(RHO,SIG,AWAVE,PATH,U4,Y)
      UA5=W5*FM(RHO,SIG,AWAVE,PATH,U5,Y)
      UA6=W6*FM(RHO,SIG,AWAVE,PATH,U6,Y)
      ANSU1=C2*(UA1+UA2+UA3+UA4+UA5+UA6)
      RETURN
      END
      SUBROUTINE YGAUSS(RHO,SIG,AWAVE,PATH,AY1,AY2,ANSYY)
      D1=(AY1+AY2)*.5
      D2=(AY2-AY1)*.5
      Y1=-.2386915*D2+D1
      Y2=.2386915*D2+D1
      Y3=-.6612094*D2+D1
      Y4=.6612094*D2+D1
```

```
      Y5=-.9324695*D2+D1
      Y6=.9324695*D2+D1
      W1=.4679139
      W2=W1
      W3=.3607616
      W4=W3
      W5=.1713245
      W6=W5
      YA1=W1*UGAUSS(PATH,RHO,SIG,AWAVE,Y1)
      YA2=W2*UGAUSS(PATH,RHO,SIG,AWAVE,Y2)
      YA3=W3*UGAUSS(PATH,RHO,SIG,AWAVE,Y3)
      YA4=W4*UGAUSS(PATH,RHO,SIG,AWAVE,Y4)
      YA5=W5*UGAUSS(PATH,RHO,SIG,AWAVE,Y5)
      YA6=W6*UGAUSS(PATH,RHO,SIG,AWAVE,Y6)
      ANSYY=D2*(YA1+YA2+YA3+YA4+YA5+YA6)
      RETURN
      END
      FUNCTION FM(RHO,SIGMAT,AWAVE,PATH,U,Y)
      IF(Y.LE.0.)  GO TO 251
      IF(ABS(U).LE..001.OR.ABS(U).GE..99)   GO TO 251
      AXXX=U*(1.-U)
      IF(AXXX.GE.0.)    GO TO 991
      WRITE(6,232) AXXX
232   FORMAT(F14.8)
991   CONTINUE
      FM14=EXP(-SIGMAT*F3(Y)*(U*(1.-U))**(5./6.))
      FM11=(U*(1.-U))**((5.)/6.)
      PHI=22./7.
      FM12X=SQRT((4.*PHI*Y*U)/(1.-U))
      FM12Y=SQRT(AWAVE*PATH)
      FM12=FM12X*RHO/FM12Y
      FM13=FF2(Y)
      FM=FM11*FM13*FM14*AJ0(FM12)*2.95*SIGMAT
      GO TO 252
251   FM=0.
252   CONTINUE
      RETURN
      END
      FUNCTION UGAUSS(PATH,RHO,SIGMAT,AWAVE,Y)
      AU=0.
      BU=1.
      NU=2
      TNSU=0.
 501  ANSU=0.
      DO 502  IU=1,NU
      ANU=NU
      A1=AU+(IU-1.)*(BU-AU)/ANU
      A2=AU+(IU)*(BU-AU)/ANU
      CALL GAUSSU(RHO,SIGMAT,AWAVE,PATH,A1,A2,Y,ANSU2)
      ANSU=ANSU+ANSU2
502   CONTINUE
      IF(ABS(ANSU-TNSU).LE.ABS(.02*ANSU))   GO TO 503
      TNSU=ANSU
      NU=NU*2
```

```
      GO TO 501
503   UGAUSS=ANSU
      RETURN
      END
      FUNCTION FX(PATH,CN2,AWAVE,ALPH0,FOCUS,PXM,A,R)
      FXX=F1(PATH,CN2,AWAVE,ALPH0,FOCUS,R)
      FX=FXX*R*AJ0(PXM*R/A)
      RETURN
      END
      FUNCTION FYY(RHO,SIGMAT,AWAVE,PATH)
      TNSX=0.
      ANSX=0.
      AY=0.
      IF(SIGMAT.LE.1.)  GO TO 721
      BY=1./(2.*SIGMAT)
      GO TO 722
721   BY=1.
722   DELTA=BY
723   NY=2
      TNSY=0.
508   ANSY=0.
      DO 509  IY=1,NY
      ANY=NY
      AY1=AY+(IY-1.)*(BY-AY)/ANY
      AY2=AY+IY*(BY-AY)/ANY
      CALL YGAUSS(RHO,SIGMAT,AWAVE,PATH,AY1,AY2,ANSY2)
      ANSY=ANSY+ANSY2
509   CONTINUE
      IF(ABS(ANSY-TNSY).LE.ABS(.02*ANSY))  GO TO 510
      TNSY=ANSY
      NY=NY*2
      WRITE(6,461)   ANSY
461   FORMAT(5X,E14.6)
      IF(NY.GE.4.AND.ABS(ANSY).LE..001)   GO TO 510
      GO TO 508
510   ANSX=ANSX+ANSY
      IF(ABS(ANSX-TNSX).LE.ABS(.02*ANSX))  GO TO 732
      AY=AY+DELTA
      BY=BY+DELTA
      TNSX=ANSX
      IF(ABS(ANSX).LE..001)   GO TO 732
      GO TO 723
732   FYY=ANSX
      RETURN
      END
      SUBROUTINE GAX(RHO,CN2,AWAVE,PATH,A1,A2,ANSU1)
      C1=(A1+A2)*.5
      C2=(A2-A1)*.5
      U1=-.2386915*C2+C1
      U2=.2386915*C2+C1
      U3=-.6612094*C2+C1
      U4=.6612094*C2+C1
      U5=-.9324695*C2+C1
      U6=.9324695*C2+C1
```

```
      W1=.4679139
      W2=W1
      W3=.3607616
      W4=W3
      W5=.1713245
      W6=W5
      UA1=W1*FMXX(RHO,CN2,AWAVE,PATH,U1)
      UA2=W2*FMXX(RHO,CN2,AWAVE,PATH,U2)
      UA3=W3*FMXX(RHO,CN2,AWAVE,PATH,U3)
      UA4=W4*FMXX(RHO,CN2,AWAVE,PATH,U4)
      UA5=W5*FMXX(RHO,CN2,AWAVE,PATH,U5)
      UA6=W6*FMXX(RHO,CN2,AWAVE,PATH,U6)
      ANSU1=C2*(UA1+UA2+UA3+UA4+UA5+UA6)
      RETURN
      END
      FUNCTION FGX(RHO,CN2,AWAVE,PATH)
      AU=0.
      BU=1.
      NU=2
      TNSU=0.
 501  ANSU=0.
      DO 502  IU=1,NU
      ANU=NU
      A1=AU+(IU-1.)*(BU-AU)/ANU
      A2=AU+(IU)*(BU-AU)/ANU
      CALL GAX(RHO,CN2,AWAVE,PATH,A1,A2,ANSU2)
      ANSU=ANSU+ANSU2
502   CONTINUE
      IF(ABS(ANSU-TNSU).LE.ABS(.02*ANSU))   GO TO 503
      TNSU=ANSU
      NU=NU*2
      GO TO 501
503   FGX=ANSU
      RETURN
      END
      FUNCTION FMXX(RHO,CN2,AWAVE,PATH,U)
      PHI=22./7.
      AK=2.*PHI/AWAVE
      A1=SQRT((U*(1.-U)*PATH)/(2.*AK))
      A2=ABS(RHO*(1.-U))
      CALL HS(A1,A2,CC)
      FMXX=.132*PHI*PHI*AK*AK*PATH*CN2*CC
      RETURN
      END
      SUBROUTINE HS(A,B,C)
      DIMENSION C2(9),C3(10)
      INTEGER F1
      DOUBLE PRECISION G2,G3,HK,BB,G,C,H
      DATA C2/9.64506E-3,-.513572E-2,.298032E-1,
     1 -.5402513E0,.2056255E2
     1  ,-1.35296E3,1.37215E5,-1.9892E7,3.9089E9/
      DATA C3/3.36111,-13.49112,-66.08151,.385934E3,
     1 .2626497E4,-.2044046E5,
     1  -.1791784E6,.1747611E7,1.877604E7,-2.203577E8/
```

```
      Z=B*B/(8*A*A)
      HH=.559167*B**(1.6666667)
      IF (Z.GT.12.56) GO TO 200
      N=31
C POWER SERIES EXPANSION OF H[A,B]
      N1=N+1
      HK=5./(36*4)
      BB=Z*Z*HK
      G2=1.+BB
      N3=N/2+1
      DZ=Z*Z
      TZ=DZ*DZ
      DO 10 J=1,N3
      I=2*J-1
      HK=-HK*(6.*I+1.)*(6.*I+7.)/((6.*(I+2.)*(I+3.))**2)
      IF(J.EQ.1) GO TO 12
      HK=HK*DZ
      GO TO 10
   12 HK=HK*TZ
 10   G2=G2+HK
      HK=5./6.
      BB=HK*Z
      G3=BB
      DO 11 J=0,N3
      I=2*J
      HK=-HK*(6.*I+1.)*(6.*I+7.)/((6.*(I+2)*(I+3))**2)
      IF(J.EQ.0) GO TO 13
      HK=HK*DZ
      GO TO 11
   13 HK=HK*DZ*Z
   11 G3=G3+HK
 100  G=(.25881904*G2+.96592583*G3)
      C=2.975414275*A**1.6666667*G
      C=-HH+C
      RETURN
C ASYMPTOTIC EXPANSION OF H[A,B]
 200  ZZ=1/Z
      D1=0.525982*B**1.666667
      G1=C2(1)*ZZ**2+C2(2)*ZZ**4+C2(3)*ZZ**6+C2(4)*ZZ**8
     1   +C2(5)*ZZ**10+C2(6)*ZZ**12+C2(7)*ZZ**14+C2(8)*ZZ**
     1 16
      G2=1+C3(2)*ZZ**2+C3(4)*ZZ**4+C3(6)*ZZ**6+C3(8)*ZZ**8
     1 +C3(10)*ZZ*10
      G3=C3(1)*ZZ+C3(3)*ZZ**3+C3(5)*ZZ**5+C3(7)*ZZ**7+
     1 C3(9)*ZZ**9
      PO=2.66666667
      H=1.0630853*G1+SIN(Z)*ZZ**PO*G2*.1497105-.1497*
     1 COS(Z)*ZZ**PO*G3
      C=-H*D1
      RETURN
      END
```

```
C      NAME OF THE PROGRAM IS RAO2FF
C      NOTATION OF THE PROGRAM VAR111 APLLIES HERE
C      CALCULATION OF <I(K1) I(K2)> VERUS RATIO
C      OF WAVELENGTHS(K1/K2) AT A GIVEN POINT
C      IN THE RECEIVER PLANE AT VARIOUS VALUES
C      OF INTEGRATED TURBULENCE. THIS IS USEFUL
C      IN STUDYING THE DEPENDENCE OF TWO FREQUENCY
C      ATMOSPHERIC PERTURBATION ON THE FREQUENCY
C      DIFFERENCE (SEE CHAPTER V ,TABLE ON THE
C      COMPARISION OF TWO FREQUENCY AND SINGLE
C      FREQUENCY ATMOSPHERIC PERTURBATION).
C      THE TWO FREQUENCY LOG-AMPLITUDE COVARIANCE
C      C(R,K1,K2) IS STUDIED IN ANOTHER PROGRAM.
C      THIS PROGRAM IS VALID ONLY AT LOW
C      TURBULENCE LEVELS (RYTOV VARIANCE<.3).
       DIMENSION PM(15),AJ1(15),CX(6)
       DIMENSION BM(10)
       DATA PM /2.4048,5.5201,8.6537,11.7915,14.9309,
      C18.0711,21.2116,24.3525,27.4935,30.6346,33.7758,
      136.9171,40.0584,43.1998,46.3412/
       DATA AJ1 /.51915,-.34206,.27145,-.23246,-.20635,
      1-.18773,.17327,-.16170,-.15218,.144166,-.1373,
      1.131325,-.12607,.1239,-.11721/
       READ(5,702) PATH,FOCUS,ALPH0,AWAVE
 702   FORMAT(2X,F7.2,2X,F7.2,2X,F6.4,2X,E11.4)
       READ(5,703)   CHOP
 703   FORMAT(F7.5)
       READ(5,707)  CN2
 707   FORMAT(E10.4)
       AK0=44./(7.*AWAVE)
       DO 99  IJJ=1,6
       BETA=IJJ*.1
       AK1=AK0+AK0*BETA*.5
       AK2=AK0-AK0*BETA*.5
       WRITE(4,40)   PATH,FOCUS,ALPH0
       WRITE(6,40)   PATH,FOCUS,ALPH0
  40   FORMAT(2X,'PATH=',F5.0,2X,'FOCUS=',3X,F5.0
      1 ,2X,'ALPH0=',F6.4)
       WRITE(4,41) CN2,AWAVE,BETA
       WRITE(6,41) CN2,AWAVE,BETA
  41   FORMAT(4X,'CN2=',4X,E10.4,2X,'AWAVE=',2X,
      1 E10.4,'BETA=',F6.3)
       PHI=22./7.
       ARHO=1.09215*CN2*AK1*AK1*PATH
C       THE NEXT STEP DECIDES THE RANGE TO GET BMS
       A1=1./(2.*ALPH0**2)
       A2=1./(ARHO**(1.2))
       A=(A1+A2)**(-.5)/100.
 22    X=F1(AK2,PATH,CN2,AK1,ALPH0,FOCUS,A)
       IF(ABS(X).LT.CHOP)   GO TO 23
       A=A*1.1
       GO TO 22
  23   WRITE(4,175) A
```

```
  175 FORMAT(2X,'A=',2X,E14.6)
C        CALCULATION OF BMS FOLLOWS
      M=1
 29   IF(M.GT.6) GO TO 25
      AR=0.
      BR=A
      DR=(BR-AR)*.5
      PXM=PM(M)
      SUM1=FX(AK2,PATH,CN2,AK1,ALPH0,FOCUS,PXM,A,AR)+
     1 2.*FX(AK2,PATH,CN2,AK1,ALPH0,FOCUS,PXM,A,DR)+
     2 FX(AK2,PATH,CN2,AK1,ALPH0,FOCUS,PXM,A,BR)
      SUMA=SUM1*DR*.5
      NR=1
 26   NR=2*NR
      TDR=DR
      DR=DR*.5
      R=AR+DR
      DO 101 IR=1,NR
      SUM1=SUM1+2.*FX(AK2,PATH,CN2,AK1,ALPH0,
     1 FOCUS,PXM,A,R)
      R=R+TDR
 101  CONTINUE
      SUM2=SUM1*DR*.5
      IF(ABS(SUM2-SUMA).LE.ABS(.01*SUM2)) GO TO 666
      SUMA=SUM2
      GO TO 26
 666  IF(NR.GT.16) GO TO 667
      SUMA=SUM2
      GO TO 26
 667  BM(M)=SUM2*2./((A*AJ1(M))**2)
      M=M+1
      GO TO 29
 25   CONTINUE
      SUMC=0.
      DO 103 M=1,6
      WRITE(4,28) M,BM(M)
      WRITE(6,28) M,BM(M)
      SUMC=SUMC+BM(M)
  28  FORMAT(4X,'M=',I4,5X,'BM(M)=',F10.7)
 103  CONTINUE
      WRITE(6,94) SUMC
      WRITE(4,94) SUMC
 94   FORMAT(10X,'SUMC=',F10.7)
C     CALCULATIONS FOR CX(M)  FOLLOW
      MC=1
 32   IF(MC.GT.6)       GO       TO 33
      RHO=PATH*PM(MC)/(A*AK2)
      SIGMAT=.124*AK0**(7./6.)*PATH**(11./6.)*CN2
      WRITE(6,93) SIGMAT
 93   FORMAT(4X,'SIGMAT=',E14.6)
      CX(MC)=FYY(AK2,RHO,CN2,AK1,PATH)
      WRITE(4,511) MC,CX(MC),RHO
      WRITE(6,511) MC,CX(MC),RHO
 511  FORMAT(4X,'MC=',I4,5X,'CX(MC)=',E14.6,
```

```
     1 2X,'RHO=',E14.6)
      IF(CX(MC).LE..001) GO TO 520
      MC=MC+1
      GO TO 32
520   MC1=MC+1
      DO 521 IM=MC1,6
      CX(IM)=0.
521   CONTINUE
33    CONTINUE
      COFFSM=0.
      DO 522 M=1,6
      COFFSM=COFFSM+BM(M)*EXP(4.*CX(M))
522   CONTINUE
      SIGMA=COFFSM+1.-SUMC
      WRITE(4,524) SIGMAT,SIGMA
      WRITE(6,524) SIGMAT,SIGMA
524   FORMAT(4X, 'SIGMAT=',E18.6,5X,'SIGMA=',E14.6)
      WRITE(4,555)
555   FORMAT('///////')
99    CONTINUE
199   CONTINUE
      STOP
      END
      FUNCTION AJ0(X)
      IF(X.GT.3.) GO TO 71
      X1=X/3.
      AJ0=1.-2.2499997*X1**2+1.2656208*X1**4-.3163866*X1**
     16+.0444479*X1**8-.0039444*X1**10+.00021*X1**12
      GO TO 72
71    X2=3./X
      FO=.79788456-.00000077*X2-.0055274*X2**2-.0000951*X2
     1**3+.00137237*X2**4-.00072805*X2**5+.00014476*X2**6
      THETA=X-.78539816-.04166397*X2-.00003954*X2**2+
     1.00262573*X2**3-.00054125*X2**4-.00029333*X2**5+
     1 .00013558*X2**6
      AJ0=FO*COS(THETA)/SQRT(X)
      GO TO 72
72    CONTINUE
      RETURN
      END
      FUNCTION F1(AK2,PATH,CN2,AK1,ALPH0,FOCUS,Z2)
      ZZ=Z2/ALPH0
      B1=AK2/AK1
      B2=AK1/AK2
      X1=EXP(-ZZ*ZZ*.25*(1.+B1*B1))
      X3=.545625*CN2*PATH*(AK2**2)*(1.+B2**(.3333333))
      Z3=Z2**(5./3.)
      X2=EXP(-X3*Z3)
      X4=AK2*(1.-PATH/FOCUS)*Z2*ALPH0/(2.*PATH)
      X5=EXP(-X4*X4*2.)
      F1=X1*X2*X5
      RETURN
      END
      SUBROUTINE GAUSSU(AK2,RHO,CN2,AK1,PATH,A1,A2,Y,ANS)
```

```
      C1=(A1+A2)*.5
      C2=(A2-A1)*.5
      U1=-.2386915*C2+C1
      U2=.2386915*C2+C1
      U3=-.6612094*C2+C1
      U4=.6612094*C2+C1
      U5=-.9324695*C2+C1
      U6=.9324695*C2+C1
      W1=.4679139
      W2=W1
      W3=.3607616
      W4=W3
      W5=.1713245
      W6=W5
      UA1=W1*FM(AK2,RHO,CN2,AK1,PATH,U1,Y)
      UA2=W2*FM(AK2,RHO,CN2,AK1,PATH,U2,Y)
      UA3=W3*FM(AK2,RHO,CN2,AK1,PATH,U3,Y)
      UA4=W4*FM(AK2,RHO,CN2,AK1,PATH,U4,Y)
      UA5=W5*FM(AK2,RHO,CN2,AK1,PATH,U5,Y)
      UA6=W6*FM(AK2,RHO,CN2,AK1,PATH,U6,Y)
      ANS=C2*(UA1+UA2+UA3+UA4+UA5+UA6)
      RETURN
      END
      SUBROUTINE YGAUSS(AK2,RHO,CN2,AK1,PATH,AY1,AY2,ANS)
      D1=(AY1+AY2)*.5
      D2=(AY2-AY1)*.5
      Y1=-.2386915*D2+D1
      Y2=.2386915*D2+D1
      Y3=-.6612094*D2+D1
      Y4=.6612094*D2+D1
      Y5=-.9324695*D2+D1
      Y6=.9324695*D2+D1
      W1=.4679139
      W2=W1
      W3=.3607616
      W4=W3
      W5=.1713245
      W6=W5
      YA1=W1*UGAUSS(AK2,PATH,RHO,CN2,AK1,Y1)
      YA2=W2*UGAUSS(AK2,PATH,RHO,CN2,AK1,Y2)
      YA3=W3*UGAUSS(AK2,PATH,RHO,CN2,AK1,Y3)
      YA4=W4*UGAUSS(AK2,PATH,RHO,CN2,AK1,Y4)
      YA5=W5*UGAUSS(AK2,PATH,RHO,CN2,AK1,Y5)
      YA6=W6*UGAUSS(AK2,PATH,RHO,CN2,AK1,Y6)
      ANS=D2*(YA1+YA2+YA3+YA4+YA5+YA6)
      RETURN
      END
      FUNCTION FM(AK2,RHO,CN2,AK1,PATH,U,Y)
      IF(Y.LE.0.) GO TO 251
      IF(ABS(U).LE..001.OR.ABS(U).GE..99) GO TO 251
      AXXX=U*(1.-U)
      IF(AXXX.GE.0.) GO TO 991
      WRITE(6,232) AXXX
232   FORMAT(F14.8)
```

```
991   CONTINUE
      FM11=(U*(1.-U))**((5.)/6.)
      PHI=22./7.
      FM12X=SQRT((4.*PHI*Y*U)/(1.-U))
      WAVEL=44./(7.*AK1)
      FM12Y=SQRT(WAVEL*PATH)
      FM12=FM12X*RHO/FM12Y
      BB=AK1/AK2
      FM13=SIN(Y)*SIN(BB*Y)/(BB*(Y**(11./6.)))
      CONS=.36558246*CN2*(AK1**(7./6.))*(PATH**(11./6.))
      FM=CONS*FM11*AJ0(FM12)*FM13
      GO TO 252
251   FM=0.
252   CONTINUE
      RETURN
      END
      FUNCTION UGAUSS(AK2,PATH,RHO,CN2,AK1,Y)
      AU=0.
      BU=1.
      NU=2
      TNSU=0.
 501  ANSU=0.
      DO 502 IU=1,NU
      ANU=NU
      A1=AU+(IU-1.)*(BU-AU)/ANU
      A2=AU+(IU)*(BU-AU)/ANU
      CALL GAUSSU(AK2,RHO,CN2,AK1,PATH,A1,A2,Y,ANSU2)
      ANSU=ANSU+ANSU2
502   CONTINUE
      IF(ABS(ANSU-TNSU).LE.ABS(.02*ANSU)) GO TO 503
      TNSU=ANSU
      NU=NU*2
      GO TO 501
503   UGAUSS=ANSU
      RETURN
      END
      FUNCTION FX(AK2,PATH,CN2,AK1,ALPH0,FOCUS,PXM,A,R)
      FXX=F1(AK2,PATH,CN2,AK1,ALPH0,FOCUS,R)
      FX=FXX*R*AJ0(PXM*R/A)
      RETURN
      END
      FUNCTION FYY(AK2,RHO,CN2,AK1,PATH)
      SIGMAT=.124*AK1**(7./6.)*(PATH**(11./6.))*CN2
      TNSX=0.
      ANSX=0.
      AY=0.
      IF(SIGMAT.LE.1.) GO TO 721
      BY=1./(2.*SIGMAT)
      GO TO 722
721   BY=1.
722   DELTA=BY
      IF(AK1.GT.AK2) BY=BY*AK2/AK1
      IF(AK1.GT.AK2) DELTA=DELTA*AK2/AK1
723   NY=2
```

```
      TNSY=0.
508   ANSY=0.
      DO 509 IY=1,NY
      ANY=NY
      AY1=AY+(IY-1.)*(BY-AY)/ANY
      AY2=AY+IY*(BY-AY)/ANY
      CALL YGAUSS(AK2,RHO,CN2,AK1,PATH,AY1,AY2,ANSY2)
      ANSY=ANSY+ANSY2
509   CONTINUE
      IF(ABS(ANSY-TNSY).LE.ABS(.02*ANSY)) GO TO 510
      TNSY=ANSY
      NY=NY*2
      WRITE(6,461) ANSY
461   FORMAT(5X,E14.6)
      IF(NY.GE.4.AND.ABS(ANSY).LE..001) GO TO 510
      GO TO 508
510   ANSX=ANSX+ANSY
      IF(ABS(ANSX-TNSX).LE.ABS(.02*ANSX)) GO TO 732
      AY=AY+DELTA
      BY=BY+DELTA
      TNSX=ANSX
      IF(ABS(ANSX).LE..001) GO TO 732
      GO TO 723
732   FYY=ANSX
      RETURN
      END
```

```
C       NAME OF PROGRAM IS RAOGXX
C       PROGRAM TO CALCULATE THE ATMOSPHERIC
C       PERTURBATION USING HILL SPECTRUM FOR THE
C       SIMULATION TANK VALID ONLY AT LOW
C       LOW TURBULENCE REGIMES.NEED TO BE CHANGED
C       FOR STRONG TURBULENCE REGIMES.
        DIMENSION PM(15),AJ1(15),CX(6),CN2I(6)
        DIMENSION BM(10)
        DATA PM /2.4048,5.5201,8.6537,11.7915,14.9309,
       C18.0711,21.2116,24.3525,27.4935,30.6346,33.7758,
       136.9171,40.0584,43.1998,46.3412/
        DATA AJ1 /.51915,-.34206,.27145,-.23246,-.20635,
       1-.18773,.17327,-.16170,-.15218,.144166,-.1373,
       1.131325,-.12607,.1239,-.11721/
        DATA CN2I/1.E-11,5.E-11,1.E-10,2.E-10,5.E-10,
       1 1.E-09/
        READ(5,444)  PATH
  444   FORMAT(F4.2)
        READ(5,445)   FOCUS
  445   FORMAT(F4.2)
        READ(5,446)   ALPH0
  446   FORMAT(F5.3)
        READ(5,447)   AWAVE
  447   FORMAT(F6.3)
        AWAVE=AWAVE*(1.E-06)
        READ(5,703)   CHOP
  703   FORMAT(F7.5)
C       REFRACTIVE INDEX IS 1.361;IT SHOULD BE
C       CHANGED FOR OTHER SIMULATING MEDIUMS
        DO 99 INDEX=1,6,1
        CN2=CN2I(INDEX)
        WRITE(4,40)   PATH,FOCUS,ALPH0
        WRITE(6,40)   PATH,FOCUS,ALPH0
   40   FORMAT(2X,'PATH=',F7.2,2X,'FOCUS=',3X,F7.2,2X,
       1 'ALPH0=',F6.4)
        WRITE(4,41) CN2,AWAVE
        WRITE(6,41) CN2,AWAVE
   41   FORMAT(4X,'CN2=',4X,E10.4,2X,'AWAVE=',2X,E10.4)
        PHI=22./7.
        AK=2.*PHI*1.361/(AWAVE)
        ARHO=1.09215*CN2*AK*AK*PATH
C        THE NEXT STEP DECIDES THE RANGE TO GET BMS
        A1=1./(2.*ALPH0**2)
        A2=1./(ARHO**(1.2))
        A=(A1+A2)**(-.5)/100.
  22    X=F1(PATH,CN2,AWAVE,ALPH0,FOCUS,A)
        IF(ABS(X).LT.CHOP)   GO TO 23
        A=A*1.1
        GO TO 22
   23   WRITE(4,175)       A
   175  FORMAT(2X,'A=',2X,E14.6)
C        CALCULATION OF BMS FOLLOWS
        M=1
```

```
29    IF(M.GT.6)       GO TO 25
      AR=0.
      BR=A
      DR=(BR-AR)*.5
      PXM=PM(M)
      SUM1=FX(PATH,CN2,AWAVE,ALPH0,FOCUS,PXM,A,AR)
     1+2.*FX(PATH,N2,AWAVE,ALPH0,FOCUS,PXM,A,DR)
     2+FX(PATH,CN2,AWAVE,ALPH0,FOCUS,PXM,A,BR)
      SUMA=SUM1*DR*.5
      NR=1
26    NR=2*NR
      TDR=DR
      DR=DR*.5
      R=AR+DR
      DO 101   IR=1,NR
      SUM1=SUM1+2.*FX(PATH,CN2,AWAVE,ALPH0,FOCUS,PXM,A,R)
      R=R+TDR
101   CONTINUE
      SUM2=SUM1*DR*.5
      IF(ABS(SUM2-SUMA).LE.ABS(.01*SUM2)) GO TO 666
      SUMA=SUM2
      GO TO 26
666   IF(NR.GT.16) GO TO 667
      SUMA=SUM2
      GO TO 26
667   BM(M)=SUM2*2./((A*AJ1(M))**2)
      M=M+1
      GO TO 29
25    CONTINUE
      SUMC=0.
      DO 103 M=1,6
      WRITE(4,28) M,BM(M)
      WRITE(6,28) M,BM(M)
      SUMC=SUMC+BM(M)
 28   FORMAT(4X,'M=',I4,5X,'BM(M)=',F10.7)
103   CONTINUE
      WRITE(6,94) SUMC
      WRITE(4,94) SUMC
 94   FORMAT(10X,'SUMC=',F10.7)
C     LOG-AMPLITUDE COVARIANCE FUNCTION OF A SPHERICAL WAV
C     AT LOW TURBULENCE LEVELS IS USED IN THE NUMERICAL
C     EVALUATION. THIS SHOULD BE MODIFIED FOR STRONG
C     TURBULENCE CONDITIONS.
C      CALCULATIONS FOR CX(M)  FOLLOW
      RYTOV=FYY(0.,CN2,AWAVE,PATH)
      WRITE(4,188)       RYTOV
      WRITE(6,188)       RYTOV
188   FORMAT(2X,'RYTOV=',E14.6)
      MC=1
32    IF(MC.GT.6) GO TO 33
      RHO=PATH*PM(MC)/(A*AK)
      CX(MC)=FYY(RHO,CN2,AWAVE,PATH)
      WRITE(4,511) MC,CX(MC),RHO
      WRITE(6,511) MC,CX(MC),RHO
```

```
511   FORMAT(4X,'MC=',I4,5X,'CX(MC)=',E14.6,2X,'RHO=',E14.
      IF(CX(MC).LE..001) GO TO 520
      MC=MC+1
      GO TO 32
520   MC1=MC+1
      DO 521 IM=MC1,6
      CX(IM)=0.
521   CONTINUE
33    CONTINUE
      COFFSM=0.
      DO 522 M=1,6
      COFFSM=COFFSM+BM(M)*EXP(4.*CX(M))
522   CONTINUE
      SIGMA=COFFSM+1.-SUMC
      WRITE(4,524) SIGMA
      WRITE(6,524) SIGMA
 524  FORMAT(4X,'SIGMA=',E14.6)
99    CONTINUE
      STOP
      END
      FUNCTION AJ0(X)
      IF(X.GT.3.) GO TO 71
      X1=X/3.
      AJ0=1.-2.2499997*X1**2+1.2656208*X1**4-.3163866*X1**
     16+.0444479*X1**8-.0039444*X1**10+.00021*X1**12
      GO TO 72
71    X2=3./X
      FO=.79788456-.00000077*X2-.0055274*X2**2-.0000951*X2
     1**3+.00137237*X2**4-.00072805*X2**5+.00014476*X2**6
      THETA=X-.78539816-.04166397*X2-.00003954*X2**2+
     1.00262573*X2**3-.00054125*X2**4-.00029333*X2**5+
     1 .00013558*X2**6
      AJ0=FO*COS(THETA)/SQRT(X)
      GO TO 72
72    CONTINUE
      RETURN
      END
      FUNCTION F1(PATH,CN2,AWAVE,ALPH0,FOCUS,Z2)
      ZZ=Z2/ALPH0
      X1=EXP(-ZZ*ZZ/2.)
      AK=44.*1.361/(7.*AWAVE)
      X3=1.09215*CN2*PATH*AK**2
      Z3=Z2**(5./3.)
      X2=EXP(-X3*Z3)
      X4=AK*(1.-PATH/FOCUS)*Z2*ALPH0/(2.*PATH)
      X5=EXP(-X4*X4*2.)
      F1=X1*X2*X5
      RETURN
      END
      SUBROUTINE GAUSSU(RHO,CN2,AWAVE,PATH,A1,A2,Y,ANSU1)
      C1=(A1+A2)*.5
      C2=(A2-A1)*.5
      U1=-.2386915*C2+C1
      U2=.2386915*C2+C1
```

```
U3=-.6612094*C2+C1
U4=.6612094*C2+C1
U5=-.9324695*C2+C1
U6=.9324695*C2+C1
W1=.4679139
W2=W1
W3=.3607616
W4=W3
W5=.1713245
W6=W5
UA1=W1*FM(RHO,CN2,AWAVE,PATH,U1,Y)
UA2=W2*FM(RHO,CN2,AWAVE,PATH,U2,Y)
UA3=W3*FM(RHO,CN2,AWAVE,PATH,U3,Y)
UA4=W4*FM(RHO,CN2,AWAVE,PATH,U4,Y)
UA5=W5*FM(RHO,CN2,AWAVE,PATH,U5,Y)
UA6=W6*FM(RHO,CN2,AWAVE,PATH,U6,Y)
ANSU1=C2*(UA1+UA2+UA3+UA4+UA5+UA6)
RETURN
END
SUBROUTINE YGAUSS(RHO,CN2,AWAVE,PATH,AY1,AY2,ANS)
D1=(AY1+AY2)*.5
D2=(AY2-AY1)*.5
Y1=-.2386915*D2+D1
Y2=.2386915*D2+D1
Y3=-.6612094*D2+D1
Y4=.6612094*D2+D1
Y5=-.9324695*D2+D1
Y6=.9324695*D2+D1
W1=.4679139
W2=W1
W3=.3607616
W4=W3
W5=.1713245
W6=W5
YA1=W1*UGAUSS(PATH,RHO,CN2,AWAVE,Y1)
YA2=W2*UGAUSS(PATH,RHO,CN2,AWAVE,Y2)
YA3=W3*UGAUSS(PATH,RHO,CN2,AWAVE,Y3)
YA4=W4*UGAUSS(PATH,RHO,CN2,AWAVE,Y4)
YA5=W5*UGAUSS(PATH,RHO,CN2,AWAVE,Y5)
YA6=W6*UGAUSS(PATH,RHO,CN2,AWAVE,Y6)
ANS=D2*(YA1+YA2+YA3+YA4+YA5+YA6)
RETURN
END
FUNCTION FM(RHO,CN2,AWAVE,PATH,U,Y)
IF(Y.LE.0.) GO TO 251
IF(ABS(U).LE..001.OR.ABS(U).GE..99) GO TO 251
AXXX=U*(1.-U)
AK=44.*1.361/(7.*AWAVE)
AL1=.00055
TERM1=((2.*AK)/(PATH*U*(1.-U)))**(.5)
F16=1.1107207*(AK**(1.5))*(PATH**(1.5))*CN2
F11=(1.+SQRT(Y)*TERM1*AL1)/(Y**(1.5))
F12=EXP(-Y*AL1*TERM1)
F13=(U*(1.-U))**(.5)
```

```
      F14=SIN(Y)**2.
      TERM2=RHO*SQRT(Y)*TERM1*U
      F15=AJ0(TERM2)
      F17=FYC(CN2,AWAVE,PATH,U,Y)
      F18=EXP(-F17)
      FM=F11*F12*F13*F14*F15*F16*F18
      GO TO 252
251   FM=0.
252   CONTINUE
      RETURN
      END
      FUNCTION UGAUSS(PATH,RHO,CN2,AWAVE,Y)
      AU=0.
      BU=1.
      NU=2
      TNSU=0.
 501  ANSU=0.
      DO 502  IU=1,NU
      ANU=NU
      A1=AU+(IU-1.)*(BU-AU)/ANU
      A2=AU+(IU)*(BU-AU)/ANU
      CALL GAUSSU(RHO,CN2,AWAVE,PATH,A1,A2,Y,ANSU2)
      ANSU=ANSU+ANSU2
502   CONTINUE
      IF(ABS(ANSU-TNSU).LE.ABS(.02*ANSU)) GO TO 503
      TNSU=ANSU
      NU=NU*2
      GO TO 501
503   UGAUSS=ANSU
      RETURN
      END
      FUNCTION FX(PATH,CN2,AWAVE,ALPH0,FOCUS,PXM,A,R)
      FXX=F1(PATH,CN2,AWAVE,ALPH0,FOCUS,R)
      FX=FXX*R*AJ0(PXM*R/A)
      RETURN
      END
      FUNCTION FYY(RHO,CN2,AWAVE,PATH)
      TNSX=0.
      ANSX=0.
      AY=0.
721   BY=1.
722   DELTA=BY
723   NY=2
      TNSY=0.
508   ANSY=0.
      DO 509  IY=1,NY
      ANY=NY
      AY1=AY+(IY-1.)*(BY-AY)/ANY
      AY2=AY+IY*(BY-AY)/ANY
      CALL YGAUSS(RHO,CN2,AWAVE,PATH,AY1,AY2,ANSY2)
      ANSY=ANSY+ANSY2
509   CONTINUE
      IF(ABS(ANSY-TNSY).LE.ABS(.02*ANSY)) GO TO 510
      TNSY=ANSY
```

```
      NY=NY*2
      WRITE(6,461) ANSY
461   FORMAT(5X,E14.6)
      IF(NY.GE.4.AND.ABS(ANSY).LE..001) GO TO 510
      GO TO 508
510   ANSX=ANSX+ANSY
      IF(ABS(ANSX-TNSX).LE.ABS(.02*ANSX)) GO TO 732
      AY=AY+DELTA
      BY=BY+DELTA
      TNSX=ANSX
      IF(ABS(ANSX).LE..001) GO TO 732
      GO TO 723
732   FYY=ANSX
      RETURN
      END
```

APPENDIX C

This appendix consists of the computer program called COVAR written to evaluate the covariance, normalized to the square of the average intensity. In order to make the data useful for a wide range of VSCR values, the coherent and incoherent parts are printed separately for each spacing and propagation data. The input is path length, wave length, beam size and focal length. The turbulence data corresponds to 9 data points where the Rytov variance is specified under SIGI(9). The spacings are .005 meters to .030 meters with an increment of .005 meters. These data points are called P1 (initial spacing), P2 (final spacing) and DELP (increment in spacing). By changing these values, the program can be used for arbitrary spacings. The coherent part in the output is called AINT2 and the incoherent part is called AINT1.

```
      DIMENSION PM(15),AJ1(15),CX1(6),CX2(6)
C     PROGRAM NAME IS COVAR
C     PROGRAM TO CALCULATE THE SPATIAL COVARIANCE AT
C     LOW TURBULENCE LEVELS.IT ALSO GIVES GOOD
C     RESULTS FOR THE STRONG TURBULENCE CONDITIONS
C     FOR REASONS EXPALINED IN THE TEXT.
C     P1 IS THE INTIAL DETECTOR SPACING, P2 IS THE FINAL
C     DETECTOR SPACING AND DELP IS THE INCREMENT.
C     P1,P2 AND DELP SHOULD BE CHANGED FOR THE
C     DESIRED VALUES OF THE SPACING, UNDER CONSIDERATION.
C     OUTPUT CONSISTS OF ALL THE PROPAGATION DATA,
C     DETECTOR SPACING VALUES AND THE COHERENT TERM(AINT2)
C     AND THE INCOHERENT TERM(AINT1). FOR DETAILED
C     MEANING OF THESE TERMS, SEE THE CHAPTER ON THE
C     COVARIANCE (CHAPTER VI).
C     PROGRAM CAN BE CHANGED , IF THE FREQUNCIES ARE
C     WIDELY SEPERATED BY USING THE PROGRAMS RAO2FF
C     AND CXX2FF.
C     SIGI IS THE RYTOV VARIANCE
C     THIS PROGRAM GENERATES DATA FOR SEVERAL VALUES
C     OF DETECTOR SPACINGS , FOR 9 VALUES OF THE
C     RYTOV VARIANCE ,SPECIFIED IN THE DATA.
C     THE INPUT CAN BE SUITABLY MODIFIED,DEPENDING
C     ON THE PROBLEM ,UNDER CONSIDERATION.
      DIMENSION CN2I(3),BM(10)
      DATA PM /2.4048,5.5201,8.6537,11.7915,14.9309,
     C18.0711,21.2116,24.3525,27.4935,30.6346,33.7758
     C,36.9171,40.0584,43.1998,46.3412/
      DATA AJ1 /.51915,-.34206,.27145,-.23246,-.20635,
     C -.167738773,.17327,-.16170,-.15218,.144166,
     C -.1373,.1313245,-.12607,.1239,-.11721/
      DATA CN2I /1.E-15,1.E-14,1.E-13/
      READ(5,77)  PATH
      READ(5,77) FOCUS
      READ(5,77) AWAVE
      READ(5,77) ALPH0
 77   FORMAT(E10.4)
      DO 99 INDEX=1,3
      PHI=22./7.
      AK=2.*PHI/AWAVE
      CONSS=.124*(AK**(7./6.))*PATH**(11./6.)
      CN2=CN2I(INDEX)
      WRITE(6,41)  PATH,FOCUS,ALPH0
      WRITE(4,41)  PATH,FOCUS,ALPH0
 41   FORMAT(2X,'PATH=',F5.0,2X,'FOCUS=',F5.0,2X,
     1 'ALPH0=',F6.4)
      WRITE(6,40)  CN2,AWAVE
      WRITE(4,40)  CN2,AWAVE
 40   FORMAT(2X,'CN2=',E14.6,5X,'AWAVE=',E14.6)
      ARHO=1.09215*CN2*AK*AK*PATH
C     THE NEXT STEP DECIDES THE RANGE TO GET BMS
      CHOP=.01
      A1=1./(2.*ALPH0**2)
```

```
      A2=1./(ARHO**(1.2))
      A=(A1+A2)**(-.5)/100.
 22   X=F1(PATH,CN2,AWAVE,ALPH0,FOCUS,1.,A)
      IF(ABS(X).LT.CHOP)   GO TO 23
      A=A*1.1
      GO TO 22
 23   WRITE(6,175) A
      WRITE(4,175) A
 175  FORMAT(5X,'A=',E14.6)
C     A IS THE RANGE WHERE F1  IS CHOPPED
      M=1
 29   IF(M.GT.6)      GO TO 25
      AR=0.
      BR=1.
      DR=(BR-AR)*.5
      PXM=PM(M)
      SUM1=FX(PATH,CN2,AWAVE,ALPH0,FOCUS,PXM,A,AR)
     C+2.*FX(PATH,CN2,AWAVE,ALPH0,FOCUS,PXM,A,DR)
     C+FX(PATH,CN2,AWAVE,ALPH0,FOCUS,PXM,A,BR)
      SUMA=SUM1*DR*.5
      NR=1
 26   NR=2*NR
      TDR=DR
      DR=DR*.5
      R=AR+DR
      DO 101  IR=1,NR
      SUM1=SUM1+2.*FX(PATH,CN2,AWAVE,ALPH0,FOCUS,PXM,A,R)
      R=R+TDR
 101  CONTINUE
      SUM2=SUM1*DR*.5
      IF(ABS(SUM2-SUMA).LE.ABS(.01*SUM2)) GO TO 666
      IF(NR.GT.2048)      GO TO 667
      SUMA=SUM2
      GO TO 26
 666  IF(NR.GT.16)      GO TO 667
      SUMA=SUM2
      GO TO 26
 667  BM(M)=SUM2*2./((AJ1(M))**2.)
      M=M+1
      GO TO 29
 25   CONTINUE
      SUMC=0.
      DO 103  M=1,6
      WRITE(6,28)  M,BM(M)
      SUMC=SUMC+BM(M)
 28   FORMAT(4X,'M=',I4,'BM(M)=',F10.7)
 103  CONTINUE
      WRITE(6,94)  SUMC
      WRITE(4,94)   SUMC
 94   FORMAT(10X,'SUMC=',F10.7)
C     CALCULATIONS FOR COVARIANCE
      P1=.005
      DELP=.005
      P2=.050
```

```
      P=P1
 830  CONTINUE
      IF(P.GT.P2) GO TO 401
C     CALCULATIONS FOR CX1(MC) FOLLOW
      SIGMAT=.124*AK**(7./6.)*PATH**(11./6.)*CN2
      WRITE(4,93)   SIGMAT
      WRITE(6,93)   SIGMAT
 93   FORMAT(4X,'SIGMAT=',E14.6)
      MC=1
 32   IF(MC.GT.6)      GO TO 33
      RHO=PATH*PM(MC)/(A*AK)
      IF(MC.EQ.1)  GO TO 908
      MC1=MC-1
      DIFF=ABS(CX1(MC1)-1.)
      IF(ABS(DIFF).LE..001)  GO TO 910
 908  CONTINUE
      CX1(MC)=FCX(RHO,P,CN2,PATH,ALPH0,FOCUS,AWAVE)
     1 *.15909091
      GO TO 911
 910  CX1(MC)=1.
 911  CONTINUE
      MC2=MC-1
      IF(MC2.GE.1.AND.ABS(BM(MC)).LE..01)   GO TO 912
      CX2(MC)=FF1(RHO,P,CN2,PATH,ALPH0,FOCUS,AWAVE)
     1 *.15909091
      GO TO 913
912   CX2(MC)=0.
 913  CONTINUE
 907  CONTINUE
      WRITE(6,511) MC,BM(MC),CX1(MC),CX2(MC)
      WRITE(4,511)  MC,BM(MC),CX1(MC),CX2(MC)
 511  FORMAT(3X,'MC=',I3,2X,'BM(MC)=',E10.4,2X,
     1 'CX1(MC)=',E10.4,3X,'CX2(MC)=',E10.4)
      MC=MC+1
      GO TO 32
 33   CONTINUE
      AINT1=0.
      AINT2=0.
      DO 522 M=1,6
      AINT1=AINT1+BM(M)*CX1(M)
      AINT2=AINT2+BM(M)*CX2(M)
 522  CONTINUE
      AINT1=AINT1+1.-SUMC
      AINT2=AINT2+1.-SUMC
      WRITE(6,524)  P,AINT1,AINT2
      WRITE(4,524)  P,AINT1,AINT2
 524  FORMAT(2X,'P=',F8.5,2X,'AINT1=',E14.6,2X,
     1 'AINT2=',E14.6)
      COVAR=AINT1+AINT2-1.
      WRITE(4,555)  P,COVAR
      WRITE(6,555) P,COVAR
555   FORMAT(3X,'P=',F5.3,5X,'COVAR=',F9.6)
      IF(ABS(COVAR).LE..1)  GO TO 401
      P=P+DELP
```

```
      GO TO 830
  401 CONTINUE
  99  CONTINUE
      STOP
      END
      FUNCTION FCX(RHO,P,CN2,PATH,ALPH0,FOCUS,AWAVE)
C     INTEGRATION OVER THETA
      ATH=0.
      BTH=44./7.
      NTH=1
      TNSTH=0.
  301 STH=0.
      DO 302 ITH=1,NTH
      ANTH=NTH
      ATH1=ATH+(ITH-1.)*(BTH-ATH)/ANTH
      ATH2=ATH+ITH*(BTH-ATH)/ANTH
      STH=STH+FCXT(RHO,P,CN2,PATH,ALPH0,AWAVE,ATH1,ATH2)
  302 CONTINUE
      IF(ABS(STH-TNSTH).LE.ABS(.02*STH)) GO TO 303
      TNSTH=STH
      NTH=NTH*2
      GO TO 301
  303 FCX=STH
      RETURN
      END
      FUNCTION FCXT(RHO,P,CN2,PATH,ALPH0,AWAVE,ATH1,ATH2)
      CTH1=(ATH1+ATH2)*.5
      CTH2=(ATH2-ATH1)*.5
      T1=-.2386915*CTH2+CTH1
      T2=.2386915*CTH2+CTH1
      T3=.6612094*CTH2+CTH1
      T4=-.6612094*CTH2+CTH1
      T5=-.9324695*CTH2+CTH1
      T6=.9324695*CTH2+CTH1
      WT1=.4679139
      WT2=WT1
      WT3=.3607616
      WT4=WT3
      WT5=.1713245
      WT6=WT5
      UT1=WT1*SXX(RHO,P,CN2,PATH,ALPH0,AWAVE,T1)
      UT2=WT2*SXX(RHO,P,CN2,PATH,ALPH0,AWAVE,T2)
      UT3=WT3*SXX(RHO,P,CN2,PATH,ALPH0,AWAVE,T3)
      UT4=WT4*SXX(RHO,P,CN2,PATH,ALPH0,AWAVE,T4)
      UT5=WT5*SXX(RHO,P,CN2,PATH,ALPH0,AWAVE,T5)
      UT6=WT6*SXX(RHO,P,CN2,PATH,ALPH0,AWAVE,T6)
      FCXT=CTH2*(UT1+UT2+UT3+UT4+UT5+UT6)
      RETURN
      END
      FUNCTION GAUSSU(RHO,P,CN2,PATH,ALPH0,AWAVE,T)
      AU=0.
      BU=1.
      NU=1
      TNSU=0.
```

```
501   ANSU=0.
      DO 502 IU=1,NU
      ANU=NU
      AU1=AU+(IU-1.)*(BU-AU)/ANU
      AU2=AU+IU*(BU-AU)/ANU
      ANSU=ANSU+UG(RHO,P,CN2,PATH,ALPH0,AWAVE,T,AU1,AU2)
502   CONTINUE
      IF(ABS(ANSU-TNSU).LE.ABS(.02*ANSU)) GO TO 503
      TNSU=ANSU
      NU=NU*2
      GO TO 501
503   GAUSSU=ANSU
      RETURN
      END
      FUNCTION UG(RHO,P,CN2,PATH,ALPH0,AWAVE,T,AU1,AU2)
      CU1=(AU1+AU2)*.5
      CU2=(AU2-AU1)*.5
      UG1=-.2386915*CU2+CU1
      UG2=.2386915*CU2+CU1
      UG3=-.6612094*CU2+CU1
      UG4=.6612094*CU2+CU1
      UG5=-.9324695*CU2+CU1
      UG6=.9324695*CU2+CU1
      WG1=.4679139
      WG2=WG1
      WG3=.3607616
      WG4=WG3
      WG5=.1713245
      WG6=WG5
      AG1=WG1*CXX(RHO,P,CN2,PATH,ALPH0,AWAVE,T,UG1)
      AG2=WG2*CXX(RHO,P,CN2,PATH,ALPH0,AWAVE,T,UG2)
      AG3=WG3*CXX(RHO,P,CN2,PATH,ALPH0,AWAVE,T,UG3)
      AG4=WG4*CXX(RHO,P,CN2,PATH,ALPH0,AWAVE,T,UG4)
      AG5=WG5*CXX(RHO,P,CN2,PATH,ALPH0,AWAVE,T,UG5)
      AG6=WG6*CXX(RHO,P,CN2,PATH,ALPH0,AWAVE,T,UG6)
      UG=CU2*(AG1+AG2+AG3+AG4+AG5+AG6)
      RETURN
      END
      FUNCTION SXX(RHO,P,CN2,PATH,ALPH0,AWAVE,T)
      SXX=EXP(4.*GAUSSU(RHO,P,CN2,PATH,ALPH0,AWAVE,T))
      RETURN
      END
      FUNCTION FF1(RHO,P,CN2,PATH,ALPH0,FOCUS,AWAVE)
      ATH=0.
      BTH=6.2856
      NTH=1
      TNSTH=0.
201   STH=0.
      DO 202 ITH=1,NTH
      ANTH=NTH
      ATH1=ATH+(ITH-1.)*(BTH-ATH)/ANTH
      ATH2=ATH+ITH*(BTH-ATH)/ANTH
      STH=STH+FFF(RHO,P,CN2,PATH,ALPH0,AWAVE,ATH1,ATH2)
202   CONTINUE
```

```
      IF(ABS(STH-TNSTH).LE.ABS(.02*STH)) GO TO 203
      TNSTH=STH
      NTH=NTH*2
      GO TO 201
203   FF1=STH
      RETURN
      END
      FUNCTION FFF(RHO,P,CN2,PATH,ALPH0,AWAVE,ATH1,ATH2)
      XTH1=(ATH1+ATH2)*.5
      XTH2=(ATH2-ATH1)*.5
      X1=-.2386915*XTH2+XTH1
      X2=.2386915*XTH2+XTH1
      X3=-.6612094*XTH2+XTH1
      X4=.6612094*XTH2+XTH1
      X5=-.9324695*XTH2+XTH1
      X6=.9324695*XTH2+XTH1
      W1=.4679139
      W2=W1
      W3=.3607616
      W4=W3
      W5=.1713245
      W6=W5
      AX1=W1*FX8(RHO,P,CN2,PATH,ALPH0,AWAVE,X1)
      AX2=W2*FX8(RHO,P,CN2,PATH,ALPH0,AWAVE,X2)
      AX3=W3*FX8(RHO,P,CN2,PATH,ALPH0,AWAVE,X3)
      AX4=W4*FX8(RHO,P,CN2,PATH,ALPH0,AWAVE,X4)
      AX5=W5*FX8(RHO,P,CN2,PATH,ALPH0,AWAVE,X5)
      AX6=W6*FX8(RHO,P,CN2,PATH,ALPH0,AWAVE,X6)
      FFF=XTH2*(AX1+AX2+AX3+AX4+AX5+AX6)
      RETURN
      END
      FUNCTION FX8(RHO,P,CN2,PATH,ALPH0,AWAVE,T)
      S1=P*RHO*COS(T)
      S2=44./(7.*AWAVE*PATH)
      AK=44./(7.*AWAVE)
      R11=.545625*CN2*PATH*AK*AK
      R12=2.*R11*P**(5./3.)
      S4=(-1.09125*CN2*AK*AK*PATH*RHO**(5./3.))
      FXXX=FX10(P,RHO,T)+FX11(P,RHO,T)
      S5=(1.455*CN2*AK*AK*PATH*FXXX)
      TR1=GAUSSU(RHO,P,CN2,PATH,ALPH0,AWAVE,T)
      PC=-RHO
      TR2=GAUSSU(PC,P,CN2,PATH,ALPH0,AWAVE,T)
      S6=(2.*(TR1+TR2))
      CONS1=-R12+S4+S5+S6
      CONS2=-CONS1
      IF(CONS2.GT.5) GO TO 310
      CC=EXP(CONS1)
      S3=COS(S1*S2)
      FX8=S3*CC
      GO TO 311
310   FX8=0.
311   CONTINUE
      RETURN
```

```
      END
      FUNCTION FX10(P,RHO,T)
      AL=0.
      BL=1.
      NL=1
      TSFX=0.
450   ANSF=0.
      DO 451 I=1,NL
      AL1=AL+(I-1.)*(BL-AL)/NL
      AL2=AL+I*(BL-AL)/NL
      ANSF=ANSF+FX10G(P,RHO,T,AL1,AL2)
451   CONTINUE
      IF(ABS(ANSF-TSFX).LE.ABS(.02*ANSF)) GO TO 452
      TSFX=ANSF
      NL=NL*2
      GO TO 450
452   FX10=ANSF
      RETURN
      END
      FUNCTION FX10G(P,RHO,T,AL1,AL2)
      C1=(AL1+AL2)/2.
      C2=(AL2-AL1)/2.
      X1=-.2386915*C2+C1
      X2=.2386915*C2+C1
      X3=-.6612094*C2+C1
      X4=.6612094*C2+C1
      X5=-.9324695*C2+C1
      X6=.9324695*C2+C1
      G1=.4679139
      G2=G1
      G3=.3607616
      G4=G3
      G5=.1713245
      G6=G5
      XX1=G1*FX1011(P,RHO,T,X1)
      XX2=G2*FX1011(P,RHO,T,X2)+G3*FX1011(P,RHO,T,X3)+
     CFX1011(P,RHO,T,X4)*G4+G5*FX1011(P,RHO,T,X5)
     C+G6*FX1011(P,RHO,T,X6)
      FX10G=C2*(XX1+XX2)
      RETURN
      END
      FUNCTION FX1011(P,RHO,T,P1)
      TE1=(P*P1)**2.
      TE2=(RHO*(1.-P1))**2.
      TE3=2.*P*RHO*P1*(1.-P1)*COS(T)
      TE4=ABS(TE1+TE2+TE3)
      FX1011=TE4**(5./6.)
      RETURN
      END
      FUNCTION FX11(P,RHO,T)
      AL=0.
      BL=1.
      NL=1
      TG=0.
```

```
460   AG=0.
      DO 461  I=1,NL
      AL1=AL+(I-1.)*(BL-AL)/NL
      AL2=AL+I*(BL-AL)/NL
      AG=AG+FX11G(P,RHO,T,AL1,AL2)
461   CONTINUE
      IF(ABS(AG-TG).LE.ABS(.02*AG)) GO TO 462
      TG=AG
      NL=NL*2
      GO TO 460
462   FX11=AG
      RETURN
      END
      FUNCTION FX11G(P,RHO,T,AL1,AL2)
      C1=(AL1+AL2)*.5
      C2=(AL2-AL1)*.5
      CX1=-.2386915*C2+C1
      CX2=.2386915*C2+C1
      CX3=.6612094*C2+C1
      CX4=-.6612094*C2+C1
      CX5=-.9324695*C2+C1
      CX6=.9324695*C2+C1
      W1=.4679139
      W2=W1
      W3=.3607616
      W4=W3
      W5=.1713245
      W6=W5
      ANS=W1*FX1101(P,RHO,T,CX1)+W2*FX1101(P,RHO,T,CX2)
     C+W3*FX1101(P,RHO,T,CX3)+W4*FX1101(P,RHO,T,CX4)
     C+W5*FX1101(P,RHO,T,CX5)+W6*FX1101(P,RHO,T,CX6)
      FX11G=ANS*C2
      RETURN
      END
      FUNCTION FX1101(P,RHO,T,X)
      TER1=(P*X)**2.
      TE2=(RHO*(1.-X))**2.
      TE3=2.*P*RHO*X*(1.-X)*COS(T)
      TX=ABS(TER1+TE2-TE3)
      FX1101=TX**(5./6.)
      RETURN
      END
      FUNCTION AJ0(X)
      IF(X.GT.1000.) GO TO 888
      IF(X.EQ.0.) GO TO 898
      IF(X.GT.3.) GO TO 71
      X1=X/3.
      AJ0=1.-2.2499997*X1**2+1.2656208*X1**4-.3163866*X1
     C**6+.0444479*X1**8-.0039444*X1**10+.00021*X1**12
      GO TO 72
71    X2=3./X
      F0=.79788456-.00000077*X2-.0055274*X2**2-.0000951*X2
     C**3+.00137237*X2**4-.00072805*X2**5+.00014476*X2**6
      THETA=X-.78539816-.04166397*X2-.00003954*X2**2+
```

```
     C.00262573*X2**3-.00054125*X2**4-.00029333*X2**5+
     1 .00013558*X2**6
      AJ0=FO*COS(THETA)/SQRT(X)
      GO TO 72
888   AJ0=SQRT(.63661977/X)*COS(X-2.3561945)
      GO TO 72
898   AJ0=1.
72    CONTINUE
      RETURN
      END
      FUNCTION F1(PATH,CN2,AWAVE,ALPH0,FOCUS,A,ZF)
      Z2=ZF*A
      ZZ=Z2/ALPH0
      X1=EXP(-ZZ*ZZ/2.)
      AK=44./(7.*AWAVE)
      X3=1.09215*CN2*AK**2*PATH
      Z3=Z2**(5./3.)
      X2=EXP(-X3*Z3)
      X4=AK*(1.-PATH/FOCUS)*Z2*ALPH0/(2.*PATH)
      X5=EXP(-X4*X4*2.)
      F1=X1*X2*X5
      RETURN
      END
      FUNCTION FX(PATH,CN2,AWAVE,ALPH0,FOCUS,PXM,A,R)
      FXX=F1(PATH,CN2,AWAVE,ALPH0,FOCUS,A,R)
      FX=FXX*R*AJ0(PXM*R)
      RETURN
      END
      FUNCTION FF2(Y)
      IF(Y.EQ.0.) GO TO 562
      IF(ABS(Y).LT..01) GO TO 560
      FF2=ABS(SIN(Y))**2./(Y**(11./6.))
      GO TO 561
560   FF2=Y**(1./6.)
      GO TO 561
562   FF2=0.
561   CONTINUE
      RETURN
      END
      FUNCTION CXX(RHO,P,CN2,PATH,ALPH0,AWAVE,T,U)
      IF(ABS(U).LE..001.OR.ABS(U).GE..999) GO TO 902
      PHI=22./7.
      AK=2.*PHI/(AWAVE)
      AUU=ABS(U*(1.-U))
      A1=AUU*PATH/(2.*AK)
      A=SQRT(A1)
      TE1=P*P*U*U+RHO*RHO*(1.-U)*(1.-U)
      TE3=2.*AUU*P*RHO*COS(T)
      TE5=ABS(TE1+TE3)
      B=SQRT(TE5)
      CALL  HS(A,B,CC)
      CXX=.132*PHI*PHI*AK*AK*CN2*PATH*CC
      GO TO 912
902   CXX=0.
```

```
      GO TO 912
 912  CONTINUE
      RETURN
      END
      SUBROUTINE HS(A,B,C)
      DIMENSION C2(9),C3(10)
      INTEGER F1
      DOUBLE PRECISION G2,G3,HK,BB,G,C,H
      DATA C2/9.64586E-3,-.513572E-2,.298032E-1,
     1  -.5402513E0,.205255E2,-1.35296E3,1.37215E5,
     1 -1.9892E7,3.9089E9/
      DATA C3/3.36111,-13.49112,-66.08151,.385934E3
     1  ,.262497E4,-.2044046E5,-.1791784E6,.1747611E7
     1 ,1.8776047E7,-2.2-3577E8/
      Z=B*B/(8*A*A)
      HH=.559167*B**(1.6666667)
      IF (Z.GT.12.56) GO TO 200
      N=31
C POWER SERIES EXPANSION OF H[A,B]
      N1=N+1
      HK=5./(36*4)
      BB=Z*Z*HK
      G2=1.+BB
      N3=N/2+1
      DZ=Z*Z
      TZ=DZ*DZ
      DO 10 J=1,N3
      I=2*J-1
      HK=-HK*(6.*I+1.)*(6.*I+7.)/((6.*(I+2.)*(I+3.))**2)
      IF(J.EQ.1) GO TO 12
      HK=HK*DZ
      GO TO 10
   12 HK=HK*TZ
 10   G2=G2+HK
      HK=5./6.
      BB=HK*Z
      G3=BB
      DO 11 J=0,N3
      I=2*J
      HK=-HK*(6.*I+1.)*(6.*I+7.)/((6.*(I+2)*(I+3))**2)
      IF(J.EQ.0) GO TO 13
      HK=HK*DZ
      GO TO 11
   13 HK=HK*DZ*Z
   11 G3=G3+HK
 100  G=(.25881904*G2+.96592583*G3)
      C=2.975414275*A**1.6666667*G
      C=-HH+C
      RETURN
CASYMPTOTIC EXPANSION OF H[A,B]
 200  ZZ=1/Z
      D1=0.525982*B**1.666667
      G1=C2(1)*ZZ**2+C2(2)*ZZ**4+C2(3)*ZZ**6
     1+C2(4)*ZZ**8+C2(5)*ZZ**10+C2(6)*ZZ**12+C2(7)
```

```
2*ZZ**14+C2(8)*ZZ**16
 G2=1+C3(2)*ZZ**2+C3(4)*ZZ**4+C3(6)*ZZ**6+C3(8)
1 *ZZ**8+C3(10)*ZZ**10
 G3=C3(1)*ZZ+C3(3)*ZZ**3+C3(5)*ZZ**5+C3(7)
1*ZZ**7+C3(9)*ZZ**9
 PO=2.66666667
 H=1.0630853*G1+SIN(Z)*ZZ**PO*G2*.149705
1-.1497*COS(Z)*ZZ**PO*G3
 C=-H*D1
 RETURN
 END
```

APPENDIX D

This appendix consists of the program, TDCCOV, designed to calculate the time delayed covariance of the intensity of speckle patterns. This program was found to be occasionally defective, the reason being that the number of coefficients required to expand the function f_2 of Chapter VII is varying by a large number. Occasionally the function f_2 is practically zero. The output of this program is very extensive, i.e., runs into several pages and this tells whether the program was executed correctly or not. After several corrections, the final output values were used to generate the theoretical values for comparison with experimental data. All the output has been preserved for the future theoretical guidance on this problem. After several steps in the program, the final output consists of two terms, AINT1 (incoherent term) and AINT2 (the coherent term), defined in Chapter VII.

```
C      PROGRAM NAME IS TDCCOV
C      PROGRAM TO EVALUATE THE TIME DELAYED COVARIANCE
C      OF THE INTENSITY OF A LASER SPECKLE PATTERN
C      INPUT DATA IS SELF EXPLANATORY
C      PROGRAM OUTPUT IS VERY EXTENSIVE. THIS IS BECAUSE
C      IT IS FOUND OCCASSIONALLY THE PROGRAM DID NOT WORK
C      OUT WELL DUE TO THE IRREGULAR NATURE OF COFFECIENTS
C      OF EXPANSION IN THE FOURIER-BESSEL SERIES. SO
C      ALL THE IMPORTANT STEPS IN THE PROGRAM OUTPUT
C      HAVE BEEN PRINTED TO CHECK IF THE PROGRAM HAD
C      BEEN EXECUTED CORRECTLY.THE EXTENSIVE OUTPUT HAS
C      BEEN PRESERVED FOR FURTHER STUDY, IF NEEDED.
C      FINAL OUTPUT IS GIVEN AS AINT1 AND AINT2.
C      MEANING OF THESE TERMS  CAN BE FOUND IN CHAPTER VII.
C      POSSIBILITY OF EXTENDING THIS TECHNIQUE TO WIDELY
C      SEPERATED FREQUENCIES WAS NOT INESTIGATED.
       DIMENSION CM(6),CX1(6),PM(15),AJ1(15)
       DATA PM /2.4048,5.5201,8.6537,11.7915,14.9309,
     C 18.0711,21.2116,24.3525,27.4935,30.6346,33.7758,
     C 36.9171,40.0584,43.1998,46.3412/
       DATA AJ1 /.51915,-.34206,.27145,-.23246,-.20635,
     C -.167738773,.17327,-.16170,-.15218,.144166,-.1373,
     C .1313245,-.12607,.1239,-.11721/
       READ(5,70)  PATH
       READ(5,70) FOCUS
 70    FORMAT(E10.4)
       READ(5,71)  ALPH0
 71    FORMAT(F6.4)
       READ(5,71) AWAVE
       AWAVE=AWAVE*(1.E-06)
       READ(5,70)  CN2
       READ(5,71)  P
       READ(5,72)  VEL
 72    FORMAT(F5.2)
       WRITE(4,60) PATH,FOCUS,ALPH0
 60    FORMAT('PATH=',E14.6,3X,'FOCUS=',E14.6,3X,
     1 'ALPH0=',F8.5)
       WRITE(4,61) AWAVE,CN2
 61    FORMAT('AWAVE=',E18.6,3X,'CN2=',E18.6)
C      NN1,NN2,NN3 ARE GIVEN SUCH THAT TD IN THE NEXT
C      FEW STEPS IS THE DESIRED POSITVE OR NEGATIVE
C      TIME DELAY
       READ(5,199) NN1,NN2,NN3
 199   FORMAT(3I3)
       DO 100  ITD=NN1,NN2,NN3
       AITD=ITD
       TD=(AITD-51.)/10000.
       WRITE(4,46) VEL,TD
 46    FORMAT('VEL=',F10.4,5X,'TD=',F10.6)
       PHI=22./7.
       AK=2.*PHI/AWAVE
       ERR=.02
       CCR=.545625*AK*AK*CN2*PATH
```

```
      RO=CCR**(-.6)
      TX=ALPH0/RO
      A0=ALPH0
110   I=0
      X=1.
30    IF(TX.LT.1.)  GO TO 25
      TFX=.5*X*X/(TX*TX)+2.*(X**(1.666667))
      GO TO 51
25    TFX=.5*X*X+2.*((X*TX)**(1.666667))
51    AFX=-TFX+6.
      IF(ABS(AFX).LE.1.E-02)      GO TO 35
      IF(AFX.GT.0.)      GO TO 45
      I=I+1
      X=X-.5**I
      GO TO 30
45    IF(I.GT.0)       GO TO 41
      X=X+1.
      GO TO 30
41    I=I+1
      X=X+.5**I
      GO TO 30
35    AX=X
      IF(TX.LT.1.)       GO TO 43
      AAX=AX*RO
      GO TO 40
43    AAX=AX*ALPH0
40    CONTINUE
      A=AAX
      WRITE(6,888) A
888   FORMAT('A=',E14.6)
      DO 501  MC=1,6
      PY=PM(MC)
      CALL TRAP(1.,AX,ERR,RO,TX,PY,1,CB)
      CM(MC)=CB*2./(AJ1(MC)*AJ1(MC))
      WRITE(6,899)      CM(MC)
899   FORMAT(E14.6)
501   CONTINUE
      AINT1=0.
      DO 506  MC=1,6
      RHO=PM(MC)*PATH/(AAX*AK)
      IF(ABS(CM(MC)).LE..001) GO TO 811
      CX1(MC)=FCX(RHO,P,CN2,PATH,AWAVE,VEL,TD)*.159091
      GO TO 812
811   CX1(MC)=0.
812   CONTINUE
      WRITE(4,815) CM(MC),CX1(MC)
815   FORMAT(2X,'CM(MC)=',E14.6,4X,'CX1(MC)=',E14.6)
      AINT1=AINT1+CM(MC)*CX1(MC)
506   CONTINUE
      WRITE(4,818) TD,AINT1
818   FORMAT(2X,'TIMEDEALY=',E14.6,2X,'AINT1=',E14.6)
      ATH=0.
      BTH=22./7.
      DTH=(BTH-ATH)*.5
```

```
      SUM1=2.*SXX(P,PATH,CN2,ALPH0,FOCUS,AWAVE,VEL,TD,DTH)
     1+SXX(P,PATH,CN2,ALPH0,FOCUS,AWAVE,VEL,TD,ATH)+
     2SXX(P,PATH,CN2,ALPH0,FOCUS,AWAVE,VEL,TD,BTH)
      SUMA=SUM1*DTH*.5
      N=1
 26   N=2*N
      TDTH=DTH
      DTH=DTH*.5
      TH=ATH+DTH
      DO 22 I=1,N
      SUM1=SUM1+2.*SXX(P,PATH,CN2,ALPH0,FOCUS,AWAVE,VEL,
     1 TD,TH)
      TH=TH+TDTH
 22   CONTINUE
      SUM2=SUM1*DTH*.5
      IF(ABS(SUM2-SUMA).LE.ABS(.01*SUMA)) GO TO 667
      SUMA=SUM2
      IF(N.GE.16.AND.ABS(SUM2).LE..001)      GO TO 667
      IF(N.GE.32)      GO TO 667
      GO TO 26
 667  FI=SUM2
      AINT2=FI*7./22.
      WRITE(4,65) TD,AINT2
 65   FORMAT(2X,'TIMEDEALY=',E14.6,4X,'AINT2=',E14.6)
      TDC=AINT1+AINT2-1.
      WRITE(4,99) TD,TDC
 99   FORMAT('***',2X,'TIMEDELAY=',E14.6,4X,'TDC=',E14.6)
 100  CONTINUE
      STOP
      END
      FUNCTION SXX(P,PATH,CN2,ALPH0,FS,AWAVE,VEL,TD,ATH)
      DIMENSION PM(15),AJ1(15),BM(15),DCX(15)
      DATA PM /2.4048,5.5201,8.6537,11.7915,14.9309,
     1 18.0711,21.2116,24.3525,27.4935,30.6346,33.7758,
     C 36.9171,40.0584,43.1998,46.3412/
      DATA AJ1 /.51915,-.34206,.27145,-.23246,-.20635,
     1 -.167738773,.17327,-.1617,-.15218,.144166,-.1373,
     1 .1313245,-.12607,.1239,-.11721/
      PHI=22./7.
      AK=2.*PHI/AWAVE
      ARHO=1.09215*CN2*AK*AK*PATH
C      THE NEXT STEP DECIDES THE RANGE TO GET BMS
      CHOP=.01
      A1=1./(2.*ALPH0**2)
      A2=1./(ARHO**(1.2))
      A=(A1+A2)**(-.5)/1000.
      DELA=.002
      IF(ABS(TD).GE..0035)      DELA=.0002
 22   X=F1(PATH,CN2,AWAVE,ALPH0,FS,ATH,VEL,TD,A)
      IF(ABS(X).LE.CHOP)      GO TO 23
      A=A+DELA
      GO TO 22
 23   WRITE(4,175) A
 175  FORMAT(5X,'A=',E14.6)
```

```
C       A IS THE RANGE WHERE F1  IS CHOPPED
      M=1
      SUMFF=EXP(-2.95*CN2*AK*AK*PATH*((ABS(VEL*TD))**
     1 1.666667))
      SUMXX=0.
 29   IF(M.GT.14) GO TO 25
      IF(M.EQ.1) GO TO 669
      MX=M-1
      IF(ABS(SUMFF-SUMXX).LE..01) GO TO 668
      IF((M.GE.2).AND.(ABS(BM(MX)).LE.1.E-05)) GO TO 668
      GO TO 669
 668  BM(M)=0.
      M=M+1
      GO TO 29
 669  CONTINUE
      AR=0.
      BR=1.
      DR=(BR-AR)*.5
      PXM=PM(M)
      PGM=AJ1(M)
      SUM1=2.*FX(PATH,CN2,AWAVE,ALPH0,FS,PXM,PGM,ATH,
     1 VEL,TD,A,DR)
      SUMA=SUM1*DR*.5
      NR=1
 26   NR=2*NR
      TDR=DR
      DR=DR*.5
      R=AR+DR
      DO 101 IR=1,NR
      SUM1=SUM1+2.*FX(PATH,CN2,AWAVE,ALPH0,FS,PXM,PGM
     C ,ATH,VEL,TD,A,R)
      R=R+TDR
 101  CONTINUE
      SUM2=SUM1*DR*.5
      IF(ABS(SUM2-SUMA).LE.ABS(.01*SUMA))  GO TO 667
      SUMA=SUM2
      GO TO 26
 667  BM(M)=SUM2*2.
      IF(ABS(BM(M)).GE.1.)       BM(M)=0.
      SUMXX=SUMXX+BM(M)
      M=M+1
      GO TO 29
 25   CONTINUE
      SUMC=0.
      DO 105 MC=1,14
      RHO=PM(MC)*PATH/(A*AK)
      DCX(MC)=0.
      IF(ABS(BM(MC)).GT.0.) DCX(MC)=FX8(RHO,P,CN2,PATH,
     1 AWAVE,VEL,TD)
      SUMC=SUMC+DCX(MC)*BM(MC)
      IF(BM(MC).EQ.0.)  GO TO 109
 109  CONTINUE
 105  CONTINUE
      SUMG=SUMFF-SUMXX
```

```
      WRITE(4,833) SUMFF,SUMXX,SUMG
833   FORMAT(1X,'SUMFF=',E14.6,2X,'SUMXX=',E14.6,2X,
     1 'SUMG=',E14.6)
      SXX=SUMC+SUMG
      WRITE(4,188) SXX
188   FORMAT(2X,'SXX=',E14.6)
      RETURN
      END
      FUNCTION FX10(RHO,ATH,VEL,TD)
      AL=0.
      BL=1.
      DL=(BL-AL)*.5
      FI1=GX(RHO,AL,ATH,VEL,TD)+GX(RHO,BL,ATH,VEL,TD)
      AAL=AL+DL
      FI2=GX(RHO,AAL,ATH,VEL,TD)
      FI3=0.
      FIP=DL*(FI1+4.*FI2)/3.
      N=1
21    N=N*2
      FI3=FI2+FI3
      FI2=0.
      TDL=DL
      DL=DL*.5
      XL=AL+DL
      DO 22 I=1,N
      FI2=FI2+GX(RHO,XL,ATH,VEL,TD)
      XL=XL+TDL
22    CONTINUE
      FI=DL*(FI1+4.*FI2+2.*FI3)/3.
      IF(ABS(FI-FIP)-(.02*ABS(FI))) 42,42,43
43    FIP=FI
      GO TO 21
42    FX10=FI
      RETURN
      END
      FUNCTION GX(RHO,P1,ATH,VEL,TD)
      TE2=RHO*RHO*(1.-P1)*(1.-P1)
      TE5=2.*VEL*RHO*TD*(1.-P1)*COS(ATH)
      TE6=VEL*TD*VEL*TD
      TE7=ABS(TE2-TE5+TE6)
      GX=TE7**(.8333333)
      RETURN
      END
      FUNCTION AJ0(X)
      IF(X.GT.1000.)      GO TO 888
      IF(X.EQ.0.)      GO TO 898
      IF(X.GT.3.)      GO TO 71
      X1=X/3.
      AJ0=1.-2.2499997*X1**2+1.2656208*X1**4-.3163866*X1**
     C6+.0444479*X1**8-.0039444*X1**10+.00021*X1**12
      GO TO 72
71    X2=3./X
      F0=.79788456-.00000077*X2-.0055274*X2**2-.0000951*X2
     C**3+.00137237*X2**4-.00072805*X2**5+.00014476*X2**6
```

```
      THETA=X-.78539816-.04166397*X2-.00003954*X2**2+
     C.00262573*X2**3-.00054125*X2**4-.00029333*X2**5+
     1 .00013558*X2**6
      AJ0=FO*COS(THETA)/SQRT(X)
      GO TO 72
888   AJ0=SQRT(.63661977/X)*COS(X-2.3561945)
      GO TO 72
898   AJ0=1.
72    CONTINUE
      END
      FUNCTION F1(PATH,CN2,AWAVE,ALPH0,FFS,ATH,VEL,TD,Z2)
      ZZ=Z2/ALPH0
      X1=EXP(-ZZ*ZZ/2.)
      AK=44./(7.*AWAVE)
      X3=2.91*CN2*AK**2*PATH
      Z21=-Z2
      X21=FX10(Z21,ATH,VEL,TD)
      X2=EXP(-X3*X21)
      X4=AK*(1.-PATH/FFS)*Z2*ALPH0/(2.*PATH)
      X5=EXP(-X4*X4*2.)
      F1=X1*X2*X5
      RETURN
      END
      FUNCTION FX(PX,CN2,AW,A0,FS,PXM,PGM,ATH,V,TD,A,R)
      ZZ=R*A/A0
      X1=EXP(-ZZ*ZZ*.5)
      AK=44./(7.*AW)
      X4=AK*(1.-PX/FS)*R*A*A0/(2.*PX)
      X5=EXP(-X4*X4*2.)
      X3=2.91*CN2*AK*AK*PX
      Z21=R*A
      X21=FX10(Z21,ATH,V,TD)
      X2=EXP(-X3*X21)
      FX=X1*X2*X5*R*AJ0(PXM*R)/(PGM*PGM)
      RETURN
      END
      FUNCTION GAUSSU(RHO,P,CN2,PATH,AWAVE,VEL,TD)
      AU=0.
      BU=1.
      DU=(BU-AU)*.5
      FIU1=CXX(RHO,P,CN2,PATH,AWAVE,AU,VEL,TD)+
     1CXX(RHO,P,CN2,PATH,AWAVE,BU,VEL,TD)
      ADU=AU+DU
      FIU2=CXX(RHO,P,CN2,PATH,AWAVE,ADU,VEL,TD)
      FIU3=0.
      FIPU=DU*(FIU1+4.*FIU2)/3.
      NU=1
31    NU=2*NU
      FIU3=FIU2+FIU3
      FIU2=0.
      TDU=DU
      DU=DU*.5
      U=AU+DU
      DO 32 I=1,NU
```

```
      FIU2=FIU2+CXX(RHO,P,CN2,PATH,AWAVE,U,VEL,TD)
      U=U+TDU
32    CONTINUE
      FIU=DU*(FIU1+4.*FIU2+2.*FIU3)/3.
      IF(ABS(FIU-FIPU)-(.02*ABS(FIU))) 43,43,33
33    FIPU=FIU
      IF(NU.GE.16.AND.ABS(FIU).LE..001)  GO TO 43
      GO TO 31
43    GAUSSU=FIU
      RETURN
      END
      FUNCTION CXX(RHO,P,CN2,PATH,AWAVE,U,VEL,TD)
      IF(ABS(U).LE..001.OR.ABS(U).GE..999)  GO TO 902
      PHI=22./7.
      AK=2.*PHI/(AWAVE)
      A1=U*(1.-U)*PATH/(2.*AK)
      A=SQRT(A1)
      TE1=P*P*U*U+VEL*VEL*TD*TD+RHO*RHO*(1.-U)*(1.-U)
      TE2=2.*U*P*VEL*TD
      TE3=2.*U*(1.-U)*P*RHO
      TE4=2.*VEL*TD*(1.-U)*RHO
      TE5=TE1-TE2+TE3-TE4
      B=SQRT(TE5)
      CALL  HS(A,B,CC)
      CXX=.132*PHI*PHI*AK*AK*CN2*PATH*CC
      GO TO 912
902   CXX=0.
      GO TO 912
912   CONTINUE
      RETURN
      END
      FUNCTION FX8(RHO,P,CN2,PATH,AWAVE,VEL,TD)
      AK=44./(7.*AWAVE)
      S1=P*RHO
      S2=AK/PATH
      R11=.545625*CN2*PATH*AK*AK
      S4=1.09125*CN2*AK*AK*PATH*RHO**(1.6666667)
      FXXX=XM10(P,RHO,VEL,TD)
      S5=1.455*CN2*AK*AK*PATH*FXXX
      PC=-RHO
      TR1=GAUSSU(RHO,P,CN2,PATH,AWAVE,VEL,TD)
      TR2=GAUSSU(PC,P,CN2,PATH,AWAVE,VEL,TD)
      S6=EXP(2.*(TR1+TR2)-S4+S5)
      S3=AJ0(S1*S2)
      FX8=S3*S6
      IF(ABS(FX8).GE.10.) FX8=0.
      WRITE(6,98) FX8
98    FORMAT(2X,'FX8=',E14.6)
      RETURN
      END
      FUNCTION XM10(P,RHO,VEL,TD)
      A=0.
      B=1.
      DX=(B-A)*.5
```

```
      FI1=XM(P,RHO,A,VEL,TD)+XM(P,RHO,B,VEL,TD)
      FI2=XM(P,RHO,DX,VEL,TD)
      FI3=0.
      FIP=DX*(FI1+4.*FI2)/3.
      N=1
 61   N=2*N
      FI3=FI2+FI3
      FI2=0.
      TDX=DX
      DX=DX*.5
      X=A+DX
      DO 62 I=1,N
      FI2=FI2+XM(P,RHO,X,VEL,TD)
      X=X+TDX
 62   CONTINUE
      FI=DX*(FI1+4.*FI2+2.*FI3)/3.
      IF(ABS(FI-FIP)-(.02*ABS(FI))) 64,64,63
 63   FIP=FI
      IF(ABS(FI).LE..001.AND.N.GE.32)  GO TO 64
      GO TO 61
 64   XM10=FI
      RETURN
      END
      FUNCTION  XM(P,RHO,X,VEL,TD)
      TE1=P*P*X*X+VEL*VEL*TD*TD+(1.-X)*(1.-X)*RHO*RHO
      TE2=2.*X*P*VEL*TD
      TE3=2.*X*P*RHO*(1.-X)
      TE4=2.*VEL*TD*RHO*(1.-X)
      TE5=ABS(TE1-TE2+TE3-TE4)
      TE9=TE5**(.8333333)
      TE10=ABS(TE1-TE2-TE3+TE4)
      TE11=TE10**(.833333)
      TE8=2.*((ABS(P*X-VEL*TD))**(1.666667))
      XM=TE9+TE11-TE8
      RETURN
      END
      FUNCTION FCX(RHO,P,CN2,PATH,AWAVE,VEL,TD)
C      INTEGRATION OVER THETA
      A=0.
      B=44./7.
      DX=(B-A)/2.
      FI1=RXX(RHO,P,CN2,PATH,AWAVE,A,VEL,TD)+RXX(RHO,
     1P,CN2,PATH,AWAVE,B,VEL,TD)
      AAX=A+DX
      FI2=RXX(RHO,P,CN2,PATH,AWAVE,AAX,VEL,TD)
      FI3=0.
      FIP=DX*(FI1+4.*FI2)/3.
      N=1
 21   N=N*2
      FI3=FI2+FI3
      FI2=0.
      TDX=DX
      DX=.5*DX
      X=A+DX
```

```
      DO 22 I=1,N
      FI2=FI2+RXX(RHO,P,CN2,PATH,AWAVE,X,VEL,TD)
      X=X+TDX
22    CONTINUE
      FI=DX*(FI1+4.*FI2+2.*FI3)/3.
      IF(ABS(FI-FIP)-(.02*ABS(FI)))  42,42,43
43    FIP=FI
      GO TO 21
42    FCX=FI
      WRITE(6,99) N,FI
99    FORMAT(I6,2X,'FI=',E14.6)
      RETURN
      END
      FUNCTION UGAUSS(RHO,P,CN2,PATH,AWAVE,T,VEL,TD)
      AU=0.
      BU=1.
      DU=(BU-AU)*.5
      FIU1=ZXX(RHO,P,CN2,PATH,AWAVE,T,AU,VEL,TD)+
     1 ZXX(RHO,P,CN2,PATH,AWAVE,T,BU,VEL,TD)
      ADU=AU+DU
      FIU2=ZXX(RHO,P,CN2,PATH,AWAVE,T,ADU,VEL,TD)
      FIU3=0.
      FIPU=DU*(FIU1+4.*FIU2)/3.
      NU=1
31    NU=NU*2
      FIU3=FIU2+FIU3
      FIU2=0.
      TDU=DU
      DU=DU*.5
      U=AU+DU
      DO 32 I=1,NU
      FIU2=FIU2+ZXX(RHO,P,CN2,PATH,AWAVE,T,U,VEL,TD)
      U=U+TDU
32    CONTINUE
      FIU=DU*(FIU1+4.*FIU2+2.*FIU3)/3.
      IF(ABS(FIU-FIPU)-(.02*ABS(FIU)))  43,43,33
33    FIPU=FIU
      IF(NU.GE.16.AND.ABS(FIU).LE..001)       GO TO 43
      GO TO 31
43    UGAUSS=FIU
      RETURN
      END
      FUNCTION ZXX(RHO,P,CN2,PATH,AWAVE,T,U,VEL,TD)
      IF(ABS(U).LE..001.OR.ABS(U).GE..999)  GO TO 902
      PHI=22./7.
      AK=2.*PHI/AWAVE
      A1=U*(1.-U)*PATH/(2.*AK)
      A=SQRT(ABS(A1))
      TE1=P*P*U*U+VEL*VEL*TD*TD+RHO*RHO*(1.-U)*(1.-U)
      TE2=2.*U*P*VEL*TD
      TE3=2.*U*(1.-U)*P*RHO*COS(T)
      TE4=2.*VEL*TD*(1.-U)*RHO*COS(T)
      TE5=TE1-TE2+TE3-TE4
      B=SQRT(ABS(TE5))
```

```
      CALL HS(A,B,CC)
      ZXX=.132*PHI*PHI*CN2*AK*AK*PATH*CC
      GO TO 912
 902  ZXX=0.
 912  CONTINUE
      RETURN
      END
      FUNCTION RXX(RHO,P,CN2,PATH,AWAVE,T,VEL,TD)
      RXX=EXP(4.*UGAUSS(RHO,P,CN2,PATH,AWAVE,T,VEL,TD))
      RETURN
      END
      FUNCTION BIX(X)
      IF(X.GT.3.)  GO TO 1
      YY=X/3.
      Y=YY*YY
      BIX=X*(.50+Y*(-.56249985+Y*(.21093573+Y*(-.03954289+
     C+Y*(.00443319+Y*(-.00031761+Y*(.00001109)))))))
      GO TO 2
1     Y=3./X
      FF1=.79788456+Y*(.00000156+Y*(.01659667+Y*(.00017105
     C+Y*(-.0024951+Y*(.00113653+Y*(-.00020033))))))
      THETA=X-2.35619449+Y*(.12499612+Y*(.00005650+Y*(
     C-.00637879+Y*(.00074348+Y*(.00079824+Y*(
     1 -.000291666))))))
      BIX=FF1*COS(THETA)/SQRT(X)
2     RETURN
      END
      SUBROUTINE TRAP(A,AX,ERR,RO,TX,FL,L,FI)
      DX=.5
      FI1=GRAN(A,AX,RO,TX,L,FL)/2.
      FI2=GRAN(DX,AX,RO,TX,L,FL)
      FIP=DX*(FI1+FI2)
      N=1
      J=0
    1 N=2*N
      TDX=DX
      DX=.5*DX
      X=DX
      DO 2 I=1,N
      FI2=FI2+GRAN(X,AX,RO,TX,L,FL)
    2 X=X+TDX
      FI=DX*(FI1+FI2)
      FI3=ABS(FI-FIP)
      FI4=ERR*ABS(FI)
      IF(FI3.LE.FI4)  GO TO 4
      IF(J.GE.9)  GO TO 5
      FIP=FI
      J=J+1
      GO TO 1
    5 WRITE(6,7)
    7 FORMAT(2X,'LIMIT(TRAP) REACHED')
    4 RETURN
      END
      FUNCTION GRAN(X,AX,RO,TX,L,FL)
```

```
      AO=RO*TX
      T1=FL*X
      IF(L.EQ.1) T2=AJ0(T1)
      IF(L.EQ.2) T2=BIX(T1)
      IF(TX.LT.1.)  GO TO 1
      T3=.5*((AX*X)**2)/(TX*TX)
      T4=2.*((AX*X)**(5./3.))
      T5=EXP(-T3-T4)
      GO TO 6
    1 T6=.5*((AX*X)**2)+2.*((AX*TX*X)**(5./3.))
      T5=EXP(-T6)
    6 GRAN=X*T2*T5
      IF(L.EQ.1)  GO TO 7
      IF(TX.LT.1.)  GO TO 8
      GRAN=GRAN*((AX*X*RO)**(2./3.))
      GO TO 7
    8 GRAN=GRAN*((AX*X*AO)**(2./3.))
    7 RETURN
      END
      SUBROUTINE HS(A,B,C)
      DIMENSION C2(9),C3(10)
      INTEGER F1
      DOUBLE PRECISION G2,G3,HK,BB,G,C,H
      DATA C2/9.64506E-3,-.513572E-2,.298032E-1,
     1  -.5402513E0,.205255E2,-1.35296E3,1.37215E5,
     1 -1.9892E7,3.9089E9/
      DATA C3/3.36111,-13.49112,-66.08151,.385934E3
     1  ,.262497E4,-.2044046E5,-.1791784E6,.1747611E7
     1 ,1.8776047E7,-2.2-3577E8/
      Z=B*B/(8*A*A)
      HH=.559167*B**(1.6666667)
      IF (Z.GT.12.56) GO TO 200
      N=31
C POWER SERIES EXPANSION OF H[A,B]
      N1=N+1
      HK=5./(36*4)
      BB=Z*Z*HK
      G2=1.+BB
      N3=N/2+1
      DZ=Z*Z
      TZ=DZ*DZ
      DO 10 J=1,N3
      I=2*J-1
      HK=-HK*(6.*I+1.)*(6.*I+7.)/((6.*(I+2.)*(I+3.))**2)
      IF(J.EQ.1) GO TO 12
      HK=HK*DZ
      GO TO 10
   12 HK=HK*TZ
 10   G2=G2+HK
      HK=5./6.
      BB=HK*Z
      G3=BB
      DO 11 J=0,N3
      I=2*J
```

```
      HK=-HK*(6.*I+1.)*(6.*I+7.)/((6.*(I+2)*(I+3))**2)
      IF(J.EQ.0) GO TO 13
      HK=HK*DZ
      GO TO 11
   13 HK=HK*DZ*Z
   11 G3=G3+HK
  100 G=(.25881904*G2+.96592583*G3)
      C=2.975414275*A**1.6666667*G
      C=-HH+C
      RETURN
CASYMPTOTIC EXPANSION OF H[A,B]
  200 ZZ=1/Z
      D1=0.525982*B**1.666667
      G1=C2(1)*ZZ**2+C2(2)*ZZ**4+C2(3)*ZZ**6
     1+C2(4)*ZZ**8+C2(5)*ZZ**10+C2(6)*ZZ**12+C2(7)
     2*ZZ**14+C2(8)*ZZ**16
      G2=1+C3(2)*ZZ**2+C3(4)*ZZ**4+C3(6)*ZZ**6+C3(8)
     1 *ZZ**8+C3(10)*ZZ**10
      G3=C3(1)*ZZ+C3(3)*ZZ**3+C3(5)*ZZ**5+C3(7)
     1*ZZ**7+C3(9)*ZZ**9
      PO=2.66666667
      H=1.0630853*G1+SIN(Z)*ZZ**PO*G2*.1497105
     1-.1497*COS(Z)*ZZ**PO*G3
      C=-H*D1
      RETURN
      END
```

APPENDIX E

This appendix consists of 2 programs. The first one is called CXX2FF. This is to generate the two frequency log-amplitude covariance function. The input is in order, the path length, the first wave length, the second wave length and the turbulence level. The program actually evaluates the log-amplitude covariance at the integral multiples of the half Fresnel zone sizes, corresponding to the first wave length. This covariance scale size is called RHO in the program. By specifying RHO, if necessary, log-amplitude covariance at any arbitrary value of RHO, can be estimated.

The second program is called SXX2FF. This evaluates the phase covariance as above except the Fresnel zone size is estimated at the center wave length. The first program uses the Kolmogorov spectrum and the latter, modified Tatarskii spectrum with an outer scale of 1 meter and an inner scale of 1 millimeter.

```
C       NAME OF THE PROGRAM IS CXX2FF
C       PROGRAM EVALUATES THE TWO FREQUENCY
C       LOG-AMPLITUDE COVARIANCE C(R,K1,K2)
        READ(5,41) PATH
 41     FORMAT(F6.1)
        READ(5,42) AWAVE1
 42     FORMAT(F6.4)
        AWAVE1=AWAVE1*(1.E-06)
        READ(5,42) AWAVE2
        AWAVE2=AWAVE2*(1.E-06)
        PHI=22./7.
        AK1=2.*PHI/AWAVE1
        AK2=2.*PHI/AWAVE2
        READ(5,43) CN2
43      FORMAT(E10.4)
        FSS=SQRT(AWAVE1*PATH)
        DO 100 J=1,4
        AJ=J*.5
        RHO=AJ*FSS
        ANS=FYY(AK2,RHO,CN2,AK1,PATH)
        WRITE(4,56)  PATH,CN2,AK1,AK2,RHO,ANS
56      FORMAT(6(E10.4,2X))
100     CONTINUE
        ANS1=FYY(AK2,RHO,CN2,AK1,PATH)
        STOP
        END
        FUNCTION AJ0(X)
        IF(X.GT.3.) GO TO 71
        X1=X/3.
        AJ0=1.-2.2499997*X1**2+1.2656208*X1**4-.3163866*
       1X1**6+.0444479*X1**8-.0039444*X1**10+.00021*X1**12
        GO TO 72
 71     X2=3./X
        F0=.79788456-.00000077*X2-.0055274*X2**2-.0000951*X
       1**3+.00137237*X2**4-.00072805*X2**5+.00014476*X2**6
        THETA=X-.78539816-.04166397*X2-.00003954*X2**2+
       1.00262573*X2**3-.00054125*X2**4-.00029333*X2**5+
       1.00013558*X2**6
        AJ0=F0*COS(THETA)/SQRT(X)
        GO TO 72
72      CONTINUE
        RETURN
        END
        SUBROUTINE GAUSSU(AK2,RHO,CN2,AK1,PT,A1,A2,Y,AN)
        C1=(A1+A2)*.5
        C2=(A2-A1)*.5
        U1=-.2386915*C2+C1
        U2=.2386915*C2+C1
        U3=-.6612094*C2+C1
        U4=.6612094*C2+C1
        U5=-.9324695*C2+C1
        U6=.9324695*C2+C1
        W1=.4679139
```

```
      W2=W1
      W3=.3607616
      W4=W3
      W5=.1713245
      W6=W5
      UA1=W1*FM(AK2,RHO,CN2,AK1,PT,U1,Y)
      UA2=W2*FM(AK2,RHO,CN2,AK1,PT,U2,Y)
      UA3=W3*FM(AK2,RHO,CN2,AK1,PT,U3,Y)
      UA4=W4*FM(AK2,RHO,CN2,AK1,PT,U4,Y)
      UA5=W5*FM(AK2,RHO,CN2,AK1,PT,U5,Y)
      UA6=W6*FM(AK2,RHO,CN2,AK1,PT,U6,Y)
      AN=C2*(UA1+UA2+UA3+UA4+UA5+UA6)
      RETURN
      END
      SUBROUTINE YGAUSS(AK2,RHO,CN2,AK1,PT,AY1,AY2,AN)
      D1=(AY1+AY2)*.5
      D2=(AY2-AY1)*.5
      Y1=-.2386915*D2+D1
      Y2=.2386915*D2+D1
      Y3=-.6612094*D2+D1
      Y4=.6612094*D2+D1
      Y5=-.9324695*D2+D1
      Y6=.9324695*D2+D1
      W1=.4679139
      W2=W1
      W3=.3607616
      W4=W3
      W5=.1713245
      W6=W5
      YA1=W1*UGAUSS(AK2,PT,RHO,CN2,AK1,Y1)
      YA2=W2*UGAUSS(AK2,PT,RHO,CN2,AK1,Y2)
      YA3=W3*UGAUSS(AK2,PT,RHO,CN2,AK1,Y3)
      YA4=W4*UGAUSS(AK2,PT,RHO,CN2,AK1,Y4)
      YA5=W5*UGAUSS(AK2,PT,RHO,CN2,AK1,Y5)
      YA6=W6*UGAUSS(AK2,PT,RHO,CN2,AK1,Y6)
      AN=D2*(YA1+YA2+YA3+YA4+YA5+YA6)
      RETURN
      END
      FUNCTION FM(AK2,RHO,CN2,AK1,PATH,U,Y)
      IF(Y.LE.0.)  GO TO 251
      IF(ABS(U).LE..001.OR.ABS(U).GE..99)   GO TO 251
      AXXX=U*(1.-U)
      IF(AXXX.GE.0.)    GO TO 991
      WRITE(6,232) AXXX
  232 FORMAT(F14.8)
991   CONTINUE
      FM11=(U*(1.-U))**((5.)/6.)
      PHI=22./7.
      FM12X=SQRT((4.*PHI*Y*U)/(1.-U))
      WAVEL=44./(7.*AK1)
      FM12Y=SQRT(WAVEL*PATH)
      FM12=FM12X*RHO/FM12Y
      BB=AK1/AK2
      FM13=SIN(Y)*SIN(BB*Y)/(BB*(Y**(11./6.)))
```

```
      CONS=.36558246*CN2*(AK1**(7./6.))*(PATH**(11./6.))
      FM=CONS*FM11*AJ0(FM12)*FM13
      GO TO 252
 251  FM=0.
 252  CONTINUE
      RETURN
      END
      FUNCTION UGAUSS(AK2,PATH,RHO,CN2,AK1,Y)
      AU=0.
      BU=1.
      NU=2
      TNSU=0.
 501  ANSU=0.
      DO 502  IU=1,NU
      ANU=NU
      A1=AU+(IU-1.)*(BU-AU)/ANU
      A2=AU+(IU)*(BU-AU)/ANU
      CALL GAUSSU(AK2,RHO,CN2,AK1,PATH,A1,A2,Y,ANSU2)
      ANSU=ANSU+ANSU2
 502  CONTINUE
      IF(ABS(ANSU-TNSU).LE.ABS(.02*ANSU))   GO TO 503
      TNSU=ANSU
      NU=NU*2
      GO TO 501
 503  UGAUSS=ANSU
      RETURN
      END
      FUNCTION FYY(AK2,RHO,CN2,AK1,PATH)
      SIGMAT=.124*AK1**(7./6.)*(PATH**(11./6.))*CN2
      TNSX=0.
      ANSX=0.
      AY=0.
      IF(SIGMAT.LE.1.)  GO TO 721
      BY=1./(2.*SIGMAT)
      GO TO 722
 721  BY=1.
 722  DELTA=BY
 723  NY=2
      TNSY=0.
 508  ANSY=0.
      DO 509  IY=1,NY
      ANY=NY
      AY1=AY+(IY-1.)*(BY-AY)/ANY
      AY2=AY+IY*(BY-AY)/ANY
      CALL YGAUSS(AK2,RHO,CN2,AK1,PATH,AY1,AY2,ANSY2)
      ANSY=ANSY+ANSY2
 509  CONTINUE
      IF(ABS(ANSY-TNSY).LE.ABS(.02*ANSY))  GO TO 510
      TNSY=ANSY
      NY=NY*2
      WRITE(6,461) ANSY
 461  FORMAT(5X,E14.6)
      IF(NY.GE.4.AND.ABS(ANSY).LE..001)   GO TO 510
      GO TO 508
```

```
510    ANSX=ANSX+ANSY
       IF(ABS(ANSX-TNSX).LE.ABS(.02*ANSX))  GO TO 732
       AY=AY+DELTA
       BY=BY+DELTA
       TNSX=ANSX
       IF(ABS(ANSX).LE..001)    GO TO 732
       GO TO 723
732    FYY=ANSX
       RETURN
       END
```

```
C       PROGRAM NAME IS SXX2FF
        DIMENSION AW(7)
C       PROGRAM EVALUATES THE TWO FREQUENCY
C       PHASE COVARIANCE FUNCTION S(R,K1,K2)
C       USING MODIFIED TATARSKI SPECTRUM FOR THE
C       REFRACTIVE INDEX FLUCTUATIONS.INNER SCALE IS
C       1 MILLIMETER AND OUTER SCALE IS A METER.
        DATA AW /2.128,1.596,1.064,.632,.488,.266,.133/
        PHI=22./7.
        PATH=500.
        AWAVE1=.532E-06
        CN2=5.0000E-14
        WRITE(4,31)  PATH,CN2
  31    FORMAT(3X,'PATH=',F6.1,4X,'CN2=',E10.4)
        DO  100  I=1,8
        WRITE(4,55)
  55    FORMAT(2X,'*****************************')
        AWAVE2=AW(I)*1.E-06
        AK1=2.*PHI/AWAVE1
        AK2=2.*PHI/AWAVE2
        FS1=SQRT(AWAVE1*PATH)
        FS2=SQRT(AWAVE2*PATH)
        WRITE(4,32)AWAVE1,AWAVE2
  32    FORMAT(2X,'AWAVE1=',E10.4,3X,'AWAVE2=',E10.4)
        WRITE(4,33) FS1,FS2
  33    FORMAT(3X,'FS1=',F10.4,4X,'FS2=',F10.4)
        WRITE(4,45)
  45    FORMAT(2X,'STUDY OF PHASE COVARIANCE FOR TWO
      1 FREQUENCY CASE')
        RHO=.001
  44    IF(RHO.GT.(5.*FS1))  GO TO 100
        ANS=FYY(AK2,RHO,CN2,AK1,PATH)
        ANS2=FYY(AK1,RHO,CN2,AK1,PATH)
        ANS3=FYY(AK2,RHO,CN2,AK2,PATH)
        R1=ANS/ANS2
        R2=ANS/ANS3
        R3=RHO/FS1
        R4=RHO/FS2
        WRITE(4,34)  RHO,ANS2,ANS,R3,R1
  34    FORMAT(2X,'RHO=',F7.3,X,'ANS2=',E10.4,X,'ANS=',
      1  E10.4,X,'R3=',F7.3,X,'R1=',F7.3)
        WRITE(4,35) RHO,ANS3,ANS,R4,R2
  35    FORMAT(3X,'RHO=',F7.3,3X,'ANS3=',E10.4,3X,'ANS=',
      1  E10.4,3X,'R4=',F7.3,3X,'R2=',F7.3)
        WRITE(4,36)
  36    FORMAT('&&&&&&&')
        RHO=RHO+.5*FS1
        GO TO 44
 100    CONTINUE
        STOP
        END
        FUNCTION AJ0(X)
        IF(X.GT.3.)       GO TO 71
```

```
      X1=X/3.
      AJ0=1.-2.2499997*X1**2+1.2656208*X1**4-.3163866*X1**
     16+.0444479*X1**8-.0039444*X1**10+.00021*X1**12
      GO TO 72
71    X2=3./X
      FO=.79788456-.00000077*X2-.0055274*X2**2-.0000951*X2
     1**3+.00137237*X2**4-.00072805*X2**5+.00014476*X2**6
      THETA=X-.78539816-.04166397*X2-.00003954*X2**2+
     1.00262573*X2**3-.00054125*X2**4-.00029333*X2**5+
     1 .00013558*X2**6
      AJ0=FO*COS(THETA)/SQRT(X)
      GO TO 72
72    CONTINUE
      RETURN
      END
      SUBROUTINE YGAUSS(AK2,RHO,CN2,AK1,PATH,AY1,AY2,ANS)
      DY=(AY2-AY1)*.5
      FY1=UX(AK2,RHO,CN2,AK1,PATH,AY1)+UX(AK2,RHO,CN2,
     1 AK1,PATH,AY2)
      ADY=AY1+DY
      FY2=UX(AK2,RHO,CN2,AK1,PATH,ADY)
      FY3=0.
      FYP=DY*(FY1+4.*FY2)/3.
      NY=1
31    NY=NY*2
      FY3=FY2+FY3
      FY2=0.
      TDY=DY
      DY=DY*.5
      Y=AY1+DY
      DO 32  I=1,NY
      FY2=FY2+UX(AK2,RHO,CN2,AK1,PATH,Y)
      Y=Y+TDY
32    CONTINUE
      FY=DY*(FY1+4.*FY2+2.*FY3)/3.
      IF(ABS(FY-FYP)-ABS(.02*FY)) 43,43,33
33    FYP=FY
      IF(NY.GE.16.AND.ABS(FY).LE..001) GO TO 43
43    ANS=FY
      RETURN
      END
      FUNCTION UX(AK2,RHO,CN2,AK1,PATH,Y)
      AU=0.
      BU=1.
      DU=(BU-AU)*.5
      FU1=FM(AK2,RHO,CN2,AK1,PATH,Y,AU)+FM(AK2,RHO,CN2,
     1 AK1,PATH,Y,BU)
      FU2=FM(AK2,RHO,CN2,AK1,PATH,Y,DU)
      ADU=AU+DU
      FU2=FM(AK2,RHO,CN2,AK1,PATH,Y,ADU)
      FU3=0.
      FUP=DU*(FU1+4.*FU2)/3.
      NU=1
51    NU=NU*2
```

```
      FU3=FU2+FU3
      FU2=0.
      TDU=DU
      DU=DU*.5
      U=AU+DU
      DO 52 J=1,NU
      FU2=FU2+FM(AK2,RHO,CN2,AK1,PATH,Y,U)
      U=U+TDU
52    CONTINUE
      FU=DU*(FU1+4.*FU2+2.*FU3)/3.
      IF(ABS(FU-FUP).LE.ABS(.02*FU)) GO TO 63
      FUP=FU
      IF(NU.GE.16.AND.ABS(FU).LE..001) GO TO 63
      GO TO 51
63    UX=FU
      RETURN
      END
      FUNCTION FM(AK2,RHO,CN2,AK1,PATH,Y,U)
      IF(ABS(U).LE..001.OR.ABS(U).GE..99) GO TO 251
      AX=ABS(U*(1.-U))
      IF(AX.GE.0.) GO TO 991
      WRITE(6,232) AXXX
232   FORMAT(F14.8)
991   CONTINUE
      AL0=1.
      ALM=5.92/(.001)
      PHI=22./7.
      FM11=AX
      FM12=(2.*AK1*Y)/(AX*PATH)+(1./AL0)**2
      FM13=FM12**(-11./6.)
      FM15=SQRT((2.*AK1*U*Y)/((1.-U)*PATH))*RHO
      FM16=AJ0(FM15)*COS(Y)*COS(Y*AK1/AK2)
      CONS=.132*PHI*PHI*CN2*AK1*AK1*AK2
      FM18=EXP(-2.*AK1*Y/(AX*PATH*ALM*ALM))
      FM=CONS*FM13*FM16*FM18/FM11
      GO TO 252
251   FM=0.
252   CONTINUE
      RETURN
      END
      FUNCTION FYY(AK2,RHO,CN2,AK1,PATH)
      THSX=0.
      ANSX=0.
      PHI=22./7.
      AY=0.
721   BY=2.
722   DELTA=BY
      AY1=AY
      AY2=BY
723   CONTINUE
      CALL YGAUSS(AK2,RHO,CN2,AK1,PATH,AY1,AY2,ANSY2)
      WRITE(6,145)       ANSY2
145   FORMAT(5X,E10.4)
510   ANSX=ANSX+ANSY2
```

```
      IF(ABS(ANSX-TNSX).LE.ABS(.02*ANSX)) GO TO 732
      AY1=AY1+DELTA
      AY2=AY2+DELTA
      TNSX=ANSX
      IF(ABS(ANSX).LE..001) GO TO 732
      GO TO 723
732   FYY=ANSX
      WRITE(6,144) FYY
144   FORMAT(15X,E10.4)
      RETURN
      END
```

APPENDIX F

This appendix consists of seven short programs. The first one is called JJJ. This evaluates the mean square error in replacing the Rice-Nakagami distribution by an equivalent M distribution as discussed in Chapter VIII. The input is M and the mean is assumed to be unity. The program can be modified to get the mean square error for an exponentially weighted distribution as suggested in that program.

The second program is called APPRX. For a given value of M, assuming mean value to be unity, this program estimates the parameters of an equivalent Rice-Nakagami distribution and prints the absolute values of both distributions and their difference for several values of intensity.

The third program, APX, uses the same set of input as earlier, and it estimates moments of intensity of both the distributions and their ratio until the 7th moment of intensity is reached.

The fourth program, KMOMENT, is designed to check whether the intensity of a monochromatic speckle pattern is following a K-distribution. The first few lines of the program explain it.

The fifth program, MOMOMENT, is used to check whether the intensity of a polychromatic speckle pattern is following an M-distribution.

The sixth program, PMOMENT, is designed to compare the validity of theoretical and experimental moments of a polychromatic speckle pattern in turbulence. This program is self-explanatory.

The seventh program is called KDEN11. This is a double precision program, designed to calculate the cumulative probability density function of the speckle intensity in the turbulent atmosphere.

All the programs in this appendix refer to Chapter VIII. All of them are self-explanatory and no detailed explanations are necessary.

```
C       PROGRAM NAME IS JJJ
C       TRAPEZOIDAL INTEGRATION TO GET RICE-NAKAGAMI
C       AND M-DISTRIBUTION
C       IN THIS PROGRAM MEAN VALUE OF M DISTRIBUTION
C       IS UNITY. GIVEN M, IT EVALUATES THEEQUIVALENT
C       ALPHA AND BETA OF RICE-NAKAGAMI DISTRIBUTION.
C       THEN IT TAKES THE DIFFERENCE BETWEEN THE TWO
C       DISTRIBUTIONS FOR EACH VALUE OF INTENSITY
C       AND SQUARES THE ERROR.THIS ERROR IS INTEGRATED
C       FOR ALL VALUES OF INTENSITY FROM ZERO TO
C       INFINITY SO THAT THE FINAL RESULT IS THE MEAN
C       SQUARE ERROR .IN THIS PROGRAM THE DISTRIBUTIONS
 C       ARE NOT WEIGHTED. THEY CAN BE WEIGHTED BY ANY
C       SUITABLE WEIGHTING FUNCTION FOR EXAMPLE,
C       AN EXPONENTIAL DISTTRIBUTION FUNCTION. MODIFICATION
C       OF THE PROGRAM IS RATHER EASY TO INCLUDE
C       THE WEIGHTING FUNCTIONS.
        READ(5,44) M
 44     FORMAT(I2)
        AM=M
        READ(5,44) II
C       II IS THE VALUE OF THE INTENSITY SUCH THAT THE
C       DIFFERENCE BETWEEN THE PDFS IS NEGLIGIBLE. THIS
C       CAN BE PRE-ESTIMATED.
        B=1.-SQRT(1.-1./AM)
        A=1.-B
        DO 121 JJ=1,100
        J1=J1-1
        AJ1=J1
        AI=AJ1/10.
        AR=0.
        BR=II
        DR=(BR-AR)*.5
        SUM1=FX(AI,A,B,AR)+2.*FX(AI,A,B,DR)+FX(AI,A,B,BR)
        SUMA=SUM1*DR*.5
        NR=1
 26     NR=2*NR
        TDR=DR
        DR=DR*.5
        R=AR+DR
        DO 101    IR=1,NR
        SUM1=SUM1+2.*FX(AI,A,B,R)
        R=R+TDR
 101    CONTINUE
        SUM2=SUM1*DR*.5
        IF(ABS(SUM2-SUMA).LE.ABS(.01*SUM2))  GO TO 666
        SUMA=SUM2
        GO TO 26
 666    IF(NR.GT.1000)  GO TO 667
        SUMA=SUM2
        GO TO 26
 667    ANS=SUM2
        WRITE(4,45)  AI,ANS
```

```
  45    FORMAT(2E14.6)
  121   CONTINUE
        STOP
        END
        FUNCTION DIFF1(M,AI)
C       PROGRAM TO CHECK THE VALIDITY OF REPLACING RICE
C       NAKAGAMI BY M DISTRIBUTION
        AM=M
        BETA=1.-SQRT(1.-1./AM)
        ALPHA=1.-BETA
        P1=(ALPHA+AI)/BETA
        P2=EXP(-P1)/BETA
        P3=2.*SQRT(AI*ALPHA)/BETA
        P4=AI0(P3)
        WEIT=EXP(-AI)
        RNX=P2*P4
        RNXW=RNX*WEIT
        G1=AM**AM
        G2=GAMMA(M)
        G3=AI**(AM-1.)
        G4=EXP(-AM*AI)
        ANM=(G1*G3*G4)/G2
        ANMW=ANM*WEIT
        DIFF1=ANM-RNX
        RETURN
        END
        FUNCTION GAMMA(M)
        N=M-1
        SUM=1.
        DO 101 I=1,N
        A=I
        SUM=SUM*A
  101   CONTINUE
        GAMMA=SUM
        RETURN
        END
        FUNCTION AI0(X)
       T=X/3.75
       IF(X.GT.3.75)  GO TO 66
       IF(X.EQ.0.)    GO TO 67
       AI0=1.+3.5156229*T*T+3.0899424*(T**4)+1.2067492*(T**
      16)+.2659732*(T**8)+.036078*(T**10)+.0045813*(T**12)
       GO TO 68
  66   A=1./T
       B=.39894228+.01328592*A+.00225319*(A**2)-.00157565*
      1(A**3)+.0091628*(A**4)-.02057706*(A**5)+.02635537
      2*(A**6)-.01647633*(A**7)+.00392377*(A**8)
       C=EXP(X)
       D=SQRT(X)
       AI0=(B*C)/D
       GO TO 68
  67   AI0=1.
  68   CONTINUE
       RETURN
```

```
      END
      FUNCTION FX(AI,A,B,X)
      IF(X.EQ.0.)  GO TO 55
      CONS=EXP(-A/B)/B
      CC=AI/X+X/B
      IF(CC.GT.15.)  GO TO 55
      C3=EXP(-CC)
      C4=2.*SQRT(X*A)/B
      C5=AI0(C4)-1.
      FX=C3*C5*CONS/X
      GO TO 56
55    FX=0.
56    CONTINUE
      RETURN
      END
```

```
C       PROGRAM NAME IS APPRX
C       PROGRAM TO CHECK THE VALIDITY OF REPLACING
C       RICE-NAKAGAMI DISTRIBUTION BY M-DISTRIBUTION
C       ASSUMES THE MEAN VALUE OF THE M-DISTRIBUTION
C       IS UNITY. GIVEN THE VALUE OF M, IT EVALUATES
C       THE EQUIVALENT ALPHA AND BETA OF RICE-NAKAGAMI
C       DISTRIBUTION BY MATCHING THE FIRST TWO MOMENTS
C       OF INTENSITY.THE PROGRAM EVALUATES BOTH THE
C       DISTRIBUTIONS, THEIR WEIGHTED VALUES AND THE
C       DIFFERENCE FOR SEVERAL VALUES OF INTENSITY.
        READ(5,21) M
 21     FORMAT(I2)
        AM=M
        BETA=1.-SQRT(1.-1./AM)
        ALPHA=1.-BETA
        AI=.01
 33     CONTINUE
        IF(AI.GT.4.)  GO TO 44
        P1=(ALPHA+AI)/BETA
        P2=EXP(-P1)/BETA
        P3=2.*SQRT(AI*ALPHA)/BETA
        P4=AI0(P3)
        WEIT=EXP(-AI)
        RNX=P2*P4
        RNXW=RNX*WEIT
        G1=AM**AM
        G2=GAMMA(M)
        G3=AI**(AM-1.)
        G4=EXP(-AM*AI)
        ANM=(G1*G3*G4)/G2
        ANMW=ANM*WEIT
        DIFF=ANMW-RNXW
        PERC=DIFF*100./(RNXW)
        DIFF1=RNX-ANM
        PERC1=DIFF1*100./RNX
        WRITE(4,55) AI, RNX,ANM,DIFF1,PERC1,RNXW,ANMW,
      1 DIFF,PERC
  55    FORMAT(9(F7.3,2X))
        AI=AI+.1
        GO TO 33
 44     CONTINUE
        STOP
        END
        FUNCTION GAMMA(M)
        N=M-1
        SUM=1.
        DO 101 I=1,N
        A=I
        SUM=SUM*A
 101    CONTINUE
        GAMMA=SUM
        RETURN
        END
```

```
      FUNCTION AI0(X)
      T=X/3.75
      IF(X.GT.3.75)  GO TO 66
      IF(X.EQ.0.)    GO TO 67
      AI0=1.+3.5156229*T*T+3.0899424*(T**4)+1.2067492*(T**
     16)+.2659732*(T**8)+.036078*(T**10)+.0045813*(T**12)
      GO TO 68
66    A=1./T
      B=.39894228+.01328592*A+.00225319*(A**2)-.00157565*(
     1A**3)+.0091628*(A**4)-.02057706*(A**5)+.02635537
     2*(A**6)-.01647633*(A**7)+.00392377*(A**8)
      C=EXP(X)
      D=SQRT(X)
      AI0=(B*C)/D
      GO TO 68
67    AI0=1.
68    CONTINUE
      RETURN
      END
```

```
C          PROGRAM TO COMPARE MOMENTS
C        PROGRAM NAME IS APX
C        PROGRAM COMPARES THE HIGHER ORDER MOMENTS
C        OF RICE-NAKAGMI DISTRIBUTION AND M-DIST.
C        ASSUMES THE MEAN VALUE OF M-DISTRIBUTION
C        IS UNITY. THEN GIVEN M, IT ESTIMATES THE
C        EQUIVALENT SET OF ALPHA AND BETA OF RICE-
C        NAKAGAMI DISTRIBUTION AND EVALUATES HIGHER
C        ORDER MOMENTS OF BOTH THE DISTRIBUTIONS AND
C        THE RATIO OF MOMENTS.
          DIMENSION C(7),D(7)
          WRITE(4,56)
 56       FORMAT(2X,'COMPARISION OF MOMENTS OF M-DIST WITH
     1 RICE-NAKAGAMI DIST')
      DO 301  M=5,20
      WRITE(4,21) M
 21   FORMAT(12X,'M=',I2)
      AM=M
      B=1.-SQRT(1.-1./AM)
      A=1.-B
      XM=1./AM
      C(1)=1.
      C(2)=C(1)*(1.+XM)
      C(3)=C(2)*(1.+2.*XM)
      C(4)=C(3)*(1.+3.*XM)
      C(5)=C(4)*(1.+4.*XM)
      C(6)=C(5)*(1.+5.*XM)
      C(7)=C(6)*(1.+6.*XM)
      D(1)=1.
      D(2)=2.*B*B+4.*A*B+A*A
      D(3)=6.*B**3+18.*A*B**2+9.*B*A**2+A**3
      D(4)=24.*B**4+96.*A*B**3+72.*(A*B)**2+16.*B*A**3+
     1 A**4
      D(5)=120.*B**5+600*A*B**4+600.*A**2*B**3+200.*A**3
     1*B**2+25.*A**4*B+A**5
      D61=720.*B**6+4320.*A*B**5+5400.*A**2*B**4
      D62=2400.*A**3*B**3
      D63=450.*A**4*B**2+36.*B*A**5+A**6
      D(6)=D61+D62+D63
      D71=5040.*B**7+35280.*A*B**6+52920.*A**2*B**5
      D72=29420.*A**3*B**4
      D73=7350.*A**4*B**3+882.*A**5*B**2+49.*A**6*B+A**7
      D(7)=D72+D71+D73
      DO 101  I=1,7
      R=D(I)/C(I)
      WRITE(4,45) I,C(I),D(I),R
 45   FORMAT(I4,2X,3E14.6)
 101  CONTINUE
 301  CONTINUE
      STOP
      END
```

```
C        PROGRAM NAME IS KMOMENT
C        AIM OF THIS PROGRAM IS TO CHECK IF THE SPECKLE
C        STATISTICS FOLLOWS A K-DISTRIBUTION ;VALID ONLY
C        FOR MONOCHROMATIC SPECKLE
C        PROGRAM TAKES NOISE DATA AND SIGNAL+NOISE DATA
C        EVALUATES THE VARIANCE AND THE CORRESPONDING
C        M OF K DISTRIBUTION AND CALCULATES THE
C        THEORETICAL K-MOMENTS AND COMPARES THEM
C        WITH EXPERIMENTAL VALUES AND THEIR ABSOLUTE
C        VALUES AND RATIOS
C        FIRST SET IS NOISE MOMENTS
C        SECOND SET IS SIGNAL+NOISE MOMENTS
      READ(5,11) AIN1
 11   FORMAT(E14.8)
      READ(5,11) AIN2
      READ(5,11) AIN3
      READ(5,11) AIN4
      READ(5,11) SN1
      READ(5,11) SN2
      READ(5,11) SN3
      READ(5,11) SN4
      WRITE(4,18)
 18   FORMAT('CALCULATION OF MOMENTS OF SPECKLE INTENSITY
      WRITE(4,19) AIN1,AIN2,AIN3,AIN4
 19   FORMAT(2X,'NOISE MOMENTS',4E14.6)
      WRITE(4,20) SN1,SN2,SN3,SN4
 20   FORMAT(2X,'SIGNAL+NOISE MOMENTS',4E14.6)
      S1=SN1-AIN1
      WRITE(4,12) S1
 12   FORMAT(2X,'AVERAGE INTENSITY=',E14.6)
      S2=SN2-2.*S1*AIN1-AIN2
      WRITE(4,13) S2
 13   FORMAT(2X,'SECOND MOMENT OF INTENSITY=',E14.6)
      S3=SN3-3.*S2*AIN1-3.*S1*AIN2-AIN3
      WRITE(4,14) S3
 14   FORMAT(2X,'THIRD MOMENT OF INTENSITY=',E14.6)
      S4=SN4-4.*S3*AIN1-6.*S2*AIN2-4.*S1*AIN3-AIN4
      WRITE(4,15) S4
 15   FORMAT(2X,'4TH MOMENT OF INTENSITY=',E14.6)
      VAR=(S2-S1*S1)/(S1*S1)
      WRITE(4,16) VAR
 16   FORMAT(2X,'NORM. VARIANCE OF INTENSITY=',E14.6)
      AM=2./(VAR-1.)
      AXX=1./AM
      AM1=S1
      AM2=2.*(1.+AXX)*S1*S1
      AM3=6.*(1.+2.*AXX)*(1.+AXX)*S1**3
      AM4=24.*(1.+AXX)*(1.+2.*AXX)*(1.+3.*AXX)*S1**4
      R1=S1/AM1
      R2=S2/AM2
      R3=S3/AM3
      R4=S4/AM4
      WRITE(4,30)
```

```
30    FORMAT(8X,'THEO.MOMENTS',5X,'EXPT.MOMENTS',5X,'RATIO
      WRITE(4,31) AM2,S2,R2
31    FORMAT(2X,'N=2',E10.4,5X,E10.4,5X,E10.4)
      WRITE(4,32)AM3,S3,R3
32    FORMAT(2X,'N=3',E10.4,5X,E10.4,5X,E10.4)
      WRITE(4,33) AM4,S4,R4
33    FORMAT(2X,'N=4',E10.4,5X,E10.4,5X,E10.4)
      STOP
      END
```

```
C        PROGRAM NAME IS KMOMENT
C        AIM OF THIS PROGRAM IS TO CHECK IF THE SPECKLE
C        STATISTICS FOLLOWS A K-DISTRIBUTION ;VALID
C        ONLY FOR MONOCHROMATIC SPECKLE
C        PROGRAM TAKES NOISE DATA AND SIGNAL+NOISE DATA
C        EVALUATES THE VARIANCE AND THE CORRESPONDING
C        M OF K DISTRIBUTION AND CALCULATES THE
C        THEORETICAL K-MOMENTS AND COMPARES THEM
C        WITH EXPERIMENTAL VALUES AND THEIR ABSOLUTE
C        VALUES AND RATIOS
C        FIRST SET IS NOISE MOMENTS
C        SECOND SET IS SIGNAL+NOISE MOMENTS
      READ(5,11) AIN1
 11   FORMAT(E14.8)
      READ(5,11) AIN2
      READ(5,11) AIN3
      READ(5,11) AIN4
      READ(5,11) SN1
      READ(5,11) SN2
      READ(5,11) SN3
      READ(5,11) SN4
      WRITE(4,18)
 18   FORMAT('CALS OF MOMENTS OF SPECKLE INTENSITY')
      WRITE(4,19) AIN1,AIN2,AIN3,AIN4
 19   FORMAT(2X,'NOISE MOMENTS',4E14.6)
      WRITE(4,20) SN1,SN2,SN3,SN4
 20   FORMAT(2X,'SIGNAL+NOISE MOMENTS',4E14.6)
      S1=SN1-AIN1
      WRITE(4,12) S1
 12   FORMAT(2X,'AVERAGE INTENSITY=',E14.6)
      S2=SN2-2.*S1*AIN1-AIN2
      WRITE(4,13) S2
 13   FORMAT(2X,'SECOND MOMENT OF INTENSITY=',E14.6)
      S3=SN3-3.*S2*AIN1-3.*S1*AIN2-AIN3
      WRITE(4,14) S3
 14   FORMAT(2X,'THIRD MOMENT OF INTENSITY=',E14.6)
      S4=SN4-4.*S3*AIN1-6.*S2*AIN2-4.*S1*AIN3-AIN4
      WRITE(4,15) S4
 15   FORMAT(2X,'4TH MOMENT OF INTENSITY=',E14.6)
      VAR=(S2-S1*S1)/(S1*S1)
      WRITE(4,16) VAR
 16   FORMAT(2X,'NORM. VARIANCE OF INTENSITY=',E14.6)
      AM=2./(VAR-1.)
      AXX=1./AM
      AM1=S1
      AM2=2.*(1.+AXX)*S1*S1
      AM3=6.*(1.+2.*AXX)*(1.+AXX)*S1**3
      AM4=24.*(1.+AXX)*(1.+2.*AXX)*(1.+3.*AXX)*S1**4
      R1=S1/AM1
      R2=S2/AM2
      R3=S3/AM3
      R4=S4/AM4
      WRITE(4,30)
```

```
30    FORMAT(8X,'THEO.MOMENTS',5X,'EXPT.MOMENTS',5X,
     1 'RATIO')
      WRITE(4,31) AM2,S2,R2
31    FORMAT(2X,'N=2',E10.4,5X,E10.4,5X,E10.4)
      WRITE(4,32)AM3,S3,R3
32    FORMAT(2X,'N=3',E10.4,5X,E10.4,5X,E10.4)
      WRITE(4,33) AM4,S4,R4
33    FORMAT(2X,'N=4',E10.4,5X,E10.4,5X,E10.4)
      STOP
      END
```

```
C       PROGRAM NAME IS MMOMENT
C       FIRST SET IS NOISE MOMENTS
C       SECOND SET IS SIGNAL+NOISE MOMENTS
C       PROGRAM CHECKS IF THE MULTIFREQUENCY OR PARTIALLY
C       COHERENT SPECKLE PATTERN IN THE TURBULENT ATMOSPHER
C       FOLLOWS  A M-DISTRIBUTIOB OR NOT.INPUT DATA IS THE
C       MOMENTS OF INTENSITY OF NOISE AND SIGNAL+NOISE.
C       BY USING THE AVERAGE AND SECOND MOMENT OF INTENSITY
C       IT CALCULATES THE PARAMETERS OF M-DISTRIBUTION
C       AND THESE VALUES ARE USED TO GET THE HIGHER
C       ORDER MOMENTS AND THE THEORETICAL VALUES ARE
C       COMPARED WITH THE EXPERIMENTAL DATA.
      READ(5,11) AIN1
 11   FORMAT(E14.8)
      READ(5,11) AIN2
      READ(5,11) AIN3
      READ(5,11) AIN4
      READ(5,11) SN1
      READ(5,11) SN2
      READ(5,11) SN3
      READ(5,11) SN4
      WRITE(4,18)
 18   FORMAT('CALS OF MOMENTS OF SPECKLE INTENSITY')
      WRITE(4,19) AIN1,AIN2,AIN3,AIN4
 19   FORMAT(2X,'NOISE MOMENTS',4E14.6)
      WRITE(4,20) SN1,SN2,SN3,SN4
 20   FORMAT(2X,'SIGNAL+NOISE MOMENTS',4E14.6)
      S1=SN1-AIN1
      WRITE(4,12) S1
 12   FORMAT(2X,'AVERAGE INTENSITY=',E14.6)
      S2=SN2-2.*S1*AIN1-AIN2
      WRITE(4,13) S2
 13   FORMAT(2X,'SECOND MOMENT OF INTENSITY=',E14.6)
      S3=SN3-3.*S2*AIN1-3.*S1*AIN2-AIN3
      WRITE(4,14) S3
 14   FORMAT(2X,'THIRD MOMENT OF INTENSITY=',E14.6)
      S4=SN4-4.*S3*AIN1-6.*S2*AIN2-4.*S1*AIN3-AIN4
      WRITE(4,15) S4
 15   FORMAT(2X,'4TH MOMENT OF INTENSITY=',E14.6)
      VAR=(S2-S1*S1)/(S1*S1)
      WRITE(4,16) VAR
 16   FORMAT(2X,'NORM. VARIANCE OF INTENSITY=',E14.6)
      AM=1./VAR
      AM1=S1
      AM2=(1.+VAR)*S1*S1
      AM3=(1.+2.*VAR)*(1.+VAR)*S1**3
      AM4=(1.+VAR)*(1.+2.*VAR)*(1.+3.*VAR)*S1**4
      R1=S1/AM1
      R2=S2/AM2
      R3=S3/AM3
      R4=S4/AM4
      WRITE(4,30)
 30   FORMAT(8X,'THEO.MOMENTS',5X,'EXPT.MOMENTS',5X,
```

```
     1 'RATIO')
      WRITE(4,31) AM2,S2,R2
31    FORMAT(2X,'N=2',E10.4,5X,E10.4,5X,E10.4)
      WRITE(4,32) AM3,S3,R3
32    FORMAT(2X,'N=3',E10.4,5X,E10.4,5X,E10.4)
      WRITE(4,33) AM4,S4,R4
33    FORMAT(2X,'N=4',E10.4,5X,E10.4,5X,E10.4)
      STOP
      END
```

```
C       PROGRAM NAME IS PMOMENT
C       FIRST SET IS NOISE MOMENTS
C       SECOND SET IS SIGNAL+NOISE MOMENTS
C       PROGRAM CHECKS IF THE MULTIFREQUENCY OR PARTIALLY
C       COHERENT SPECKLE PATTERN IN THE TURBULENT ATMOSPHER
C       FOLLOWS  A K-DISTRIBUTION OR NOT.INPUT DATA IS THE
C       MOMENTS OF INTENSITY OF NOISE AND SIGNAL+NOISE
C      IN VACUUM.THE VALUES OF EXPERIMENTAL MOMENTS
C      OF INTENSITY (SIGNAL+NOISE AND NOISE)
C      IN THE TURBUELNT ATMOSPHERE ARE GIVEN AS INPUT
C      IN THE SECOND STAGE OF THE PROGRAM.
       READ(5,11) AIN1
 11    FORMAT(E14.8)
       READ(5,11) AIN2
       READ(5,11) AIN3
       READ(5,11) AIN4
       READ(5,11) SN1
       READ(5,11) SN2
       READ(5,11) SN3
       READ(5,11) SN4
       WRITE(4,18)
 18    FORMAT('CALS OF MOMENTS OF SPECKLE INTENSITY')
       WRITE(4,19) AIN1,AIN2,AIN3,AIN4
 19    FORMAT(2X,'NOISE MOMENTS',4E14.6)
       WRITE(4,20) SN1,SN2,SN3,SN4
 20    FORMAT(2X,'SIGNAL+NOISE MOMENTS',4E14.6)
       S1=SN1-AIN1
       WRITE(4,12) S1
 12    FORMAT(2X,'AVERAGE INTENSITY=',E14.6)
       S2=SN2-2.*S1*AIN1-AIN2
       WRITE(4,13) S2
 13    FORMAT(2X,'SECOND MOMENT OF INTENSITY=',E14.6)
       S3=SN3-3.*S2*AIN1-3.*S1*AIN2-AIN3
       WRITE(4,14) S3
 14    FORMAT(2X,'THIRD MOMENT OF INTENSITY=',E14.6)
       S4=SN4-4.*S3*AIN1-6.*S2*AIN2-4.*S1*AIN3-AIN4
       WRITE(4,15) S4
 15    FORMAT(2X,'4TH MOMENT OF INTENSITY=',E14.6)
       VAR1=(S2-S1*S1)/(S1*S1)
       WRITE(4,16) VAR1
 16    FORMAT(2X,'NORM. VARIIANCE OF INTENSITY=',E14.6)
       AM1=1./VAR1
       A1=S1
       A2=(1.+VAR1)*S1*S1
       A3=(1.+2.*VAR1)*(1.+VAR1)*S1**3
       A4=(1.+VAR1)*(1.+2.*VAR1)*(1.+3.*VAR1)*S1**4
       R1=S1/A1
       R2=S2/A2
       R3=S3/A3
       R4=S4/A4
       WRITE(4,30)
 30    FORMAT(8X,'THEO.MOMENTS',5X,'EXPT.MOMENTS',5X,
      1 'RATIO')
```

```
      WRITE(4,31) A2,S2,R2
 31   FORMAT(2X,'N=2',E10.4,5X,E10.4,5X,E10.4)
      WRITE(4,32) A3,S3,R3
 32   FORMAT(2X,'N=3',E10.4,5X,E10.4,5X,E10.4)
      WRITE(4,33) A4,S4,R4
 33   FORMAT(2X,'N=4',E10.4,5X,E10.4,5X,E10.4)
C     FIRST SET IS NOISE MOMENTS IN TURBULENCE FOR
C     THE POLYCHROMATIC SPECKLE PATTERN
C     SECOND SET IS THE SIGNAL+NOISE MOMENTS FOR
C     THE POLYCHROMATIC SPECKLE PATTERN IN THE
C     TURBULENT ATMOSPHERE
      READ(5,11) BIN1
      READ(5,11) BIN2
      READ(5,11) BIN3
      READ(5,11) BIN4
      READ(5,11) BSN1
      READ(5,11) BSN2
      READ(5,11) BSN3
      READ(5,11) BSN4
      WRITE(4,70)
 70   FORMAT(4X,'CALS FOR SPECKLE IN TURBULENCE')
      WRITE(4,68)
 68   FORMAT('CALS FOR MOENTS OF SPECKLE IN TURBULENCE')
      WRITE(4,49) BIN1,BIN2,BIN3,BIN4
 49   FORMAT(2X,'NOISE MOMENTS' ,4E14.6)
      WRITE(4,50) BSN1,BSN2,BSN3,BSN4
 50   FORMAT(2X,'SIGNAL+NOISE MOMENTS',4E14.6)
      B1=BSN1-BIN1
      WRITE(4,52) B1
 52   FORMAT(2X,'AVERAGE INTENSITY=',E14.6)
      B2=BSN2-2.*B1*BIN1-BIN2
      WRITE(4,53) B2
 53   FORMAT(2X,'SECOND MOMENT OF INTENSITY=',E14.6)
      B3=BSN3-3.*B2*BIN1-3.*B1*BIN2-BIN3
      WRITE(4,54) B3
 54   FORMAT(2X,'THIRD MOMENT OF INTENSITY=',E14.6)
      B4=BSN4-4.*B3*BIN1-6.*B2*BIN2-4.*B1*BIN3-BIN4
      WRITE(4,55) B4
 55   FORMAT(2X,'FOURTH MOMENT OF INTENSITY=',E14.6)
      VAR2=(B2-B1*B1)/(B1*B1)
      WRITE(4,56) VAR2
 56   FORMAT(2X,'NORM.VARIANCE OF INTENSITY=',E14.6)
      AXX=(1.+VAR2)/(1.+VAR1)-1.
      AM2=1./AXX
      C1=B1
      C2=(1.+VAR1)*(1.+AXX)*B1*B1
      C3=(1.+2.*VAR1)*(1.+VAR1)*(1.+2.*AXX)*(1.+AXX)*B1**3
      C4=(1.+3.*AXX)*(1.+3.*VAR1)*B1*C3
      G2=B2/C2
      G3=B3/C3
      G4=B4/C4
      WRITE(4,60)
 60   FORMAT(5X,'THEO. MOMENTS=',5X,'EXPT. MOMENTS',5X,
     1 'RATIO')
```

```
      WRITE(4,61) C2,B2,G2
61    FORMAT(2X,'N=2',E10.4,5X,E10.4,5X,E10.4)
      WRITE(4,62) C3,B3,G3
62    FORMAT(2X,'N=3',E10.4,5X,E10.4,5X,E10.4)
      WRITE(4,64) C4,B4,G4
64    FORMAT(2X,'N=4',E10.4,5X,E10.4,5X,E10.4)
      STOP
      END
```

```
C       PROGRAM CALCULATES THE CUMULATIVE PDF OF
C       A K-DISTRIBUTION GIVEN M1 AND M2.
        IMPLICIT DOUBLE PRECISION (A-H,O-Z)
        DIMENSION X(8),W(8)
        DATA X/.1531506616D00,.2872644039D00,.4346274067D00,
       1.5845185666D00,.7251264097D00,.8451894879D00,
       2.9350435075D00,.9874605085D00/
        DATA W/.1053011D-04,.2783586D-03,.23353415D-02,
       1.01000446144000,.0264853011D00,.0458856532D00,
       2.0515342238D00,.0300926424D00/
        READ(5,41) AM1,AM2
 41     FORMAT(2X,D22.14,2X,D22.14)
        PHI=3.14159265358979
        COFF1=4.**(AM1-AM2+1.)*DSQRT(PHI)
        COFF2=(AM1*AM2)**(AM1)
        COFF3=GAMMA(AM1)*GAMMA(AM2)*GAMMA(AM2-AM1+.5)
        COFF4=COFF1*COFF2/COFF3
        C2=2.*AM1-1.
        C3=2.*DSQRT(AM1*AM2)
        C4=AM2-AM1-.5
        C5=2.*C3
        G=.1D00
        DELG=.1D00
 29     CONTINUE
        IF(G.GT.1.) DELG=.5D00
        IF(G.GT.3.)  DELG=1.D00
        IF(G.GT.10.)  GO TO 30
        COFF=(G**(3.04225933))*COFF4
        WRITE(5,44) COFF
 44     FORMAT(D22.14)
        SUM1=0.
        DO 31 I=1,8
        X1=X(I)
        W1=W(I)
        S1=SXX(C2,C3,C4,C5,G,X1)
        SUM1=SUM1+COFF*S1*W1
 31     CONTINUE
        WRITE(4,32) G,SUM1
 32     FORMAT(2X,'G=',F6.3,2X,'SUM1=',D22.14)
        G=G+DELG
        GO TO 29
 30     CONTINUE
        STOP
        END
        FUNCTION SXX(C2,C3,C4,C5,G,X)
        IMPLICIT DOUBLE PRECISION (A-H,O-Z)
        S2=X**(C2-5.)
        S3=DEXP(-C3*DSQRT(G)*X)
        S4=FT(C4,C5,G,X)
        SXX=S2*S3*S4
        RETURN
        END
        FUNCTION FT(C4,C5,G,X)
```

```
      IMPLICIT DOUBLE PRECISION (A-H,O-Z)
      DIMENSION T(12),W2(12)
      DATA T /.115722117358D0,.611757484515D0,
     11.51261026977600,2.83375177774400,4.59922763941800,
     26.84452545311500,9.62131684245700,13.00605499330600,
     317.11685518746200,22.15109037939700,
     428.48796725098400,37.09912104446700/
      DATA W2/2.64731371955D-01,3.77759275873D-01,
     12.44082011132D-01,9.04492222117D-02,
     1 2.01023811546D-02,2.66397354187D-03,
     22.03231592663D-04,8.36505585682D-06,
     31.66849387654D-07,1.34239103052D-09,
     43.06160163504D-12,8.14807746743D-16/
      SUM2=0.
      DO 33 I=1,12
      T1=T(I)
      W3=W2(I)
      SUM2=SUM2+W3*FTT(C4,C5,G,X,T1)
33    CONTINUE
      FT=SUM2
      RETURN
      END
      FUNCTION FTT(C4,C5,G,X,T)
      IMPLICIT DOUBLE PRECISION (A-H,O-Z)
      H2=T**C4
      H3=T+C5*DSQRT(G)*X
      H4=H3**C4
      FTT=H2*H4
      RETURN
      END
      FUNCTION GAMMA(Z)
      IMPLICIT DOUBLE PRECISION (A-H,O-Z)
      DIMENSION T(12),W2(12)
      DATA T /.115722117358D0,.611757484515D0,
     11.51261026977600,2.83375177774400,4.59922763941800,
     26.84452545311500,9.62131684245700,13.00605499330600,
     317.11685518746200,22.15109037939700,
     428.48796725098400,37.09912104446700/
      DATA W2/2.64731371955D-01,3.77759275873D-01,
     12.44082011132D-01,9.04492222117D-02,
     12.01023811546D-02,2.66397354187D-03,
     22.03231592663D-04,8.36505585682D-06,
     31.66849387654D-07,1.34239103052D-09,
     43.06160163504D-12,8.14807746743D-16/
      SUM2=0.
      DO 33 I=1,12
      T1=T(I)
      S1=T1**(Z-1.)
      W3=W2(I)
      SUM2=SUM2+W3*S1
33    CONTINUE
      GAMMA=SUM2
      RETURN
      END
```

REFERENCES

1. J. L. Lumley and H. A. Panofsky, The Structure of the Atmospheric Turbulence, Wiley-Inter Science, New York, 1964.
2. A. S. Monin and Y. M. Yaglom, Statistical Fluid Mechanics, MIT Press, Cambridge, Massachusetts 1971.
3. R. J. Hill, "Models of the Scalar Spectrum for Turbulent Advection," J. Fluid Mech. 88, 541 (1978).
4. R. J. Hill, "Spectra of Fluctuations in Refractivity, Temperature, Humidity and Temperature-Humidity Cospectrum in the Inertial and Dissipation Ranges," Radio Sci. 13, 953 (1978).
5. R. A. Elliott, J. R. Kerr and P. A. Pincus," Optical Propagation in Laboratory Generated Turbulence," Appl. Opt. 18, 3315 (1979).
6. L. A. Chernov, Wave Propagation in a Random Medium (Trans. R. A. Silverman), McGraw Hill, New York, 1960.
7. V. I. Tatarskii, Wave Propagation in a Turbulent Medium (Trans. R. A. Silverman), McGraw Hill, New York, 1961.
8. R. W. Lee and J. C. Harp, "Weak Scattering in Random Media, with Applications to Remote Sensing," Proc. IEEE 57, 375 (1969).

9. R. S. Lawrence and J. W. Strohbehn, "A Survey of Clean Air Propagation Effects Relevant to Optical Communications," Proc. IEEE 58, 1523 (1970).

10. R. L. Fante, "Electromagnetic Beam Propagation in Turbulent Media," Proc. IEEE 63, 1669 (1975).

11. A. M. Prokhorov, F. V. Bunkin, K. S. Gochelashvily and V. I. Shishov, "Laser Irradiance Propagation in Turbulent Media," Proc. IEEE 63, 790 (1975).

12. R. L. Fante, "Electromagnetic Beam Propagation in Turbulent Media: An Update," Proc. IEEE 68, 1424 (1980).

13. V. I. Tatarskii, "The Effect of the Turbulent Atmosphere on Wave Propagation, Springfield, U.S. Dept. commerce, 1971.

14. A. Ishimaru, Wave Propagation and Scattering in Random Media, Vols. 1 and 2. Academic Press, New York 1978.

15. J. W. Strohbehn, Ed., Laser Beam Propagation in the Atmosphere (Topics in Applied Physics, Vol. 25) Springer Verlag 1978.

16. P. M. Livingstone, "Multiple Scattering of Light in a Turbulent Atmosphere," J. Opt. Soc. Am. 56 1660 (1966).

17. R. Dashen, "Path Integrals for Waves in Random Media," J. Math. Phys. 20, 894 (1979).

18. M. H. Lee, J. F. Holmes and J. R. Kerr, "Statistics of Speckle Propagation Through the Turbulent Atmosphere," J. Opt. Soc. Am. 66, 1164 (1976).

19. J. F. Holmes, M. H. Lee and J. R. Kerr, "Effect of the Log-amplitude Covariance Function on the Statistics of Speckle Propagation Through the Turbulent Atmosphere," J. Opt. Soc. Am. 70, 355 (1980).

20. J. F. Holmes, J. R. Kerr, M. H. Lee and M. E. Fossey, "Experimental Feasibility-Pulsed Laser Remote Crosswind Measurement System Feasibility and Design," USAARC, Research and Development Tech. Report, FA-TR 76065, November 1975.

21. R. L. Fante, "Multiple Frequency Mutual Coherence Function for a Beam in a Random Medium," IEEE Trans. on Antennas and Propag. Vol. AP-26, 621-623 (1978).

22. J. Carl Leader, "Intensity Fluctuations Resulting from Partially Coherent Light Propagating Through Atmospheric Turbulence," J. Opt. Soc. Am. 69, 73 (1979).

23. H. T. Yura, "Mutual Coherence Function of a Finite Cross Section Optical Beam Propagating in a Turbulent Atmosphere," Appl. Opt. 11, 1399 (1972).

24. A. Ishimaru, "Temporal Frequency Spectra of Multifrequency Waves in Turbulent Atmosphere," IEEE Trans. on Antennas and Propag. Vol. AP-20, 10 (1972).

25. L. Mandel, "Fluctuations of Photon Beams: The Distribution of Photoelectrons," Proc. Phys. Soc. 74, 233 (1950).

26. D. Middleton, Statistical Communication Theory, McGraw Hill, New York, 1960.

27. M. Nakagami, "The M-distribution - A General Formula of Intensity Distribution of Rapid Fading," in Statistical Methods in Radio Wave Propagation, edited by W. C. Hoffman, pages 3-36, Pergamon, New York, 1965.

28. G. N. Ramachandran, "Fluctuations of Light Intensity in Coronae, Formed by Diffraction," Proc. Indian Acad. of Sci., Vol. A18, 190 (1943).

29. J. W. Goodman, "Statistical Properties of Laser Sparkle Patterns," Tech. Report No. 2303-1, Systems Laboratory, Stanford Electronics Laboratories, Stanford, California (1963).

30. G. Parry, "Some Effects of Temporal Coherence on the First Order Statistics of Speckle," Opt. Acta 21, 763 (1974).

31. G. Parry, "The Scattering of Polychromatic Light from Rough Surfaces: The First Order Statistics," Opt. and Quant. Electron. 7, 311 (1975).

32. H. M. Pedersen, "On the Contrast of Polychromatic Speckle Patterns and its Dependence on Surface Roughness," Opt. Acta 22, 15 (1975).

33. H. M. Pedersen, "Second Order Statistics of Light Diffracted from Gaussian Rough Surfaces with Applications to the Roughness Dependence of Speckles," Opt. Acta 22, 523 (1975).

34. T. S. McKechnie, "Speckle Reduction," Chap. 4 in Laser Speckle and Related Phenomena, edited by J. C. Dainty (Springer Verlag, New York, 1975).

35. J. C. Dainty, "Some Statistical Properties of Random Speckle Patterns in Coherent and Partially Coherent Illumination," Opt. Acta 17, 761 (1970).

36. J. C. Dainty (ed.), Laser Speckle and Related Phenomena (Springer Verlag, New York, 1975).

37. P. Beckman and A. Spizzichino, Scattering of Electromagnetic Waves from Rough Surfaces, (Pergamon Press, New York, 1963).

38. A. Papoulis, Probability, Random Variables and Stochastic Processes (McGraw Hill, New York, 1965).

39. H. L. Van Trees, Detection Estimation and Modulation Theory, Part I (Wiley, New York, 1968).

40. G. Parry, "Speckle Patterns in Partially Coherent Light," in Laser Speckle and Related Phenomena, edited by J. C. Dainty, Chap. 3 (Springer Verlag, New York, 1975).

41. K. Fukunaga, Introduction to Statistical Pattern Recognition, Chap. 8 (Academic Press, New York, 1972).

42. J. W. Goodman, "Probability Density Function of the Sum of N Partially Correlated Speckle Patterns," Opt. Commun. 13, 244 (1975).

43. R. Barakat, "First Order Probability Densities of Laser Speckle Patterns Observed Through Finite Scanning Apertures," Opt. Acta 20, 729 (1973).

44. P. A. Pierre, "Characteristics of Gaussian Random Processes by Representations in Terms of Independent Random Variables," IEEE Trans. on Inf. Theory, Vol. IT-15, 648 (1969).

45. W. D. Ray and R. M. Driver, "Further Decomposition of the Karhunen-Loeve Series Representation of a Stationary Random Process," IEEE Trans. on Inf. Theory, Vol. IT-16, 663 (1970).

46. R. J. Collins, D. F. Nelson, A. L. Schalow, W. Bond, C. G. B. Garret and W. Kaiser, "Coherence, Narrowing, Directionality and Relaxation Oscillations in the Light Emission from Ruby," Phys. Rev. Lett. 5, 303 (1960).

47. D. A. Berkeley and G. J. Wolga, "Coherence Studies of Emission from a Pulsed Ruby Laser," Phys. Rev. Lett. 9, 479 (1962).

48. W. S. C. Chang and N. R. Kilcoyne, "A Study of Partial Coherence and its Application to the Collimation of Pulsed Multimode Laser Radiation," Appl. Opt. 4, 1404 (1965).

49. J. W. Foreman, Jr., "Optical Path Length Difference Effects in Photomixing with Multimode Gas Laser Radiation," Appl. Opt. 6, 821 (1967).

50. W. T. Cathey, Jr., "Multiple Frequency Wavefront Recording," Opt. Acta 15, 35 (1968).

51. R. J. Collier, C. B. Buekhardt and C. H. Lin, Optical Holography, (Academic Press, New York, 1971).

52. B. A. Sotskii and A. M. Goncharenko, "On the Relationship Between the Radiation Coherence and the Number of Modes of a Laser," Opt. and Spectrosc. 19, 435 (1965).

53. M. Born and E. Wolf, Principles of Optics (Pergamon Press, New York, 1977) Chapter X.

54. J. F. Holmes, J. R. Kerr, R. A. Elliott, M. H. Lee, P. A. Pincus and M. E. Fossey, "Experimental Feasibility Pulsed Laser Remote Crosswind Measurement Systems - Feasibility and Design (Part V)," USAARDC Report No. ARSCD-CR-79-007, Dover, New Jersey, September 1978.

55. M. Fossey, "Statistical Measurements of Speckle Propagation Through The Turbulent Atmosphere," M.S. Thesis, Department of Applied Physics and Electronic Science, Oregon Graduate Center, 1976.

56. R. J. Glauber, "Photon Correlations," Phys. Rev. Lett. 10, 84 (1963).

57. L. Mandel and E. Wolf, "Coherence of Optical Fields," Rev. Mod. Phys. 37, 231 (1965).

58. J. W. Goodman, "Role of Coherence Concepts in the Study of Speckle," SPIE Vol. 194, Applications of Optical Coherence, 86 (1979).

59. Ref. 7, page 16.

60. Ref. 7, Chapter 7.

61. Ref. 7, Chapter 9.

62. R. F. Lutomirski and H. T. Yura, "Wave Structure Function and Mutual Coherence Function of an Optical Wave in a Turbulent Atmosphere," J. Opt. Soc. Am. 61, 482 (1971).

63. S. F. Clifford, "The Classical Theory of Wave Propagation in Turbulent Medium." Chapter 2 in Ref. 15.

64. S. F. Clifford, G. R. Ochs and R. S. Lawrence, "Saturation of Optical Scintillations by Strong Turbulence," J. Opt. Soc. Am. 64, 148 (1974).

65. D. L. Fried, "Spectral and Angular Covariance of Scintillation for Propagation in a Randomly Homogeneous Medium," Appl. Opt. 10, 721 (1971).

66. P. Pincus and J. R. Kerr, "Spectral Covariance of Scintillations," Appl. Opt. 15, 2305 (1976).

67. M. H. Lee, J. F. Holmes and J. R. Kerr, "Generalized Spherical Wave Mutual Coherence Function," J. Opt. Soc. Am. 67, 1279 (1976).

68. M. Abramowitz and I. A. Stegun, Handbook of Mathematical Functions, AMS 55, NBS, U. S. Dept. of Commerce, 1972, page 363.

69. J. Fred Holmes, "Speckle Propagation Through the Turbulent Atmosphere," SPIE Proc., Vol. 243, Applications of Speckle Phenomena, 20 (1980).

70. G. Arfken, Mathematicl Methods for Physicists, (Academic Press, New York) page 494.

71. H. T. Yura, "Physical Model for Strong Optical Amplitude Fluctuations in a Turbulent Medium," J. Opt. Soc. Am. 64, 59 (1974).

72. S. F. Clifford and H. T. Yura, "Equivalence of Two Theories of Strong Optical Scintillation," J. Opt. Soc. Am. 64, 1641 (1974).

73. R. J. Hill and S. F. Clifford, "Modified Spectrum of Atmospheric Temperature Fluctuations and its Application to Optical Propagation," J. Opt. Soc. Am. 68, 892 (1978).

74. R. J. Hill and S. F. Clifford, "The Theory of Saturation of Optical Scintillation by Strong Turbulence for Refractive Index Spectra," J. Opt. Soc. Am. 71, 675 (1981).

75. P. A. Pincus, M. E. Fossey, J. F. Holmes and J. R. Kerr, "Speckle Propagation Through Turbulence: Experimental," J. Opt. Soc. Am. 68, 760 (1978).

76. Ref. 68, page 361.

77. D. A. deWolf, "Are Strong Irradiance Fluctuations Log-normal or Rayleigh Distributed," J. Opt. Soc. Am. 59, 1455 (1969).

78. J. W. Strohbehn, Ting-i Wang and J. P. Speck, "On the Probability Distribution of Line of Sight Fluctuations of Optical Signals," Radio Sci. 10, 59 (1975).

79. M. H. Lee, R. A. Elliott, J. F. Holmes and J. R. Kerr, "Variance of Irradiance for Saturated Scintillations," J. Opt. Soc. Am. 66, 1389 (1976).

80. I. S. Gradshteyn and I. M. Ryzhik, Tables of Integrals, Series and Products, page 340 (Academic Press, New York 1965).

81. Sir M. Kendall and A. Stuart, The Advanced Theory of Statistics, Vol. 1, 156-159 (McMillan Publishing Company, Inc., New York, 1977).

82. E. Jakeman and P. N. Pusey, "Significance of K-distributions in Scattering Experiments," Phys. Rev. Lett. 40, 546 (1978).

83. G. Parry and P. N. Pusey, "K-distributions in Atmospheric Propagation of Laser Light," J. Opt. Soc. Am. 69, 796 (1978).

84. S. F. Clifford and R. J. Hill, "Relation Between Irradiance and Log-amplitude Variance for Optical Scintillation Described by K-distribution," J. Opt. Soc. Am. 71, 112 (1981).

85. G. R. Ochs, S. F. Clifford and Ting-i Wang, "Laser Wind Sensing: The Effects of Saturation of Scintillation," Appl. Opt. 15, 403 (1976).

BIOGRAPHY

The author was born in Nandigama, Andhra Pradesh (India), on June 1, 1949 and attended the R.C.M. St. Anthony School, Visakhapatnam, India. He received his bachelor's degree in Electronics and Communication Engineering from the Andhra University, Waltair, India in 1971 and his M. Tech. in Electronics and Electrical Communication Engineering from the Indian Institute of Technology, Kharagpur, India in 1975. Thereafter, he worked as a senior research assistant at the Radar and Communication Center of IIT, Kharagpur until November 1975, and then joined Tata Institute of Fundamental Research, Bombay as scientific officer in the Radio Astronomy Group. He joined the Oregon Graduate Center in 1977 and completed all requirements for his Ph.D. in April 1982.